N-trimethyl chitosan (TMC) carriers for nasal and pulmonary delivery of therapeutic proteins and vaccines

Maryam Amidi

N-trimethyl chitosan (TMC) carriers for nasal and pulmonary delivery of therapeutic proteins and vaccines
Maryam Amidi
Ph.D. Thesis, with a summary in Dutch
Utrecht University, The Netherlands
April 2007
ISBN: 90-393-4492-7

Cover design: Martijn Pieck
Produced by F&N Boekservice/Eigen Beheer, Amsterdam

N-trimethyl chitosan (TMC) carriers for nasal and pulmonary delivery of therapeutic proteins and vaccines

N-trimethyl chitosan dragersystemen voor de nasale en pulmonale toediening van therapeutische eiwitten en vaccins

(met een samenvatting in het Nederlands)

Proefschrift

ter verkrijging van de graad van doctor aan de Universiteit Utrecht
op gezag van de rector magnificus, prof.dr. W.H. Gispen,
ingevolge het besluit van het college voor promoties
in het openbaar te verdedigen
op maandag 16 april 2007 des middags te 4.15 uur

door

Maryam Amidi

geboren op 5 mei 1974, te Tehran, Iran

Promotors: Prof. Dr. W.E. Hennink

Prof. Dr. W. Jiskoot

Prof. Dr. D.J.A. Crommelin

Printing of this thesis was financially supported by:

OctoPlus B.V., Leiden, The Netherlands

Feyecon D & I B.V., Weesp, The Netherlands

Utrecht University

If a man will begin with certainties,
he shall end in doubts;
but if he will be content to begin with doubts
he shall end in certainties.

Sir Francis Bacon
(1561 - 1626)

To my parents

Table of contents

Aim and outline of the thesis

1 General introduction

Recombinant DNA technology has resulted in the availability of a large number of therapeutic proteins and proteins-based antigens, which are almost exclusively administered by parenteral injections or infusions. This is rather inconvenient for patients, usually requires medical personnel and/or hospitalization and is therefore expensive. Consequently, alternative routes for the administration of protein pharmaceuticals including oral, buccal, vaginal, nasal and pulmonary administration are being explored. In particular, the respiratory tract including nasal mucosa and pulmonary epithelium are attractive sites for the delivery of therapeutic protein and antigens, because they have large absorptive surfaces, especially in the lungs, and low proteolytic activity (1-4). Importantly, pulmonarily and intranasally administered antigens can induce both local and systemic immune responses. A local immune response can be induced by efficient delivery of an antigen to the mucosal associated lymphoid tissue (MALT) as well as antigen presenting cells (APC) lining between the respiratory epithelial cells.

The inherent physical, chemical and proteolytic instability and the large size are major factors for poor absorption of proteins across mucosal surfaces. Moreover, soluble antigens are hardly taken up by the MALT. The nasal mucosa and the central respiratory tract are covered by a mucous coat, which is constantly removed by mucociliary clearance. This in turn causes an additional obstacle for the mucosal delivery of proteins (3, 5). To overcome these barriers, proteins should be formulated with proper delivery systems that protect them against degradation, prevent their rapid elimination from administration sites and enhance their absorption and/or uptake across epithelial barriers. Because the nasal mucosa and the lungs have their own specific barriers in terms of accessibility, epithelial cell type and presence or absence of a mucous layer in different parts of the respiratory tract, the properties of delivery systems for therapeutic proteins and antigens have to be tailored according to the route of administration.

In recent years, particulate carriers based on chitosan and its derivatives have received particular interest for the delivery of proteins via mucosal routes (6-11). Chitosan based polymers are mucoadhesive and are capable of opening the tight junctions between epithelial cells (6-11). Both properties may help to stimulate the absorption of protein/antigen and/or uptake of the protein/antigen loaded chitosan-based nano and microparticles. In contrast to chitosan, which is insoluble and inactive as mucoadhesive and permeation enhancer at neutral pH, N-trimethyl chitosan chloride (TMC), a partially quaternized chitosan derivative, shows good water solubility over a wide pH range with mucoadhesive properties and excellent absorption enhancing effects even at neutral pH (12, 13). Therefore, TMC is an excellent candidate for preparation of protein-loaded particles for nasal and pulmonary administration.

2 Aim and outline of the thesis

The aim of this thesis was to evaluate the potential of TMC based particulate carriers systems for their suitability for nasal and pulmonary delivery of therapeutic proteins and antigens. To this end, protein-loaded TMC nanoparticles and microparticles were prepared and characterized. Their efficacy for nasal and pulmonary delivery of different model proteins as well as a therapeutically relevant protein (insulin) and antigens (influenza subunit antigen and diphtheria toxoid) was investigated in animal models.

In **Chapter one** an overview is given of non-parenteral protein delivery, focusing on nasal and pulmonary routes of administration. The recent literature on mucoadhesive polymeric carriers, in particular chitosan-based polymers and TMC for protein and antigen delivery is discussed. The available techniques for the preparation of protein/antigen-loaded nano/microparticles (in particular those based on chitosan/TMC) are summarized. Finally, the applications and in vivo evaluations of the chitosan-based particulate delivery systems for peptide/protein, antigens and DNA are discussed.

Chapter two describes the preparation and characterization of TMC nanoparticle suspensions as carrier for the nasal delivery of proteins, using (ov)albumin as a model protein. Protein-loaded nanoparticles are prepared by mixing an aqueous solution containing TMC and ovalbumin with an aqueous tripolyphosphate (TPP) solution, at ambient temperature and pH 7.4. The antigenicity of the loaded protein as well as the biocompatibility of the nanoparticles are assessed in vitro and in vivo. Finally, the ability of the nanoparticles to cross nasal mucosal barriers will be shown in a study in rats.

To demonstrate the potential of TMC nanoparticles as a nasal vaccine delivery system, an immunization study using influenza hemagglutinin antigen is described in **Chapter three**. Mice are vaccinated intranasally with a monovalent influenza subunit antigen associated with TMC nanoparticles. The potency of the TMC vaccine formulation in comparison with conventional intramuscularly administered subunit vaccine is assessed by measuring both systemic and local immune responses (IgG and IgA antibody titers) in serum and nasal washes.

Chapter four reports on the physicochemical characteristics of insulin-loaded microparticles for pulmonary delivery prepared by a supercritical CO^2 drying process. TMC20, as a mucoadhesive, TMC60, as a mucoadhesive and an absorption enhancer (12, 14) and dextran, as a non-mucoadhesive and non-permeation enhancer, were selected as polymeric carriers. The insulin-containing particles are characterized for their geometric and aerodynamic size distribution, which are important characteristics for pulmonary delivery of therapeutic proteins. The powder characteristics and the structural integrity of insulin in the freshly prepared formulations as well as in aged powders are evaluated using chromatographic and spectroscopic techniques.

In **Chapter five**, the therapeutic potential of the insulin-TMC powders as described in Chapter four is investigated in diabetic rats. Furthermore, the pharmacological

activity of the administered insulin is determined by using a population PKPD model. Finally, possible acute adverse effects of these microparticles are examined by histological studies of the lungs of the treated rats.

Chapter six describes the preparation of diphtheria toxoid (DT) loaded TMC50 (as a mucoadhesive and an absorption enhancer) and dextran (as a non-permeation enhancer) microparticles by a supercritical CO_2 drying process. The efficiency of the DT-containing particles to induce local and systemic immune responses after pulmonary immunization is investigated in guinea pigs.

In **Chapter seven,** the results and conclusions of this thesis are summarized and, in addition, perspectives on future research are given.

References

1. S. S. Davis. Nasal Vaccines. *Drug Del. Rev*. 51: 21-42. (2001).

2. J. S. Patton, C. S. Fishburn, and J. G. Weers. The lungs as a portal of entry for systemic drug delivery. *Proc Am Thorac Soc* 1: 338-44 (2004).

3. J. S. Patton. Mechanisms of macromolecules absorption by the lungs. *Adv Drug Del Rev* 19: 3-36 (1996).

4. A. J. Almeidaand H. O. Alpar. Nasal delivery of vaccines. *J. Drug Target.* 3: 455-467 (1996).

5. R. J. Soane, M. Hinchcliffe, S. S. Davis, and L. Illum. Clearance characteristics of chitosan based formulation in the sheep nasal cavity. *Int J pharm* 217: 183-191 (2001).

6. I. M. van der Lubben, G. Kersten, M. M. Fretz, C. Beuvery, J. C. Verhoef, and H. E. Junginger. Chitosan microparticles for mucosal vaccination against diphtheria: oral and nasal efficacy studies in mice. *Vaccine* 28: 1400-1408 (2003).

7. I. M. van der Lubben, F. A. Konings, G. Borchard, J. C. Verhoef, and H. E. Junginger. In vivo uptake of chitosan microparticles by murine Peyer's patches: visualization studies using confocal laser scanning microscopy and immunohistochemistry. *J Drug Target*. 9: 39-47 (2001).

8. P. Calvo, C. Remunan-Lopez, J. L. Vila-Jato, and M. J. Alonso. Chitosan and chitosan/ethylene oxide-propylene oxide block copolymer nanoparticles as novel carriers for proteins and vaccines. *Pharm Res* 14: 1431-1436 (1997).

9. R. Fernandez-Urrusuno, P. Calvo, C. Remunan-Lopez, J. L. Vila-Jato, and J. A. Alonso. Enhancement of nasal absorption of Insulin using chitosan nanopartocles. *Pharm Res* 16: 1576-1581 (1999).

10. M. Amidi, S. G. Romeijn, G. Borchard, H. E. Junginger, W. E. Hennink, and W. Jiskoot. Preparation and characterization of protein-loaded N-trimethyl chitosan nanoparticles as nasal delivery system. *J Control Release* 111: 107-116 (2006).

11. A. Vila, A. Sanchez, K. Janes, I. Behrens, T. Kissel, J. L. Vila Jato, and M. J. Alonso. Low molecular weight chitosan nanoparticles as new carriers for nasal vaccine delivery in mice. *Eur J Pharm Biopharm* 57: 123-131 (2004).

12. J. H. Hamman, M. Stander, and A. F. Kotzé. Effect of the degree of quaternization of N-trimethyl chitosan chloride on absorption enhancement: in vivo evaluation in rat nasal epithelia. *Int J Pharm* 232: 235-242 (2002).

13. M. Thanou, J. C. Verhoef, J. H. M. Verheijden, and H. E. Junginger. Intestinal absorption of octeriotide: N-trimethyl chitosan chloride (TMC) ameliorates the permeability and absorption properties of the somatostatin analogue in vitro and in vivo. *J Pharm Sci* 89: 951-957 (2000).

14. D. Snyman, J. H. Hamman, and A. F. Kotze. Evaluation of the mucoadhesive properties of N-trimethyl chitosan chloride. *Drug Dev Ind Pharm* 29: 61-9 (2003).

Chapter one

1 A literature review on non-parenteral delivery systems based on chitosan and its derivatives for protein therapeutics and antigens

1 Non-parenteral protein delivery

Significant advances in biotechnology have resulted in the discovery and availability of therapeutic proteins as well as protein-based antigens. Proteins and vaccines are regularly delivered by parenteral routes, because of their low bioavailability and/or poor immunogenicity when administered via non-parenteral routes of administrations (15). However, injections are inconvenient for patients and injectable formulations normally have high production costs. Therefore, in recent years considerable research has been focused on non-invasive routes, such as mucosal (oral, buccal, nasal, pulmonary and vaginal) and transdermal ones, for delivery of proteins and vaccines (16-27). However, the delivery of these macromolecules via non-invasive routes remains a challenge because of their poor absorption and their susceptibility to enzymatic degradation. Because of the latter, both the nose and the lungs are particularly attractive sites as the local proteolytic activity is relatively low (1, 3, 28-30). The nose is easily accessible but has a relatively small absorptive surface area (150 cm^2), whereas the lungs have a large surface area (~ 75 m^2), extensive vasculature and a thin membrane, but are less well accessible. Importantly, intranasally and pulmonarily administered vaccines can induce both systemic and local immune responses (1, 26, 31). The potential of nasal and pulmonary delivery of macromolecular therapeutics and vaccines is very high, although, as pointed out in the next sections, a number of challenges still have to be overcome.

2 The respiratory epithelium and mucosal surfaces

After a mucus or a surfactant layer, the second barrier of the respiratory tract that proteins encounter is formed by a monolayer of epithelial cells, which comprises two completely different epithelia, namely, the airway and alveolar epithelium. The airway epithelium consists of pseudostratified columnar ciliated cells, basal cells and mucus-secreting goblet cells (figure 1). The epithelial cells are tightly sealed by intercellular junctions (named as the 'tight junctions'), which make them essentially impermeable for macromolecules. This pseudostratified columnar epithelium is found in the nasal cavity, the trachea, the bronchi and the bronchioles, and is covered by a thick mucus layer, which is propelled by beating cilia to the glottis and is removed from the airways (1, 3). The thickness of the epithelium and also the mucus layer decreases from the upper respiratory tract toward the lower part.

The epithelium at the mucosal surfaces of the respiratory tract is associated with immunological active compartments, the mucosal-associated lymphoid tissue (MALT) (32-34), which is an important site for antigen sampling and that mucosal surfaces represent a major entry portal for pathogens. The mucosal lymphoid follicles in the nasal-associated lymphoid tissue (NALT) and bronchus-associated lymphoid tissue (BALT) are homing several immunological cells such as dendritic cells (DCs), T and B lymphocytes, which participate in induction of immune responses against

pathogens entered through the respiratory mucosa (31). The epithelial cells covering the NALT and BALT are equipped with microfold cells (M-cell) which are involved in uptake, transport and presentation of antigens present in the respiratory lumen. Transport of the antigens to the subepithelial compartment (sub-mucosa) within the MALT is a prerequisite for inducing local and subsequent systemic immune responses (35-37).

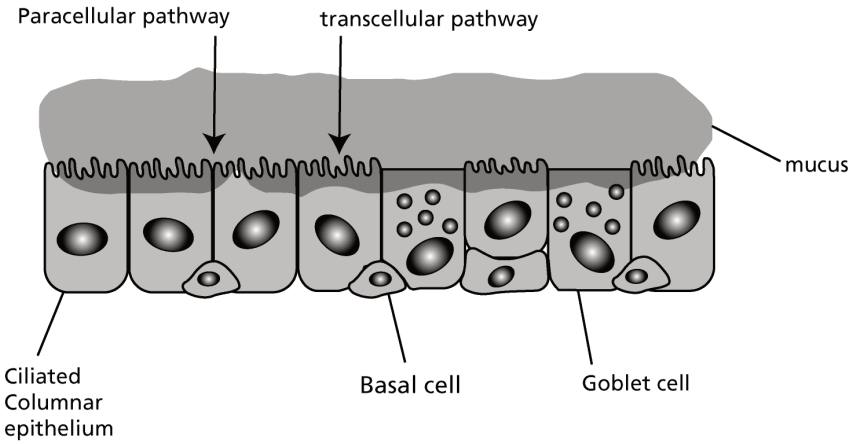

Figure 1. Lateral view of the air way epithelia at the upper and the central respiratory tract.

In the distal respiratory tract, the epithelium becomes less columnar and the alveolar epithelial cells are rather thin (0.1-0.5 μm) and devoid of a mucus barrier. The respiratory epithelium at the alveolar region comprises two cell types, namely extremely broad and thin cells (called Type I cells) and compact surfactant-secreting Type II cells (3, 38) (figure 2). The alveolar epithelium of the lung is opposed to extensive capillaries where gas-exchange and absorption of molecules occurs.

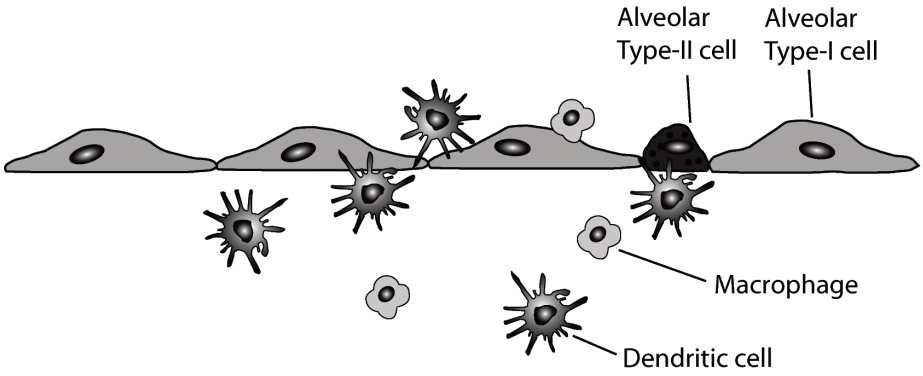

Figure 2. Lateral view of the alveolar epithelia at the distal respiratory tract.

2.1 Absorption of proteins and antigens/vaccines through the respiratory epithelium

Macromolecules can pass the respiratory epithelia via two different pathways, namely, paracellularly through tight junctions between the cells or transcellularly by endocytosis (3, 29) (figure 1). As pointed out in the previous section, the airway epithelium has firmly closed tight junctions, which made them essentially impermeable for macromolecules (29). Moreover, the mucus layer, which covers the upper respiratory (nasal cavity, conductive airways) and the central respiratory tract, as well as the mucociliary clearance and mucociliary escalator, are extra barriers that limit the uptake of proteins in the respiratory lumen. Therefore, agents, called 'penetration enhancers', that reversibly open the tight junctions may facilitate the transition of macromolecules across the epithelium to the sub-mucosa and subsequently to the systemic and/or the lymphatic circulation. Contrary to the airways epithelium, at the alveoli the tight junctions between the alveolar epithelial cells are loose and macromolecules up to 22 kDa can passively diffuse via paracellular pathways (39, 40). Moreover, the mucus barrier and mucociliary escalator mechanism are absent in the alveoli region, which is additionally advantageous for protein absorption. Besides the paracellular route by which relatively small proteins are absorbed, larger proteins can be absorbed from the respiratory tract by the transcellular pathway, which includes both nonspecific and receptor-mediated endocytosis (41). The transport of antibodies and plasma proteins, like albumin, across the epithelial barrier from the systemic circulation to the respiratory lumen and vice versa occurs by receptor-mediated endocytosis. However, macromolecular therapeutics, antigens as well as particulate protein and antigen formulations might pass the epithelial barrier by nonspecific endocytosis, although the precise mechanism is not well known, yet (3, 42, 43).

2.2 Induction of immune responses in the respiratory tract

At the mucosal surfaces, M-cells of the epithelium overlaying NALT and BALT are involved in the uptake and transport of antigens, especially in particulate form, to the sub-mucosa where antigen-presenting cells (APCs) and T cells are present (31, 33, 35-37). This results in generation of IgG as well as secretory IgA antibodies. The latter cross the epithelial cells and contribute to protection of mucosal sites from further binding and entry of pathogens (figure 3). However, the exact mechanisms of immune induction, such as the function of BALT and antigen sampling by M-cells, are not fully unraveled yet. The presence of BALT in humans is well established. BALTs are not organized structures in human lungs and it is believed that lungs can develop classical BALT structures when exposed to a high antigen load (44). At the alveolar region, phagocytic cells like alveolar macrophages and DCs are crucial for protection and induction of immunity against particulate antigens (45-48). They phagocytose, process, present and translocate the antigen to the lymph nodes and subsequently activate naïve T cells and B lymphocytes to induce immune responses (45-47, 49).

3A

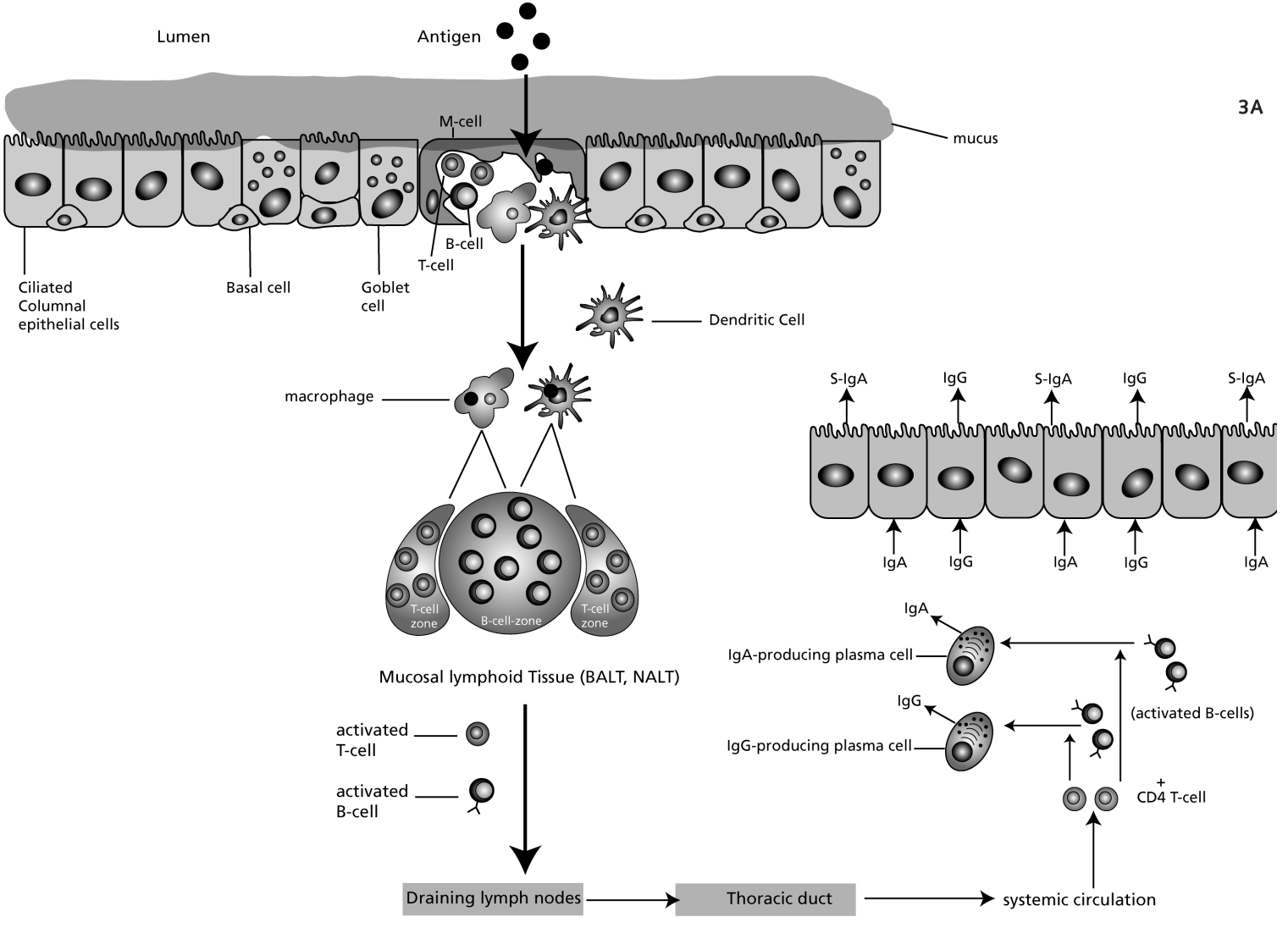
Lumen
Antigen
M-cell
mucus
B-cell
T-cell
Ciliated
Columnal
epithelial cells
Basal cell
Goblet
cell
Dendritic Cell
macrophage
S-IgA
IgG
S-IgA
IgG
S-IgA
IgA
IgG
IgA
IgG
IgA
T-cell
zone
B-cell-zone
T-cell
zone
Mucosal lymphoid Tissue (BALT, NALT)
IgA
IgA-producing plasma cell
IgG
IgG-producing plasma cell
(activated B-cells)
+
CD4 T-cell
activated
T-cell
activated
B-cell
Draining lymph nodes
Thoracic duct
systemic circulation

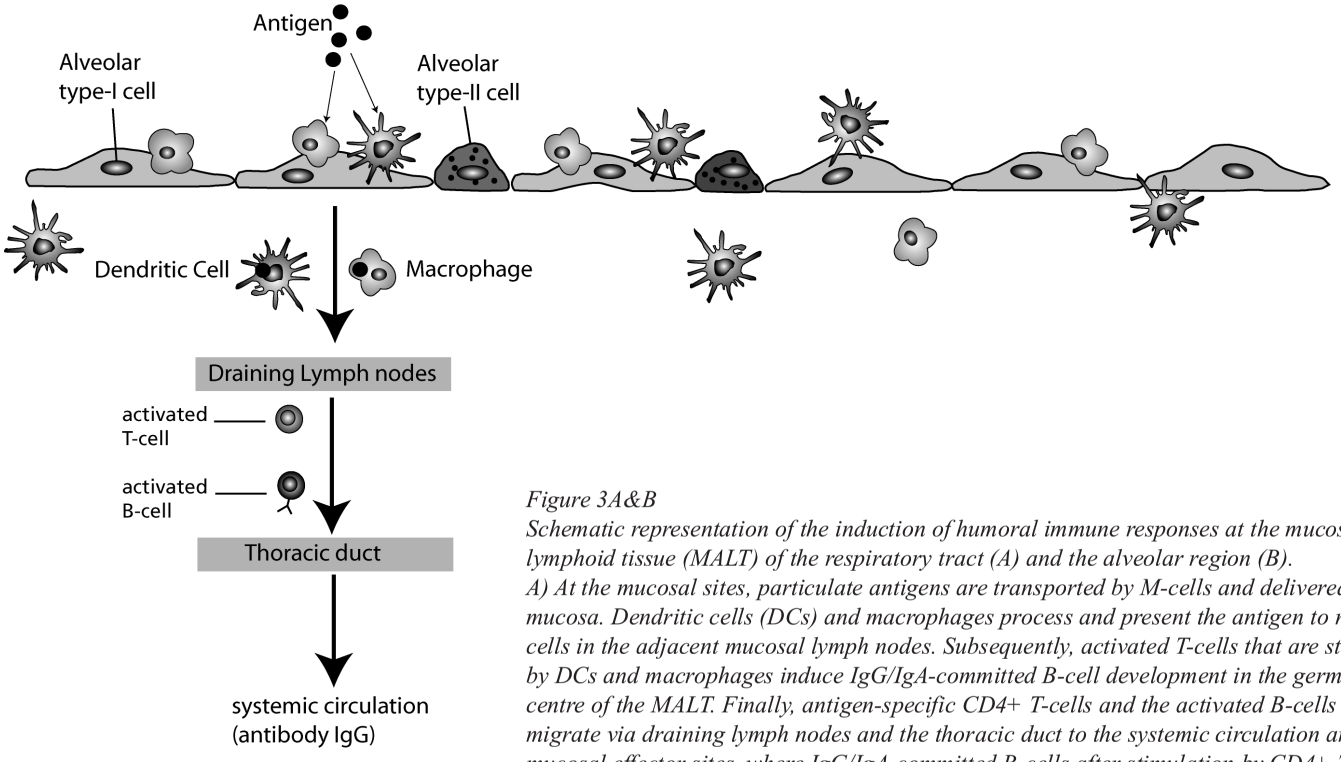

Figure 3A&B
Schematic representation of the induction of humoral immune responses at the mucosal lymphoid tissue (MALT) of the respiratory tract (A) and the alveolar region (B).
A) At the mucosal sites, particulate antigens are transported by M-cells and delivered to sub-mucosa. Dendritic cells (DCs) and macrophages process and present the antigen to naïve T-cells in the adjacent mucosal lymph nodes. Subsequently, activated T-cells that are stimulated by DCs and macrophages induce IgG/IgA-committed B-cell development in the germinal centre of the MALT. Finally, antigen-specific CD4+ T-cells and the activated B-cells will migrate via draining lymph nodes and the thoracic duct to the systemic circulation and other mucosal effector sites, where IgG/IgA-committed B-cells after stimulation by CD4+ T-helper cells differentiate to antibody secreting plasma cells, which produce IgG and IgA antibodies.
B) At the alveoli, particulate antigens are taken up and processed by alveolar DCs and macrophages which migrate to the nearest draining lymph node to present the antigens to naïve T-cells. The activated T-cells and B-cells will migrate via the thoracic duct to the systemic circulation, where IgG-committed B-cells after stimulation by CD4+ T-cells differentiate to antibody secreting plasma cells, which produce IgG antibodies.

3 Practical issues for nasal and pulmonary delivery of therapeutic proteins and vaccines

Despite the advantages and potentials of nasal and pulmonary protein delivery, there are still a number of issues that have to be tackled. The low permeability of the respiratory epithelium, poor delivery at the site of the absorption and short residence time of proteins in the upper and central respiratory tract, due to the mucociliary clearance in the nasal cavity and in the lungs, are severe limitations for protein/vaccine delivery in the respiratory tract (5, 28, 50). Moreover, for pulmonary delivery the poor deposition of protein formulations to the alveoli is another major limitation. This implies that proper delivery systems are needed that efficiently deliver protein/antigen formulations to the absorption sites that increase the absorption/uptake of the proteins/protein-loaded particles from the epithelium and prevent rapid elimination of the formulations from the respiratory tract.

To deposit proteins efficiently into the lungs they must be inhaled as particles with aerodynamic diameters preferably between 1.5-3 μm (2, 24). Mucoadhesive microparticles with permeation-enhancing properties and a suitable aerodynamic diameter are the most studied systems for pulmonary delivery of macromolecules (1, 22, 26, 27, 51, 52). For nasal delivery both mucoadhesive micro- and nanoparticles, which can interact with the epithelial cells, are applied to enhance protein/antigen absorption. These particulate carrier systems prolong the residence time of proteins in the respiratory tract, enhance the paracellular passage of the macromolecules through the respiratory epithelium and improve significantly the uptake of encapsulated protein/antigen by epithelial cells, M-cells present in MALT (NALT or BALT) (31, 33, 35-37, 53) and alveolar DCs and macrophages (45-48). The size of the particles, which can be controlled by the formulation conditions, is crucial for efficient pulmonary and nasal delivery of proteins and vaccines (1, 2, 22-24). Intranasally delivered antigen-loaded nanoparticles are taken up efficiently by M-cells and epithelial cells, subsequently activate the immune cells in the NALT and draining lymph nodes (53), whereas for efficient pulmonary delivery, an average aerodynamic size of 1-3 μm is essential to reach the absorptive area.

4 Mucoadhesive delivery systems

As pointed out in the previous sections, a candidate pulmonary or nasal delivery system should have mucoadhesive properties. A great variety of neutral and anionic polysaccharides such as starch, cellulose derivatives (e.g. carboxymethylcellulose), aliginate and hyaluronic acid are mucoadhesive. Moreover, synthetic polymers including anionic polyacrylates such as Carbopol and polycarbophil, noncharged polyethers, among which poloxamers and poly(ethylene oxide), have been used for the preparation of mucoadhesive systems (5, 54-58). Besides non-ionic and anionic polymers, cationic polymers, particularly, chitosan and chitosan derivatives have excellent mucoadhesive properties (further elaborated in section five). The mucoadhesion of the mentioned polymers is based on non-covalent interactions (hydrogen bonds, van der Waals' forces and electrostatic interactions) between the polymers on the one hand and mucus and structures present in the membranes of epithelial cells on the other.

It has been reported that Carbopol and starch/maltodextrin increase the bioavailability of nasally administered insulin because of their mucoadhesive properties and protease inhibition effects (56). It should be mentioned that besides for nasal and pulmonary administration of proteins/vaccines, mucoadhesive systems are also used to enhance their absorption after oral administration (57, 58). Among the mucoadhesive polysaccharides, hyaluronic acid microparticles have shown significant potential for the development of nasal and pulmonary administered vaccines (55, 59). Furthermore, it was shown that hyaluronic acid is an activator of T-cells and natural killer cells (60, 61). Hydroxypropylcellulose has been successfully used as a mucoadhesive carrier for the pulmonary delivery of proteins (62, 63).Hydroxypropylcellulose has been successfully used as mucoadhesive carrier for the pulmonary delivery of proteins (62, 63). Poloxamers and polyethylene oxide effectively improve the retention and absorption of intranasally administered macromolecular therapeutics as well as the delivery of a papillomavirus vaccine after vaginal administration (64, 65).

Although mucoadhesion increases the residence time of biotherapeutics, this does not necessarily have to result in a high absorption. This is especially the case when they are formulated as simple solutions. Generally speaking, non-charged and negatively charged polymers only stick to the mucus, but are unable to open the tight junctions. In contrast, cationic polymers like chitosan and its derivatives not only interact with the mucus and/or epithelial cells but also increase the paracellular permeability of the epithelium (66-68). Besides their charge, other structural elements of chitosan and its quaternized derivatives likely contribute to their penetration-enhancing activity, since other cationic polysaccharides such as quaternized diethyl aminoethyl (DEAE)-dextran with high a charge density were ineffective as enhancer (69).

In many studies, it was demonstrated that chitosan-based formulations were superior in enhancing absorption of therapeutic proteins as well as induction of antibodies after mucosal vaccination (59, 70-72). Recently, a new generation of mucoadhesive

polymers with thiol ligands has been introduced. These so-called thiomers can be covalently grafted to the mucus through disulphide bonds formed between the thiol ligands and cysteine residues of mucus glycol proteins (73). Poly (acrylic-acid)-cysteine and chitosan-4-thio-butyl-amidine are examples of anionic and cationic mucoadhesive thiomers, respectively (74).

5 Chitosan-based delivery systems

5.1 Chitosan and derivatives

Chitosan [α (1-4) 2-amino 2-deoxy β-D glucan,], a copolymer of glucosamine and N-acetylglucosamine (figure 4), is obtained by deacetylation of chitin, a naturally abundantly available polymer (e.g. in crustaceans).

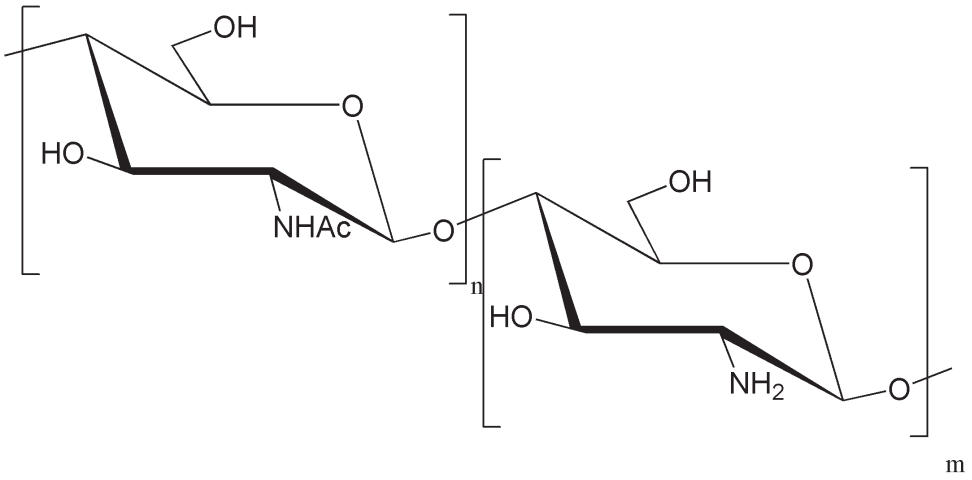

Figure 4. Chemical structure of chitosan. The degree of de-acetylation (m) is variable.

Chitosan has been studied as a biomaterial and as a pharmaceutical excipient for drug delivery, because of its favorable properties (66-68, 75-77). The primary amine groups render special properties that make chitosan very useful for pharmaceutical applications. The interaction of the protonated amine groups of chitosan with the cell membrane results in a reversible structural re-organization of tight junction-associated proteins which is followed by opening of the tight junctions.
Chitosan has been used for the preparation of mucoadhesive formulations (51, 52, 78, 79), for drug targeting systems (80), and for formulations that enhance the absorption of macromolecular therapeutics (proteins, peptides and plasmid DNA) (51, 52, 79, 81, 82). Chitosan is soluble, mucoadhesive and active as an absorption enhancer in its protonated form at low pH (83-85). Because the pKa of the amine groups of chitosan is 6.2 (84), at neutral pH chitosan does hardly carry charge, has a

low solubility and is therefore essentially inactive. Because of the presence of functional groups (amine and hydroxyl) various chemical chitosan derivatives have been synthesized and studied for different applications. Aiedeh et al. used chitosan succinate and chitosan phthalate for the design of colon-specific delivery systems of drugs (86). They used these compounds to formulate poorly soluble drugs in the form of solid dispersions (86). Thiolated chitosans, obtained by modification of the primary amine groups with thiol compounds, are another class of derivatives that showed improved mucoadhesive properties. Modified chitosans, obtained by reaction with cysteine, thioglycolic acid and 2-iminothiolane, have been evaluated as new mucoadhesive oral and nasal drug delivery systems. These thiolated chitosans have shown in situ gelling properties due to the formation of inter- and intramolecular disulfide bonds at physiological pH values (87-89). The strong mucoadhesive properties of the thiolated chitosans make them in particular highly suitable carriers for prolonged protein delivery at the mucosal sites. Further, chitosan was conjugated with the protease inhibitors chymostatin and it was shown that the formed conjugate acted as protease inhibitor. A mixture of the chitosan-chymostatin conjugate and EDTA-derivatized chitosan strongly improved the bioavailability of orally administered peptide drugs (90).

Chitosan with different degrees of palmitoyl glycol derivatization and thus different hydrophobicities have been synthesized by Martin et al. These polymers form hydrogels and were used for the controlled release of hydrophilic macromolecules. The release of a model compound (FITC-dextran) from the gel, as well as the hydration, erosion and bioadhesiveness of the hydrogels were dependent on the hydrophobicity of the polymer and the presence of the amphiphilic additives. It should be noticed, however, that these chitosan derivatives were less bioadhesive as compared to non-modified chitosan (91).

Mono-N-carboxymethyl chitosan (MCC) was synthesized by chemical modification of amine groups of chitosan with glyoxylic acid and sodium borohydride as reducing agent (92). In this way even negatively charged chitosan derivatives can be obtained. Whereas chitosan forms precipitates with polyanions, MCC is compatible with anionic compounds. MCC showed a significant decrease of Transepithelial electrical resistance (TEER) of Caco-2 cell monolayers when it was applied apically at concentrations of 3-5% (w/v). Moreover, MCC was used to enhance the permeation of low molecular weight heparin in rats after oral administration (92).

Quaternary chitosan derivatives are, because of their permanent cationic charge, soluble over a wide pH range. Importantly, these derivatives have mucoadhesive and penetration-enhancing properties also at neutral pH. The first quaternized chitosan was synthesized by alkylation of the primary amine groups of chitosan with various aldehydes and sodium borohydride. These N-alkylated chitosan derivatives were used as antibacterial and anti-fungal materials (93, 94). N-trimethyl chitosan (TMC) is a partially quaternized and well water-soluble derivative of chitosan, which has been extensively studied for its mucoadhesive and absorption-enhancing effects for hydrophilic macromolecules. The permeation-enhancing activity of TMC as well as

other properties, among which its biocompatibility, will be discussed in more detail in the next section. Another group of quaternary chitosan derivatives has been prepared by attaching a quaternary ammonium moiety to the amine groups of chitosan. Several of these derivatives were synthesized by reacting N-chloroacyl-6-*O*-triphenylmethyl modified chitosan, with suitable tertiary amine compounds. Chitosan derivatives with various degree of quaternization can be prepared by using N-chloroacyl-6-*O*-triphenylmethyl chitosans having various degrees of N-chloroacylation as starting materials (95). Xu et al. synthesized a quaternary derivative of chitosan, N-(2-hydroxyl) propyl-3-trimethyl ammonium chitosan chloride (HTCC), by reaction of chitosan with glycidyl trimethyl ammonium. Further, this chitosan derivative was used to prepare albumin-loaded nanoparticles by ionic gelation of HTCC and sodium tripolyphosphate (TPP). The HTCC nanoparticles had a size between 110-180 nm and their encapsulation efficiency was up to 90%. *In vitro* release studies showed a burst effect followed by a slow release. Adding polyethylene glycol (PEG) or significantly decreased the burst effect and also the encapsulation efficiency, whereas the addition of alginate also reduced the burst effect while protein loading was increased (96).

5.2 N-trimethyl chitosan (TMC)

N-trimethyl chitosan (TMC) is synthesized by methylation of amine groups of chitosan with methyl iodide (97). It was shown that the methylation of chitosan with CH_3I leads to some chain scission which is likely due to the harsh reaction conditions (~4 M NaOH and a high temperature of 60 ^oC) (98).

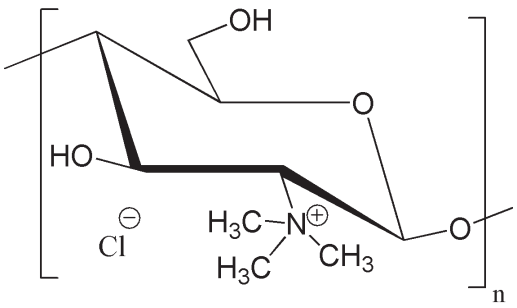

Figure 5. The chemical structure of TMC

By varying the degree of methylation, the water-solubility of TMC can be tailored. Soluble TMC has both mucoadhesive properties and excellent absorption-enhancing effects (the latter depending on its degree of quaternization (DQ)) even at neutral pH (12, 13, 99). It has been shown in many studies that TMCs enhance the permeation of hydrophilic macromolecules across the mucosal epithelia by opening the tight junctions (12, 13, 99-104). The degree of quaternization of TMC plays an important

role in its ability to open tight junctions of epithelial cells. At physiological pH, only TMC with a degree of quaternization above 36% increased the absorption of hydrophilic model compounds such as mannitol and poly(ethylene glycol) 4000 across intestinal epithelia and nasal mucosa. The permeation-enhancing effect of TMC increased with increasing degree of quaternization (105-107). It has been shown that TMC can enhance the permeation of hydrophilic high molecular weight compounds across stratified epithelia such as buccal mucosa which lack tight junctions (108). In these studies, TMC with higher DQs showed stronger mucoadhesive and penetration-enhancing properties. Moreover, transcorneal permeation-enhancing activities of TMC polymers, differing in DQ, have been shown for permeation of oflaxocin across rabbit corneal epithelium *in vitro* and *in vivo* in rabbit eyes. TMC with a DQ of 46% showed the best absorption-enhancing properties. In contrast, fully quaternized diethyl aminoethyl (DEAE)-dextran with high a charge density was ineffective as enhancer (69). This indicates that the overall properties of TMC rather than solely its charge contribute to its role as absorption enhancer. The mucoadhesive properties of TMC with different DQs were investigated by Snyman et al. They found that the mucoadhesiveness of TMC decreased with increasing DQ, which was explained by a decreased flexibility of TMC and decreased interpenetration into the mucus (14). In contrast to Snyman et al., in a recent study Sandri et al. found an increase in mucoadhesivity of TMC with increasing DQ. However, Sandri et al. normalized the mucoadhesion parameters. Sandri et al. showed that TMC synthesized from a low Mw chitosan and with a high DQ showed the best mucoadhesive and absorption-enhancing properties (108).

For evaluation of the practical use of TMC as a mucoadhesive and permeation enhancer, safety studies are required to guarantee the absence of cytotoxicity and tissue damage. (10, 109-112). Thanou et al. incubated monolayers of Caco-2 cells with different TMC solutions. The fluorescent probe YO-PRO-1, which is able to stain nuclei if the cell membrane is damaged, was added to the cells. Confocal scanning microscopy (CLSM) study showed no nuclei staining after 4 hours incubation with TMCs (109), which indicates that TMCs do not cause cell membrane damage. In other studies, the viability of Calu-3 cell monolayers, as a model for mucus-secreting respiratory epithelial cells, COS-7 (monkey kidney fibroblast) and MCF-7 (epithelial breast cancer) cells after exposure to various soluble TMCs and TMC-nanoparticles were examined by measuring the mitochondrial dehydrogenase activity of the cells (10, 104, 111, 112). TMCs with a low DQ were non-toxic. Moreover, these studies showed that with increasing DQ the cytotoxicity increases. However, the cytotoxicity of TMC with different DQ was substantially less than that of linear poly(ethylene imine) (PEI), a polymer frequently used for gene delivery purposes (113). Ciliary beat frequency (CBF) of chicken embryo trachea has proven to be a valuable *ex vivo* model to evaluate the safety of nasal drug formulations. The measurement of the CBF is very precise, but because this excised tissue is devoid of a protective mucus layer, it may result in an overestimation of the ciliotoxicity *in vivo*. Several studies have shown that TMCs made of high-molecular-weight chitosan

and with a high DQ decreased the CBF more than low-molecular weight TMCs. Importantly, this cilio-static effect is mostly reversible (10, 103, 109, 110).
The toxicity of TMC formulations have also been investigated *in vivo*. Haffegee et al. showed that intranasally administered TMC solutions did not cause any tissue damage in rats' nasal mucosa (110). Furthermore, histological evaluation of rats' lungs after intratracheal instillation of TMC, differing in DQ, solutions (104) and pulmonary administration of TMC powder formulations (Chapter 5) did not show any tissue damage and/or infiltration of immune cells such as neutrophils.
From the studies above it can be concluded that a high charge density of TMC is able to safely interact with cell membranes and to induce paracellular permeabilization of the epithelium. Taken together, from the penetration and toxicity studies it appears that TMC is a safe mucoadhesive and absorption enhancer for hydrophilic macromolecules across respiratory and other mucosal sites.

5.3 Techniques for the preparation of chitosan-based micro/nanoparticle formulations

Different methods have been used to prepare chitosan-based particulate carrier systems. When selecting a method for the preparation of a particulate dosage form of an active compound, the physicochemical properties and stability of both the active substance and the excipients, the aimed release kinetics of the active compound, and aimed particle size of the carrier should be taken into consideration. Furthermore, the route of administration, the target area and the aimed pharmacological effects as well as the safety of the product are crucial factors which should be taken into account. In this section the most frequently used methods for preparation of chitosan-based micro/nanoparticles are summarized and discussed.
Chitosan-based particles can be formed by chemical processes, e.g. by reacting the primary amine groups of chitosan with an aldehyde (mostly glutaraldehyde) crosslinker. Here, first a water-in-oil (w/o) emulsion of chitosan with the drug in liquid paraffin is formed, after which glutaraldehyde is added to crosslink chitosan which subsequently resulted in the formation of drug-loaded microspheres (114). In another study, insulin-loaded chitosan microspheres were prepared by dissolving the protein and the polymer in an acetic acid solution. This solution was emulsified in mineral oil and chitosan was chemically crosslinked with dehydroascorbyl palmitate. This preparation method produced microparticles characterized by high loading levels of insulin, and they completely released the drug in about 80 h at an almost constant release rate (115). Chemical crosslinking methods have major drawbacks for the preparation of protein formulations. Firstly, the organic phases used to make the w/o emulsions may adversely affect the stability of proteins and, most importantly, the applied crosslinking agents can react with proteins. Finally, complete removal of the unreacted and toxic crosslinker is difficult. Consequently, methods by which chitosan and its derivatives are crosslinked by physical methods are preferred to prepare protein-loaded particles.

Spray-drying has been applied for the preparation of protein-loaded chitosan microparticles. It is a relatively protein friendly technique and suitable to prepare microparticle powder formulations of protein-loaded chitosan nanoparticles suitable e.g. for pulmonary delivery (116, 117). Also other techniques, such as ionic crosslinking methods and supercritical drying processes have been used for the preparation of protein-loaded chitosan-based particles. These techniques are discussed in more detail in the following sections.

5.3.1 Ionic crosslinking methods

The complexation between chitosan-based polymers and oppositely charged macromolecules results in micro/nanoparticles suitable for drug delivery. The particles can be prepared by an ionic crosslinking through self-assembly of chitosan and oppositely charged macromolecules or by the addition of an extra anionic crosslinker, such as tripolyphophate (TPP) or sodium sulfate, to chitosan solutions. These ionic crosslinking methods have received much attention for the preparation of protein formulations because the used processes are simple, and mild to proteins, as they do not involve the use of chemical crosslinkers and avoid the use organic solvents and high temperatures, (96, 118, 119). Coacervation/precipitation has been used to prepare different protein-loaded chitosan microparticles. In this method, a coacervate, e.g. sodium sulfate, is added dropwise to an acidic solution of chitosan under stirring and sonication to prepare ionically crosslinked particles. Using this method, chitosan-based microparticles loaded with interleukin-2 (IL-2) have been prepared. (120). Although the coacervation/precipitation method seems more protein friendly than the chemical crosslinking preparation technologies, sonication may harm the protein structure.

Schatz et al. synthesized a partially N-sulfated chitosan. Upon acidification of an aqueous solution of this amphoteric chitosan, nanoparticles were formed by electrostatic interactions between the non-sulfated protonated amine groups of chitosan and the negatively charged N-sulfated chitosan amines. These polyelectrolyte complexes can be used for encapsulation of macromolecules but loading and releases studies have not been reported (121).

Glucomannan can interact with mannose receptors on M-cells and macrophages and can be used for the targeted delivery of mucosal vaccines. Phosphorylated glucomannan-chitosan nanoparticles were prepared by ionic crosslinking with and without using (TPP) as a crosslinker. These nanoparticles exhibited high loading efficiencies for insulin and immunomodulatory protein P1. Moreover, the release of the proteins could be modulated by varying the composition of the nanoparticles. No immunization studies with these nanoparticles have been reported so far (122).

A chitosan-based nanoparticulate system has been prepared by electrostatic complexation of poly-γ-glutamic acid (γ-PGA) and chitosan. The particle size and zeta potential of the nanoparticles were mainly dependent on the amount and concentration of γ-PGA added to chitosan solution. γ-PGA was selected as negatively charged crosslinking agent because it has been shown that nanoparticles containing

this polymer have the capacity to target hepatocytes. Chitosan-γ-PGA nanoparticles were able to decrease efficiently and reversibly the TEER of Caco-2 cell monolayers. The uptake of FITC-labeled chitosan-γ-PGA nanoparticles *in vitro* was shown by CLSM studies (123). Mao et al. reported self-assembly polyelectrolyte complexes (PEC) formed from chitosan, (pegylated)-TMC and insulin. Complexation of the polymers and insulin occurred only above the pI (5.3) of insulin. PECs were spherical, had a smooth surface and their size was in the range of 200-500 nm. The characteristics of PEC did not change after lyophilization (119).

The ionic gelation of chitosan with a polyanion such as TPP has been extensively used for the preparation of protein and antigen-loaded nanoparticles (8, 10, 71, 72, 118, 124, 125). In this process, an aqueous solution of TPP is added dropwise to an aqueous solution of chitosan at ambient temperature under stirring. Due to complexation of the oppositely charged components, chitosan nanoparticles are formed (71, 72). Using this method, chitosan nanoparticles loaded with insulin and tetanus toxoid have been prepared and investigated as nasal delivery vehicles (9, 11). Fernandez-Urrusuno et al. prepared insulin-loaded chitosan nanoparticles by ionic gelation of chitosan with TPP. Chitosan nanoparticles had a size 300-400 nm and a positive surface charge. Insulin release *in vitro* occurred rapidly under sink conditions. Chitosan nanoparticles enhanced the nasal absorption of insulin to a greater extent than an aqueous solution of chitosan (71). In another study, tetanus toxoid (TT)-loaded chitosan nanoparticles, with an average size about 350 nm and a positive surface charge, showed a high loading efficiency for TT. *In vitro* release studies showed an initial burst followed by a sustained release of antigenically active toxoid. Intranasal administration with TT-loaded nanoparticles elicited a high and long-lasting humoral immune response as well as a mucosal IgA response till 6 months post-administration (72). Recently, there have been many studies focusing on the intranasal or oral delivery of proteins and vaccines using TMC nanoparticles prepared by ionic gelation (10, 125-128).

5.3.2 Supercritical fluid CO_2 (SCF-CO_2) drying process

With increasing pharmaceutical interest in particulate carrier systems for proteins/antigens, there is a need for alternative particle-formation processes over conventional techniques. Such processes should be simple and protein friendly, improve the shelf-life of the proteins and offer the possibility to produce formulations with different particle sizes.

Supercritical fluid (SCF) drying process has been recently used as an alternative technique for producing powder formulations (129-133). SCF drying is a fast and mild process, is cost effective and offers the possibility to produce small microparticles suitable for inhalation (129-133). Above the critical points (temperature and pressure), a SCF has liquid-like viscosity and density, and gas-like diffusivity properties, and can therefore penetrate into substances like a gas and dissolve materials like a liquid (134).

The most widely used SCF for pharmaceutical applications is carbon dioxide (CO_2)

because it has a low critical temperature (31.2 °C) and pressure (75.8 bar), and it is non-flammable, non-toxic and inexpensive (133). Because proteins have a very low solubility in supercritical CO_2 (SC-CO_2), this fluid has been used as an antisolvent to precipitate proteins from their solutions. (135). It is possible to modify the solvent power of SC-CO_2 by adding volatile co-solvents such as ethanol (136).
Pérez de Diego et al. prepared protein-loaded TMC microparticles by spraying a water/DMSO solution of albumin/polymer into SC-CO_2 as an antisolvent. Adding water to DMSO/CO_2 was necessary to dissolve protein and TMC in the mixture. The experimental conditions resulted in protein-TMC spherical microspheres with a size between 1-10 μm and devoid of agglomeration, potentially suitable for inhalation. No stabilization studies on the dried protein have been reported yet (132).

5.4 Chitosan-based nanoparticles and microparticles for protein delivery

The mucoadhesive and/or absorption enhancing properties of chitosan and its derivatives are important factors for enhancing protein absorption/uptake across epithelial barriers (51, 66-68, 78, 79). Moreover, particulate carrier systems intensify the interaction of proteins with epithelial cell membranes and/or mucus at the site of administration, protect labile proteins from enzymatic degradation and promote the uptake of the encapsulated proteins by cells. Importantly, it has been shown that insulin-loaded chitosan nanoparticles enhanced nasal and intestinal absorption of this protein to a greater extent than chitosan solutions (70, 71). The effects of molecular weight and degree of deacetylation (DD) of chitosan and nanoparticles based on cellular uptake were studied using A549 cells. The uptake of nanoparticles was a saturable event for the chitosan varying in molecular weight and DD. Importantly, cell-associated chitosan nanoparticles were internalized, but not the cell-associated chitosan polymers. Chitosan DD had an influence on particle uptake because of its effect on the zeta potential of the nanoparticles. The nanoparticles prepared using a low DD chitosan contained more primary amines available for protonation. Consequently they were more positively charged and taken up by cells more efficiently (137). Chitosan-nanocapsules with either solid lipid or oily cores coated with chitosan have shown interesting features as mucoadhesive delivery systems for peptides and proteins. The chitosan-coated nanoemulsion and lipid nanoparticles had a size of about 300-500 nm with a positive surface charge and showed a slow release of a model protein, salmon calcitonin, which was attributed to the affinity of the peptide for the lipid core. Importantly, these nanocapsules improved the intestinal absorption of salmon calcitonin in rats (138, 139). Furthermore, a pegylated chitosan nanocapsule as an oral peptide delivery system was studied by Prego et al. (140). Pegylation increased the stability of the nanocapsules in gastro-intestinal fluids and decreased their toxicity *in vitro*. Studies in rats showed a prolonged and enhanced intestinal absorption of salmon calcitonin.
Pulmonary delivery of proteins is a potential delivery route, which needs to be more investigated for designing suitable and safe delivery systems. Powder formulations of

protein-loaded chitosan nanoparticles for pulmonary delivery were prepared by spray drying. Insulin-loaded nanoparticles were obtained by ionic gelation of a chitosan solution with a TPP solution containing insulin. The nanoparticles were suspended in a solution of mannitol and lactose. Spray-drying yielded microparticle powders with a suitable aerodynamic diameter for alveolar deposition. The insulin-loaded chitosan nanoparticles had a good loading capacity (65–80%) and were fully recovered from the powder formulations after contact with an aqueous medium and showed a fast release of insulin (116). However, there are no *in vivo* pulmonary delivery data with these powder formulations published so far. Yang et al. prepared an inhalable chitosan-based powder formulation of salmon calcitonin-containing mannitol (as a protecting agent) using a spray drying process. The effect of chitosan on the physicochemical stability of the protein was investigated with chromatographic and spectrometric techniques. The dissolution rate of the protein decreased when formulated with chitosan, which might be due to irreversible complex formation between the protein and chitosan during the drying process (117). Yamamoto et al. showed that chitosan-coated poly(lactide-co-glycolide) (PLGA) nanoparticle suspensions improved the absorption of calcitonin after pulmonary administration. A chitosan-coated PLGA nanoparticle suspension was aerosolized with a nebulizer. The elimination of the chitosan-coated nanoparticles from the lungs was retarded due to the mucoadhesive properties of chitosan. It was shown that after pulmonary administration of the calcitonin-loaded particles the pharmacological action of calcitonin was prolonged compared to that of the protein loaded in the unmodified nanoparticles (141). In another study, the potential of chitosan oligomers and polymers for pulmonary delivery of proteins was studied. The absorption of interferon-α (INF) in rats was improved after pulmonary administration of aqueous solutions of the oligomers and INF. Among various oligomers, glucoseamine hexamers at a concentration of 0.5% (w/v) were the most effective. Chitosan polymers were less efficient than oligomers in increasing the systemic level of INF due to their lower solubility in lung fluids (142).

As pointed out in the section 5.2. TMC, a partially quaternized chitosan derivative, is an attractive alternative for chitosan for the design of protein-loaded particles. Although mucosal peptide delivery with TMC solutions has been extensively studied, there are few studies that report mucosal delivery of protein-loaded TMC particles. In a study, Mao et al. synthesized a series of copolymers by grafting activated poly(ethylene glycol) (PEG) onto TMC polymers (DQ: 40%) with different molecular weights to improve the biocompatibility of TMC. Pegylation reduced substantially the toxicity of low molecular weight TMCs. Complexation of pegylated-TMC with insulin masked the toxicity of the polymers (112).

In another study, polyelectrolyte nanocomplexes (PEC) consisting of chitosan or chitosan derivatives and insulin were prepared and characterized. The stability of nanocomplexes was dependent on the molecular weight of chitosan. Only when the molecular weight of the polymers was above 25 kDa, PEC precipitation could be avoided. Using TMC and pegylated-TMC improved the stability of insulin

significantly. Additionally, PEC protected insulin from chemical degradation even at 50 °C. All complexes could be lyophilized without influencing the particle size and stability of insulin. These PECs were aimed for nasal protein delivery, however, no *in vivo* studies were reported (119). The effect of TMC with various DQ on nanoparticle characteristics, protein loading and release of two model proteins with different isoelectric points (pI) values, bovine serum albumin (pI = 4.8) and bovine hemoglobin (pI 6.8), were studied. TMC nanoparticles had a low loading efficiency for hemoglobin, presumably because of the weak negative charge of the protein at neutral pH. Nanoparticles of TMC with a lower DQ showed slower release kinetics, because the lower positively charged TMC has a slower ionic exchange between polymer and release medium. The burst release observed for TMC nanoparticles was reduced by incorporating alginate during preparation, probably by forming a polyelectrolyte complex layer with cationic TMC on the particle surface (126). Sandri at al. investigated TMC nanoparticles, using TMC polymers with different DQs, for intestinal peptide delivery. The permeation-enhancing properties of the TMC nanoparticles and chitosan nanoparticles (as a control) were studied in an *in vitro* Caco-2 cell model and an *ex vivo* rat jejunum model. All TMC nanoparticles enhanced the absorption of a model compound, fluorescein isocyanate dextran, comparable or superior to that of chitosan nanoparticles except TMC particles with a high DQ (90%), which were internalized and remained trapped inside the cells. Similar results were seen with *ex vivo* absorption enhancement studies. The higher mucoadhesion and internalization of TMC-nanoparticles in comparison chitosan nanoparticles make TMC nanosystems, in particular those made with intermediate DQ TMC, suitable carriers for mucosal peptide/protein delivery (127).

5.5 Chitosan-based particulates for vaccine delivery

Chitosan-based carriers have been extensively studied for mucosal delivery of antigens (6, 7, 52, 72, 143-145). In these studies nasal immunizations with various antigen-loaded chitosan powders, micro/nanoparticle and chitosan-coated poly(lactic acid) nanospheres demonstrated various levels of both systemic and local immune responses. Moreover, in a phase I clinical study, intranasal immunization with solutions of chitosan glutamate plus influenza vaccine showed positive effects of the polymer on the immune responses raised in the vaccinees (146). The type of chitosan formulation may have a great influence on the immune response because of differences in absorption across nasal mucosa and uptake of antigen-loaded particles by M-cells as well as epithelia.

The immunostimulating effect of chitosan plus its mucoadhesive and/or absorption enhancing properties make the polymer as a potential carrier for vaccine delivery. The adjuvant activities of chitin and chitosan with DD of 30 and 70% after intraperitoneal administration in mice and guinea pigs was shown in terms of induction of cytokines, long-lasting circulating antibodies and cell-based immunity against bacterial alpha-amylase and *Escherichia coli* infection (147, 148). In another

study, chitosan (DD 70%) showed induction of cytokines, interleukin-1 and colony-stimulating factor (CSF) in macrophages *in vitro* (149). Moreover, particulate chitosan systems can protect antigens from degradation and enhance the uptake of the particles by APCs, macrophages and M-cells at mucosal sites and the other sites of administration. Nishimura et al. have shown that porous chitosan (DD 80%) microspheres with a mean diameter of 2.5 micron enhanced the cytolytic activity of peritoneal macrophages and the production of CSF *in vitro* and in mice. Porous chitin microspheres showed no effect on the activation of peritoneal macrophages, but slightly enhanced the production of CSF *in vivo* (150). Shibata et al. showed that only phagocytosed chitin or chitosan particles were able to induce interferon gamma levels after intravenous administration and priming alveolar microphages (151).

Van der Lubben et al. prepared ovalbumin-loaded chitosan microparticles and their uptake by murine Peyer's patches was shown by confocal microscopy (7). Furthermore, they investigated the potential of chitosan particles loaded with diphtheria toxoid (DT) for nasal and oral immunization. After both administration routes, the DT chitosan formulation induced high neutralizing antibody as well as secretory IgA antibody levels (6). In another study, intranasal immunization with DT-loaded TMC microparticles induced the formation of both IgG and IgA similar to that of TMC solution co-administered with DT antigen (152). Contrary to this, in this thesis it is demonstrated that influenza hemagglutinin loaded in TMC nanoparticles elicited much stronger systemic and local immune responses than those obtained after intranasal administration of TMC solution plus antigen, or after intramuscular immunization with influenza antigen (125). In other studies, intranasal immunization with either a TMC solution containing a group C meningococcal conjugate vaccine (CRM-MenC) and LTK63 (a mucosal adjuvant) or a suspension of TMC microparticles loaded with CRM-MenC antigen or LTK63, induced bactericidal antibodies in mice superior to those by parenteral immunizations (126, 153). In chapter six of this thesis, the potential of TMC as an adjuvant for vaccination in guinea pigs is shown for pulmonarily administered DT-loaded TMC microparticle powders prepared by a supercritical drying process. The animals that received TMC-DT powders showed comparable or superior systemic and local immune responses compared to the animals that received a subcutaneously administered alum-adsorbed DT vaccine.

Nagamoto et al. prepared chitosan particles and chitosan-coated emulsions with different particle diameters. A model antigen, albumin, and cholera toxin, as an adjuvant, were loaded into the particles and they were administered either intranasally (i.n.) or intraperitoneally (i.p.). The chitosan-coated emulsion and nanoparticle formulations induced the formation of high serum IgG and mucosal IgA antibody titers in rats (144). A chitosan-based nanoparticle system for oral vaccination was reported by Jain et al. (154). albumin-loaded nanoparticles were prepared and encapsulated in vesicles (liposomes and niosomes) to make them acid resistant upon oral administration. The nanoparticles were characterized for their size, surface charge, protein loading and stability in simulated gastrointestinal fluid (pH 1.2) and

simulated intestinal fluid (pH 7.5). Oral administration of modified albumin-nanoparticles induced significantly higher IgG and mucosal IgA titers as compared to unmodified chitosan nanoparticles (154).

6 Conclusions

Chitosan has many attractive properties for pharmaceutical application, in particular for the delivery of macromolecular therapeutics and antigens. Chitosan has functional groups for chemical modifications, which has resulted in a large variety of chitosan derivatives with several tailored properties, such as solubility, hydrophobicity, etc. In contrast to chitosan, N-trimethyl chitosan (TMC), a partially quaternized chitosan derivative, is water-soluble at neutral pH. Moreover, TMC has mucoadhesive and absorption enhancing properties. Particulate carrier systems based on chitosan and its derivatives have attractive features for the delivery of delicate pharmaceutical macromolecules via mucosal surfaces.

References

1. S. S. Davis. Nasal Vaccines. *Drug Deliv Rev* 51: 21-42. (2001).

2. J. S. Patton, C. S. Fishburn, and J. G. Weers. The lungs as a portal of entry for systemic drug delivery. *Proc Am Thorac Soc* 1: 338-44 (2004).

3. J. S. Patton. Mechanisms of macromolecules absorption by the lungs. *Adv Drug Del Rev* 19: 3-36 (1996).

4. A. J. Almeidaand H. O. Alpar. Nasal delivery of vaccines. *J Drug Target* 3: 455-467 (1996).

5. R. J. Soane, M. Hinchcliffe, S. S. Davis, and L. Illum. Clearance characteristics of chitosan based formulation in the sheep nasal cavity. *Int J Pharm* 217: 183-191 (2001).

6. I. M. van der Lubben, G. Kersten, M. M. Fretz, C. Beuvery, J. C. Verhoef, and H. E. Junginger. Chitosan microparticles for mucosal vaccination against diphtheria: oral and nasal efficacy studies in mice. *Vaccine* 28: 1400-1408 (2003).

7. I. M. van der Lubben, F. A. Konings, G. Borchard, J. C. Verhoef, and H. E. Junginger. In vivo uptake of chitosan microparticles by murine Peyer's patches: visualization studies using confocal laser scanning microscopy and immunohistochemistry. *J Drug Target* 9: 39-47 (2001).

8. P. Calvo, C. Remunan-Lopez, J. L. Vila-Jato, and M. J. Alonso. Chitosan and chitosan/ethylene oxide-propylene oxide block copolymer nanoparticles as novel carriers for proteins and vaccines. *Pharm Res* 14: 1431-1436 (1997).

9. R. Fernandez-Urrusuno, P. Calvo, C. Remunan-Lopez, J. L. Vila-Jato, and J. A. Alonso. Enhancement of nasal absorption of Insulin using chitosan nanopartocles. *Pharm. Res.* 16: 1576-1581 (1999).

10. M. Amidi, S. G. Romeijn, G. Borchard, H. E. Junginger, W. E. Hennink, and W. Jiskoot. Preparation and characterization of protein-loaded N-trimethyl chitosan nanoparticles as nasal delivery system. *J Control Release* 111: 107-116 (2006).

11. A. Vila, A. Sanchez, K. Janes, I. Behrens, T. Kissel, J. L. Vila Jato, and M. J. Alonso. Low molecular weight chitosan nanoparticles as new carriers for nasal vaccine delivery in mice. *Eur. J. Pharm. Biopharm.* 57: 123-131 (2004).

12. J. H. Hamman, M. Stander, and A. F. Kotzé. Effect of the degree of quaternization of N-trimethyl chitosan chloride on absorption enhancement: in vivo evaluation in rat nasal epithelia. *Int J Pharm* 232: 235-242 (2002).

13. M. Thanou, J. C. Verhoef, J. H. M. Verheijden, and H. E. Junginger. Intestinal absorption of octeriotide: N-trimethyl chitosan chloride (TMC) ameliorates the permeability and absorption properties of the somatostatin analogue in vitro and in vivo. *J Pharm Sci* 89: 951-957 (2000).

14. D. Snyman, J. H. Hamman, and A. F. Kotze. Evaluation of the mucoadhesive properties of N-trimethyl chitosan chloride. *Drug Dev. Ind. Pharm.* 29: 61-9 (2003).

15. E. L. Giudiceand J. D. Campbell. Needle-free vaccine delivery. *Adv Drug Deliv Rev* 58: 68-89 (2006).

16. J. Blanchette, N. Kavimandan, and N. A. Peppas. Principles of transmucosal delivery of therapeutic agents. *Biomed Pharmacother* 58: 142-51 (2004).

17. N. A. Peppas, K. M. Wood, and J. O. Blanchette. Hydrogels for oral delivery of therapeutic proteins. *Expert Opin Biol Ther* 4: 881-7 (2004).

18. N. Salamat-Millerand T. P. Johnston. Current strategies used to enhance the paracellular transport of therapeutic polypeptides across the intestinal epithelium. *Int J Pharm* 294: 201-16 (2005).

19. H. J. Dean. Epidermal delivery of protein and DNA vaccines. *Expert Opin Drug Deliv* 2: 227-36 (2005).

20. G. M. Glenn, R. T. Kenney, S. A. Hammond, and L. R. Ellingsworth. Transcutaneous immunization and immunostimulant strategies. *Immunol Allergy Clin North Am* 23: 787-813 (2003).

21. Y. Sudhakar, K. Kuotsu, and A. K. Bandyopadhyay. Buccal bioadhesive drug delivery—a promising option for orally less efficient drugs. *J Control Release* 114: 15-40 (2006).

22. L. Illum. Nanoparticulate systems for nasal delivery of drugs: A real improvement over simple systems? *J Pharm Sci* (2006).

23. M. Koping-Hoggard, A. Sanchez, and M. J. Alonso. Nanoparticles as carriers for nasal vaccine delivery. *Expert Rev Vaccines* 4: 185-96 (2005).

24. S. A. Cryan. Carrier-based strategies for targeting protein and peptide drugs to the lungs. *AAPS J* 7: E20-41 (2005).

25. I. Gonda. Systemic delivery of drugs to humans via inhalation. *J Aerosol Med* 19: 47-53 (2006).

26. H. O. Alpar, S. Somavarapu, K. N. Atuah, and V. W. Bramwell. Biodegradable mucoadhesive particulates for nasal and pulmonary antigen and DNA delivery. *Adv Drug Deliv Rev* 57: 411-30 (2005).

27. V. J. Sullivan, J. A. Mikszta, P. Laurent, J. Huang, and B. Ford. Noninvasive delivery technologies: respiratory delivery of vaccines. *Expert Opin Drug Deliv* 3: 87-95 (2006).

28. R. J. Soane, M. Ferier, A. C. Perkins, N. S. Jones, S. S. Davis, and L. Illum. Evaluation of the clearance characteristics of bioadhesive system in humans. *Int J Pharm* 178: 55-65 (1999).

29. L. Illum. Nasal drug delivery—possibilities, problems and solutions. *J Control Release* 87: 187-98 (2003).

30. T. K. Mandal. Inhaled insulin for diabetes mellitus. *Am J Health Syst Pharm* 62: 1359-64 (2005).

31. J. Bienenstockand M. R. McDermott. Bronchus- and nasal-associated lymphoid tissues. *Immunol Rev* 206: 22-31 (2005).

32. J. Bienenstock, N. Johnston, and D. Y. Perey. Bronchial lymphoid tissue. I. Morphologic characteristics. *Lab Invest* 28: 686-92 (1973).

33. J. Bienenstock, N. Johnston, and D. Y. Perey. Bronchial lymphoid tissue. II. Functional characterisitics. *Lab Invest* 28: 693-8 (1973).

34. J. Bienenstockand N. Johnston. A morphologic study of rabbit bronchial lymphoid aggregates and lymphoepithelium. *Lab Invest* 35: 343-8 (1976).

35. L. J. Hathawayand J. P. Kraehenbuhl. The role of M cells in mucosal immunity. *Cell Mol Life Sci* 57: 323-32 (2000).

36. J. P. Kraehenbuhland M. R. Neutra. Epithelial M cells: differentiation and function. *Annu Rev Cell Dev Biol* 16: 301-32 (2000).

37. A. Gebertand R. Pabst. M cells at locations outside the gut. *Semin Immunol* 11: 165-70 (1999).

38. K. C. Stone, R. R. Mercer, P. Gehr, B. Stockstill, and J. D. Crapo. Allometric relationships of cell numbers and size in the mammalian lung. *Am J Respir Cell Mol Biol* 6: 235-43 (1992).

39. S. Kobayashi, S. Kondo, and K. Juni. Permeability of peptides and proteins in human cultured alveolar A549 cell monolayer. *Pharm Res* 12: 1115-9 (1995).

40. K. Morimoto, H. Yamahara, V. H. Lee, and K. J. Kim. Transport of thyrotropin-releasing hormone across rat alveolar epithelial cell monolayers. *Life Sci* 54: 2083-92 (1994).

41. J. Gil. Number and distribution of plasmalemmal vesicles in the lung. *Fed Proc* 42: 2414-8 (1983).

42. A. T. Jones, M. Gumbleton, and R. Duncan. Understanding endocytic pathways and intracellular trafficking: a prerequisite for effective design of advanced drug delivery systems. *Adv Drug Deliv Rev* 55: 1353-7 (2003).

43. S. D. Xiang, A. Scholzen, G. Minigo, C. David, V. Apostolopoulos, P. L. Mottram, and M. Plebanski. Pathogen recognition and development of particulate vaccines: does size matter? *Methods* 40: 1-9 (2006).

44. T. Tschernigand R. Pabst. Bronchus-associated lymphoid tissue (BALT) is not present in the normal adult lung but in different diseases. *Pathobiology* 68: 1-8 (2000).

45. T. Thepen, E. Claassen, K. Hoeben, J. Breve, and G. Kraal. Migration of alveolar macrophages from alveolar space to paracortical T cell area of the draining lymph node. *Adv Exp Med Biol* 329: 305-10 (1993).

46. L. W. Poulter. Pulmonary macrophages, *Pulmonary defences*, John Willey & sons Ltd., Chichester, 1997, pp. 77-92.

47. P. G. Holt, M. A. Schon-Hegrad, J. Oliver, B. J. Holt, and P. G. McMenamin. A contiguous network of dendritic antigen-presenting cells within the respiratory epithelium. *Int Arch Allergy Appl Immunol* 91: 155-9 (1990).

48. P. G. Holt, M. A. Schon-Hegrad, and P. G. McMenamin. Dendritic cells in the respiratory tract. *Int Rev Immunol* 6: 139-49 (1990).

49. W. Xia, C. E. Pinto, and R. L. Kradin. The antigen-presenting activities of Ia+ dendritic cells shift dynamically from lung to lymph node after an airway challenge with soluble antigen. *J Exp Med* 181: 1275-83 (1995).

50. L. Illum. Nasal drug delivery- possibilities, problems and solutions. *J. Control. Release* 87: 187-98 (2003).

51. L. Illum, N. F. Farraj, and S. S. Davis. Chitosan as a novel nasal delivery system for peptide drugs. *Pharm Res* 11: 1186-1189 (1994).

52. L. Illum, I. Jabbal-Gill, M. Hinchcliffe, A. N. Fisher, and S. S. Davis. Chitosan as a novel nasal delivery system for vaccines. *Adv Drug Deliv Rev* 51: 81-96 (2001).

53. P. L. Heritage, M. A. Brook, B. J. Underdown, and M. R. McDermott. Intranasal immunization with polymer-grafted microparticles activates the nasal-associated lymphoid tissue and draining lymph nodes. *Immunology* 93: 249-56 (1998).

54. A. Garcia-Arieta, S. Torrado-Santiago, L. Goya, and J. J. Torrado. Spray-dried powders as nasal absorption enhancers of cyanocobalamin. *Biol Pharm Bull* 24: 1411-6 (2001).

55. S. T. Lim, B. Forbes, G. P. Martin, and M. B. Brown. In vivo and in vitro characterization of novel microparticulates based on hyaluronan and chitosan hydroglutamate. *AAPS PharmSciTech* 2: 20 (2001).

56. C. Callensand J. P. Remon. Evaluation of starch-maltodextrin-Carbopol 974 P mixtures for the nasal delivery of insulin in rabbits. *J Control Release* 66: 215-20 (2000).

57. S. Kockisch, G. D. Rees, S. A. Young, J. Tsibouklis, and J. D. Smart. Polymeric microspheres for drug delivery to the oral cavity: an in vitro evaluation of mucoadhesive potential. *J Pharm Sci* 92: 1614-23 (2003).

58. H. Takeuchi, Y. Matsui, H. Yamamoto, and Y. Kawashima. Mucoadhesive properties of carbopol or chitosan-coated liposomes and their effectiveness in the oral administration of calcitonin to rats. *J Control Release* 86: 235-42 (2003).

59. M. Singh, M. Briones, and D. T. O'Hagan. A novel bioadhesive intranasal delivery system for inactivated influenza vaccines. *J Control Release* 70: 267-76 (2001).

60. R. Galandrini, E. Galluzzo, N. Albi, C. E. Grossi, and A. Velardi. Hyaluronate is costimulatory for human T cell effector functions and binds to CD44 on activated T cells. *J Immunol* 153: 21-31 (1994).

61. R. Galandrini, R. De Maria, M. Piccoli, L. Frati, and A. Santoni. CD44 triggering enhances human NK cell cytotoxic functions. *J Immunol* 153: 4399-407 (1994).

62. M. Sakagami, K. Sakon, W. Kinoshita, and Y. Makino. Enhanced pulmonary absorption following aerosol administration of mucoadhesive powder microspheres. *J Control Release* 77: 117-29 (2001).

63. M. Sakagami, W. Kinoshita, K. Sakon, J. Sato, and Y. Makino. Mucoadhesive beclomethasone microspheres for powder inhalation: their pharmacokinetics and pharmacodynamics evaluation. *J Control Release* 80: 207-18 (2002).

64. J. S. Park, Y. K. Oh, M. J. Kang, and C. K. Kim. Enhanced mucosal and systemic immune responses following intravaginal immunization with human papillomavirus 16 L1 virus-like particle vaccine in thermosensitive mucoadhesive delivery systems. *J Med Virol* 70: 633-41 (2003).

65. J. S. Park, Y. K. Oh, H. Yoon, J. M. Kim, and C. K. Kim. In situ gelling and mucoadhesive polymer vehicles for controlled intranasal delivery of plasmid DNA. *J Biomed Mater Res* 59: 144-51 (2002).

66. N. G. Schipper, S. Olsson, J. A. Hoogstraate, A. G. deBoer, K. M. Varum, and P. Artursson. Chitosans as absorption enhancers for poorly absorbable drugs 2: mechanism of absorption enhancement. *Pharm Res* 14: 923-9 (1997).

67. P. Artursson, T. Lindmark, S. S. Davis, and L. Illum. Effect of chitosan on the permeability of monolayers of intestinal epithelial cells (Caco-2). *Pharm Res* 11: 1358-61 (1994).

68. G. Borchard, H. L. Lueßen, A. G. de Boer, J. C. Verhoef, C. M. Lehr, and H. E. Junginger. The potential of mucoadhesive polymers in enhancing intestinal peptide drug absorption III: Effects of chitosan glutamate and carbomer on epithelial tight junctions in vitro,. *J. Control. Release* 39: 131-138 (1996).

69. G. Di Colo, S. Burgalassi, Y. Zambito, D. Monti, and P. Chetoni. Effects of different N-trimethyl chitosans on in vitro/in vivo ofloxacin transcorneal permeation. *J Pharm Sci* 93: 2851-62 (2004).

70. Y. Pan, Y. J. Li, H. Y. Zhao, J. M. Zheng, H. Xu, G. Wei, J. S. Hao, and F. D. Cui. Bioadhesive polysaccharide in protein delivery system: chitosan nanoparticles improve the intestinal absorption of insulin in vivo. *Int J Pharm* 249: 139-147 (2002).

71. R. Fernandez-Urrusuno, P. Calvo, C. Remunan-Lopez, J. L. Vila-Jato, and M. J. Alonso. Enhancement of nasal absorption of insulin using chitosan nanoparticles. *Pharm Res* 16: 1576-81 (1999).

72. A. Vila, A. Sanchez, K. Janes, I. Behrens, T. Kissel, J. L. Vila Jato, and M. J. Alonso. Low molecular weight chitosan nanoparticles as new carriers for nasal vaccine delivery in mice. *Eur J Pharm Biopharm* 57: 123-31 (2004).

73. V. M. Leitner, G. F. Walker, and A. Bernkop-Schnurch. Thiolated polymers: evidence for the formation of disulphide bonds with mucus glycoproteins. *Eur J Pharm Biopharm* 56: 207-14 (2003).

74. A. Bernkop-Schnurch, M. Hornof, and D. Guggi. Thiolated chitosans. *Eur J Pharm Biopharm* 57: 9-17 (2004).

75. O. Felt, P. Buri, and R. Gurny. Chitosan: a unique polysaccharide for drug delivery. *Drug Dev. Ind. Pharm.* 24: 979-993 (1998).

76. L. Illum. Chitosan and its use as a pharmaceutical excipient. *Pharm. Res.* 15: 1326-1331 (1998).

77. H. E. Jungingerand J. C. Verhoef. Macromolecules as safe penetration enhancers for hydrophilic drugs-a fiction? *Pharm. Sci. Tech. Today* 1: 370-376 (1998).

78. C. M. Lehr, J. A. Browstra, E. H. Schacht, and H. E. Junginger. In vitro evaluation of mucoadhesive properties of chitosan and some other natural polymers. *Int J Pharm* 78: 43-48 (1992).

79. H. L. Luessen, B. J. de Leeuw, M. W. Langemeyer, A. B. de Boer, J. C. Verhoef, and H. E. Junginger. Mucoadhesive polymers in peroral peptide drug delivery. VI. Carbomer and chitosan improve the intestinal absorption of the peptide drug buserelin in vivo. *Pharm Res* 13: 1668-72 (1996).

80. E. E. Hassan, R. C. Parish, and J. M. Gallo. Optimized formulation of magnetic chitosan microspheres containing the anticancer agent, oxantrazole. *Pharm Res* 9: 390-7 (1992).

81. H. Q. Mao, K. Roy, V. L. Troung-Le, K. A. Janes, K. Y. Lin, Y. Wang, J. T. August, and K. W. Leong. Chitosan-DNA nanoparticles as gene carriers: synthesis, characterization and transfection efficiency. *J Control Release* 70: 399-421 (2001).

82. M. Bivas-Benita, K. E. van Meijgaarden, K. L. Franken, H. E. Junginger, G. Borchard, T. H. Ottenhoff, and A. Geluk. Pulmonary delivery of chitosan-DNA nanoparticles enhances the immunogenicity of a DNA vaccine encoding HLA-A*0201-restricted T-cell epitopes of Mycobacterium tuberculosis. *Vaccine* 22: 1609-15 (2004).

83. A. F. Kotzé, H. L. Lueßen, B. J. de Leeuw, A. G. de Boer, J. C. Verhoef, and H. E. Junginger. Chitosan for enhanced intestinal permeability: prospects for derivatives soluble in neutral and basic environments. *Eur J Pharm Sci* 7: 145-151 (1999).

84. A. F. Kotzé, H. L. Lueßen, B. J. de Leeuw, A. G. de Boer, J. C. Verhoef, and H. E. Junginger. N-trimethyl chitosan chloride as a potential absorption enhancer across mucosal surfaces: in vitro evaluation in intestinal epithelial cells (Caco-2). *Pharm Res* 14: 1197-202 (1997).

85. A. F. Kotzé, H. L. Lueßen, B. J. de Leeuw, A. G. de Boer, J. C. Verhoef, and H. E. Junginger. Enhancement of paracellular drug transport with highly quaternised N-trimethyl chitosan chloride in neutral environments: in vitro evaluation in intestinal epithelial cells (Caco-2). *J Pharm Sci* 88: 253-257 (1999).

86. K. Aiedehand M. O. Taha. Synthesis of chitosan succinate and chitosan phthalate and their evaluation as suggested matrices in orally administered, colon-specific drug delivery systems. *Arch Pharm (Weinheim)* 332: 103-7 (1999).

87. A. Bernkop-Schnurch, M. Hornof, and T. Zoidl. Thiolated polymers—thiomers: synthesis and in vitro evaluation of chitosan-2-iminothiolane conjugates. *Int J Pharm* 260: 229-37 (2003).

88. M. D. Hornof, C. E. Kast, and A. Bernkop-Schnurch. In vitro evaluation of the viscoelastic properties of chitosan-thioglycolic acid conjugates. *Eur J Pharm Biopharm* 55: 185-90 (2003).

89. M. Roldo, M. Hornof, P. Caliceti, and A. Bernkop-Schnurch. Mucoadhesive thiolated chitosans as platforms for oral controlled drug delivery: synthesis and in vitro evaluation. *Eur J Pharm Biopharm* 57: 115-21 (2004).

90. A. Bernkop-Schnurchand C. E. Kast. Chemically modified chitosans as enzyme inhibitors. *Adv Drug Deliv Rev* 52: 127-37 (2001).

91. L. Martin, C. G. Wilson, F. Koosha, L. Tetley, A. I. Gray, S. Senel, and I. F. Uchegbu. The release of model macromolecules may be controlled by the hydrophobicity of palmitoyl glycol chitosan hydrogels. *J Control Release* 80: 87-100 (2002).

92. M. Thanou, M. T. Nihot, M. Jansen, J. C. Verhoef, and H. E. Junginger. Mono-N-carboxymethyl chitosan (MCC), a polyampholytic chitosan derivative, enhances the intestinal absorption of low molecular weight heparin across intestinal epithelia in vitro and in vivo. *J Pharm Sci* 90: 38-46 (2001).

93. Z. Jia, D. shen, and W. Xu. Synthesis and antibacterial activities of quaternary ammonium salt of chitosan. *Carbohydr Res* 333: 1-6 (2001).

94. R. Muzzarelli, R. Tarsi, O. Filippini, E. Giovanetti, G. Biagini, and P. E. Varaldo. Antimicrobial properties of N-carboxybutyl chitosan. *Antimicrob Agents Chemother* 34: 2019-23 (1990).

95. J. Holappa, T. Nevalainen, P. Soininen, M. Elomaa, R. Safin, M. Masson, and T. Jarvinen. N-Chloroacyl-6-O-triphenylmethylchitosans: useful intermediates for synthetic modifications of chitosan. *Biomacromolecules* 6: 858-63 (2005).

96. Y. Xu, Y. Du, R. Huang, and L. Gao. Preparation and modification of N-(2-hydroxyl) propyl-3-trimethyl ammonium chitosan chloride nanoparticle as a protein carrier. *Biomaterials* 24: 5015-22 (2003).

97. A. B. Sieval, M. Thanou, A. F. Kotzé, J. C. Verhoef, J. Brussee, and H. E. Junginger. Preparation and NMR- characterisation of highly substituted N-trimethyl chitosan chloride. *Carbohydr Polym* 36: 157-165 (1998).

98. D. Snyman, T. Govender, and A. F. Kotze. Low molecular weight quaternised chitosan (I): synthesis and characterisation. *Pharmazie* 58: 705-8 (2003).

99. M. Thanou, J. C. Verhoef, J. H. Verheijden, and H. E. Junginger. Intestinal absorption of octreotide using trimethyl chitosan chloride: studies in pigs. *Pharm Res* 18: 823-8 (2001).

100. A. F. Kotze, M. M. Thanou, H. L. Luessen, B. G. de Boer, J. C. Verhoef, and H. E. Junginger. Effect of the degree of quaternization of N-trimethyl chitosan chloride on the permeability of intestinal epithelial cells (Caco-2). *Eur J Pharm Biopharm* 47: 269-74 (1999).

101. J. H. Hamman, C. M. Schultz, and A. F. Kotze. N-trimethyl chitosan chloride: optimum degree of quaternization for drug absorption enhancement across epithelial cells. *Drug Dev Ind Pharm* 29: 161-72 (2003).

102. S. M. van der Merwe, J. C. Verhoef, J. H. Verheijden, A. F. Kotze, and H. E. Junginger. Trimethylated chitosan as polymeric absorption enhancer for improved peroral delivery of peptide drugs. *Eur J Pharm Biopharm* 58: 225-35 (2004).

103. C. Jonker-Venter, D. Snyman, C. Janse van Rensburg, E. Jordaan, C. Schultz, J. H. Steenekamp, J. H. Hamman, and A. F. Kotze. Low molecular weight quaternised chitosan (11): in vitro assessment of absorption enhancing properties. *Pharmazie* 61: 301-5 (2006).

104. B. I. Florea, M. Thanou, H. E. Junginger, and G. Borchard. Enhancement of bronchial octreotide absorption by chitosan and N-trimethyl chitosan shows linear in vitro/in vivo correlation. *J Control Release* 110: 353-61 (2006).

105. A. F. Kotzé, M. M. Thanou, H. L. Lueßen, B. J. de Leeuw, A. G. de Boer, J. C. Verhoef, and H. E. Junginger. Effect of the degree quaternisation of N-trimethyl chitosan chloride on the permeability of intestinal epithelial cells (Caco-2). *Eur J Pharm Biopharm* 47: 269-274 (1999).

106. J. H. Hamman, C. M. Schultz, and A. F. Kotzé. N-trimethyl chitosan chloride: optimum degree of quaternization for drug absorption enhancement across epithelial cells. *Drug Dev Ind Pharm* 29: 161-172. (2003).

107. C. Jonker, J. H. Hamman, and A. F. Kotzé. Intestinal paracellular permeation enhancement with quaternized chitosan: in situ and in vitro evaluation. *Int J Pharm* 238: 205-213 (2002).

108. G. Sandri, S. Rossi, M. C. Bonferoni, F. Ferrari, Y. Zambito, G. Di Colo, and C. Caramella. Buccal penetration enhancement properties of N-trimethyl chitosan: Influence of quaternization degree on absorption of a high molecular weight molecule. *Int J Pharm* 297: 146-55 (2005).

109. M. M. Thanou, J. C. Verhoef, S. G. Romeijn, J. F. Nagelkerke, F. W. Merkus, and H. E. Junginger. Effects of N-trimethyl chitosan chloride, a novel absorption enhancer, on caco-2 intestinal epithelia and the ciliary beat frequency of chicken embryo trachea. *Int J Pharm* 185: 73-82 (1999).

110. N. Haffejee, J. Du Plessis, D. G. Muller, C. Schultz, A. F. Kotze, and C. Goosen. Intranasal toxicity of selected absorption enhancers. *Pharmazie* 56: 882-8 (2001).

111. T. Kean, S. Roth, and M. Thanou. Trimethylated chitosans as non-viral gene delivery vectors: cytotoxicity and transfection efficiency. *J. Control. Release* 103: 643-53 (2005).

112. S. Mao, X. Shuai, F. Unger, M. Wittmar, X. Xie, and T. Kissel. Synthesis, characterization and cytotoxicity of poly(ethylene glycol)-graft-trimethyl chitosan block copolymers. *Biomaterials* 26: 6343-56 (2005).

113. T. Kean, S. Roth, and M. Thanou. Trimethylated chitosans as non-viral gene delivery vectors: cytotoxicity and transfection efficiency. *J Control Release* 103: 643-53 (2005).

114. S. R. Jameela, T. V. Kumary, A. V. Lal, and A. Jayakrishnan. Progesterone-loaded chitosan microspheres: a long acting biodegradable controlled delivery system. *J Control Release* 52: 17-24 (1998).

115. F. Bugamelli, M. A. Raggi, I. Orienti, and V. Zecchi. Controlled insulin release from chitosan microparticles. *Arch Pharm (Weinheim)* 331: 133-8 (1998).

116. A. Grenha, B. Seijo, and C. Remunan-Lopez. Microencapsulated chitosan nanoparticles for lung protein delivery. *Eur J Pharm Sci* 25: 427-437 (2005).

117. M. Yang, S. Velaga, H. Yamamoto, H. Takeuchi, Y. Kawashima, L. Hovgaard, M. van de Weert, and S. Frokjaer. Characterisation of salmon calcitonin in spray-dried powder for inhalation Effect of chitosan. *Int J Pharm* in press (2006).

118. P. Calvo, C. Remunan-Lopez, J. L. Vila-Jato, and M. J. Alonso. Novel Hydrophilic chitosan polyethylene oxide nanoparticles as protein carriers. *J Appl Polym Sci* 63: 125-132 (1997).

119. S. Mao, U. Bakowsky, A. Jintapattanakit, and T. Kissel. Self-assembled polyelectrolyte nanocomplexes between chitosan derivatives and insulin. *J Pharm Sci* 95: 1035-48 (2006).

120. S. Ozbas-Turan, J. Akbuga, and C. Aral. Controlled release of interleukin-2 from chitosan microspheres. *J Pharm Sci* 91: 1245-51 (2002).

121. C. Schatz, A. Bionaz, J. M. Lucas, C. Pichot, C. Viton, A. Domard, and T. Delair. Formation of polyelectrolyte complex particles from self-complexation of N-sulfated chitosan. *Biomacromolecules* 6: 1642-7 (2005).

122. M. Alonso-Sande, M. Cuna, C. Remunan-Lopez, Teijerio-Osorio, J. L. Alonso-Lebrero, and A. M. J. Formation of new glucomannan-chitosan nanoparticles and study of their ability to associate and deliver proteins. *Biomacromolecules* 39: 4152-58 (2006).

123. Y. H. Lin, C. K. Chung, C. T. Chen, H. F. Liang, S. C. Chen, and H. W. Sung. Preparation of nanoparticles composed of chitosan/poly-gamma-glutamic acid and evaluation of their permeability through Caco-2 cells. *Biomacromolecules* 6: 1104-12 (2005).

124. Z. Ma, T. M. Lim, and L. Y. Lim. Pharmacological activity of peroral chitosan-insulin nanoparticles in diabetic rats. *Int J Pharm* 293: 271-80 (2005).

125. M. Amidi, S. G. Romeijn, J. C. Verhoef, H. E. Junginger, L. Bungener, A. Huckriede, D. J. Crommelin, and W. Jiskoot. N-Trimethyl chitosan (TMC) nanoparticles loaded with influenza subunit antigen for intranasal vaccination: Biological properties and immunogenicity in a mouse model. *Vaccine* 25: 144-53 (2007).

126. F. Chen, Z. R. Zhang, and Y. Huang. Evaluation and modification of N-trimethyl chitosan chloride nanoparticles as protein carriers. *Int J Pharm* in press (2006).

127. G. Sandri, M. C. Bonferoni, S. Rossi, F. Ferrari, S. Gibin, Y. Zambito, G. Di Colo, and C. Caramella. Nanoparticles based on N-trimethylchitosan: Evaluation of absorption properties using in vitro (Caco-2 cells) and ex vivo (excised rat jejunum) models. *Eur J Pharm Biopharm* 65: 68-77 (2007).

128. X. J. Yuan, Z. R. Zhang, Q. G. Song, and Q. He. Research on thymopentin loaded oral N-trimethyl chitosan nanoparticles. *Arch Pharm Res* 29: 795-9 (2006).

129. S. D. Yeo, G. B. Lim, P. G. Debenedetti, and H. Bernstein. Formation of microparticulate protein powders using a supercritical fluid antisolvent. *Biotech Bioeng* 41: 341-346 (1993).

130. N. Elvassore, A. Bertucco, and P. Caliceti. Production of insulin-loaded poly(ethylene glycol)/poly(l-lactide) (PEG/PLA) nano-particles by gas antisolvent techniques. *J Pharm Sci* 90: 1628–1636 (2001).

131. H. Okamoto, S. Nishida, H. Todo, Y. Sakakura, K. Iida, and K. Danjo. Pulmonary gene delivery by chitosan-pDNA complex powder prepared by a supercritical carbon dioxide process. *J Pharm Sci* 92: 371-80 (2003).

132. Y. Pérez de Diego, H. C. Pellikaan, F. E. Wubbolts, G. Borchard, G. J. Witkamp, and P. J. Jansens. Opening new operating windows for polymer and protein micronisation using the PCA process. *J Supercrit Fluids* 36: 216-224 (2006).

133. N. Jovanovic, A. Bouchard, G. W. Hofland, G. J. Witkamp, D. J. A. Crommelin, and W. Jiskoot. Stabilization of proteins in dry powder formulations using supercritical fluid technology. *Pharm Res* 21: 1955-69 (2004).

134. E. Reverchon. Supercritical antisolvent precipitation of micro-and nano-particles. *J Supercrit Fluids* 15: 1-21 (1999).

135. P. M. Gallagher, M. P. Coffey, V. J. Krukonis, and N. Klasutis. Gas antisolvent recrystallization: new process to recrystallize compounds insoluble in supercritical fluids. *ACS Symp Ser* 406: 334–354 (1989).

136. S. Palakodatyand P. York. Phase behavioral effects on particle formation processes using supercritical fluids. *Pharm Res* 16: 976-85 (1999).

137. M. Huang, E. Khor, and L. Y. Lim. Uptake and cytotoxicity of chitosan molecules and nanoparticles: effects of molecular weight and degree of deacetylation. *Pharm Res* 21: 344-53 (2004).

138. M. Garcia-Fuentes, D. Torres, and M. J. Alonso. New surface-modified lipid nanoparticles as delivery vehicles for salmon calcitonin. *Int J Pharm* 296: 122-32 (2005).

139. C. Prego, M. Garcia, D. Torres, and M. J. Alonso. Transmucosal macromolecular drug delivery. *J Control Release* 101: 151-62 (2005).

140. C. Prego, D. Torres, E. Fernandez-Megia, R. Novoa-Carballal, E. Quinoa, and M. J. Alonso. Chitosan-PEG nanocapsules as new carriers for oral peptide delivery. Effect of chitosan pegylation degree. *J Control Release* 111: 299-308 (2006).

141. H. Yamamoto, Y. Kuno, S. Sugimoto, H. Takeuchi, and Y. Kawashima. Surface-modified PLGA nanosphere with chitosan improved pulmonary delivery of calcitonin by mucoadhesion and opening of the intercellular tight junctions. *J Control Release* 102: 373-81 (2005).

142. K. Yamada, M. Odomi, N. Okada, T. Fujita, and A. Yamamoto. Chitosan oligomers as potential and safe absorption enhancers for improving the pulmonary absorption of interferon-alpha in rats. *J Pharm Sci* 94: 2432-40 (2005).

143. B. C. Baudner, M. M. Giuliani, J. C. Verhoef, R. Rappuoli, and H. E. Junginger. The concomitant use of the LTK63 mucosal adjuvant and of chitosan-based delivery system enhances the immunogenicity and efficacy of intranasally administered vaccines. *Vaccine* 28: 3837-3844. (2003).

144. T. Nagamoto, Y. Hattori, K. Takayama, and Y. Maitani. Novel chitosan particles and chitosan-coated emulsions inducing immune response via intranasal vaccine delivery. *Pharm Res* 21: 671-4 (2004).

145. K. S. Jaganathanand S. P. Vyas. Strong systemic and mucosal immune responses to surface-modified PLGA microspheres containing recombinant hepatitis B antigen administered intranasally. *Vaccine* 24: 4201-11 (2006).

146. R. C. Read, S. C. Naylor, C. W. Potter, J. Bond, I. Jabbal-Gill, A. Fisher, L. Illum, and R. Jennings. Effective nasal influenza vaccine delivery using chitosan. *Vaccine* 23: 4367-74 (2005).

147. K. Nishimura, S. Nishimura, N. Nishi, I. Saiki, S. Tokura, and I. Azuma. Immunological activity of chitin and its derivatives. *Vaccine* 2: 93-9 (1984).

148. K. Nishimura, S. Nishimura, N. Nishi, F. Numata, Y. Tone, S. Tokura, and I. Azuma. Adjuvant activity of chitin derivatives in mice and guinea-pigs. *Vaccine* 3: 379-84 (1985).

149. K. Nishimura, C. Ishihara, S. Ukei, S. Tokura, and I. Azuma. Stimulation of cytokine production in mice using deacetylated chitin. *Vaccine* 4: 151-6 (1986).

150. K. Nishimura, S. Nishimura, H. Seo, N. Nishi, S. Tokura, and I. Azuma. Effect of multiporous microspheres derived from chitin and partially deacetylated chitin on the activation of mouse peritoneal macrophages. *Vaccine* 5: 136-40 (1987).

151. Y. Shibata, I. Honda, J. P. Justice, M. R. Van Scott, R. M. Nakamura, and Q. N. Myrvik. Th1 adjuvant N-acetyl-D-glucosamine polymer up-regulates Th1 immunity but down-regulates Th2 immunity against a mycobacterial protein (MPB-59) in interleukin-10-knockout and wild-type mice. *Infect Immun* 69: 6123-30 (2001).

152. I. M. van der Lubben, J. C. Verhoef, M. M. Fretz, F. A. C. van Opdorp, I. Mesu, G. Kersten, and H. E. Junginger. Trimethyl chitosan chloride (TMC) as novel excipient for oral and nasal immunization against diphtheria. *STP Pharm Sci* 12: 235-242 (2002).

153. B. C. Baudner, J. C. Verhoef, M. M. Giuliani, S. Peppoloni, R. Rappuoli, G. Del Giudice, and H. E. Junginger. Protective immune responses to meningococcal C conjugate vaccine after intranasal immunization of mice with the LTK63 mutant plus chitosan or trimethyl chitosan chloride as novel delivery platform. *J Drug Target* 13: 489-98 (2005).

154. S. Jain, R. K. Sharma, and S. P. Vyas. Chitosan nanoparticles encapsulated vesicular systems for oral immunization: preparation, in-vitro and in-vivo characterization. *J Pharm Pharmacol* 58: 303-10 (2006).

Chapter two

Preparation and characterization of protein-loaded N-trimethyl chitosan nanoparticles as nasal delivery system

Maryam Amidi[1,2]
Stefan G. Romeijn[1]
Gerrit Borchard[1]
Hans E. Junginger[1]
Wim E. Hennink[2]
Wim Jiskoot[2]

[1] Department of Pharmaceutical Technology, Leiden/Amsterdam Center for Drug Research (LACDR), Leiden University, PO Box 9502, 2300 RA Leiden, The Netherlands

[2] Department of Pharmaceutics, Utrecht Institute for Pharmaceutical Sciences, Utrecht University, PO Box 80082, 3508 TB Utrecht, The Netherlands

J Control Release 111: 107-116 (2006)

Abstract

In this study, the potential of N-trimethyl chitosan (TMC) nanoparticles as a carrier system for the nasal delivery of proteins was investigated. TMC nanoparticles were prepared by ionic crosslinking of TMC solution (with or without ovalbumin) with tripolyphosphate, at ambient temperature while stirring. The size, zeta-potential and morphology of the nanoparticles were investigated as a function of the preparation conditions. Protein loading, protein integrity and protein release were studied. The toxicity of the TMC nanoparticles was tested by ciliary beat frequency measurements of chicken embryo trachea and *in vitro* cytotoxicity assays. The *in vivo* uptake of FITC-albumin-loaded TMC nanoparticles by nasal epithelia tissue in rats was studied by confocal laser scanning microscopy. The nanoparticles had an average size of about 350 nm and a positive zeta-potential. They showed a loading efficiency up to 95% and a loading capacity up to 50% (w/w). The integrity of the entrapped ovalbumin was preserved. Release studies showed that more than 70% of the protein remained associated with the TMC nanoparticles for at least 3 hours on incubation in PBS (pH 7.4) at 37 °C. Cytotoxicity tests with Calu-3 cells showed no toxic effects of the nanoparticles, whereas a partially reversible cilio-inhibiting effect on the ciliary beat frequency of chicken trachea was observed. *In vivo* uptake studies indicated the transport of FITC-albumin-associated TMC nanoparticles across the nasal mucosa. In conclusion, TMC nanoparticles are a potential new delivery system for transport of proteins through the nasal mucosa.

Keywords: N-Trimethyl chitosan nanoparticles; Nasal protein delivery; Calu-3 cells; Ciliary beat frequency

1 Introduction

Recent advances in biotechnology have resulted in the availability of a large number of protein-based antigens. Up till now, most vaccines are administered by injection because of their low stability in the gastrointestinal tract after oral administration and a low absorption at mucosal sites. Obvious disadvantages of parenteral administration are the high production costs, low compliance of vaccinees because of fear for injections by parents and children, and need for trained personnel to administer the vaccine. Consequently, alternative routes of administration are being explored. In particular, the nasal mucosa is an attractive site for the delivery of vaccines, because it has a relatively large absorptive surface and low proteolytic activity (1-6). Importantly, nasally administered vaccines can induce both local and systemic immune responses. However, most proteins are not well absorbed from the nasal cavity when administered as simple solutions. Major factors limiting the absorption of nasally administered proteins are their poor ability to cross nasal membranes and the mucociliary clearance mechanism, which rapidly removes protein solutions from the absorption site (1, 2, 7). Bioadhesive delivery systems have been used to overcome these obstacles (2, 3, 5, 7).

Mucoadhesive, hydrophilic nanoparticles have received much attention to deliver protein antigens via the nasal route. Mucoadhesive nanoparticulate systems improve mucosal absorption, because they strongly attach to the mucosa and increase the viscosity of mucin. Thereby they significantly decrease the nasal mucociliary clearance rate and thus increase the residence time of the formulation in the nasal cavity (1, 2). Moreover, nanoparticles cross the mucosal epithelium better than microspheres do, since not only microfold (M) cells overlaying the mucosal associated lymphoid tissue (MALT) but also the epithelial cells are involved in the transport of nanoparticles (8-11).

Among the various bioadhesive materials that have been proposed for nasal delivery of proteins, chitosan, a copolymer of glucosamine and N-acetylglucosamine, has received particular interest. Chitosan has been studied as a biomaterial and as a pharmaceutical excipient for drug delivery, because of its favorable biological properties (12-14). Besides its ability to facilitate paracellular transport of peptides and proteins across mucosal barriers (3, 5, 14, 15), it is biodegradable and has a very low toxicity (16-20). Moreover, chitosan microparticles or nanoparticles loaded with macromolecules are able to enhance the absorption of these molecules at mucosal sites (21-27). Several studies have shown the ability of chitosan microparticles to enhance both systemic and local immune responses against various antigens after oral or nasal administration (23-25). Also, insulin-loaded chitosan nanoparticles prepared by ionic gelation have shown enhanced nasal and intestinal absorption of insulin in rabbits and rats, resulting in a reduction of plasma glucose levels (26-29). And recently, Vila et al reported that low-molecular-weight chitosan nanoparticles containing tetanus toxoid could induce long-lasting immune responses after nasal administration in mice (30).

In spite of its reported successes, a major drawback of chitosan is that it is insoluble at physiological pH, whereas it is soluble and active as an absorption enhancer only in its protonated form in acidic environments (31-33). In contrast, N-trimethyl chitosan chloride (TMC), a partially quaternized chitosan derivative, shows good water solubility over a wide pH range. Hence, soluble TMC has mucoadhesive properties and excellent absorption enhancing effects even at neutral pH (34, 35). Moreover, TMC is an attractive alternative over chitosan for the design of protein loaded particles by ionic crosslinking. Importantly, the pH at which the TPP-TMC particles are prepared can be adjusted to provide maximum stability of the protein of interest and/or to enhance electrostatic interactions between the protein and cationic TMC for improving loading efficiency. At present only a few studies have reported on TMC solutions and TMC *micro*particles in nasal protein and vaccine delivery (35-37). Although mucoadhesive nanoparticles offer many advantages over microparticles or other nasal dosage forms (1, 2, 8-11), no research has been published about TMC *nano*particles as mucosal delivery system. Moreover, although there have been some reports about the toxicity of TMC (38-41), only limited toxicity data are available for particulate TMC carrier systems (40).

The aim of the present work was to explore the potential of novel TMC nanoparticles as a vehicle for the nasal administration of antigens. Therefore, TMC nanoparticles were prepared by an ionic gelation technique and their potential to encapsulate the model antigen ovalbumin was studied. After optimization of the preparation method and characterization of the obtained ovalbumin-loaded TMC nanoparticles, the safety of the TMC nanoparticles as a nasal delivery system was evaluated with several *in vitro* and *in vivo* toxicity tests. Finally, for the first time, the ability of protein-loaded TMC nanoparticles to cross nasal mucosal barriers in an *in vivo* model was demonstrated.

2 Materials and methods

2.1 Materials

Chitosan (M_n = 40 kDa, M_w = 177 kDa determined by gel permeation chromatography (GPC) using poly(ethylene glycol) (PEG) standards and degree of deacetylation 93%) used for synthesizing the TMC (see below) was a generous gift from Primex (Avaldsnes, Norway). Bodipy 665/676 was purchased from Molecular Probes (Leiden, Netherlands). Tripolyphosphate (TPP), Tween 80, branched poly(ethylene imine) (PEI) 25 kDa, ovalbumin, Dulbecco's Modified Eagle's Medium (DMEM), mouse monoclonal anti-ovalbumin IgG, FITC-labeled ovalbumin and FITC-labeled albumin were obtained from Sigma (Sigma, Bornem, Belgium). Fluorescent-labeled (Cy-5) goat IgG anti-mouse immunoglobulin was supplied by Jackson laboratories (Jackson ImmunoResearch Europe Ltd. UK). All other materials used were of analytical or pharmaceutical grade.

2.2 TMC synthesis and characterization by NMR spectroscopy

TMC with a degree of quaternization of 25% was synthesized by methylation of chitosan by using CH_3I in the presence of a strong base (NaOH) as described previously (42). The obtained polymer was purified by dialysis against water for 4 days at 4 °C and then freeze-dried. The purified TMC was analyzed by ^{1}H-nuclear magnetic resonance (NMR) spectroscopy. The NMR spectrum of the TMC in D_2O at 80 ºC was recorded with a NMR spectrometer (AV-400, Brucker, Switzerland). The degree of quaternization (DQ) and dimethylation was calculated according to a previously described method (42) using the following equations:

$$DQ= [[(CH_3)_3]/[H] \times 1/9] \times 100 \quad (1)$$

$$DM= [[(CH_3)_2]/[H] \times 1/6] \times 100 \quad (2)$$

where DQ and DM are the degree of the quaternization and dimethylation, respectively, in mole percentage of free amine; $[(CH_3)_3]$ and $[(CH_3)_2]$ are the integrals of the chemical shift of the hydrogens of the trimethyl amino group at 3.3 ppm and the dimethylated amino group at 3.1 ppm, respectively; [H] is the integral of the H-1 peaks between 4.7 and 5.7 ppm, related to hydrogen atoms bound to carbon 1 of the chitosan molecule, which is taken as the reference signal.

2.3 Determination of the pKa of TMC and TPP

The pKa and the amount of titratable amines (mainly dimethylated amine) of the TMC were measured by titration of 50 mg of TMC dissolved in 3 ml 189 mM hydrochloric acid with an aqueous solution of sodium hydroxide (170 mM). The pKa's of the phosphate groups of TPP were assessed by titration of 25 mg TPP dissolved in 3 ml 200 mM NaOH with HCl (210 mM). Based on the results of these titrations, the molar charge ratio of TPP and TMC used for the preparation of the nanoparticles was calculated.

2.4 Preparation of TMC nanoparticles

TMC nanoparticles were prepared in the presence of Tween 80 as a re-suspending agent to prevent particle aggregations during purification. Briefly, an aqueous solution of TMC 2 mg/ml (5 ml) containing 1% (w/v) Tween 80 was prepared in water. Subsequently, 1.8 ml (1 mg/ml) of TPP solution (pH 8) was slowly added drop-wise to the TMC solution (pH 6) while stirring at ambient temperature, yielding a final pH of around 7. Ovalbumin-loaded TMC nanoparticles were prepared as described above by dissolving ovalbumin (0.1, 0.2, 0.3, 0.5 or 1 mg/ml) in 5 ml TMC solution (2 mg/ml) containing 1% (w/v) Tween 80 before adding TPP. The nanoparticle suspensions were then concentrated and purified (from free TMC, TPP, Tween 80

and unbound protein) by centrifugation. Aliquots of 1.5 ml particle suspensions were centrifuged on 10 µl of a glycerol bed at 10000 g for 15 minutes. The supernatants were discarded and the pellets were resuspended in phosphate buffered saline (PBS: 10 mM Na_2HPO_4, 18 mM KH_2PO_4, 3 mM KCl, 138 mM NaCl; pH 7.4) or 5 mM HEPES, pH 7.4.

2.5 Loading efficiency and loading capacity of ovalbumin-loaded nanoparticles

Ovalbumin-loaded TMC nanoparticles were prepared and purified as described above. The amount of protein entrapped in the nanoparticles was calculated from the difference between the total amount added to the loading solution and the amount of non-entrapped protein remaining in the supernatant. Ovalbumin concentrations in the supernatants were measured by the micro BCA protein assay (Pierce, USA). Since Tween 80 in the supernatant interfered with the protein assay, for initial optimization studies the ovalbumin-loaded nanoparticles were prepared without Tween 80. Aliquots of the resulting nanoparticle suspension were centrifuged for 20 minutes at 18000 g and 10 °C and the supernatants were then separated from the nanoparticles. The amount of non-entrapped protein remaining in the supernatant was measured by the micro BCA protein assay (Pierce, USA). A non-loaded nanoparticle suspension without Tween 80 was used as a blank to correct for interference by TMC.
To investigate the effect of Tween 80 on protein loading, FITC labeled ovalbumin-loaded nanoparticles were prepared as described above in presence of Tween 80 and the amount of the protein was determined by measuring fluorescence (excitation wavelength: 488 nm, emission wavelength: 520 nm) in the supernatant using a Perkin-Elmer 3000 fluorescence spectrometer (Gouda, The Netherlands). An empty nanoparticle suspension was used as blank to correct for interferences by TMC and Tween 80. Loading efficiency (LE) and loading capacity (LC) for both protein and fluorescence assay were calculated as follows.

$$LE = \frac{\text{Total amount of ovalbumin} - \text{Free ovalbumin}}{\text{Total amount of ovalbumin}} \times 100\% \quad (3)$$

$$LC = \frac{\text{Total amount of ovalbumin} - \text{Free ovalbumin}}{\text{Nanoparticles dry weight}} \times 100\% \text{ (w/w)} \quad (4)$$

2.6 In vitro release of ovalbumin from TMC nanoparticles

Aliquots of 1 ml ovalbumin-loaded TMC nanoparticle suspension prepared with Tween were centrifuged at 10000 g on a 10 µl glycerol bed for 15 minutes. The supernatant was decanted and the pellet was re-suspended in 1 ml phosphate buffered saline (PBS, 0.1 M, pH 7.4). The tubes were incubated at 37 °C, under agitation (50

rpm), for 3 hours. At time 0 and at different time intervals, a tube was taken and centrifuged (at 18000 g for 10 min). The released ovalbumin in the supernatant was determined by the micro BCA protein assay. A sample consisting of only nanoparticles re-suspended in PBS was used as background. The experiments were performed in triplicate.

2.7 Characterization of TMC-nanoparticles

The nanoparticles were characterized for their size and zeta-potential with a Zetasizer 3000 (Malvern Instruments Ltd., Malvern, UK) in 5 mmol HEPES pH 7.4 buffer. The particle size distribution of the nanoparticles is reported as a polydispersity index (PDI), ranging from 0 for an entire monodisperse up to 1 for a completely heterodisperse system. Morphological examination of the nanoparticles was performed by scanning electron microscopy (SEM). A drop of the TMC nanoparticles suspension was placed on a gold disk. After air-drying overnight at ambient temperature, the dried nanoparticles were coated with gold in a gold-sputter device MED 010 (Balzer, Liechtenstein) and studied with a JOEL 6700F scanning electron microscope (JOEL BV, Schiphol-Rijk, The Netherlands).

2.8 SDS-polyacrylamide gel electrophoresis and Western blotting

SDS-polyacrylamide gel electrophoresis and Western blotting were done to evaluate the effect of the preparation process on protein integrity and antigenicity. Ovalbumin-loaded TMC nanoparticles were destabilized by adding 1 ml of 10% (w/v) NaCl to 6.8 ml of the nanoparticle suspension, resulting in a solution with a protein concentration of 0.3 mg/ml. The protein was electrophoresed at 125 V under reducing conditions, in a 7.5% SDS-polyacrylamide gel. The protein sample was prepared in electrophoresis loading-buffer (60 mM Tris-HCl, pH 6.8, with 25% glycerol and 2% SDS containing 0.1% bromophenol blue solution, and β-mercaptoethanol) and heated for 5 min at 95 ºC. After electrophoresis, the protein bands were visualized by staining with Coomassie Blue R-250. For Western blotting, antigen bands were transferred to a nitrocellulose membrane by using a semi-dry Western blotting system operating at a constant current of 100 mA for 1 h in blotting buffer consisting of Tris buffer (25 mM Tris, 1.4% glycine, 20% (v/v) methanol, pH 8.3). After blotting the free sites were blocked with 1% non-fat milk-powder in phosphate buffer saline (10 mM Na_2HPO_4, 18 mM KH_2PO_4, 3 mM KCl, 138 mM NaCl; pH 7.4) containing 0.05% Tween 20 (PBS-T). Next, the membrane was incubated with a solution of mouse anti-ovalbumin monoclonal antibody in PBS-T containing 0.1% non-fat milk powder. The membrane was then washed to remove the unbound antibody and incubated with Cy-5-labeled, goat IgG anti-mouse immunoglobulin. The blotted antigen-antibody complexes were visualized by a fluorescence Western blotting system (Amersham Corporation, IL, USA).

2.9 In vitro toxicity assays

2.9.1 Ciliary beat frequency measurements

The effect of the TMC nanoparticles on the ciliary beat frequency (CBF) was studied as described previously (43-45). Briefly, a chicken embryo trachea was dissected and sliced into small rings of 1 mm thickness. The tissue slices were put in Locke-Ringer solution (LR, pH 7.0) at 33 °C to recover for 30 minutes. Then the LR was replaced by a suspension of purified TMC nanoparticles in LR. After starting the incubation, the CBF was measured at 5, 10 and 15 minutes. Thereafter, the formulations were replaced by L.R and the reversibility of the CBF was assessed every 5-10 minutes during 45 minutes. The degree of the reversibility was classified into three categories: cilio-friendly (>75%), cilio-inhibiting (25-75%), or cilio-static (<25% of initial value) (45). The purified TMC nanoparticles (40 mg/ml) prepared with and without Tween 80 and an aqueous TMC solution (2 mg/ml) in LR were studied for their influence on the CBF in undiluted and 5-fold diluted form, which equals the estimated physiological dilution factor in the nasal cavity (45). The CBF of each formulation and the LR (negative control) were measured for six independent batches and the area under the curve (AUC) of each measurement during incubation (0-15 min) and during the reversibility test period (15-60 min) were calculated separately. The effect of the formulations on the CBF and the reversibility of the CBF were compared to that of LR. The data were statistically analyzed by using one-way analysis of variance (ANOVA) with Bonferroni's multiple comparison test.

2.9.2 Cell viability assay

The cytotoxicity of the purified TMC nanoparticles was tested *in vitro* on the differentiated human, mucus-producing, submucosal gland carcinoma cell line Calu-3. Calu-3 cells were seeded at a density $5x10^5$ cells per well into 96-well culture plates in DMEM supplemented with 10% fetal calf serum (FCS) and 50 µg/ml penicillin and streptomycin. The cells were incubated for two days at 37 ºC in 95% air and 5% CO_2. The formulations were prepared in Hank´s balanced salt solution (HBSS) buffered with 30 mM N-[2-hydroxyethyl] piperazine-N´-[2-ethanesulphonic acid] (HEPES), adjusted with 0.1 M NaOH to pH 7.2. Then the cells were exposed to HBSS-HEPES buffer, a suspension of TMC nanoparticles (40 mg/ml), TMC solutions (2 and 20 mg/ml) or poly(ethylene imine) (PEI) solutions (0.02 and 0.2 mg/ml) in HBSS-HEPES and incubated for two hours at 37 ºC. Thereafter, the formulation and polymers were replaced by 100 ml of DMEM and 20 µl cell proliferation reagent [3-(4,5-dimethylthiazole-2-yl)-5-(3-carboxymethoxyphenyl)-2-(4-sulfophenyl)-2H-tetra zolium, inner salt; MTS[a]], Promega Benelux B.V. (Leiden, The Netherlands), and the cells were incubated for 1-2 hours at 37°C. Finally, the absorbance was measured at 490 nm using a 96-well microplate reader (46, 47)]. As a positive control (cytotoxic), cells were incubated with SDS (0.01% w/v) in NaOH (1% (w/v) for 10 minutes. The data were statistically analyzed by using one-way analysis of variance (ANOVA) with Bonferroni's multiple comparison test.

2.9.3 Measurement of the transepithelial electrical resistance (TEER)

Calu-3 cells were seeded at a seeding density of $4x10^5$ cells/cm^2 on collagen-coated 12-Transwell plates with a microporous membrane (Costar Europe, Badhoevedorp, The Netherlands). One ml of the culture medium (DMEM) supplemented with 10% FCS and 50 µg/ml penicillin and streptomycin was added to both the basolateral and apical side. The medium at the apical side was removed after one day and the cells were grown at an air interface at 37 °C, 90% humidity and 5% CO_2. The medium was changed every two days and cultivation was continued for 14 days until a confluent cell layer was formed. The medium was then replaced with 1.5 ml HBSS-HEPES at the basolateral side 30 minutes before starting the experiments. Thereafter, the TMC solutions (2 mg/ml) and the purified nanoparticles (40 mg/ml) in HBSS-HEPES (0.5 ml) were applied at the apical site of the cell monolayers. The TEER of Calu-3 cells was measured at certain time intervals (0, 15, 30, 45, 60, 90, 120, 135 and 150 min). After 150 min of incubation, the formulations were replaced by HBSS-HEPES to determine the recovery of TEER to its initial value (48, 49).

2.10 In vivo uptake of TMC nanoparticles in rat nasal epithelia

Male Wistar rats (~380 g) were anesthetized by intramuscular administration of 0.5 ml/kg of Hypnorm and 0.5 ml/kg of Dormicum. A 5 cm silicone cannula was inserted into the trachea to enable the animal to breath. An incision was made in the esophagus to insert a silicone cannula of 20 cm into the posterior part of the nasal cavity and to perfuse the fixative and prevent drainage of the formulation caused by mucociliary clearance in the nasal cavity. A suspension of TMC nanoparticles loaded with FITC-albumin was prepared and purified as described before. Briefly, an aqueous solution of TMC 2 mg/ml (5 ml) containing 1% (w/v) Tween 80 and 0.5 mg/ml FITC-albumin was prepared in water. Thereafter 1.8 ml 1 mg/ml TPP solution was added drop-wise. FITC-albumin loaded nanoparticles dispersed in PBS and a 0.5 mg/ml FITC-albumin solution were administered into the rats' nares (50 µl per nostril) by a 100 µl pipette tip with a PVC-tube attached. The tube was inserted at least 0.5 cm into the nostril to deposit the formulations into the nasal cavity. During dosing and subsequent exposure the rats were in the supine position.

The animals were sacrificed 30 minutes after intranasal administration of the formulations and the nasal cavity of the rats was flushed with 5 ml 4% (v/v) formaldehyde in PBS pH 7.4 via the esophageal cannula. The septum and the nasal associated lymphoid tissue (NALT) situated at the posterior part of the rat nose were excised and immersed in the same fixative for at least 90 min.

Prior to CLSM examination, the septum and nasal tissues were permeabilized in 0.1% Triton X-100 solution in PBS for 20 minutes. The tissues (epithelia) were stained with BODIPY 665/676 in methanol for 60 minutes and visualized by a confocal laser scanning microscope (Bio-Rad, Alphen a/d Rijn, The Netherlands). The confocal pictures were obtained by scanning the nasal epithelia in the x, y plane with a z-step of 500 nm (11, 50).

3 Results and discussion

3.1 NMR characterization of TMC and pKa measurements of TMC and TPP

Chitosan was methylated with CH_3I to yield TMC. From NMR analysis a degree of quaternization of about 25% and an average degree of di- plus mono-methylation of about 75% was calculated. Titration of an acidified aqueous solution of TMC with dilute sodium hydroxide (see materials and methods) showed an average pKa of 6.2 for the mono- and di-methylated amines, which is almost equal to the pKa reported for the amines in chitosan (32).
TPP has in principle five titratable protons. Titration of TPP with dilute NaOH, however revealed two pKa values, namely 8.8 and 6.2, consuming one equivalent of NaOH per titratable group. This indicates that two out of the five hydroxyl groups of TPP are very weak acids which could not be deprotonated in the dilute NaOH solution, and one is strongly acidic and could not be protonated by dilute HCl.

3.2 Preparation and characterization of TMC nanoparticles

The TMC nanoparticles were prepared by ionotropic gelation of cationic TMC with TPP anions. This mild technique involves the mixing of two aqueous solutions at ambient temperature while stirring without using sonication or organic solvents. Since proteins are very labile molecules sensitive to several stress factors (51), this mild preparation method is very suitable to prepare protein loaded nanoparticles. Various formulations were made with different initial concentrations of TMC (1-6 mg/ml) and TPP solutions (0.25- 3 mg/ml) to establish preparation conditions at which nanoparticles are formed. Since smaller particles generally show a higher uptake by nasal epithelia than larger ones (8-11), the criteria size, size distribution, colloidal stability and reproducibility of nanoparticle production were used to select the best formulation parameters to prepare nanoparticles. The optimal TMC nanoparticles were formed when the TMC/TPP ratio was 5.5 (w/w) which is close to the optimal ratio of 3-5 for chitosan/TPP (w/w) found by Calvo et al. (28, 29). At very low or high TMC/TPP ratios either a clear solution was seen (almost no particle formation) or larger nanoparticles with a low colloidal stability were obtained, respectively. Among the formulations that led to formation of nanoparticle suspensions, one formulation that resulted in stable colloidal particles with a narrow size distribution (table 1) was selected for successive studies. Table 1 displays the characteristics of empty and ovalbumin-loaded TMC nanoparticles and shows that rather small particles with a slightly positive zeta-potential were formed.
The positive zeta-potential of the TMC-TPP nanoparticles can be explained by the molar ratio of the positive charge of TMC (which at pH 7 is almost exclusively due to quaternized amines, yielding an average charge of ca. + 0.25 per aminosugar unit) and the negative charge of TPP (ca**.** –2 per molecule). This molar ratio as was calculated to be 1.1 for the nanoparticles mentioned in table 1, when assuming that all TPP and TMC molecules participate in the formation of the nanoparticles.

Table 1. Characteristics of TMC nanoparticles

Formulations / TMC nanoparticles	Final TMC conc. mg/ml	Final TPP conc. mg/ml	TMC/TPP (w/w)	Size (nm) before purification (mean ± SD) n=3	PDI	Size (nm) after purification (mean ± SD) n=3	PDI	Zeta-potential (mV) (mean ± SD) n=3
unloaded	1.470	0.265	5.5	254 ± 9	0.157	360 ± 26	0.242	20 ± 2
loaded with ovalbumin [1]	1.470	0.265	5.5	366 ± 23	0.230	479 ± 32	0.327	16 ± 4

[1] LE = 79.8%, LC = 28.6%

Both unloaded and loaded nanoparticles showed a slight increase in size and PDI after purification, which is most probably due to slight aggregation of particles. Scanning electron microscopy (figure 1) confirmed that the nanoparticles had a narrow size distribution and their size was in agreement with the size as obtained from DLS measurements. The size and morphology of the nanoparticles were not affected by protein loadings up to LC of 50% and LE of ca 90%. Higher protein concentrations (i.e., initial protein/TMC ratios substantially exceeding the maximum LC; see section 3.3, below) resulted in lower LE and particle aggregation, which may be due to high concentrations of free ovalbumin in the nanoparticle suspension under these conditions.

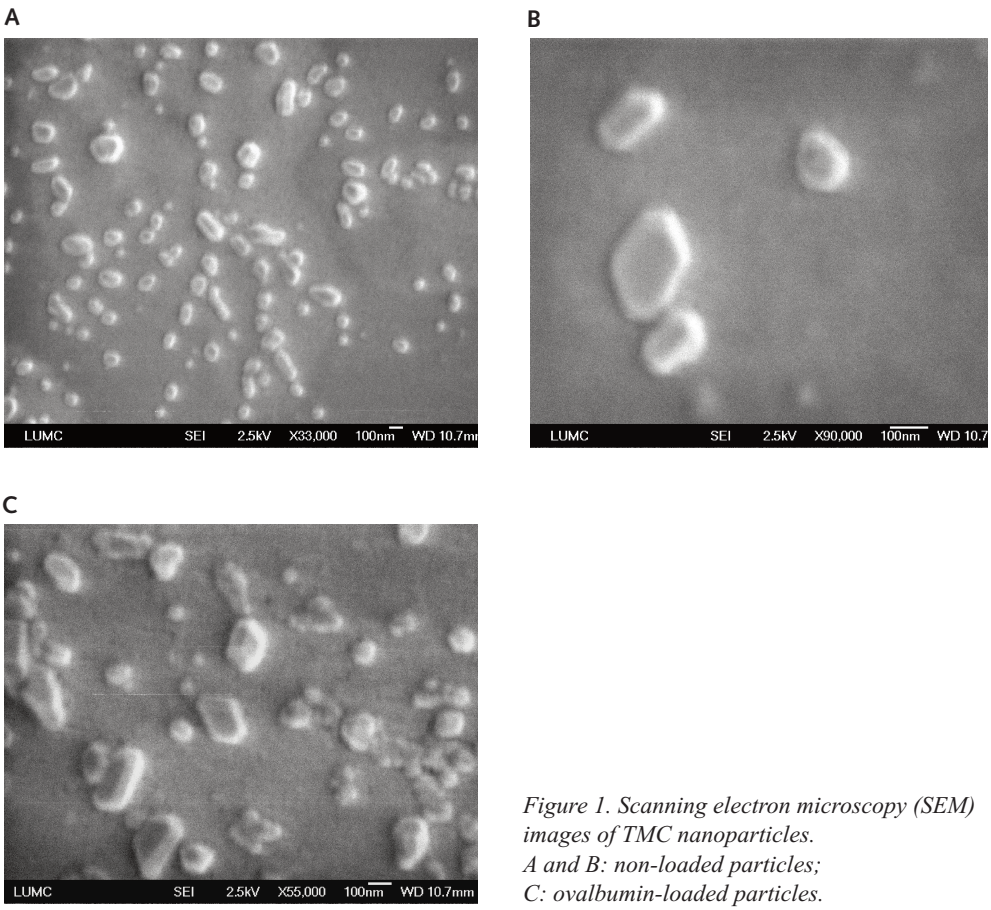

Figure 1. Scanning electron microscopy (SEM) images of TMC nanoparticles.
A and B: non-loaded particles;
C: ovalbumin-loaded particles.

3.3 Loading and release study of ovalbumin from TMC nanoparticles

Figure 2 shows the LE and LC of ovalbumin- and FITC-labeled ovalbumin-loaded nanoparticles. Both ovalbumin (preparation without Tween) and FITC-labeled ovalbumin (preparation with Tween) showed almost 100% LE up to a concentration of 0.5 mg/ml where the loading capacity (LC) for ovalbumin reached a maximum of about 50% w/w (figure 2). The LC of TMC nanoparticles for ovalbumin and FITC-ovalbumin was influenced by the initial concentration of the protein in the loading solutions. At lower protein/TMC ratios, the LC linearly increased with the protein/TMC ratio (figure 2). The loading efficiency and capacity of ovalbumin-loaded TMC nanoparticles was not affected by Tween 80, since comparable values of LE and LC for FITC-ovalbumin prepared in the presence of Tween 80 were obtained. The high loading efficiency for ovalbumin is likely due to electrostatic interactions between the positively charged TMC and negatively charged ovalbumin (pI = 4.5) at pH 7.

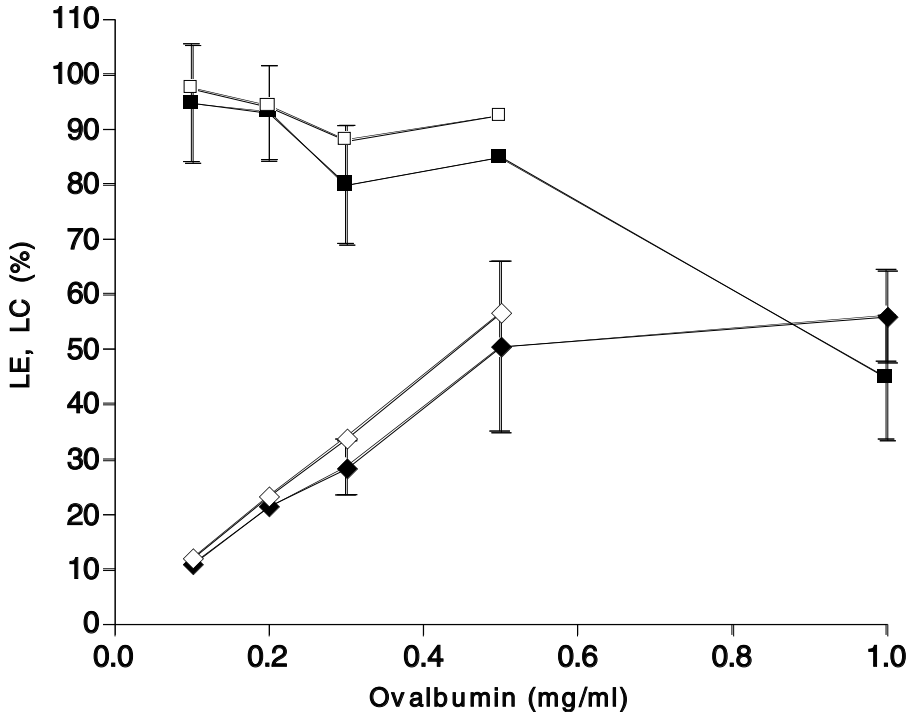

Figure 2. Loading efficiency (LE) and loading capacity (LC) of TMC nanoparticles as a function of the ovalbumin concentration used for preparation in the absence of Tween 80 (data are expressed as mean ± SD of 5 independent experiments) and the FITC-ovalbumin concentration used for preparation in presence of Tween 80 (data are expressed as mean ± SD of 3 independent experiments). (■) LE% and (◆)LC% (ovalbumin). (□) LE% and (◊) LC% (FITC-ovalbumin).

In vitro release studies showed that around 30% of the loaded protein was immediately released into PBS. The observed burst might be ascribed to protein molecules that were loosely bound to TMC (presumably at the particle surface). The remaining 70% of loaded protein was stably associated with the TMC nanoparticles for at least 3 hours. The loading and release characteristics are similar to those of albumin-loaded N-(2-hydroxy) propyl-3-trimethyl ammonium chitosan nanoparticles reported by Xu et al. (52). It is important that the protein is not released to a large extent before the protein loaded-nanoparticles pass the nasal epithelial barrier during their residence in the nasal cavity. The normal mucociliary clearance rate in healthy human's nose is about 20 min (7). Soane et al. reported that mucoadhesive chitosan microspheres were cleared from the human nasal cavity with a half-time (time taken for 50% clearance; $t_{50\%}$) of about 80 min (1).

3.4 SDS-PAGE and Western blotting analysis of ovalbumin entrapped in the TMC particles

SDS-PAGE revealed that besides the band corresponding to monomeric ovalbumin, there were no additional bands that would indicate the presence of covalent aggregates or fragments. Western blot analysis confirmed that the antigenicity of ovalbumin was not altered following its entrapment in nanoparticles (data not shown).

3.5 In vitro toxicity assays

The influence of TMC nanoparticles on the ciliary beat frequency (CBF) of chicken embryo trachea was studied to examine possible toxic effects of the TMC formulations. Figure 3A shows that during 15 min incubation a significant decrease of the CBF (to ca. 40% of the initial value) was seen for both undiluted TMC nanoparticles (40 mg/ml), prepared either in the presence or in the absence of Tween 80, and soluble TMC (2 mg/ml) as compared to the reference ($p < 0.001$). For 5-fold diluted TMC nanoparticle suspensions (8 mg/ml), prepared either in the presence or in the absence of Tween 80, a less prominent but still significant ($p < 0.05$) decrease of the CBF (to 70-90% of the initial value) was observed (figure 3B). The reversibility test showed that both the soluble TMC (0.4, 2 mg/ml) and the nanoparticles (40 mg/ml) prepared in the presence of Tween 80 could be classified as cilio-inhibiting compared to LR as a negative control ($P < 0.01$), whereas the undiluted and 5-fold diluted TMC nanoparticle suspensions (40 and 8 mg/ml) without Tween 80 and the 5-fold diluted TMC nanoparticles (8 mg/ml) prepared in the presence of Tween 80 were classified as cilio-friendly (figure 3B) ($p > 0.05$). From these results, it can be concluded that the TMC nanoparticles are less toxic than a solution of the TMC polymer. Five-fold dilution of soluble TMC did not reduce the toxicity effect of the polymer, which may be due to the strong interaction of the cationic molecules with cell membranes of the cilia. The undiluted TMC nanoparticles prepared in the presence of Tween 80 had a stronger effect on the CBF than the nanoparticles prepared without Tween, which might originate from trace amounts of Tween 80 in the formulation.

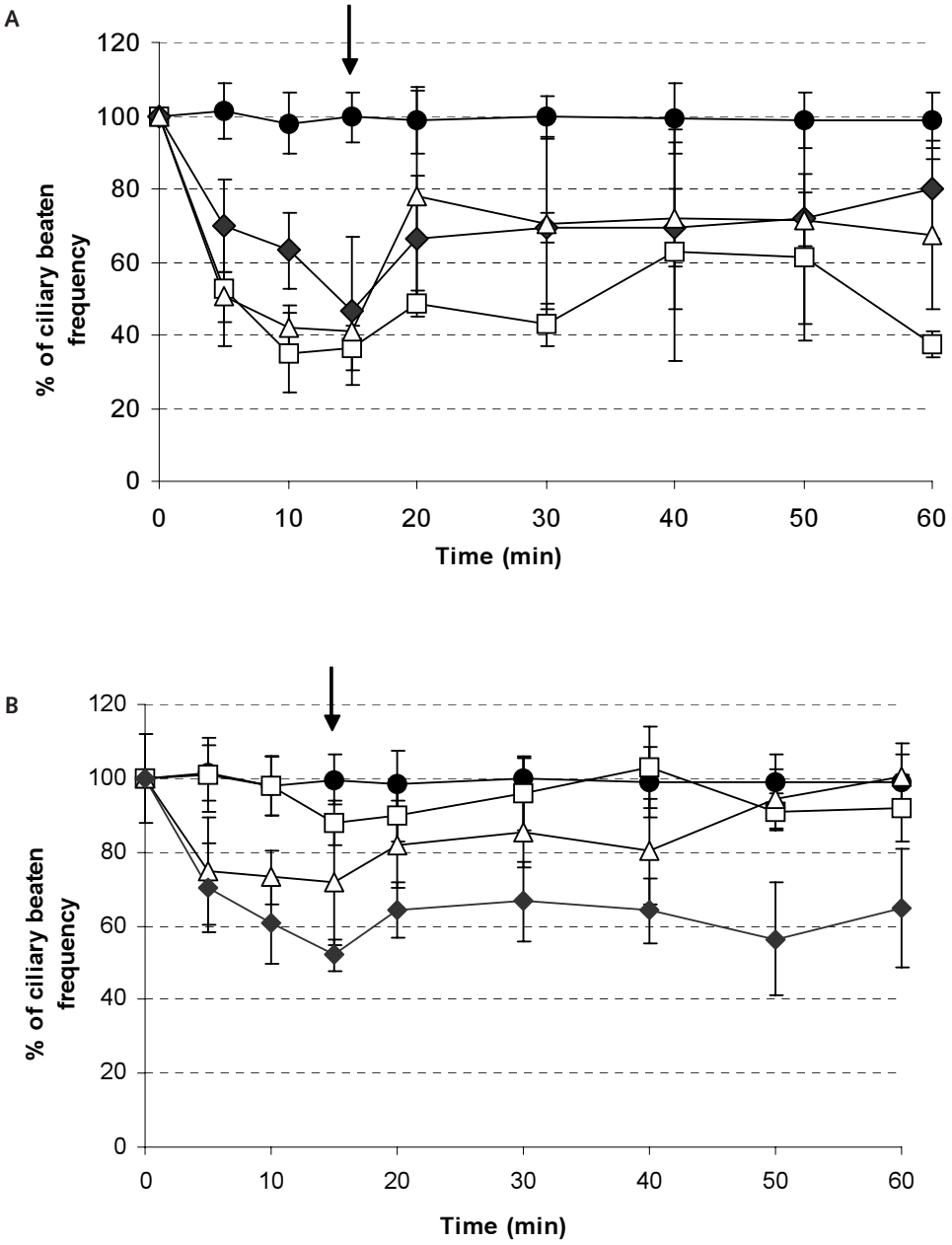

Figure 3. The effects of soluble TMC (2 mg/ml) and TMC nanoparticles (40 mg/ml) on the ciliary beat frequency (CBF) for (A) undiluted and (B) 5 fold diluted samples. Symbols: soluble TMC (◆), TMC nanoparticles prepared with Tween 80 (□), TMC nanoparticles prepared without Tween 80 (△) and LR, negative control (●). The CBF is expressed as a percentage of the initial frequency (100) and the reported data are the mean ± SD of 6 experiments. The arrow shows the time point at which the formulations were replaced by LR buffer.

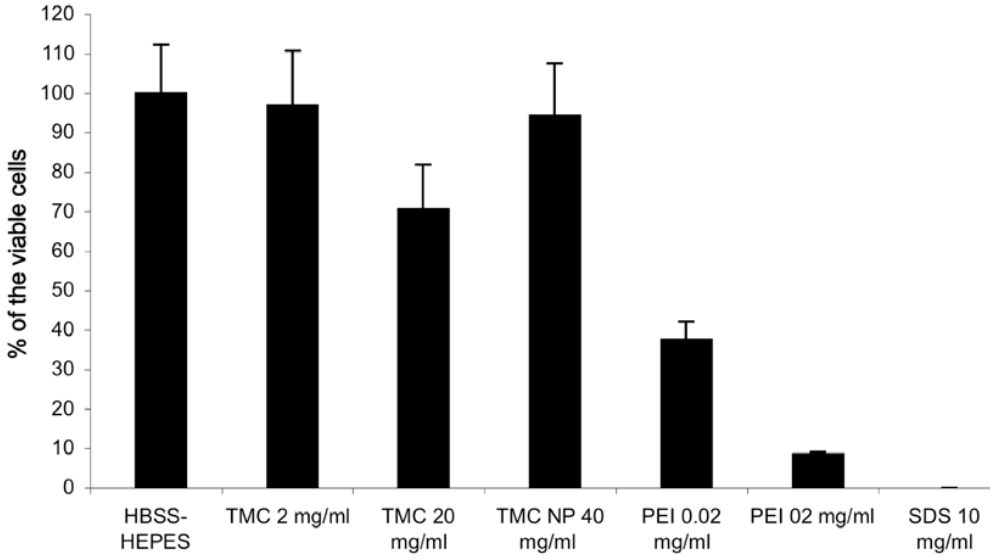

Figure 4. The effect of soluble TMC (2 and 20 mg/ml), TMC nanoparticle suspension (NP) (40 mg/ml) and soluble PEI (0.02, 0.2 mg/ml), on mitochondrial dehydrogenase activity of Calu-3 cells. Data are the mean ± SD of 8 experiments.

The results of CBF measurements should be interpreted with care, because CBF measurements may overestimate the ciliotoxicity *in vivo*. Firstly, direct exposure of the excised ciliated tissue to the formulations is probably not representative for the situation *in vivo,* because the ciliated epithelium is protected by a mucus layer secreted in the nasal cavity and the administered formulations are diluted. Secondly, the epithelial cells in the nasal mucosa are constantly replaced by cells at the basement membrane *in vivo,* a situation which cannot be mimicked *in vitro*. It has been shown that during incubation of ciliated tissue in PBS and normal saline, a substantial decrease of CBF was seen which was reversible (cilio-friendly) (45, 53). Furthermore, a human nose contains about 0.4 ml mucus and most frequently used nasal sprays have a volume of about 0.1 ml. Therefore the 5-fold lower concentration of the TMC formulations used in this study may give a more realistic view of their effect on CBF (43-45).

The effect of TMC nanoparticles and solutions on the mitochondrial dehydrogenase activity of Calu-3 cells is shown in figure 4. Calu-3 cells are known as a relevant model for respiratory epithelium; they form tight monolayers and secrete components of mucus and surfactant (48, 49, 54, 55). This cytotoxicity assay did not show significant toxic effects of TMC nanoparticle suspension (40 mg/ml), made in the presence of Tween 80, and soluble TMC (2 mg/ml) ($p > 0.05$). We only observed a decrease of the cell viability when the cells were incubated with soluble TMC at relatively high concentration (20 mg/ml) ($p < 0.001$).

It is known that cationic macromolecules like PEI can exhibit substantial cell toxicity (56). To illustrate the safety of TMC, its effect on the cell viability was directly compared with that of PEI. Whereas a substantial decrease of the cell viability was

observed after incubation with PEI at a concentration as low as 0.02 mg/ml compared to HBSS-HEPES ($P < 0.001$), soluble TMC at up to a 1000-fold higher concentration (20 mg/ml) showed a less damaging effect ($p < 0.001$). The differences between the cytotoxicity of TMC and PEI may be ascribed to differences in chemistry, charge density, 3D structure of the polymer backbone, molecular weight distribution, etc., all of which may affect the interactions of the polymers with cell membranes, and thus their toxicity.

Cytotoxicity might be associated with an irreversible decrease in TEER due to destruction of the tight junctions of the epithelial cells. The results of the TEER measurements of a confluent Calu-3 cell layer after exposure to a TMC nanoparticle suspension (40 mg/ml) made in the presence Tween 80 and soluble TMC (2 mg/ml) showed no decrease of the initial TEER values during incubation of the cells for 150 min (data not shown). These results are in line with previous observations that TMC with a low DQ is unable to open the tight junctions (57-59) and demonstrate the safety and thus the potential applicability of the TMC nanoparticles for nasal delivery.

3.6 CLSM visualization of fluorescently labeled TMC nanoparticles in nasal epithelia

FITC-albumin was used to prepare fluorescent TMC nanoparticles and to investigate the transport of these nanoparticles through the nasal mucosa. The uptake of nanoparticles by nasal epithelial and NALT cells depends in particular on their size and charge (10, 60). FITC-albumin loaded TMC nanoparticles had the same average size and zeta-potential as the ovalbumin-TMC nanoparticles. CLSM images of nasal epithelia and NALT incubated with FITC-albumin loaded TMC nanoparticles showed the presence of fluorescent nanoparticles throughout the cytoplasm of these cells (figure 5). In contrast, in the rat nasal epithelia incubated with soluble FITC-albumin, no fluorescence was detected (figure 6), which indicates that uptake of soluble FITC-albumin was negligible. Z-scan images of the nasal epithelia incubated with the fluorescently labeled nanoparticles in different steps (0.5 μm) indicated that the nanoparticles were not only internalized by the nasal epithelial cells, but also transported to the cell layers underneath (data not shown). The transport of encapsulated protein is unlikely to occur via the paracellular pathway, because soluble TMC (DQ: 25%) is not able to enhance efficiently the paracellular transport of proteins by opening the tight junctions of the epithelial cells (57-59). Moreover, the results of the TEER studies indicated the absence of paracellular permeability effects of TMC nanoparticles. Therefore, the presence of FITC-albumin loaded TMC nanoparticles in the nasal mucosa is likely due to intracellular uptake by epithelial and NALT cells.

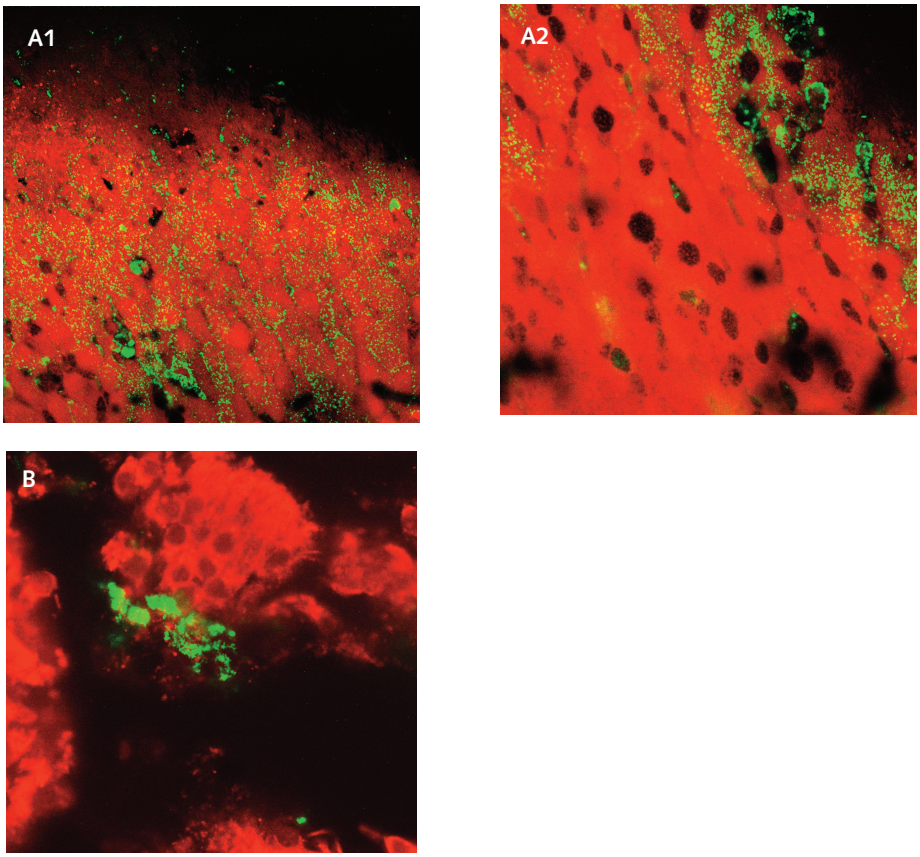

Figure 5. CLSM images of rat nasal epithelia (A) and NALT (B) following administration of a suspension of FITC-albumin loaded TMC nanoparticles.

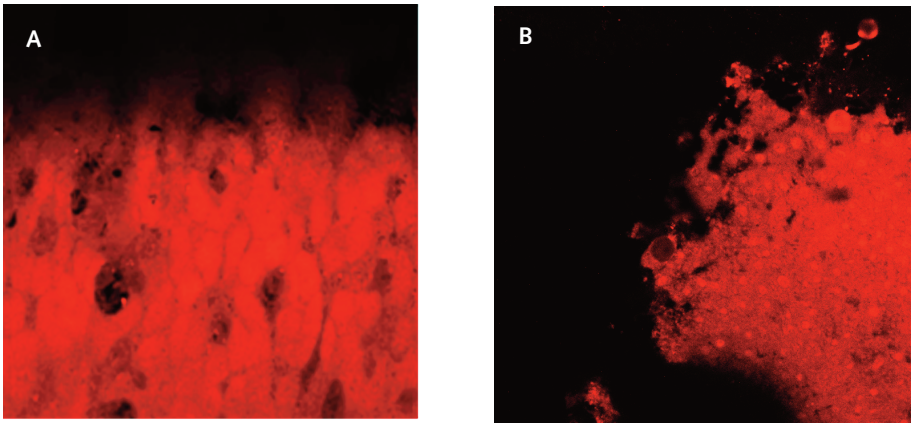

Figure 6. CLSM images of the rat nasal epithelia (A) and the NALT (B) following administration of a solution of FITC-albumin in PBS.

4 Conclusions

In this study N-trimethyl chitosan nanoparticles were prepared under mild conditions using TPP as crosslinker and investigated as a vehicle for nasal delivery of proteins. When properly prepared, stable TMC particles with a small size and a narrow size distribution were obtained. The TMC nanoparticles have an excellent loading capacity for proteins, and a positive surface charge, suitable to attach to nasal mucosa. The TMC nanoparticles showed no cytotoxicity on Calu-3 cells, whereas a cilio-inhibiting effect on the CFB of chicken trachea was seen *in vitro*. *In vivo* experiments showed that TMC nanoparticles loaded with FITC-albumin, when administered in the nasal cavity, were able to cross the mucosal layer, taken up by rat nasal epithelia and NALT cells, and transported to sub-mucosal layers. These interesting features make this novel system a promising vehicle for nasal delivery of proteins. Further studies such as *in vitro* and *in vivo* toxicity tests and *in vivo* studies with an antigen should be performed to evaluate the applicability of these nanoparticles as a nasal vaccine delivery system.

Acknowledgments

We thank Dr. H.K. Koerten (Faculty of Medicine , Leiden University) for his support with SEM, H. De Bout (Division of Toxicology, Leiden/Amsterdam Center for Drug Research (LACDR), Leiden University) for his technical help in CLSM. We are grateful to Dr. X. Jiang and Dr. R. Schiffelers (Department of Pharmaceutics, Utrecht Institute for Pharmaceutical Sciences (UIPS), Utrecht University) for the GPC measurements of chitosan and help in statistics, respectively.

References

1. R. J. Soane, M. Ferier, A. C. Perkins, N. S. Jones, S. S. Davis, and L. Illum. Evaluation of the clearance characteristics of bioadhesive system in humans. *Int J Pharm* 178: 55-65 (1999).

2. R. J. Soane, M. Hinchcliffe, S. S. Davis, and L. Illum. Clearance characteristics of chitosan based formulation in the sheep nasal cavity. *Int J Pharm* 217: 183-191 (2001).

3. L. Illum, N. F. Farraj, and S. S. Davis. Chitosan as a novel nasal delivery system for peptide drugs. *Pharm Res* 11: 1186-1189 (1994).

4. S. S. Davis. Nasal Vaccines. *Drug Deliv Rev* 51: 21-42. (2001).

5. L. Illum, I. Jabbal-Gill, M. Hinchcliffe, A. N. Fisher, and S. S. Davis. Chitosan as a novel nasal delivery system for vaccines. *Adv Drug Deliv Rev* 51: 81-96 (2001).

6. A. J. Almeidaand H. O. Alpar. Nasal delivery of vaccines. *J Drug Target* 3: 455-467 (1996).

7. L. Illum. Nasal drug delivery- possibilities, problems and solutions. *J Control Release* 87: 187-98 (2003).

8. M. P. Desai, V. Labhasetwar, G. L. Amidon, and R. J. Levy. Gastrointestinal uptake of biodegradable microparticles: effect of particle size. *Pharm Res* 13: 1838-45 (1996).

9. F. Delie. Evaluation of nano- and microparticle uptake by the gastrointestinal tract. *Adv Drug Deliv Rev* 34: 221-233 (1998).

10. Y. Huangand M. D. Donovan. Large molecule and particulate uptake in the nasal cavity: the effect of size on nasal absorption. *Adv Drug Deliv Rev* 29: 147-155 (1998).

11. J. Brooking, S. S. Davis, and L. Illum. Transport of nanoparticles across the rat nasal mucosa. *J Drug Target* 9: 267-279 (2001).

12. L. Illum. Chitosan and its use as a pharmaceutical excipient. *Pharm. Res.* 15: 1326-1331 (1998).

13. O. Felt, P. Buri, and R. Gurny. Chitosan: a unique polysaccharide for drug delivery. *Drug Dev Ind. Pharm* 24: 979-993 (1998).

14. H. E. Jungingerand J. C. Verhoef. Macromolecules as safe penetration enhancers for hydrophilic drugs-a fiction? *Pharm. Sci. Tech. Today* 1: 370-376 (1998).

15. G. Borchard, H. L. Lueßen, A. G. de Boer, J. C. Verhoef, C. M. Lehr, and H. E. Junginger. The potential of mucoadhesive polymers in enhancing intestinal peptide drug absorption III: Effects of chitosan glutamate and carbomer on epithelial tight junctions in vitro,. *J Contro. Release* 39: 131-138 (1996).

16. K. Y. Lee, W. S. Ha, and W. H. Park. Blood compatibility and biodegradability of partially N-acylated chitosan derivatives. *Biomaterials* 16: 1211-1216 (1995).

17. R. A. A. Muzzarelli. Human enzymatic activities related to the therapeutic administration of chitin derivative. *Cell Mol Life Sc* 53: 131-140 (1997).

18. H. Onishiand Y. Machida. Biodegradation and distribution of water-soluble chitosan in mice. *Biomaterials* 20: 175-182 (1999).

19. T. Chandyand C. P. Sharma. Chitosan as a biomaterial. *Artif. Cells Artif. Organs* 18: 1-24 (1990).

20. T. J. Aspeden, J. D. Mason, N. S. Jones, J. Lowe, O. Skaugrud, and L. Illum. Chitosan solutions on in vitro and in vivo mucociliary transport rates in human turbinates and volunteers. *J. Pharm. Sci.* 86: 509-513 (1997).

21. C. Sankar, M. Rani, A. K. Srivastava, and B. Mishra. Chitosan based pentazocine microspheres for intranasal systemic delivery: development and biopharmaceutical evaluation. *Pharmazie* 56: 223-226 (2001).

22. I. M. van der Lubben, F. A. Konings, G. Borchard, J. C. Verhoef, and H. E. Junginger. In vivo uptake of chitosan microparticles by murine Peyer's patches: visualization studies using confocal laser scanning microscopy and immunohistochemistry. *J Drug Target* 9: 39-47 (2001).

23. I. M. van der Lubben, G. Kersten, M. M. Fretz, C. Beuvery, J. C. Verhoef, and H. E. Junginger. Chitosan microparticles for mucosal vaccination against diphtheria: oral and nasal efficacy studies in mice. *Vaccine* 28: 1400-1408 (2003).

24. M. Bivas-Benita, M. Laloup, S. Versteyhe, J. Dewit, J. De Braekeleer, E. Jongert, and G. Borchard. Generation of Toxoplasma gondii GRA1 protein and DNA vaccine loaded chitosan particles: preparation, characterization, and preliminary in vivo studies. *Int J Pharm* 266: 17-27 (2003).

25. B. C. Baudner, M. M. Giuliani, J. C. Verhoef, R. Rappuoli, and H. E. Junginger. The concomitant use of the LTK63 mucosal adjuvant and of chitosan-based delivery system enhances the immunogenicity and efficacy of intranasally administered vaccines. *Vaccine* 8: 3837-3844. (2003).

26. R. Fernandez-Urrusuno, P. Calvo, C. Remunan-Lopez, J. L. Vila-Jato, and J. A. Alonso. Enhancement of nasal absorption of Insulin using chitosan nanopartocles. *Pharm. Res* 16: 1576-1581 (1999).

27. Y. Pan, Y. J. Li, H. Y. Zhao, J. M. Zheng, H. Xu, G. Wei, J. S. Hao, and F. D. Cui. Bioadhesive polysaccharide in protein delivery system: chitosan nanoparticles improve the intestinal absorption of insulin in vivo. *Int J Pharm* 249: 139-147 (2002).

28. P. Calvo, C. Remunan-Lopez, J. L. Vila-Jato, and M. J. Alonso. Novel Hydrophilic chitosan polyethylene oxide nanoparticles as protein carriers. *J Appl Polym Sci* 63: 125-132 (1997).

29. P. Calvo, C. Remunan-Lopez, J. L. Vila-Jato, and M. J. Alonso. Chitosan and chitosan/ethylene oxide-propylene oxide block copolymer nanoparticles as novel carriers for proteins and vaccines. *Pharm Res* 14: 1431-1436 (1997).

30. A. Vila, A. Sanchez, K. Janes, I. Behrens, T. Kissel, J. L. Vila Jato, and M. J. Alonso. Low molecular weight chitosan nanoparticles as new carriers for nasal vaccine delivery in mice. *Eur. J Pharm Biopharm* 57: 123-131 (2004).

31. A. F. Kotzé, H. L. Lueßen, B. J. de Leeuw, A. G. de Boer, J. C. Verhoef, and H. E. Junginger. Chitosan for enhanced intestinal permeability: prospects for derivatives soluble in neutral and basic environments. *Eur J Pharm Sci* 7: 145-151 (1999).

32. A. F. Kotzé, H. L. Lueßen, B. J. de Leeuw, A. G. de Boer, J. C. Verhoef, and H. E. Junginger. N-trimethyl chitosan chloride as a potential absorption enhancer across mucosal surfaces: in vitro evaluation in intestinal epithelial cells (Caco-2). *Pharm Res* 14: 1197-202 (1997).

33. A. F. Kotzé, H. L. Lueßen, B. J. de Leeuw, A. G. de Boer, J. C. Verhoef, and H. E. Junginger. Enhancement of paracellular drug transport with highly quaternised N-trimethyl chitosan chloride in neutral environments: in vitro evaluation in intestinal epithelial cells (Caco-2). *J Pharm Sci* 88: 253-257 (1999).

34. M. Thanou, J. C. Verhoef, J. H. M. Verheijden, and H. E. Junginger. Intestinal absorption of octeriotide: N-trimethyl chitosan chloride (TMC) ameliorates the permeability and absorption properties of the somatostatin analogue in vitro and in vivo. *J Pharm Sci* 89: 951-957 (2000).

35. J. H. Hamman, M. Stander, and A. F. Kotzé. Effect of the degree of quaternization of N-trimethyl chitosan chloride on absorption enhancement: in vivo evaluation in rat nasal epithelia. *Int J Pharm* 232: 235-242 (2002).

36. B. C. Baudner, M. Morandi, M. M. Giuliani, J. C. Verhoef, H. E. Junginger, P. Costantino, R. Rappuoli, and G. Del Giudice. Modulation of immune response to group C meningococcal conjugate vaccine given intranasally to mice together with trimethyl chitosan delivery system. *J Infect Dis* 189: 828-832 (2004).

37. I. M. van der Lubben, J. C. Verhoef, M. M. Fretz, F. A. C. van Opdorp, I. Mesu, G. Kersten, and H. E. Junginger. Trimethyl chitosan chloride (TMC) as novel excipient for oral and nasal immunization against diphtheria. *STP Pharm Sci* 12: 235-242 (2002).

38. M. M. Thanou, J. C. Verhoef, S. G. Romeijn, J. F. Nagelkerke, F. W. Merkus, and H. E. Junginger. Effects of N-trimethyl chitosan chloride, a novel absorption enhancer, on caco-2 intestinal epithelia and the ciliary beat frequency of chicken embryo trachea. *Int J Pharm* 185: 73-82 (1999).

39. N. Haffejee, J. Du Plessis, D. G. Muller, C. Schultz, A. F. Kotze, and C. Goosen. Intranasal toxicity of selected absorption enhancers. *Pharmazie* 56: 882-8 (2001).

40. T. Kean, S. Roth, and M. Thanou. Trimethylated chitosans as non-viral gene delivery vectors: cytotoxicity and transfection efficiency. *J Control Release* 103: 643-53 (2005).

41. S. Mao, X. Shuai, F. Unger, M. Wittmar, X. Xie, and T. Kissel. Synthesis, characterization and cytotoxicity of poly(ethylene glycol)-graft-trimethyl chitosan block copolymers. *Biomaterials* 26: 6343-56 (2005).

42. A. B. Sieval, M. Thanou, A. F. Kotzé, J. C. Verhoef, J. Brussee, and H. E. Junginger. Preparation and NMR- characterisation of highly substituted N-trimethyl chitosan chloride. *Carbohydr Polym* 36: 157-165 (1998).

43. H. J. M. van de Donk, I. P. Muller-Plantema, J. Zuidema, and F. W. H. M. Merkus. The effects of perservatives on the ciliary beat frequency of chicken embryo tracheas. *Rhinology* 18: 119-130 (1980).

44. S. G. Romeijn, J. C. Verhoef, E. Marttin, and F. W. H. M. Merkus. The effect of nasal drug formulations on ciliary beating in vitro. *Int J Pharm* 135: 137-145. (1996).

45. P. Merkus, S. G. Romeijn, J. C. Verhoef, F. W. H. M. Merkus, and P. F. Schouwenburg. Classification of cilio-inhibiting effects of nasal drugs. *Laryngoscope* 111: 595-602 (2001).

46. T. J. Moosman. Rapid colorimetric assay for cellular growth and survival: application to proliferation and cytotoxicity assays. *J Immunol Meth* 65: 55-65 (1983).

47. T. L. Rissand R. A. Moravec. Comparison of MTT, XTT, and a novel tetra-zolium compound for MTS for in vitro proliferation and chemosensitivity assays. *Mol Biol Cell (Suppl)* 3: 207 (1992).

48. K. A. Foster, M. L. Avery, M. Yazdanian, and K. L. Audus. Characterization of the Calu-3 cell line as a tool to screen pulmonary delivery. *Int J Pham* 208: 1-11 (2000).

49. N. R. Mathias, J. Timoszyk, P. I. Stetsko, J. R. Megill, R. L. Smith, and D. A. Wall. Permeability characteristics of Calu-3 human bronchial epithelial cells: in vitro-in vivo correlation to predict lung absorption in rats. *J Drug Target* 10: 31-40 (2002).

50. E. Marttin, J. C. Verhoef, C. Cullander, S. G. Romeijn, J. F. Nagelkerke, and F. W. H. M. Merkus. Confocal laser scanning Microscopic visualisation of the transport of dextran after nasal administration to rat effects of Absorption Enhancers. *Pharm Res* 14: 631-637 (1997).

51. M. van der Weert, W. E. Hennink, and W. Jiskoot. Protein instability poly (lactic-co-glycolic acid) microparticles. *Pharm Res* 17: 1159-1167 (2000).

52. Y. Xu, Y. Du, R. Huang, and L. Gao. Preparation and modification of N-(2-hydroxyl) propyl-3-trimethyl ammonium chitosan chloride nanoparticle as a protein carrier. *Biomaterials* 24: 5015-22 (2003).

53. B. M. Wilbert, K. Nesil, K. Graamans, and E. H. Huizing. Physiologic and hypertonic saline solutions impair ciliary activity in vitro. *Laryngoscope* 109: 396-399 (1999).

54. J. Fiegel, C. Ehrhardt, U. F. Schaefer, C. M. Lehr, and J. Hanes. Large porous particle impingement on lung epithelial cell monolayers—toward improved particle characterization in the lung. *Pharm Res* 20: 788-96 (2003).

55. C. Witschiand R. J. Mrsny. In vitro evaluation of microparticles and polymer gels for use as nasal platforms for protein delivery. *Pharm Res* 16: 382-90 (1999).

56. B. I. Florea, C. Meaney, H. E. Junginger, and G. Borchard. Transfection efficiency and toxicity of polyethylenimine in differentiated Calu-3 and non differentiated COS-1 cell cultures. *AAPS Pharm Sci* 4: E12 (2002).

57. A. F. Kotzé, M. M. Thanou, H. L. Lueßen, B. J. de Leeuw, A. G. de Boer, J. C. Verhoef, and H. E. Junginger. Effect of the degree quaternisation of N-trimethyl chitosan chloride on the permeability of intestinal epithelial cells (Caco-2). *Eur J Pharm Biopharm* 47: 269-274 (1999).

58. J. H. Hamman, C. M. Schultz, and A. F. Kotzé. N-trimethyl chitosan chloride: optimum degree of quaternization for drug absorption enhancement across epithelial cells. *Drug Dev Ind Pharm* 29: 161-172. (2003).

59. C. Jonker, J. H. Hamman, and A. F. Kotzé. Intestinal paracellular permeation enhancement with quaternized chitosan: in situ and in vitro evaluation. *Int J Pharm* 238: 205-213 (2002).

60. T. Gershanik, S. Benzeno, and S. Benita. Interaction of a self-emulsifying lipid drug delivery system with the everted rat intestinal mucosa as a function of droplet size and surface charge. *Pharm Res* 15: 863-869 (1998).

Chapter three

N-trimethyl chitosan (TMC) nanoparticles loaded with influenza subunit antigen for intranasal vaccination: Biological properties and immunogenicity in a mouse model

Maryam Amidi[1]
Stefan G. Romeijn[1]
J. Coos Verhoef[1]
Hans E. Junginger[1]
Laura Bungener[3]
Anke Huckriede[3]
Daan J.A. Crommelin[2]
Wim Jiskoot[1,2]

[1] Department of Pharmaceutics, Utrecht Institute for Pharmaceutical Sciences, Utrecht University, PO Box 80082, 3508 TB Utrecht, The Netherlands

[2] Division of Drug Delivery Technology, Leiden/Amsterdam Center for Drug Research (LACDR), Leiden University, P.O. Box 9502, 2300 RA Leiden, The Netherlands

[3] Department of Microbiology, Molecular Virology Section, University Medical Center Groningen, University of Groningen, Groningen, The Netherlands

Vaccine 25: 144-153 (2007)

Abstract

In this study, the potential of N-trimethyl chitosan (TMC) nanoparticles as a carrier system for the nasal delivery of a monovalent influenza subunit vaccine was investigated. The antigen-loaded nanoparticles were prepared by mixing a solution containing TMC and monovalent influenza A subunit H3N2 with a tripolyphosphate (TPP) solution, at ambient temperature and pH 7.4 while stirring. The nanoparticles had an average size of about 800 nm with a narrow size distribution and a positive surface charge. The nanoparticles showed a loading efficiency of 78% and a loading capacity of 13% (w/w). It was shown that more than 75% of the protein remained associated with the TMC nanoparticles upon incubation of the particles in PBS for 3 hours. The molecular weight and antigenicity of the entrapped hemagglutinin was maintained as shown by polyacrylamide gel electrophoresis and Western blotting, respectively. Single i.n. or i.m. immunization with antigen-loaded TMC nanoparticles resulted in strong hemagglutination inhibition and total IgG responses. These responses were significantly higher than those achieved after i.m. administration of the subunit antigen, whereas the IgG1/IgG2a profile did not change substantially. The i.n. administered antigen-TMC nanoparticles induced higher immune responses compared to the other i.n. antigen formulations, and these responses were enhanced by i.n. booster vaccinations. Moreover, among the tested formulations only i.n. administered antigen-containing TMC nanoparticles induced significant IgA levels in nasal washes of all mice. In conclusion, these findings demonstrate that TMC nanoparticles are a potent new delivery system for i.n. administered influenza antigens.

Keywords: N-trimethyl chitosan (TMC) nanoparticles; nasal vaccine delivery; influenza subunit vaccine

1 Introduction

Influenza virus infections cause considerable mortality and morbidity world wide each year, particularly in elderly people and children. Prophylactic vaccination is the most effective means to prevent the infection. Both humoral and cellular immune responses are essential for protection against influenza infection (1-4). Virus-specific secretory IgA (S-IgA) antibodies in the respiratory tract are of particular importance for the prevention and control of infection at the mucosal sites (5). Numerous studies in humans and mice have shown that S-IgA-based mucosal immunity obtained from natural infection is more effective in cross protection against virus infection than systemic immunity induced by parenterally administered vaccine (6-12). Current commercially available parenteral influenza vaccines include formulations of inactivated virus (whole virus vaccines), split virus, and purified viral surface proteins (subunit vaccines). Hemagglutinin (HA) and neuraminidase (NA) are the most important antigens for the induction of virus-neutralizing antibodies and subunit vaccines are as potent and efficacious as whole virus and split virus but elicit fewer side effects (13). However, these vaccines have in common that, although they do induce neutralizing serum IgG antibodies, they are poor stimulators of local immune responses and S-IgA production at respiratory mucosa (14, 15). Moreover, obvious disadvantages of parenteral vaccination are low immunization coverage, infection risk and need for trained personnel to administer the vaccine. Thus, non-parenteral influenza vaccines capable of inducing strong serum IgG as well as mucosal S-IgA responses are highly desirable.

The nasal mucosa is an attractive site for the delivery of vaccines and has certain advantages over other mucosal sites. It is highly vascularized and has a relatively large absorptive surface and low proteolytic activity. Importantly, nasal immunization was reported to be more efficient than oral immunization at inducing secretory in addition to systemic antibody responses (16). The local and systemic immune responses are initiated by targeting the nasal associated lymphoid tissue (NALT) at the base of the nasal cavity (Waldeyer's ring in humans). The nasal epithelium covering the NALT contains nonciliated microfold cells (M-cells), which are mainly responsible for antigen uptake and delivery to the sub mucosal lymphoid tissues (16-20). However, in spite of these attractive features, most vaccines are not well absorbed from the nasal cavity when administered as simple solutions. Major factors limiting the absorption of nasally administered vaccines are their poor ability to cross nasal barriers and the mucociliary clearance mechanism, which removes soluble antigens from the nasal cavity (21-23).

Mucoadhesive particulate carrier systems such as starch, hyaluronic acid and chitosan offer a significant potential for the development of mucosally administered antigens (18, 24). Such carriers can be designed to prolong the residence time in the nasal cavity (21-23), to protect entrapped antigens against degradation, to enhance uptake by M-cells, and to target the antigens more specifically to antigen presenting cells (APC) (25-31). Particulate carriers based on chitosan, a copolymer of glucosamine

and N-acetylglucosamine, have received particular interest for the delivery of macromolecules via mucosal routes (18, 25-27). Besides its favorable biological properties (18, 32-35), chitosan is biodegradable and has a very low toxicity (36-38). A major drawback of chitosan is, however, its poor solubility at physiological pH, whereas it is soluble and active as an absorption enhancer only in its protonated form in acidic environments (39, 40). In contrast, N-trimethyl chitosan chloride (TMC), a partially quaternized chitosan derivative, shows good water solubility over a wide pH range. Hence, soluble TMC has mucoadhesive properties and excellent absorption enhancing effects even at neutral pH (41, 42). Because of these properties, TMC is an attractive alternative to chitosan for the design of protein-loaded particles by ionic crosslinking. At present only a few studies have reported the use of TMC solutions and TMC *micro*particles in nasal vaccine delivery (43, 44). Several studies have shown *nano*particles to offer many advantages over microparticles or other nasal dosage forms (21, 22, 45, 46). It has been shown that particles below 1 μm (nanoparticles) are taken up by nasal epithelia and NALT more efficiently than larger ones (45-48).
In a previous study, we showed that TMC nanoparticles have interesting features suitable for nasal antigen delivery, such as high protein loading capacity, low cytotoxicity, and *in vivo* uptake by the nasal epithelium and NALT (49). In the present study, we investigated the potential of TMC nanoparticles loaded with influenza antigen to elicit local and systemic immune responses after intranasal administration in mice. It is shown that the antigen-loaded nanoparticles, when administered intranasally, are capable of eliciting strong systemic as well as local antibody responses.

2 Materials and methods

2.1 Materials

Chitosan (M_n = 40 kDa, M_w = 177 kDa, determined by gel permeation chromatography (GPC) using poly(ethylene glycol) (PEG) standards; degree of deacetylation 93%) used for synthesizing the TMC was a generous gift from Primex (Avaldsnes, Norway). TMC with a degree of quaternization (DQ) of 25% was synthesized by methylation of chitosan by using CH_3I in the presence of a strong base (NaOH) and analyzed by ^{1}H-nuclear magnetic resonance (NMR) spectroscopy as previously described (50). Monovalent A/Panama (H3N2) influenza subunit vaccine and A/Panama influenza virus were kindly donated by Solvay Pharmaceuticals (Weesp, the Netherlands). Sodium tripolyphosphate (TPP), Tween 80, and mouse monoclonal anti-hemagglutinin IgG and goat anti-mouse IgA were obtained from Sigma (Sigma, Bornem, Belgium). Cy-5 conjugated goat IgG anti-mouse immunoglobulin was supplied from Jackson ImmunoResearch Europe Ltd. (Cambridgeshire, UK). Horseradish peroxidase-conjugated immunoglobulin class and subtype-specific antibodies were from Southern Biotechnology Asc. (Birmingham, Al). All other materials used were of analytical or pharmaceutical grade.

2.2 Preparation and characterization of influenza antigen-loaded TMC nanoparticles

TMC nanoparticles were prepared at ambient temperature in the presence of Tween 80 to prevent particle aggregation during purification. Briefly, TMC (6 mg) was dissolved in 3 ml of phosphate buffer (2.5 mM Na_2HPO_4, 4.5 mM KH_2PO_4, 0.8 mM KCl, 34 mM NaCl; pH 7.4.) containing monovalent A/Panama (H3N2) influenza antigens (380 µg) and 0.5% (w/w) Tween 80. Thereafter, 1.5 ml of an aqueous TPP solution (1 mg/ml) was added dropwise to the TMC-antigen solution while stirring. Aliquots of 1 ml of the resulting antigen-loaded TMC nanoparticle suspensions were centrifuged for 15 minutes at 10000 g and 4 °C on a 10-µl glycerol bed. The supernatants were then discarded and the pellets were resuspended in 100 µl of phosphate buffered saline (PBS: 10 mM Na_2HPO_4, 18 mM KH_2PO_4, 3 mM KCl, 138 mM NaCl; pH 7.4). For the i.n. immunizations, 10 µl of suspension containing one dose of influenza antigen-loaded TMC nanoparticles in PBS (pH 7.4) was administered in mice. The size and zeta-potential of the nanoparticles were measured with a Zeta-sizer 3000 (Malvern Instruments Ltd., Malvern, UK) in 5 mM HEPES (pH 7.4). The particle size distribution of the nanoparticles is reported as a polydispersity index, ranging from 0 for an entirely monodisperse suspension to 1 for a completely heterodisperse system. The amount of protein entrapped in the nanoparticles was determined as described before (49). Loading efficiency (LE) and loading capacity (LC) for hemagglutinin were calculated as follows.

$$LE = \frac{\text{Total amount of hemaglutinin} - \text{Free hemaglutinin}}{\text{Total amount of hemaglutinin}} \times 100\% \quad (1)$$

$$LC = \frac{\text{Total amount of hemaglutinin} - \text{Free hemaglutinin}}{\text{Nanoparticles dry weight}} \times 100\% \text{ (w/w)} \quad (2)$$

2.3 Short-term in vitro release of influenza antigens from TMC nanoparticles

After centrifugation of the suspensions, the nanoparticles were resuspended in 1 ml PBS in microfuge tubes. The tubes were incubated at 37 °C, under agitation (50 rpm), for 3 hours. At time 0 and at different time intervals, a tube was taken and centrifuged (at 18000 g for 10 min). The released protein was determined in the supernatant by micro BCA protein assay. To eliminate background interference, a blank sample consisting of only nanoparticles resuspended in PBS was used. The experiments were performed in triplicate.

2.4 SDS-polyacrylamide gel electrophoresis and Western blotting

Antigen-loaded TMC nanoparticles were destabilized by adding 1 ml of 10% (w/v) NaCl to 4.5 ml of the nanoparticle suspension. SDS-PAGE was performed under reducing conditions following a standard procedure (51). After electrophoresis, the protein bands were visualized by staining with Silver Stain Plus (Bio-Rad laboratories B.V., Veenendaal, The Netherlands). For Western blotting, antigen bands were transferred to a nitrocellulose membrane by using a semi-dry Western blotting system operating at a constant current of 100 mA for 1 h in blotting buffer (25 mM Tris, 1.4% glycine, 20% (v/v) methanol, pH 8.3). After blotting the free sites were blocked with 1% non-fat milk-powder in PBS containing 0.05% Tween 20 (PBS-T). Next, the membrane was incubated with a solution of mouse anti-hemagglutinin monoclonal antibody in PBS-T containing 0.1% non-fat milk powder. The membrane was then washed to remove the unbound antibody and incubated with Cy-5-labeled, goat IgG anti-mouse immunoglobulin. The blotted antigen-antibody complexes were visualized by a fluorescence using a Typhoon imager (Amersham Corporation, Arlington Heigths, IL, USA).

2.5 Immunization studies

Female C57BL/6 (B6) mice, 6-8 weeks old (Charles River, Netherlands), were housed in groups of 4 mice and maintained in the animal facility of Leiden University with a 12 h day and night schedule, while food and water were ad libitum. The experiments were approved by the Ethical Committee for Animal Experimentation of Leiden University. Single i.m. vaccinations and a three successive intranasal (i.n.) immunization with three-week intervals were performed in mice (8 per group). Before each immunization, the mice were lightly anesthetized with an inhaled gaseous mixture of 3% (v/v) isoflorane in oxygen (300 cm^3min^{-1}) and nitrous oxide (100 cm^3min^{-1}), and then immunized i.n. or i.m. with different formulations (table 1). For each i.n. administered formulation, three groups of mice were used, except for PBS or empty nanoparticles. One group received only a single i.n. immunization. The second and the third groups received two and three i.n. immunizations respectively. The i.n. administered formulations were given by instillation in a total volume of 10 µl (5 µl into each nostril) with a micropipette tip, which is an appropriate volume to prevent variable bioavailability due to the deposition of the formulation in the lung and lower respiratory tract (52).
For i.m. immunizations, lightly anesthetized mice received 50 µl of the conventional subunit antigen solution or antigen-loaded TMC nanoparticle suspension by injection into their left or right hind leg (table 1).

Table 1. Immunization study design[1]

Formulation	Antigen H3N2 dose (µg)	Volume (µl)	Immunization schedule (day)	Route of administration	Serum sampling (day)	Nasal washes (day)
1. Antigen -TMC nanoparticles	15	10	1, 22, 43	i.n.	1, 22, 43, 64	64
2. TMC + antigen solution	15	10	1, 22, 43	i.n.	1, 22, 43, 64	64
3. Antigen solution	15	10	1, 22, 43	i.n.	1, 22, 43, 64	64
4. Antigen solution	15	50	1	i.m.	1, 22	22
5. Antigen -TMC nanoparticles	15	50	1	i.m.	1, 22	22
6. Empty TMC nanoparticles	-	10	1	i.n.	1, 22	22
7. PBS	-	10	1	i.n.	1, 22	22

[1] Groups of 8 mice were immunized with the formulations indicated in the table. All formulations were prepared and/or re-suspended in PBS.

Three weeks after the last immunization, mice were anesthetized by subcutaneous injection of a mixture of ketamine (200 mg/kg) and xylazine (10 mg/kg) and bled from a leg vein. Then they were sacrificed through cervical dislocation. Individual serum samples were separated from blood cells and coagulated proteins by centrifugation for 5 min at 14000 g and 4 ºC, and stored at -20 ºC. Only in the groups of mice which were immunized i.m. or three times i.n., after blood sampling, the trachea of each mouse was opened and cannulated with a 0.5 × 1 mm PVC tube toward the nasopharyngeal duct. Then a volume of 500 µl of PBS containing 0.1% (w/v) BSA was flushed through the nasal cavity and collected from the nostrils. The nasal lavages were stored at -20 ºC till the day of analysis.

2.6 Hemagglutination inhibition assay

For determination of hemagglutination inhibition (HI) titers in serum, 100 µl of mouse sera were incubated with 500 µl cholera filtrate over night at 37 ºC to remove nonspecific anti-hemagglutination activity. Then the mixtures were heated at 56 ºC for 30 minutes to inactivate the residual cholera activity. Next, 45 µl of the pre-treated sera were transferred in duplicate to a 96-well round-bottom plate (Greiner, Alphen

a/d Rijn, Netherlands) containing 105 µl PBS/well, resulting in an initial dilution of 1:20. Subsequently, two-fold serial dilutions were made in PBS. Next, 4 hemagglutination units (HAU) of A/Panama influenza virus in a volume of 25 µl were added to each well. As a control for nonspecific hemagglutination activity, 25 µl PBS (instead of influenza virus) were added to each well of one of the dilution series. The content of each well was gently mixed and incubated for 30 min at 37 ºC. Finally, 25 µl of 1% (v/v) turkey red blood cells were added to the wells and hemagglutination was allowed to proceed for 1 h at 4 °C. The HI titer was expressed as the reciprocal value of the highest serum dilution capable of inhibiting the agglutination of the turkey erythrocytes by the influenza virus. Comparison between different experimental groups was made by a one-way ANOVA test.

2.7 Antibody assays (ELISA)

Influenza subunit antigen-specific antibody responses were determined by using an enzyme-linked immunoabsorbent assay (ELISA) as previously described (53, 54). Briefly, ELISA plates (Greiner, Alphen a/d Rijn, Netherlands) were coated overnight at 37 °C with 200 ng of influenza subunit antigen (H3N2) per well in coating buffer (0.05 M carbonate/bicarbonate, pH 9.6). Plates were washed and blocked by incubation with 2.5% (w/v) milk powder in coating buffer for 45 min at 37°C. Subsequently, the plates were washed with PBS/Tween (PBS containing 0.05% Tween, pH 7.6). Appropriate dilutions of sera and non-diluted nasal lavages of each individual mouse were applied to the plates, serially diluted two-fold in PBS/Tween and incubated for 1.5 h at 37 °C. Plates were then washed and incubated with horseradish peroxidase-conjugated goat antibodies directed against either mouse IgG, IgG1, IgG2a or IgA (all diluted 1:5000 in PBS/Tween) for 1 h at 37 °C. Thereafter, the plates were washed twice with PBS/Tween and once with PBS. Specific antibodies were detected by staining with *O*-phenyl-diamine dihydro-chloride, as described previously (53). Antibody titers are expressed as the reciprocal of the calculated sample dilution corresponding with an A_{492} of 0.2 above the background. Comparison between different groups was made by a one-way ANOVA test.

3 Results

3.1 Characterization of influenza antigen-loaded TMC nanoparticles

The influenza antigen-loaded TMC nanoparticles had an average diameter of 0.85 +/- 0.03 µm with a polydispersity index of 0.33 +/- 0.12 (n=3). The zeta-potential of the antigen-loaded nanoparticles was +13 +/- 1 mV (n=3). Influenza subunit antigens were efficiently associated with TMC nanoparticles, as they showed a loading efficiency of 78% and a loading capacity of about 13% (w/w).
SDS-PAGE revealed for both free and entrapped antigen bands corresponding to HA_1

(62 kDa) and HA_2 (22 kDa). No additional bands that would indicate the presence of aggregates or fragments were visible (figure 1A). There were no visible bands corresponding to neuraminidase (48 kDa), indicating that the neuraminidase content was negligible. Western blot analysis confirmed that the antigenicity of HA was not altered following its entrapment in nanoparticles (figure 1B).

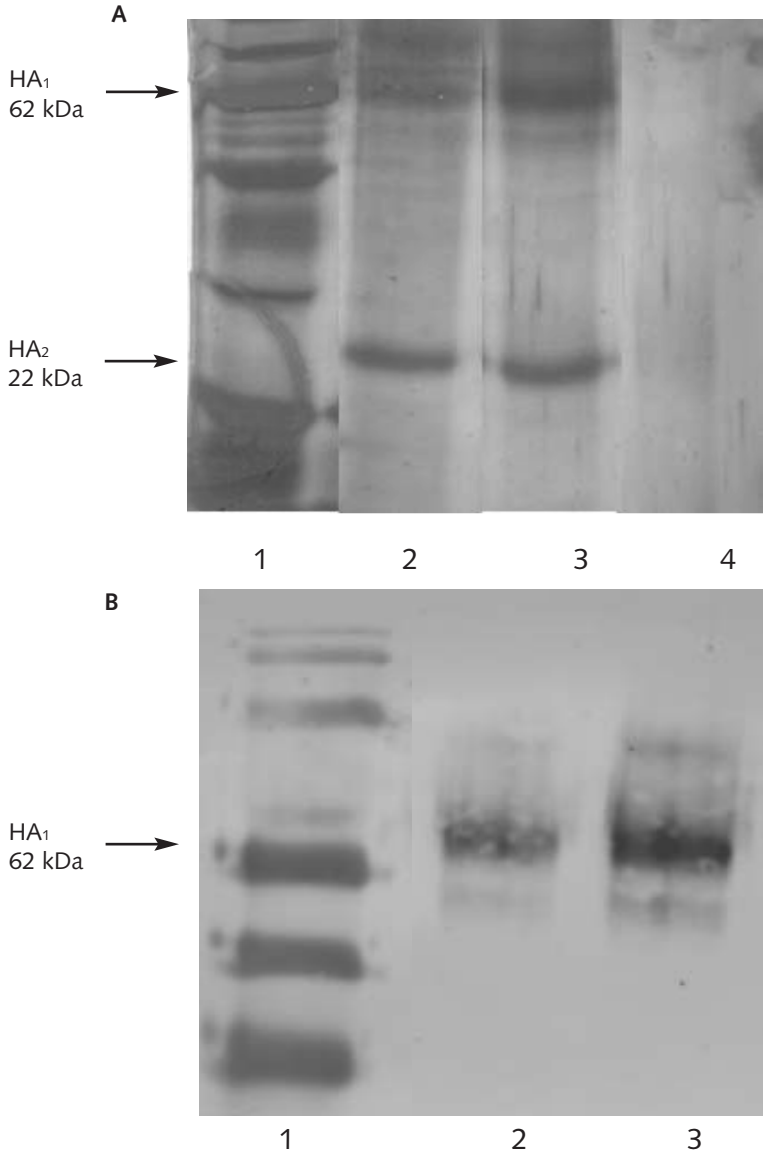

Figure 1. (A) SDS-PAGE under reducing conditions. Lane 1: molecular weight markers, lane 2: free influenza antigen in PBS (700 ng), lane 3: influenza antigen extracted from the nanoparticles (700 ng), lane 4: empty TMC nanoparticles. (B) Western blotting after SDS-PAGE under reducing conditins. Lane 1: protein markers, lane 2: free influenza antigen in PBS (1 µg), lane 3: influenza antigen extracted from the nanoparticles (1 µg).

In vitro release studies showed that about 25% of the loaded protein was immediately released into PBS (pH 7.4; 37 ºC). No further release was observed when the particles were incubated for at least three hours (results not shown).

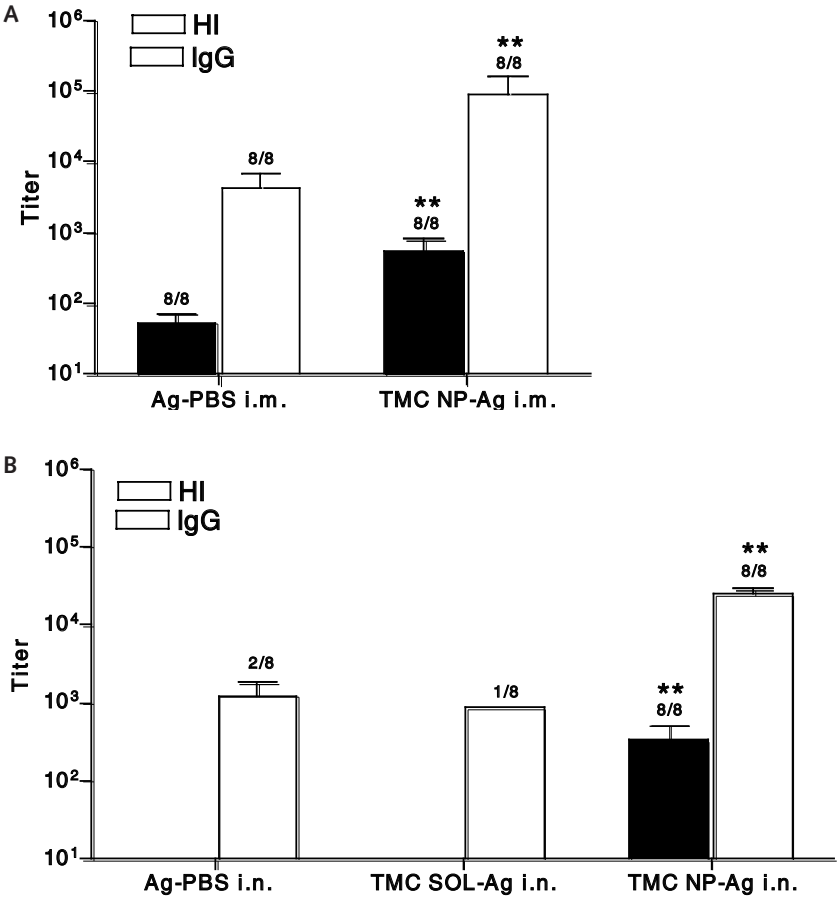

*Figure 2. Serum HI titers and anti-influenza (H3N2) antigen-specific total serum IgG responses in mice immunized once i.m. (panel A) or i.n. (panel B). Formulations: antigen in phosphate buffer saline (Ag-PBS), antigen co-administered with TMC solution (TMC SOL-Ag), antigen incorporated in TMC nanoparticles (TMC NP-Ag). Sera were collected 21 days after the immunization. Antibody titers are expressed as mean of the responding mice; the bars represent the 95% confidence intervals. The numbers above the columns indicate the number of responders per group. Asterisks indicate titers significantly (** $P < 0.001$) higher than those of the group immunized i.m. with Ag-PBS.*

3.2 Systemic antibody responses in i.m. immunized mice

In order to elucidate whether encapsulating the antigen into TMC nanoparticles altered the immunological properties of influenza subunit vaccine, we first evaluated the immune responses of mice to conventional subunit antigen alone or associated with TMC nanoparticles upon i.m. immunization. The antigen-loaded TMC nanoparticles fully retained the immunogenicity of the original subunit vaccine. In fact, significantly higher HI and anti-influenza antigen-specific serum IgG titers were induced after i.m. administration of antigen-TMC nanoparticles ($p< 0.001$) (figure 2A). This result indicates that the procedure of TMC nanoparticle preparation did not negatively affect the immunogenicity of the antigen. Moreover, TMC nanoparticles appear to have immunostimulating properties when administered via the intramuscular route.

3.3 Systemic antibody responses in i.n. immunized mice

To investigate the suitability of the antigen-loaded TMC nanoparticles for i.n. vaccination, we compared the serum responses of mice after a single i.n. vaccination with antigen alone, soluble antigen co-administered with TMC solution or antigen-loaded TMC nanoparticles. After a single i.n. immunization free antigen or a mixture of subunit antigen and TMC solution were poorly immunogenic, showing undetectable HI titers and low serum IgG titers in only some of the vaccinated animals (figure 2B). In contrast, antigen-TMC nanoparticles were able to generate strong HI and IgG antibody titers in all mice (figure 2B). Moreover, the serum antibody responses elicited by i.n. immunization with antigen-TMC nanoparticles were significantly higher than those achieved after conventional i.m. injection of soluble antigen ($p<0.001$) (figure 2). Altogether, these results point to a strong immunostimulating effect of TMC nanoparticles upon i.n. administration.
Since i.n. vaccination usually requires booster immunizations in order to induce strong immune responses (24, 26, 53, 54), the effect of i.n. booster vaccinations on the systemic antibody response was studied. As shown in figure 3, even after two booster immunizations, i.n. administered free antigen induced weak systemic immune responses with only a fraction of the mice showing HI and IgG titers. When subunit antigen was co-administered with TMC solution, the HI and IgG responses increased with slow kinetics: after the third immunization all animals showed significant HI and IgG titers. This underlines that TMC polymer has some adjuvant properties. For mice immunized i.n. with antigen-loaded TMC nanoparticles, the first booster vaccination increased the HI and IgG responses significantly ($p<0.001$). The second booster induced a further raise in total IgG immune response but not in HI titers (figure. 3). Empty TMC nanoparticles did not show any titers after i.n. administration (data not shown).

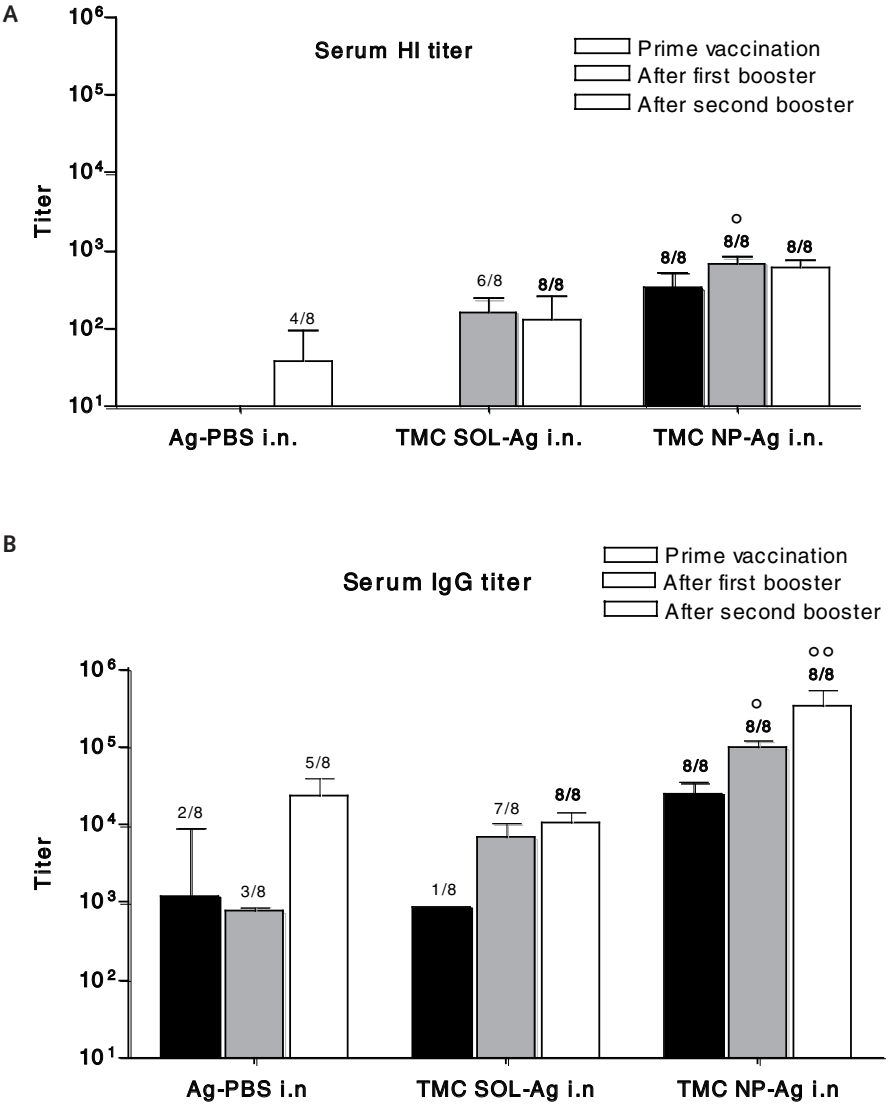

Figure 3. HI titers (panel A) and anti-influenza (H3N2) antigen-specific total serum IgG (panel B) responses in mice immunized i.n. with antigen in phosphate buffer saline (Ag-PBS), antigen co-administered with TMC solution (TMC SOL-Ag) or antigen incorporated in TMC nanoparticles (TMC NP-Ag). Animals were immunized i.n. on day 1, 22 and 43. Sera were collected 21 days after each immunization. Antibody titers are expressed as mean of the responding mice; the bars represent the 95% confidence intervals. The numbers above the columns indicate the number of responders per group. Statistical analyses are shown only between the groups showing 8/8 responders. Circles indicate titers that are significantly (° $P < 0.01$; °° $P < 0.001$) higher than those of the group immunized i.n. once (prime vaccination) with antigen-loaded TMC nanoparticles.

3.4 IgG subtype profiling

To investigate the influence of the subunit antigen-TMC nanoparticles on the quality of the immune response, the IgG subtype (IgG1/IgG2a) profile of the influenza-specific antibodies was determined. I.m. vaccination with soluble antigen resulted in predominant IgG1 responses in all mice, with low IgG2a levels detectable in a few (3/8) mice. As compared to i.m. administered soluble antigen, i.m. administered antigen-loaded TMC nanoparticles increased the IgG1 as well as the IgG2a response (the majority of the mice (6/8) developed IgG2a titers), but did not substantially change the profile, i.e., the IgG1 response remained much stronger than the IgG2a response (figure 4).

A single i.n. vaccination with antigen-TMC nanoparticles induced strong IgG1 titers as compared to those of mice immunized i.m. with conventional subunit vaccine ($p<0.001$). This response was further enhanced by repeated antigen administration ($p<0.001$). The induction of IgG2a antibodies occurred with substantially slower kinetics: one or two i.n. vaccinations with antigen-TMC nanoparticles did not induce detectable titers (1/8 responder), but three successive immunizations resulted in substantial IgG2a responses in all mice, which were comparable or superior to those obtained after i.m. administration of a single dose of soluble antigen or antigen-loaded TMC-particles (figure 4).

Altogether, these results indicate that association of the antigen with TMC nanoparticles changed the quantity but not the quality of the immune response as compared to conventional i.m. vaccination with soluble antigen.

3.5 Local S-IgA responses

Since mucosal immunization has the potential of inducing local immune responses, particularly S-IgA, the IgA levels were measured in the nasal lavages of the mice after one i.m. immunization or three i.n. vaccinations, respectively. Figure 5 shows the specific anti-influenza S-IgA titers in the nasal lavages of the mice immunized i.n. with different formulations. High S-IgA titers were detected in all mice after i.n. immunizations with the antigen loaded-nanoparticles. In contrast, mice immunized i.n. with free antigen or antigen mixed with soluble TMC gave low IgA titers in 1/8 and 2/8 mice, respectively. No detectable S-IgA response was obtained after i.m. immunization with either soluble subunit antigen or associated with TMC nanoparticles (data not shown). In conclusion, i.n. administered antigen-loaded TMC nanoparticles can induce an S-IgA response at the site of virus entry.

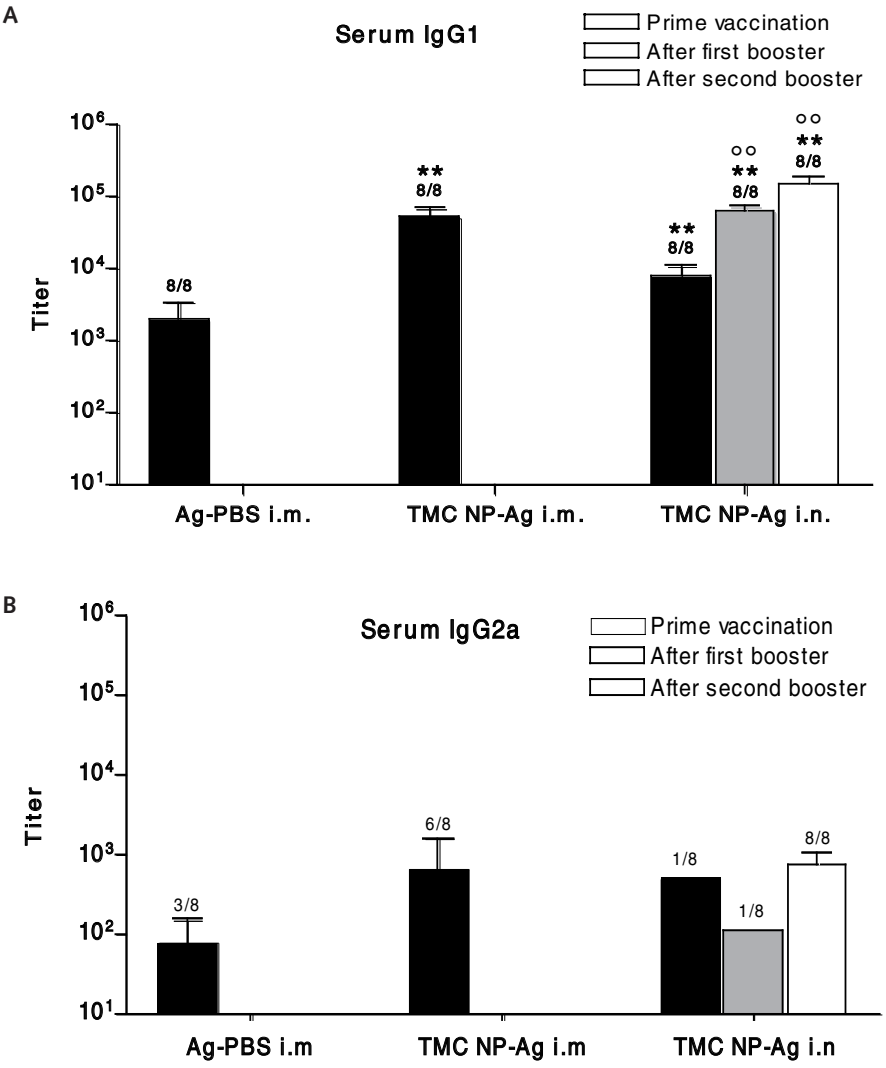

Figure 4. Anti-influenza (H3N2) antigen-specific serum IgG1 (panel A) and IgG2a (panel B) responses in mice immunized i.m. or i.n. with antigen in phosphate buffer saline (Ag-PBS) or incorporated to TMC nanoparticles (TMC NP-Ag). Animals were immunized i.m. on day 1 or i.n. on days 1, 22 and 43 Sera were collected 21 days after each immunization. Antibody titers are expressed as mean of the responding mice; the bars represent the 95% confidence intervals. The numbers above the columns indicate the number of responders per group. Statistical analyses are shown only between the groups showing 8/8 responders. Asterisks indicate titers that are significantly ($P < 0.01$; ** $P < 0.001$) higher than those of the group immunized i.m. with antigen alone. Circles indicate titers that are significantly (° $P < 0.01$; °° $P < 0.001$) higher than those of the group immunized i.n. once (prime vaccination) with antigen-loaded TMC nanoparticles.*

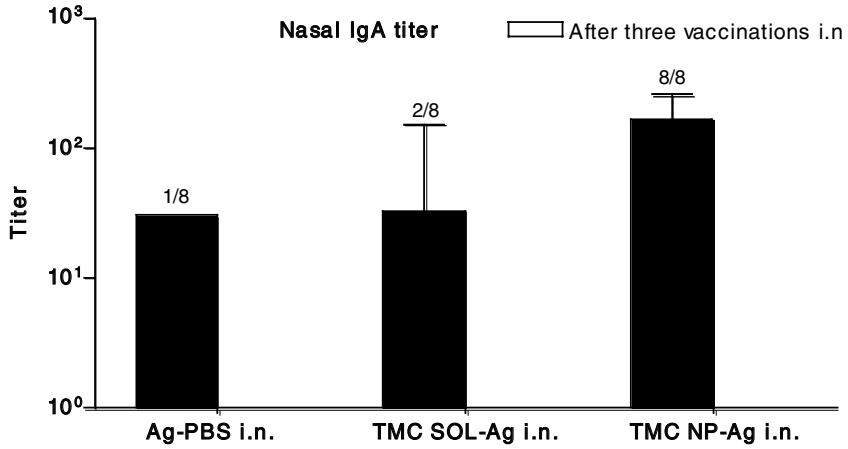

Figure 5. Anti influenza (H3N2) antigen-specific S-IgA titers in nasal lavages of mice immunized i.n. with 15 µg of antigen in phosphate buffer saline (Ag-PBS), co-administered with TMC solution (TMC SOL-Ag) or/and incorporated to TMC nanoparticles (TMC NP-Ag). Animals were immunized i.n. on day 1, 22 and 43. Nasal washes were collected 21 days after the third immunization. Antibody titers are expressed as mean of the responding mice; the bars represent the 95% confidence intervals. The numbers above the columns indicate the number of responders per group

4 Discussion

The results presented here demonstrate that TMC nanoparticles hold great promise as a delivery system for i.n. vaccination. Influenza hemagglutinin was successfully associated with TMC nanoparticles and SDS-PAGE and Western blotting indicated that the structure of the incorporated antigen remained intact. Moreover, the antigens used in our study were shown to remain largely associated with the TMC nanoparticles for at least 3 hours under physiological conditions. This is likely to be pivotal for their success as nasal vaccine, because antigens associated with nanoparticles are taken up by the nasal epithelium and more specifically by the M-cells covering the NALT (16, 46, 55). Therefore, it is important that the antigen is not released to a large extent before the antigen loaded-nanoparticles pass the nasal mucosal barrier during their residence in the nasal cavity. The normal mucociliary clearance time in healthy human's nose is about 20 min (23), whereas mucoadhesive chitosan microspheres were cleared from the human nasal cavity with a half-time (time taken for 50% clearance; $t_{50\%}$) of about 80 min (21, 22).

I.m. immunizations with antigen-loaded TMC nanoparticles resulted in strong systemic immune responses with significantly higher specific influenza antibody levels than obtained with the i.m. administered soluble vaccine (figure 2). This clearly demonstrates that TMC particles have an intrinsic immunostimulating effect, which is in line with previous results (2, 4, 8, 56, 57). The particulate nature of TMC presumably contributes to improve uptake and processing of the encapsulated antigen by APC as well as a more efficient delivery to peripheral lymph nodes (29, 30, 58-61).

Single i.n. vaccination with antigen-loaded TMC nanoparticles resulted in strong IgG and HI immune responses, in contrast to free antigen and polymer solution co-administered with soluble antigen. This indicates that TMC nanoparticles can act as a strong immunostimulator for locally administered vaccines. The high serum IgG titers correlated well with the HI response, which is in line with the notion that IgG is crucial in virus neutralization (62). Moreover, a single i.n. immunization of the antigen-TMC nanoparticles induced significantly higher serum HI and IgG antibody titers than i.m. administered conventional vaccine. This makes the TMC nanoparticles especially attractive as a nasal vaccine delivery system because most i.n. administered influenza vaccines and other vaccines need booster vaccinations to reach high antibody titers comparable to those of i.m. immunization (24, 26, 43, 63). Moreover, although the serum HI and IgG titers were further increased after repeated i.n. immunizations, the prime vaccination was sufficient to strongly stimulate an immune response superior to that of i.m. soluble vaccine.

Factors that most probably contribute to the immunostimulating effect of TMC nanoparticles on i.n. administration include prolonged exposure of the antigen to nasal mucosa, improved uptake by M-cells and APC at the nasal mucosa, more efficient delivery to mucosal lymph nodes, and/or more efficient stimulation of APC after uptake. Although after a single i.n. immunization antigen co-administered with soluble TMC was much less immunogenic than antigen-loaded TMC nanoparticles, after three successive immunizations it gave higher systemic antibody titers than i.m. conventional vaccine. This shows a moderate adjuvant effect of TMC solution. According to previous studies with TMC (DQ: 20%), the polymer is not able to efficiently enhance the paracellular transport of proteins by opening the tight junctions of the epithelial cells (64, 65). Thus, the immune responses after 3 immunizations induced by the antigen co-administered with TMC solution is most probably due to mucoadhesive properties of TMC (66). TMC is positively charged and there are likely electrostatic interactions between TMC and the negatively charged antigen. TMC attaches to mucosa and thereby can prolong the residence of the antigen in nasal cavity. Consequently, more time is available for the antigen to be taken up in nasal tissues. The immune responses elicited by the antigen-loaded TMC nanoparticles were probably based on cellular uptake of the nanoparticles in the nasal epithelium and NALT and subsequent access of the vaccine to sub-mucosal lymphoid tissues. The strong muco-adhesiveness and the particulate nature of TMC nanoparticles are probably important for this immunostimulating effect.

The impact of the TMC nanoparticles on the antibody subtype profile was investigated in vaccinated mice. Protection against influenza virus infection is mainly mediated by neutralizing immunoglobulins that bind to the viral hemagglutinin. In mice IgG1 and IgG2a antibodies are known to contribute to virus neutralization. IgG2a has been reported to play a role in complement activation and antibody-dependent cell-mediated immunity and is more effective than IgG1 in protection against viral infections by preventing virus replication (1-3). On the other hand, it has been shown that IgG1 is very effective in neutralizing virus and thus the absolute

concentration of IgG is important for reducing the viral shedding (2, 62). Therefore, induction of a combined IgG1/IgG2a response may improve vaccine efficacy against viral infections. In this study i.n. or i.m. administered antigen-loaded TMC nanoparticles did not change the subtype profile compared to i.m conventional vaccine, but were able to markedly enhance both the IgG1 and the IgG2a response after the first booster vaccination (see figure 4). The highest IgG2a antibody level was achieved only after a second i.n. booster vaccination (see figure 4B), which infers that IgG2a likely needs a longer time period and/or more administrations to be induced by the subunit vaccine. I.m. administered antigen-loaded TMC nanoparticles also induced a strong IgG1 and a weaker IgG2a response. Altogether, these data suggest that the quality of the immune response to influenza subunit vaccine is not affected by loading of the antigen onto nanoparticles.

A major advantage of i.n. vaccination is the potential induction of S-IgA antibodies at the mucosal epithelium. S-IgA not only has an important role as the first defense line against influenza viruses at the portal of virus entry in the respiratory tract but also has been proven to elicit cross-protective immunity more effectively than serum IgG (12). The S-IgA in the nasal lavages indicates vaccine-induced stimulation of IgA-secreting cells of the NALT and/or the cervical draining lymph nodes. It has been shown that i.n. antigen exposure elicited IgA responses in salivary, respiratory, intestinal and vaginal secretions suggesting trafficking of NALT lymphocytes especially to distant mucosae and to peripheral lymph nodes (20, 67). It is clear from the results that the i.n. administered antigen-loaded TMC nanoparticles were the only formulation that induced S-IgA titers after three immunizations in all mice (figure 5). In contrast, i.m. administered antigen formulations did not show S-IgA response, which is consistent with published observations that i.m. administrations of antigen formulations were not able to induce any S-IgA response, not even after several booster immunizations (24, 54).

In conclusion, i.n. administration of encapsulated influenza antigen in TMC nanoparticles enhanced significantly the systemic and local immune response, compared to i.m. or i.n. administration of soluble (conventional) influenza vaccine. This makes the TMC nanoparticles a promising vehicle for nasal delivery of influenza antigens and, most likely, other antigens.

Acknowledgments

We thank Solvay Pharmaceuticals BV for providing the influenza antigen. Guido van der Net (ViroClinics BV) and Wouter ter Veer (Molecular Virology Section, University Medical Center Groningen) are acknowledged for their technical help and Dr. Raymond Schiffelers (Department of Pharmaceutics, Utrecht Institute for Pharmaceutical Sciences, Utrecht University) for his help in statistics.

References

1. J. P. Coutelier, J. T. van der Logt, F. W. A. Heessen, G. Warnier, and J. van Snick. IgG2a restriction of murine antibodies elicited by viral infections. *J Exp Med* 165: 64-69 (1987).

2. M. J. Hocart, J. S. Mackenzie, and G. A. Stewart. The immunoglobulin G subclass response of mice to influenza A virus: the effect of mouse strain, and the neutralizing abilities of individual protein A-purified subclass antibodies. *J Gen Virol* 70: 2439–2448 (1989).

3. M. J. Hocart, J. S. Mackenzie, and G. A. Stewart. The IgG subclass responses to influenza virus haemagglutinin in the mouse: effect of route of inoculation. *J Gen Virol* 70: 809-818 (1989).

4. C. A. Benne, M. Harmsen, W. van der Graaff, A. F. M. Verheul, H. Snippe, and C. A. Kraaijeveld. Influenza virus neutralizing antibodies and IgG isotype profiles after immunization of mice with influenza A subunit vaccine using various adjuvants. *Vaccine* 15: 1039-1044 (1997).

5. X. Lu, J. D. Clements, and J. M. Katz. Mutant Escherichia coli heat-labile enterotoxin [LT(R192G)] enhances protective humoral and cellular immune responses to orally administered inactivated influenza vaccine. *Vaccine* 20: 1019-1029 (2002).

6. Y. A. S. Shavartsmanand M. P. Zykov. Secretory anti-influenza immunity. *Adv Immunol* 22: 291-330 (1976).

7. R. B. Couchand J. A. Kasel. Immunity to influenza in man. *Ann Rev Microbiol* 37: 529-549 (1983).

8. M. L. Clements, S. O'Donnel, M. M. Levine, R. M. Chanock, and B. R. Murphy. Dose response of A/Alaska/6/77 (H3N2) cold-adapted reassortant vaccine virus in adult volunteers: role of local antibody in resistance to infection with vaccine virus. *Infect Immun* 40: 1044-1051 (1983).

9. F. Y. Liew, S. M. Russel, G. Appleyard, C. M. Brand, and J. Beale. Cross protection in mice infected with influenza A virus by the respiratory route is corrected with local IgA antibody rather than serum antibody or cytotoxic T cell reactivity. *Eur J Immunol* 14: 350-356 (1984).

10. B. J. Underdownand J. M. Schiff. Immunoglobulin A:strategic defense initiative at the mucosal surface. *Annu Rev Immunol* 4: 389-417 (1986).

11. B. Murphyand M. L. Clements. The systemic and mucosal immune response of humans to influenza A virus. *Curr Top Microbiol Immunol* 146: 107-116 (1989).

12. R. Ito, Y. A. Ozaki, T. Yoshikawa, H. Hasegawa, Y. Sato, Y. Suzuki, R. Inoue, T. Morishima, N. Kondo, T. Sata, T. Kurata, and S. Tamura. Roles of anti-hemagglutinin IgA and IgG antibodies in different sites of the respiratory tract of vaccinated mice in preventing lethal influenza pneumonia. *Vaccine* 21: 2362-2371 (2003).

13. W. E. P. Beyer, A. M. Palache, and A. D. M. E. Osterhaus. Comparison of serology and reactogenicity between influenza subunit vaccines and whole virus or split vaccines. A review and meta-analysis of the literature. *Clin Drug Invest* 15: 1-12 (1998).

14. T. R. Cate, R. B. Couch, D. Parker, and B. Baxter. Reactogenicity, immunogenicity, and antibody persistence in adults given inactivated influenza virus vaccines - 1978. *Rev Infect Dis* 5: 737-747 (1983).

15. M. L. Clementsand B. R. Murphy. Development and persistence of local and systemic antibody responses in adults given live attenuated or inactivated influenza A virus vaccine. *J Clin Microbiol* 23: 66-72 (1986).

16. S. S. Davis. Nasal Vaccines. *Drug Deliv Rev* 51: 21-42. (2001).

17. A. J. Almeidaand H. O. Alpar. Nasal delivery of vaccines. *J Drug Target* 3: 455-467 (1996).

18. L. Illum, I. Jabbal-Gill, M. Hinchcliffe, A. N. Fisher, and S. S. Davis. Chitosan as a novel nasal delivery system for vaccines. *Adv Drug Deliv Rev* 51: 81-96 (2001).

19. C. F. Kuper, P. J. Koornstra, D. M. Hameleers, J. Biewenga, B. J. Spit, A. M. Duijvestijn, P. J. van Breda Vriesman, and T. Sminia. The role of nasopharyngeal lymphoid tissue. *Immunol Today* 13: 219-24 (1992).

20. H. Kiyonoand S. Fukuyama. NALT- versus Peyer's-patch-mediated mucosal immunity. *Nat Rev Immunol* 4: 699-710 (2004).

21. R. J. Soane, M. Ferier, A. C. Perkins, N. S. Jones, S. S. Davis, and L. Illum. Evaluation of the clearance characteristics of bioadhesive system in humans. *Int J Pharm* 178: 55-65 (1999).

22. R. J. Soane, M. Hinchcliffe, S. S. Davis, and L. Illum. Clearance characteristics of chitosan based formulation in the sheep nasal cavity. *Int J Pharm* 217: 183-191 (2001).

23. L. Illum. Nasal drug delivery- possibilities, problems and solutions. *J. Control. Release* 87: 187-98 (2003).

24. M. Singh, M. Briones, and D. T. O'Hagan. A novel bioadhesive intranasal delivery system for inactivated influenza vaccines. *J Control Release* 70: 267-76 (2001).

25. M. Bivas-Benita, M. Laloup, S. Versteyhe, J. Dewit, J. De Braekeleer, E. Jongert, and G. Borchard. Generation of Toxoplasma gondii GRA1 protein and DNA vaccine loaded chitosan particles: preparation, characterization, and preliminary in vivo studies. *Int J Pharm* 266: 17-27 (2003).

26. I. M. van der Lubben, G. Kersten, M. M. Fretz, C. Beuvery, J. C. Verhoef, and H. E. Junginger. Chitosan microparticles for mucosal vaccination against diphtheria: oral and nasal efficacy studies in mice. *Vaccine* 28: 1400-1408 (2003).

27. A. Vila, A. Sanchez, K. Janes, I. Behrens, T. Kissel, J. L. Vila Jato, and M. J. Alonso. Low molecular weight chitosan nanoparticles as new carriers for nasal vaccine delivery in mice. *Eur. J. Pharm. Biopharm.* 57: 123-131 (2004).

28. W. Morris, M. C. Steinhoff, and P. K. Russell. Potential of polymer microencapsulation technology for vaccine innovation. *Vaccine* 12: 5-11 (1994).

29. P. G. Jenkins, A. G. Coombes, M. K. Yeh, N. W. Thomas, and S. S. Davis. Aspects of the design and delivery of microparticles for vaccine applications. *J Drug Target* 3: 79-81 (1995).

30. A. G. Coombes, E. C. Lavelle, P. G. Jenkins, and S. S. Davis. Single dose, polymeric, microparticle-based vaccines: the influence of formulation conditions on the magnitude and duration of the immune response to a protein antigen. *Vaccine* 14: 1429-1438 (1996).

31. I. Jabbal-Gill, W. Lin, P. Jenkins, P. Watts, M. Jimenez, L. Illum, S. S. Davis, J. M. Wood, D. Major, P. D. Minor, X. Li, E. C. Lavelle, and A. G. Coombes. Potential of polymeric lamellar substrate particles (PLSP) as adjuvants for vaccines. *Vaccine* 18: 238-250 (1999).

32. L. Illum. Chitosan and its use as a pharmaceutical excipient. *Pharm. Res.* 15: 1326-1331 (1998).

33. O. Felt, P. Buri, and R. Gurny. Chitosan: a unique polysaccharide for drug delivery. *Drug Dev. Ind. Pharm.* 24: 979-993 (1998).

34. H. E. Jungingerand J. C. Verhoef. Macromolecules as safe penetration enhancers for hydrophilic drugs-a fiction? *Pharm. Sci. Tech. Today* 1: 370-376 (1998).

35. L. Illum, N. F. Farraj, and S. S. Davis. Chitosan as a novel nasal delivery system for peptide drugs. *Pharm Res* 11: 1186-1189 (1994).

36. K. Y. Lee, W. S. Ha, and W. H. Park. Blood compatibility and biodegradability of partially N-acylated chitosan derivatives. *Biomaterials* 16: 1211-1216 (1995).

37. R. A. A. Muzzarelli. Human enzymatic activities related to the therapeutic administration of chitin derivative. *Cell Mol. Life Sci.* 53: 131-140 (1997).

38. T. Chandyand C. P. Sharma. Chitosan as a biomaterial. *Artif. Cells Artif. Organs* 18: 1-24 (1990).

39. A. F. Kotzé, H. L. Lueßen, B. J. de Leeuw, A. G. de Boer, J. C. Verhoef, and H. E. Junginger. Chitosan for enhanced intestinal permeability: prospects for derivatives soluble in neutral and basic environments. *Eur J Pharm Sci* 7: 145-151 (1999).

40. A. F. Kotzé, H. L. Lueßen, B. J. de Leeuw, A. G. de Boer, J. C. Verhoef, and H. E. Junginger. N-trimethyl chitosan chloride as a potential absorption enhancer across mucosal surfaces: in vitro evaluation in intestinal epithelial cells (Caco-2). *Pharm Res* 14: 1197-202 (1997).

41. M. Thanou, J. C. Verhoef, J. H. M. Verheijden, and H. E. Junginger. Intestinal absorption of octeriotide: N-trimethyl chitosan chloride (TMC) ameliorates the permeability and absorption properties of the somatostatin analogue in vitro and in vivo. *J Pharm Sci* 89: 951-957 (2000).

42. J. H. Hamman, M. Stander, and A. F. Kotzé. Effect of the degree of quaternization of N-trimethyl chitosan chloride on absorption enhancement: in vivo evaluation in rat nasal epithelia. *Int J Pharm* 232: 235-242 (2002).

43. I. M. van der Lubben, J. C. Verhoef, M. M. Fretz, F. A. C. van Opdorp, I. Mesu, G. Kersten, and H. E. Junginger. Trimethyl chitosan chloride (TMC) as novel excipient for oral and nasal immunization against diphtheria. *STP Pharm Sci* 12: 235-242 (2002).

44. B. C. Baudner, M. Morandi, M. M. Giuliani, J. C. Verhoef, H. E. Junginger, P. Costantino, R. Rappuoli, and G. Del Giudice. Modulation of immune response to group C meningococal conjugate vaccine given intranasally to mice together with trimethyl chitosan delivery system. *J Infect Dis* 189: 828-832 (2004).

45. Y. Huangand M. D. Donovan. Large molecule and particulate uptake in the nasal cavity: the effect of size on nasal absorption. *Adv Drug Deliv Rev* 29: 147-155 (1998).

46. J. Brooking, S. S. Davis, and L. Illum. Transport of nanoparticles across the rat nasal mucosa. *J Drug Target* 9: 267-279 (2001).

47. A. J. Almeida, H. O. Alpar, and M. R. W. Brown. Immune response to nasal delivery of antigenically intact tetanus toxoid associated with poly(L-lactic acid) microspheres in rats, rabbits and guinea-pigs. *J Pharm Pharmacol* 45: 198-203 (1993).

48. H. O. Alpar, A. J. Almeida, and M. R. W. Brown. Microsphere absorption by the nasal mucosa of the rat. *J Drug Target* 2: 147-149 (1994).

49. M. Amidi, S. G. Romeijn, G. Borchard, H. E. Junginger, W. E. Hennink, and W. Jiskoot. Preparation and characterization of protein-loaded N-trimethyl chitosan nanoparticles as nasal delivery system. *J Control Release* 111: 107-116 (2006).

50. A. B. Sieval, M. Thanou, A. F. Kotzé, J. C. Verhoef, J. Brussee, and H. E. Junginger. Preparation and NMR- characterisation of highly substituted N-trimethyl chitosan chloride. *Carbohydr Polym* 36: 157-165 (1998).

51. D. M. Bollagand S. J. Edelstein. Protein Methods. *New York: Wiley-Liss Publications, 1991.*

52. S. Gizurarson. Animal models for intranasal drug delivery studies. *Acta Pharm Nord* 2: 105-122 (1990).

53. W. R. Verweij, L. de Haan, M. Holtrop, E. Agsteribbe, R. Brands, G. J. van Scharrenburg, and J. Wilschut. Mucosal immunoadjuvant activity of recombinant Escherichia coli heat-labile enterotoxin and its B subunit: induction of systemic IgG and secretory IgA responses in mice by intranasal immunization with influenza virus surface antigen. *Vaccine* 16: 2069-2076 (1998).

54. L. de Haan, W. R. Verweij, M. Holtrop, R. Brands, G. J. van Scharrenburg, A. M. Palache, E. Agsteribbe, and J. Wilschut. Nasal or intramuscular immunization of mice with influenza subunit antigen and the B subunit of Escherichia coli heat-labile toxin induces IgA- or IgG-mediated protective mucosal immunity. *Vaccine* 19: 2898-2907 (2001).

55. J. E. Eyles, V. W. Bramwell, E. D. Williamson, and H. O. Alpar. Microsphere translocation and immunopotentiation in systemic tissues following intranasal administration. *Vaccine* 19: 4732-4742 (2001).

56. B. C. Baudner, M. M. Giuliani, J. C. Verhoef, R. Rappuoli, and H. E. Junginger. The concomitant use of the LTK63 mucosal adjuvant and of chitosan-based delivery system enhances the immunogenicity and efficacy of intranasally administered vaccines. *Vaccine* 8: 3837-3844. (2003).

57. M. J. Hocart, J. S. Mackenzie, and G. A. Stewart. The immunoglobulin G subclass responses of mice to influenza A virus: the effect of mouse strain, and the neutralizing abilities of individual protein A-purified subclass antibodies. *J Gen Virol* 70: 2439-2448 (1989).

58. I. Jabbal-Gill, W. Lin, P. Jenkins, P. Watts, M. Jimenez, L. Illum, S. Davis, J. Wood, D. Major, P. Minor, X. Li, E. Lavelle, and A. Coombes. Potential of polymeric lamellar substrate particles (PLSP) as adjuvants for vaccines. 18: 238-250 (2000).

59. Q. Vu, K. M. McCarthy, M. McCormack, and E. E. Schneeberger. Lung dendritic cells are primed by inhaled particulate antigens, and retain MHC class II/antigenic peptide complexes in hilar lymph nodes for a prolonged period of time. *Immunology* 105: 488–498 (2002).

60. K. D. Newman, P. Elamanchili, G. S. Kwon, and J. Samuel. Uptake of poly(d,l-lactic-co-glycolic acid) microspheres by antigen-presenting cells in vivo. *J. Biomed. Materi. Res.* 60: 480–486 (2002).

61. R. Audran, K. Peter, J. Dannull, Y. Men, E. Scandella, M. Groettrup, B. Gander, and G. Corradin. Encapsulation of peptides in biodegradable microspheres prolongs their MHC class-I presentation by dendritic cells and macrophages in vitro. *Vaccine* 21: 1250–1255 (2003).

62. A. O. Hovden, R. J. Cox, A. Madhun, and L. R. Haaheim. Two doses of parenterally administered split influenza virus vaccine elicited high serum IgG concentrations which effectively limited viral shedding upon challenge in mice. *Scand J Immunol* 62: 342-52 (2005).

63. A. Coulter, R. Harris, R. Davis, D. Drane, J. Cox, D. Ryan, P. Sutton, S. Rockman, and M. Pearse. Intranasal vaccination with ISCOMATRIX adjuvanted influenza vaccine. *Vaccine* 21: 946-9 (2003).

64. A. F. Kotzé, M. M. Thanou, H. L. Lueßen, B. J. de Leeuw, A. G. de Boer, J. C. Verhoef, and H. E. Junginger. Effect of the degree quaternisation of N-trimethyl chitosan chloride on the permeability of intestinal epithelial cells (Caco-2). *Eur J Pharm Biopharm* 47: 269-274 (1999).

65. J. H. Hamman, C. M. Schultz, and A. F. Kotzé. N-trimethyl chitosan chloride: optimum degree of quaternization for drug absorption enhancement across epithelial cells. *Drug Dev Ind Pharm* 29: 161-172 (2003).

66. D. Snyman, J. H. Hamman, and A. F. Kotze. Evaluation of the mucoadhesive properties of N-trimethyl chitosan chloride. *Drug Dev. Ind. Pharm.* 29: 61-9 (2003).

67. J. Bienenstockand M. R. McDermott. Bronchus- and nasal-associated lymphoid tissues. *Immunol Rev* 206: 22-31 (2005).

Chapter four

Preparation and physicochemical characterization of supercritically dried insulin-loaded microparticles for pulmonary delivery

Maryam Amidi[1]
Hubert C. Pellikaan[2]
Anne H. de Boer[3]
Daan J.A. Crommelin[1]
Wim E. Hennink[1]
Wim Jiskoot[1,4]

[1] Department of Pharmaceutics, Utrecht Institute for Pharmaceutical Sciences, Utrecht University, PO Box 80082, 3508 TB Utrecht, The Netherlands

[2] Feyecon D & I B.V. Rijnkade 17A, 1382 GS, Weesp, The Netherlands

[3] Department of Pharmaceutical Technology and Biopharmacy, University of Groningen, Ant. Deusinglaan 1, 9713 AV Groningen, The Netherlands

[4] Division of Drug Delivery Technology, Leiden/Amsterdam Center for Drug Research (LACDR), Leiden University, P.O. Box 9502, 2300 RA Leiden, The Netherlands

Submitted for publication

Abstract

Therapeutic proteins have become essential in the treatment of diseases. Up to now, most of these proteins are administered by injection. In the search for non-invasive delivery options, pulmonary administration is an attractive route, because the lungs have a large surface area, extensive vasculature, a thin membrane and low enzymatic activity. Supercritical fluid (SCF) drying processes offer the possibility to produce dry protein formulations suitable for inhalation. In this study, insulin-loaded microparticles suitable for pulmonary administration were prepared and characterized. N-trimethyl chitosan (TMC), a polymeric mucoadhesive absorption enhancer and dextran, as a non-permeation enhancer, were used as carriers for insulin. The particles were prepared by spraying an acidic water/DMSO solution of insulin and TMC into supercritical carbon dioxide. The mean size of the particles as determined by laser diffraction analysis was between 6-10 μm and their volume median aerodynamic diameter (VMAD) as determined by time-of-flight measurement was ca. 4 μm. The water content of the particles as measured by Karl Fischer titration was ca. 4% (w/w), but this neither resulted in collapse nor aggregation of the particles. In the freshly prepared dried insulin powders, no insulin degradation products were detected by HPLC and GPC. Moreover, the secondary and tertiary structure of insulin as determined by circular dichroism (CD) and fluorescence spectroscopy was preserved in all formulations. After one year storage at 4 ºC, the particle characteristics were maintained and the insulin structure was largely preserved in the TMC powders. In conclusion, SCF drying is a promising, protein-friendly technique for the preparation of inhalable insulin-loaded particles.

Keywords: N-Trimethyl chitosan microparticles; supercritical carbon dioxide; pulmonary delivery; insulin; physicochemical characterization

1 Introduction

The advances in biotechnology have resulted in the availability of a large number of protein-based drugs. Up until now, most therapeutic proteins are administered by injection because of their low stability and bioavailability after oral administration and poor absorption at other mucosal sites. Recently, pulmonary delivery has attracted much attention as a non-invasive administration route for macromolecules such as proteins and peptides, because the respiratory tree has a large surface area (~75 m^2), extensive vasculature, a thin membrane and low enzymatic activity (1-3). The transport of macromolecules across the absorptive area, the alveolar wall, occurs by transcytosis for proteins > 22 kDa and through tight-junctional paracellular processes for smaller molecules (1-3). However, the clearance rate of transcytosis is so slow that it is of little importance for pulmonary delivery of protein drugs.

Protein-containing particles in the aerodynamic size range 1.5 to 3 micron (in combination with a short breathhold period) may yield a more effective alveolar deposition (1, 3, 4). The major factors limiting pulmonary absorption of the proteins are the poor deposition of the protein formulations at the alveolar region, low absorption from the respiratory epithelial barriers and the mucociliary escalator, which rapidly removes protein solution or particles from the central respiratory tract and prevent the access of the protein to the alveoli. Therefore, a suitable delivery system is required for efficient administration of protein deeply into the lungs. Moreover, the biological activity and structural stability of proteins are of crucial importance during pharmaceutical manufacturing of protein formulations. Proteins can undergo different chemical and physical degradation reactions particularly when formulated as a solution. It has been shown that the long-term stability of proteins can be greatly enhanced when they are stored in a dried state (5, 6). Importantly, proteins from dried formulations are more efficiently absorbed in the lung compared to proteins in solutions (7).

Supercritical fluid (SCF) drying is an attractive technique to prepare dried protein formulations (8-11). SCF drying is a fast and mild process, is cost effective and offers the possibility to produce small microparticles suitable for inhalation (8, 10-12). A fluid is defined as supercritical when its pressure and temperature exceed their critical values. Above the critical points, the SCF has a liquid-like viscosity and density and gas-like diffusivity properties and can therefore penetrate into substances like a gas and dissolve materials like a liquid (13). Supercritical carbon dioxide (SC-CO_2) has been commonly used as a SCF for drying pharmaceutical proteins, because proteins have a very low solubility in SC-CO_2. Consequently, it can act as an anti-solvent which results in the precipitation of the protein from its solution (14). Moreover, CO_2 is inexpensive, non-toxic and has a moderate critical temperature (31 °C) (9, 10, 15).

Dried proteins and peptides are often formulated with sugars as carriers for pulmonary administration and as stabilizers to protect proteins from degradation during processing and storage (10, 15). However, the pulmonary bioavailability of proteins is still low as compared to the intravenous and subcutaneous bioavailability (3). Therefore, polymeric

particles with absorption-enhancing properties may be suitable alternative carriers for pulmonary protein delivery. Particles consisting of peptides and proteins associated with polymeric chitosan and chitosan derivatives have been shown to enhance the absorption of these macromolecules across mucosal epithelia (16-21). Chitosan based polymers are mucoadhesive and are capable of opening the tight junctions. Both properties may help to stimulate the uptake of the encapsulated protein (16-21). In contrast to chitosan, which is soluble at low pH and insoluble at neutral pH, N-trimethyl chitosan chloride (TMC), a partially quaternized chitosan derivative, shows good water solubility over a wide pH range. Hence, TMC has mucoadhesive properties and excellent absorption enhancing effects even at neutral pH (22, 23). Because of these properties, TMC could be an attractive alternative to chitosan for the design of protein-loaded particles.

The aim of the present work was to prepare insulin loaded microparticles for pulmonary delivery using a SCF drying process. TMC20 (as a mucoadhesive), TMC60 (as a mucoadhesive and an absorption enhancer) (22, 24) and dextran (as a non-mucoadhesive and non-permeation enhancer) were selected as polymeric carriers. After preparation of TMC- and dextran-insulin microparticles, their physical characteristics such as shape, geometric and aerodynamic size distributions, water content, and insulin content were studied. Moreover, the structural integrity of insulin as well as the long-term stability of the dry powders was evaluated.

2 Materials and methods

2.1 Materials

Chitosan (M_n = 40 kDa, M_w = 177 kDa, determined by gel permeation chromatography (GPC) using poly [ethylene glycol] (PEG) standards (25), degree of deacetylation 93%) was a generous gift from Primex (Avaldsnes, Norway). N-Trimethyl chitosan with two degrees of quaternization (DQ) of 20% (TMC20) and 60% (TMC60) was synthesized by methylation of chitosan by using CH_3I in the presence of a strong base (NaOH) and analyzed by ^{1}H-nuclear magnetic resonance (NMR) spectroscopy as previously described (26). Dextran (Mw: 64-76 kDa), recombinant human insulin (M_w = 5.807 kDa, 29 IU/mg) and FITC-labeled human insulin were purchased from Sigma-Aldrich (Schnelldorf, Germany). DMSO was purchased from Across Organics. All other chemicals used were obtained from commercial suppliers and were of analytical grade.

2.2 Preparation of insulin-loaded microparticles

Insulin-loaded dextran and TMC microparticles were prepared by spraying a HCl/DMSO solution of insulin/polymer into SC-CO_2. First, 30 mg insulin was dissolved in 2.7 ml of HCl 0.01 M. Then dextran or TMC (270 mg) was dissolved in

this solution. The percentage of insulin/TMC or insulin/dextran was 10% (w/w). After TMC or dextran was fully dissolved, 2.7 ml polymer-insulin solution was mixed with 93.7 g of DMSO.

A scheme of the experimental setup is presented in figure 1 and details about the apparatus and the method were reported before (27).

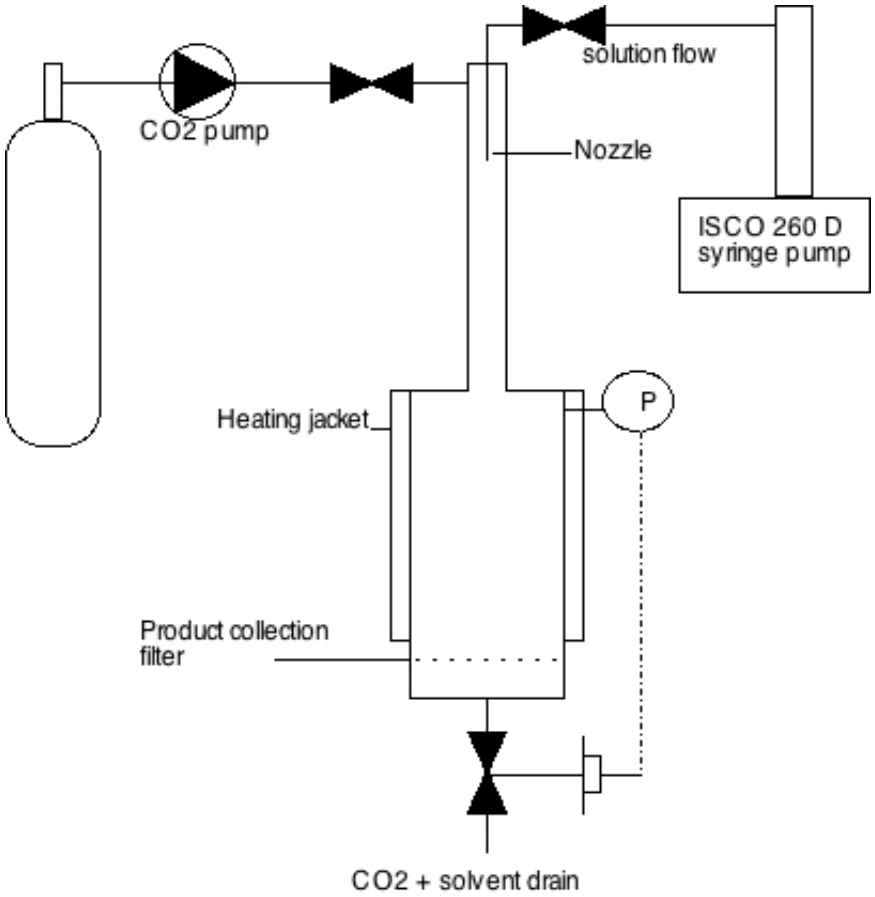

Figure 1. Scheme of experimental set-up of the SCF drying system.

At the selected operating temperature (40 °C), pressure (110 bar) and mixing ratios CO_2, water and DMSO are fully miscible resulting in a single phase in the supercritical region. The following experimental conditions gave spherical microparticles. First, at 40 °C SC-CO_2 was introduced with a constant flow rate of 333 g/min using a diaphragm pump (Lewa) into a 1-liter precipitation vessel until the pressure reached 110 bar. Next, the polymer-insulin solution (total volume around 100 ml; flow rate 4.5 ml/min) and SC-CO_2 (333 g/min) were directly fed into an atomization device (a nozzle, diameter 0.08 mm) using two ISCO 260 syringe pumps.

The ongoing co-current flow of supercritical CO_2 (333 g/min) dispersed the sprayed polymer-insulin solution. The mixture was passed through a residence-time tube (internal diameter 2 cm; length 70 cm) into the precipitation vessel. The use of a residence-time tube was crucial, because the supersaturation level was very high and phase split took place at the same time as mixing of the solution and SC-CO_2 (28). A water jacket was used to maintain the pumps and vessel at a temperature of 40 °C. Electrical heating was used to keep the temperature of the nozzle and residence tube at 40 °C. The pressure in the vessel (110 bar) and CO_2 flow (333 g/min) were controlled by exit valves and maintained at 40 °C and 110 bar during the whole experiment. Once the solution of polymer-insulin in HCl/DMSO was entirely sprayed into the precipitation vessel, the solution line was closed. Subsequently, SC-CO_2 at a flow rate of 200 g/min and ethanol at a flow rate of 4 ml/min were mixed and sprayed into the precipitation vessel for 12 min in order to remove the residual solvents (H_2O and DMSO). Finally, the vessel was flushed for 30 min with SC-CO_2 (200 g/min) to further extract residual solvents including ethanol. The dry powder was collected from the filter at the bottom of the vessel, once the pressure was released and stored in closed containers at 4 °C. To test the real-time stability, a part of each batch was stored in a separate container and stored for one year at 4 °C.

2.3 Characterization of the insulin-loaded microparticles

2.3.1 Particle morphology

The morphology of the TMC microparticles was determined using a JEOL JSM-5400 scanning electron microscope (SEM) (Peabody, USA). Samples of the particles were fixed onto aluminum SEM stubs using self-adhesive carbon disks, and were subsequently sputter-coated with a conducting gold layer.

2.3.2 Particle size analysis

The volume-mean particle diameter and size distribution were determined with a laser diffraction analyzer (HELOS BF MAGIC, Clausthal-Zellerfeld, Germany) equipped with a dry powder dispersion system RODOS (Sympatec GmbH, Germany). Approximately 2 mg of bulk powder was placed into the RODOS ring and dispersed through a laser beam (628 nm) with 3 bar of air pressure. Measurements were ×performed with a 100 mm lens and calculations were based on the Fraunhofer theory. In another measurement the particles were introduced via a DP-4 insufflator (PENN CENTURY Inc, Philadelphia, USA) designed for *in vivo* studies in rats, into the LD particle analyzer.

2.3.3 Aerodynamic particle size analysis

The volume median aerodynamic diameter (VMAD) of the microparticles was assessed by aerolization of the powders in an Aerosizer™ (TIS Inc., Minneapolis, USA) based on direct time-of-flight measurements. Half a milligram of each powder was introduced into the Aerosizer using a DP-4 insufflator (see above). The volume

median aerodynamic diameters (VMADs) of the particles were calculated from the particle number distributions presented by the Aerosizer. The mass mean aerodynamic diameter (MMAD) of particles is equal to the VMAD when particles of different sizes all have the same density.

2.3.4 Confocal laser scanning microscopy (CLSM)

FITC-insulin-loaded TMC microparticles were prepared by drying in SC-CO_2, as described in section 2.2. The particles were suspended in dichloromethane (DCM) and mounted on a slide. After evaporation of the DCM, the particles were visualized with a confocal laser scanning microscope (Bio-Rad, Alphen a/d Rijn, The Netherlands). The distribution of the FITC-insulin within the particles was investigated by scanning the particles in the x, y plane with a z-step of 0.2 μm.

2.3.5 Water content analysis

The water content of the different TMC- and dextran-insulin particles was determined by Karl-Fischer titration. In brief, 2-3 mg powder, accurately weighed, were dissolved (TMC particles) or suspended (dextran particles) in 500 μl methanol. Fifty μl of sample were injected into the titration cell and the amount of water of the powders was calculated after subtraction of the background (methanol only) signal.

2.4 Quantification and characterization of insulin

2.4.1. Reversed-phase HPLC

The insulin content of the TMC microparticles was determined by reversed-phase HPLC. This technique also allows the detection of insulin degradation products. A Prosphere C_{18} (300 Å; 5 μm, 250 X 4.6 mm) column (Alltech Breda, The Netherlands) in combination with an All-guard C_{18} pre-column (Alltech, Breda, The Netherlands) was used. The column was equilibrated with a solvent mixture consisting of 25% acetonitrile/75% H_2O/0.1% trifluoro acetic acid (TFA) for one hour at a flow rate of 1 ml/min. The microparticles were dissolved in 0.01 M HCl (1 mg/ml containing 0.1 mg insulin) and 50 μl of the solutions were injected onto the column. A calibration curve was made by injecting volumes of 0.5-50 μl of a freshly prepared insulin (1 mg/ml) solution in 0.01 M HCl onto the column.

A gradient was run from the starting composition, acetonitrile/H_2O (25/75%)/TFA 0.1%, to acetonitrile/H_2O (38/62%)/TFA 0.1% in 25 minutes. The mobile phase was delivered to the column at a flow rate of 1 ml/min by a Waters 600 gradient pump equipped with a Waters 717 plus autosampler (Waters Corporation, Milford, MA, USA). Chromatograms were recorded with a Waters 600 absorbance detector set at 280 nm.

2.4.2 Gel permeation chromatography (GPC)

GPC analyses were performed with a method adapted from (29) and (30) on a GPC max, VE 2001 instrument (Viscotek, Oss, The Netherlands) equipped with a Superdex

75 10/300 GL column, exclusion limit 1×10^5 Da (GE Healthcare Europe GmbH, Amsterdam, The Netherlands). The insulin-loaded particles were dissolved in acetic acid 20% (w/w) in water at a concentration of 1 mg/ml of insulin. Then the samples were centrifuged at high speed for 1 min to remove insoluble particles, if any. The mobile phase was 100 mM phosphate buffered saline (pH 7.4). Two hundred µl of each sample was injected onto the column; elution was done at a flow rate of 0.5 ml/min. Chromatograms were recorded with a TDA 302 tetra detector (Viscotek, Oss, The Netherlands). UV (at 280 nm) and right angle light scattering (RALS) signals were used to analyze the data. A dn/dc value of 0.189 ml/g (31) was assumed for calculation of the molecular weight of insulin from the light scattering data.

2.4.3 Circular dichroism (CD)

The secondary and tertiary structures of insulin were monitored by far-UV and near-UV circular dichroism (CD) spectroscopy, respectively. Insulin, a physical mixture of insulin and dextran/TMC 1/10 w/w and insulin-loaded TMC/dextran microparticles were dissolved in 0.01 M HCl. The final concentration of insulin was ca 0.5 mg/ml. Prior to CD spectroscopy, all samples were centrifuged for 1 min at 10000 g to remove particulate matter, if any. Far-UV (200-260 nm) CD and near-UV (250-320 nm) CD spectroscopy were performed at room temperature, in a 0.02-cm quartz cuvette and a 0.5-cm quartz cuvette, respectively, using a dual beam DSM 1000 CD spectrophotometer (On-Line Instrument Systems, Bogart, GA, USA). The subtractive double-grating monochromator was equipped with a fixed disk, holographic grating (2400 lines/nm, blaze wave-length 230 nm) and 1.24 mm slits. Each spectrum is the average of 5 scans. Spectra of 0.01 M HCl, empty TMC20, TMC60 and dextran particles dissolved in 0.01 M HCl were recorded and subtracted from the corresponding sample spectrum. The measured CD signals were corrected for concentration differences and converted into delta molar extinction ($\Delta\varepsilon$), based on a mean residual weight of 113.86 (Mw/51 amino acids) (32).

2.4.4 Fluorescence spectroscopy

Insulin, a physical mixture of insulin and dextran or TMC (1/10 w/w) and insulin-loaded microparticles were dissolved in 0.01 M HCl. Fluorescence emission spectra (290-450 nm, 1-nm step) of the different samples were measured in 1-cm quartz cuvettes in a Fluorolog III Fluorimeter (Jobin Yvon-Horriba, Edison, NJ, USA) at 25 °C while stirring. Excitation was at 280 nm and the slits (excitation and emission) were set at 3 nm. The integration time per data point was 0.1 s and the average of the 5 scans was taken. Spectra of 0.01 M HCl, empty TMC20, TMC60 and dextran particles dissolved in 0.01 M HCl and plain polymer solutions were subtracted from the corresponding sample spectrum. Before analysis, the solutions were diluted with 0.01 M HCl to obtain an absorbance < 0.1 at 280 nm and the spectra were normalized for concentration differences.

3 Results and discussion

3.1 Preparation of insulin-loaded dextran and TMC microparticles

In this study we have investigated the preparation and characterization of polymeric particles suitable for the pulmonary delivery of insulin. Particles based on TMC, a mucoadhesive absorption enhancer, and dextran, an inert polymer, were prepared using a SCF process with SC-CO_2 as an anti-solvent. The experimental conditions were based on a previous study in which the drying of a solution of dextran in DMSO resulted in small dextran microparticles, suitable for inhalation (33). The yield of particle production was about 60%. The optimum polymer concentration was found to be 0.3% (w/w) in HCl/DMSO. At lower polymer concentrations agglomerated particles were collected, whereas at higher concentrations TMC20 and TMC60 were not fully soluble in the HCl/DMSO mixture. Because of the poor solubility of the TMCs and insulin in DMSO, insulin and the polymers were first dissolved in an acidic aqueous solution (0.01 M HCl). Then, the protein/polymer solution was mixed with DMSO. The ratio of 0.01 M HCl/DMSO of 2.7/97.3 (w/w) was chosen based on the phase behavior of the water/DMSO/CO_2 mixture reported before (27). Lower or higher ratios resulted in agglomerated particles or wet materials, respectively.

3.2 Particle characterization

Figure 2 shows representative SEM photographs of insulin-loaded TMC and dextran microparticles. This figure shows that the size distributions of the three particle formulations were comparable and in the micrometer range (ca 1-30 μm). The TMC20 and TMC60 microparticles were spherical with a smooth surface (figure 2A and B), whereas the shape of the dextran microparticles was somewhat irregular (figure 2C). The volumetric size distributions of the freshly prepared TMCs and dextran particles directly after preparation and as measured by laser diffraction technique are shown in figure 3A. The cumulative volume distributions of the particles as a function of aerodynamic diameter are shown in figure 3B. All three different insulin powders showed a fairly narrow, unimodal size distribution, indicating the absence of agglomerates. From figure 3A it appears that 90% of the particles have a size between 1 and 30 μm, which is in excellent agreement with SEM analysis. The size distribution of the particles introduced into the analyzer with a DP-4 insufflator was similar to that of the particles introduced with the dry-powder air dispersion system using an air-pressure of 3 bar (data not shown). This comparison is important to evaluate the potential of the insufflator in order to properly disperse and introduce the powders into the Aerosizer for the further aerodynamic size measurements.

Table 1. Particle characteristics of the dried insulin formulation

Dried formulations	Characteristic laser diffraction diameters X10, X50, X90 (μm)[1]			VMAD (μm)[2]	Water content (%)[3]
TMC60-insulin particles	2.6	7.9	14.9	4.0	4.1
TMC20-insulin particles	2.7	9.9	30.0	4.1	4.1
Dextran-insulin particles	2.2	6.1	14.8	3.9	4.2

[1] Determined by laser diffraction (LD) analyses (n=2)
[2] Determined by time-of-flight measurements (n=2)
[3] According to Karl Fischer titration (n=2)

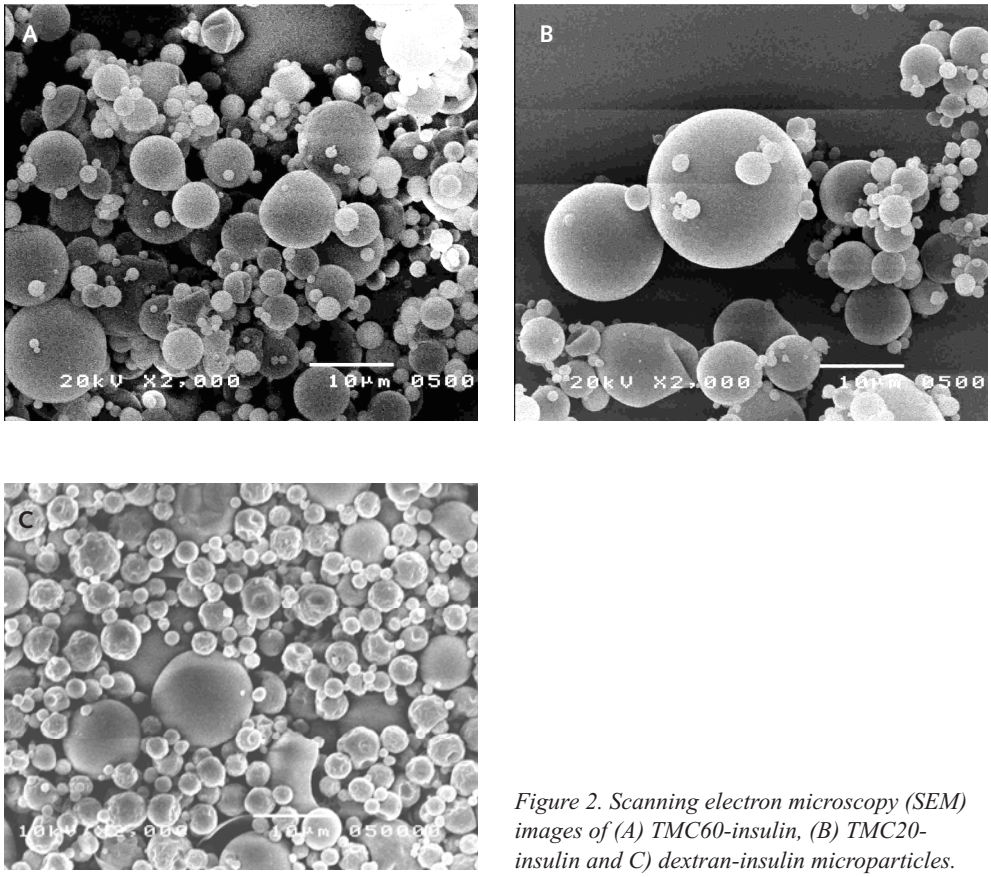

Figure 2. Scanning electron microscopy (SEM) images of (A) TMC60-insulin, (B) TMC20-insulin and C) dextran-insulin microparticles.

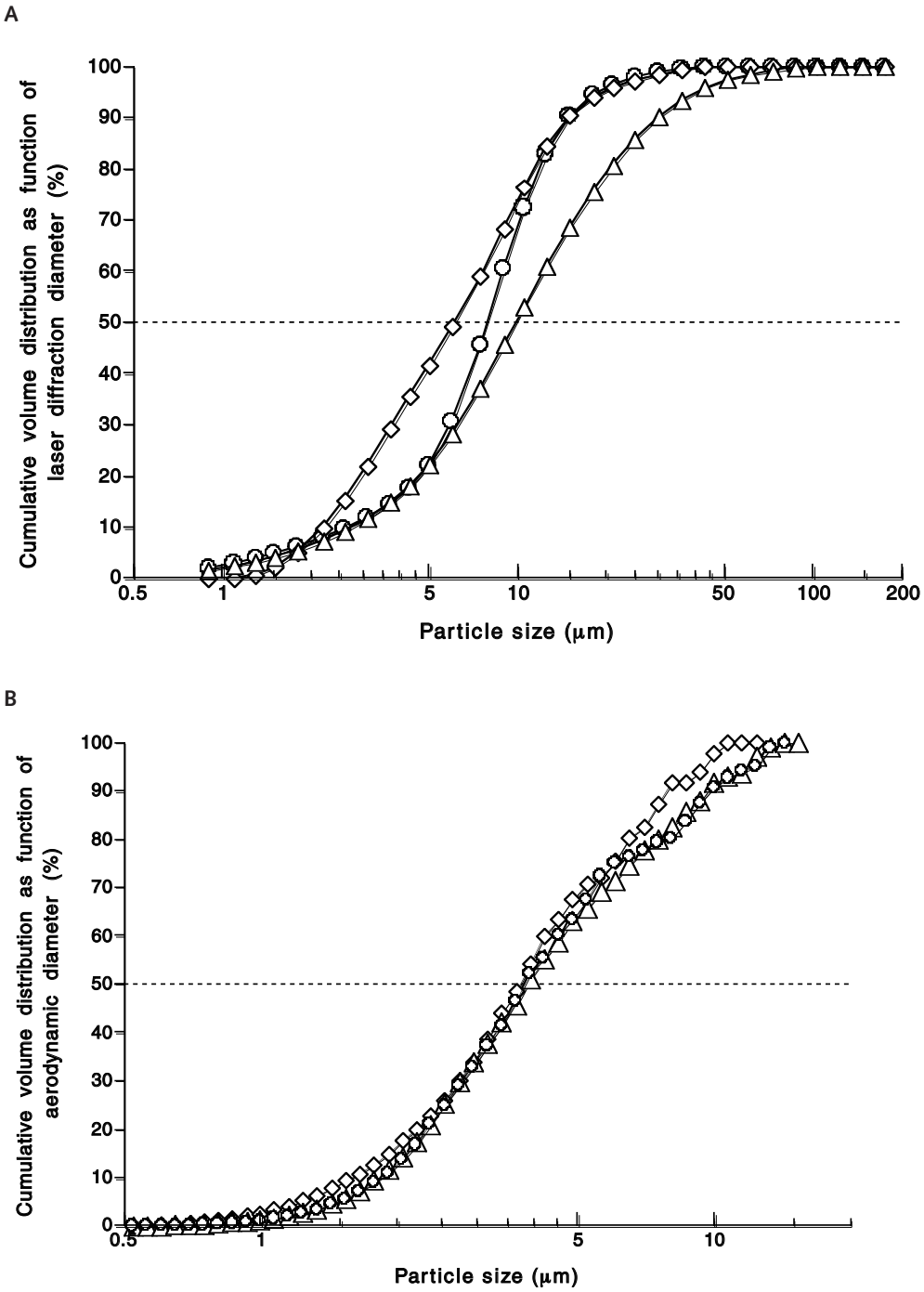

Figure 3. (A) Cumulative volume distribution curves as function of laser diffraction diameter and (B) cumulative volume distribution curves as function of aerodynamic diameter measured with APS of dried insulin formulations. (○) TMC60-insulin; (△) TMC20-insulin; (◊) dextran-insulin particles.

The VMADs of the microparticles, as determined by the time-of-flight technique and the mean volume diameters (VMD), as determined by laser diffraction are given in table 1. The VMADs of the TMC and dextran particles were about 4 μm, which is suitable for reaching peripheral respiratory tract (1, 4, 34). The VMADs of the TMC20-insulin and TMC60-insulin particles were significantly smaller than their VMDs (table 1), which indicates that the TMC-insulin particles were either porous or hollow and consequently had a density below one. The VMAD of the dextran-insulin powders was also smaller than the VMD. However, the difference between VMAD and VMD is substantially smaller for the dextran-insulin particles than observed for the TMC-insulin particles, which indicates that the dextran particles are less porous than TMC particles. CLSM images of the FITC-insulin TMC microparticles (figure 4) shows that both small and large particles were loaded with FITC-insulin. Z-scan images of the FITC-insulin particles (figure 4) indicated that the FITC-insulin was homogeneously distributed over the individual particles. From the CLSM analysis and aerodynamic size characterization it can be concluded that the particles are porous but not hollow, because, FITC-insulin was distributed over the whole particles and not solely present in the shell.

Table 1 shows the water content of the freshly prepared particles. The water content of the powders was around 4% (w/w). However, water content neither resulted in particle agglomeration nor collapse (see section 3.4.1.).

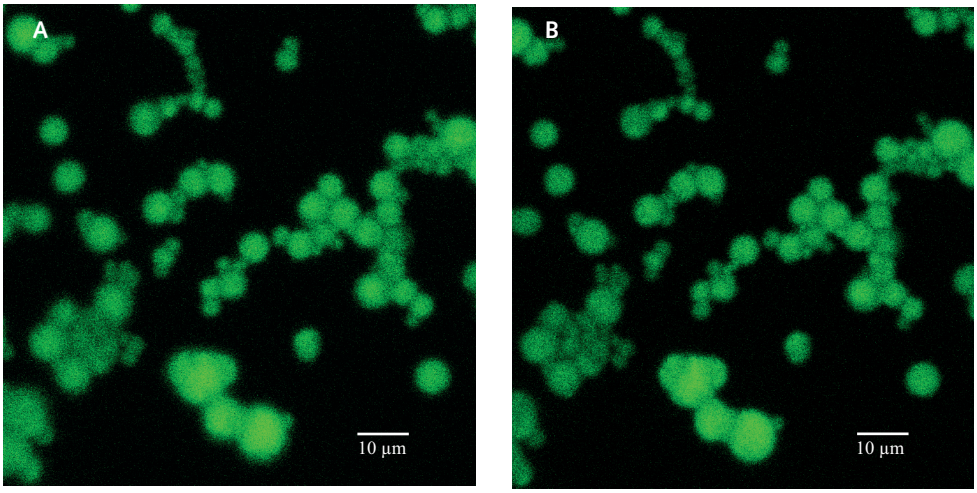

Figure 4. CLSM images of FITC-labeled insulin-TMC microparticles (image B is one μm deeper inside the microparticles than image A).

3.3 Insulin loading and structural integrity

HPLC analyses of insulin after dissolution of the powders showed that the loading was 9.0-9.7% which is close to the feed ratio (10%). Moreover, no peaks indicative for chemical degradation products were detected.
Possible formation of covalent insulin aggregates (e.g. due to disulfide reshuffling) as a result of the SCF process was studied with GPC analysis. For GPC analysis, the particles were dissolved in 20% (v/v) acetic acid in water, a solvent in which non-covalent dimers dissociate (29). The recovery of insulin was 100% for the TMC60 and dextran formulations, which means that all insulin present in these formulations was dissolved and eluted afterwards. It was not possible to analyze the TMC20-insulin formulation with GPC because of the low solubility of TMC20 in the elution buffer (PBS, pH 7.4). Figure 5 shows the GPC chromatograms of the insulin formulations. Both UV and RALS detection revealed a peak with an elution volume of ca. 15.5 ml for native insulin, and insulin formulated in dextran and TMC60 microparticles. This elution volume corresponds to monomeric insulin (6000 g/mol). No additional peaks that would indicate the presence of covalent dimers were detected. TMC60-insulin particles showed a broad peak at a retention volume of 8.5 ml. This peak was also seen for TMC60 polymer alone, which showed tailing and was partly overlapped with the insulin peak (figure 5).

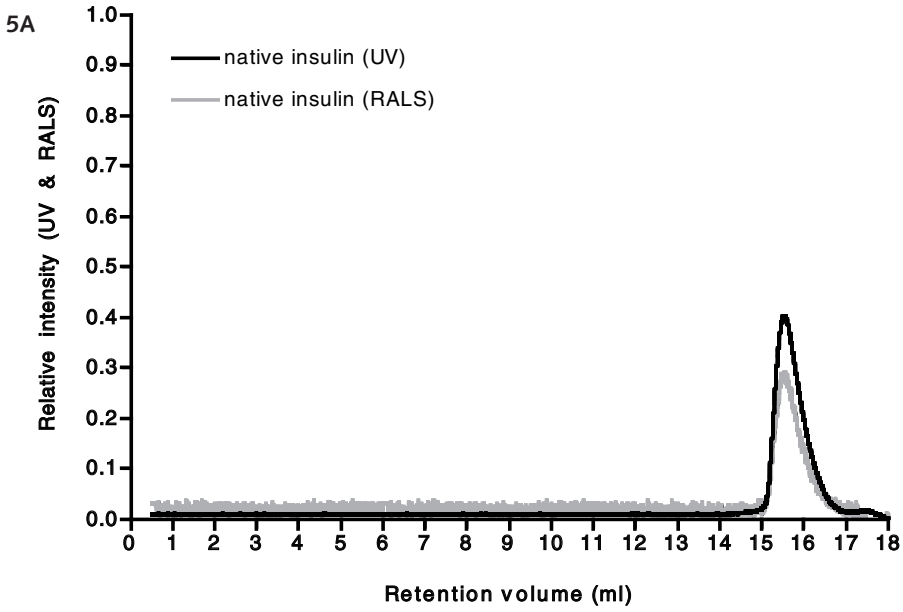

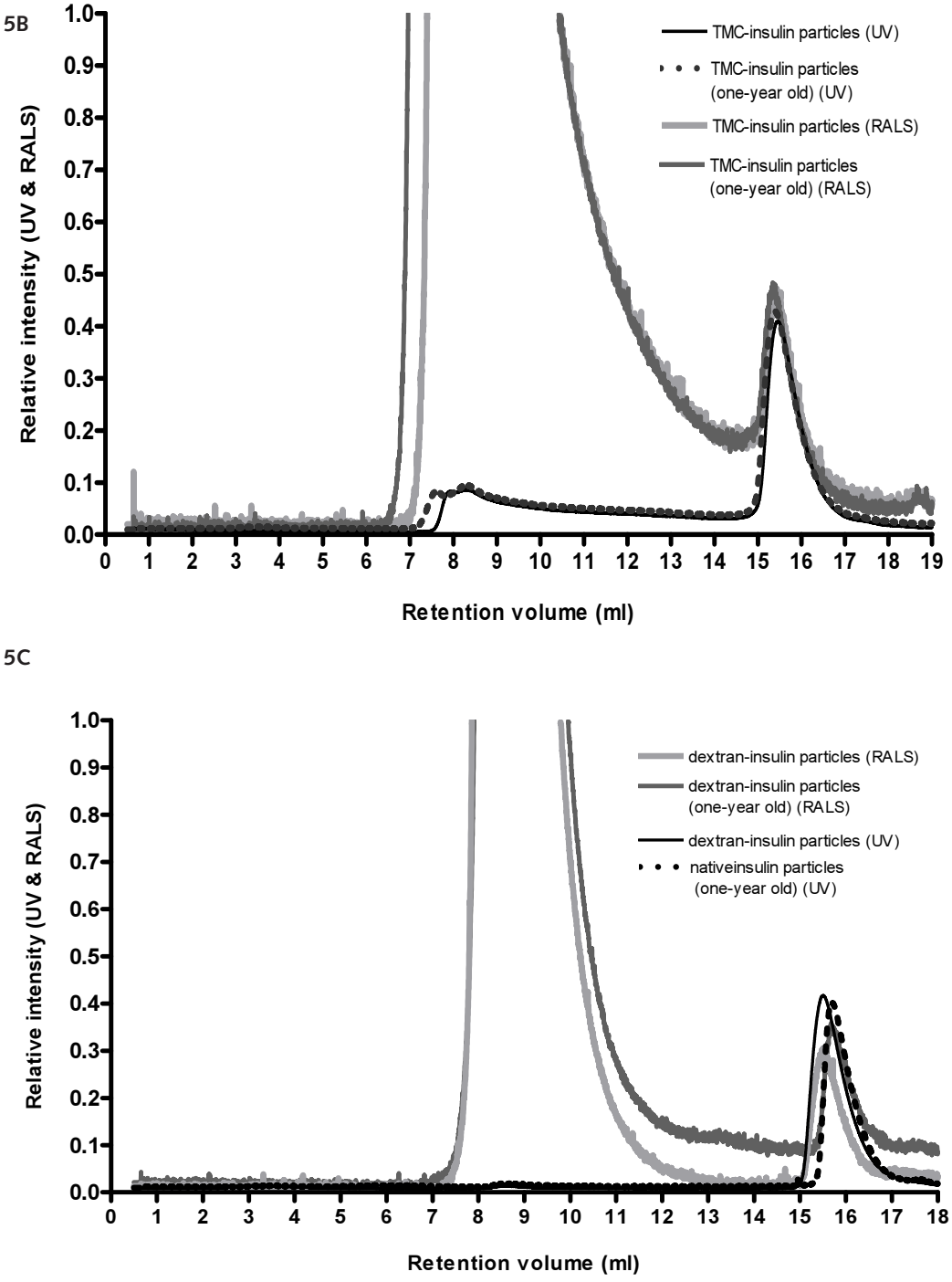

Figure 5. GPC chromatograms of the dried insulin formulations. (A) native insulin; (B) TMC60-insulin particles; (C) dextran-insulin particles.

Possible changes in the three-dimensional structure of insulin due to the drying process were monitored by circular dichroism (CD) spectroscopy. Near-UV CD was used to gain information about the tertiary structure, whereas far-UV CD gives information about the secondary structure (32). Insulin-loaded TMC/dextran particles and native insulin were dissolved in 0.01 M HCl. At pH 2, insulin (pI = 5.3) is positively charged and consequently electrostatic interactions with TMC are minimized. Furthermore, at this pH equilibrium exists between insulin in its monomeric and dimeric form (30, 35). The CD spectra obtained after dissolution of freshly prepared insulin formulations are shown in figures 6A and B. Figure 6A shows the near-UV CD spectra of the different insulin samples. Insulin exhibits one peak at 255 nm characteristic for phenylalanines (3 per insulin molecule) and a broad peak around 276 nm, characteristic for tyrosines (4 per insulin molecule) (35, 36). These signals are mainly attributed to the interactions in the monomer-monomer interface of the dimers (35). The CD spectrum of insulin in the presence of TMC20 or TMC60 was the same as that of native insulin (data not shown). In comparison with native insulin, the CD spectrum of the dissolved insulin-loaded TMC and dextran particles shows an increase of the signal at a vicinity of 276 nm, indicating subtle changes in the tyrosine environments (35-37). There were no significant spectral changes at 255 nm characteristic of phenylalanine in insulin (figure 6A). The overall spectral shape was essentially retained, which indicates that the tertiary structure was largely preserved.

Far-UV CD spectra are shown in figure 6B. Native insulin exhibits a spectrum with minima at 210 and 222 nm, which is typical for a protein with an α-helical structure. No significant spectral changes in shape and intensity were observed after dissolution of TMC60-insulin particles compared to native insulin (figure 6B). Small increases were observed in the vicinity of 224 and 210 nm in the spectra of the insulin-dextran and TMC20-insulin particles (figure 6B), which indicates minor increases in the α-helical structure. The results of near-UV and far-UV CD indicate that the secondary and the tertiary structure of the insulin were mainly preserved during the drying sprocess.

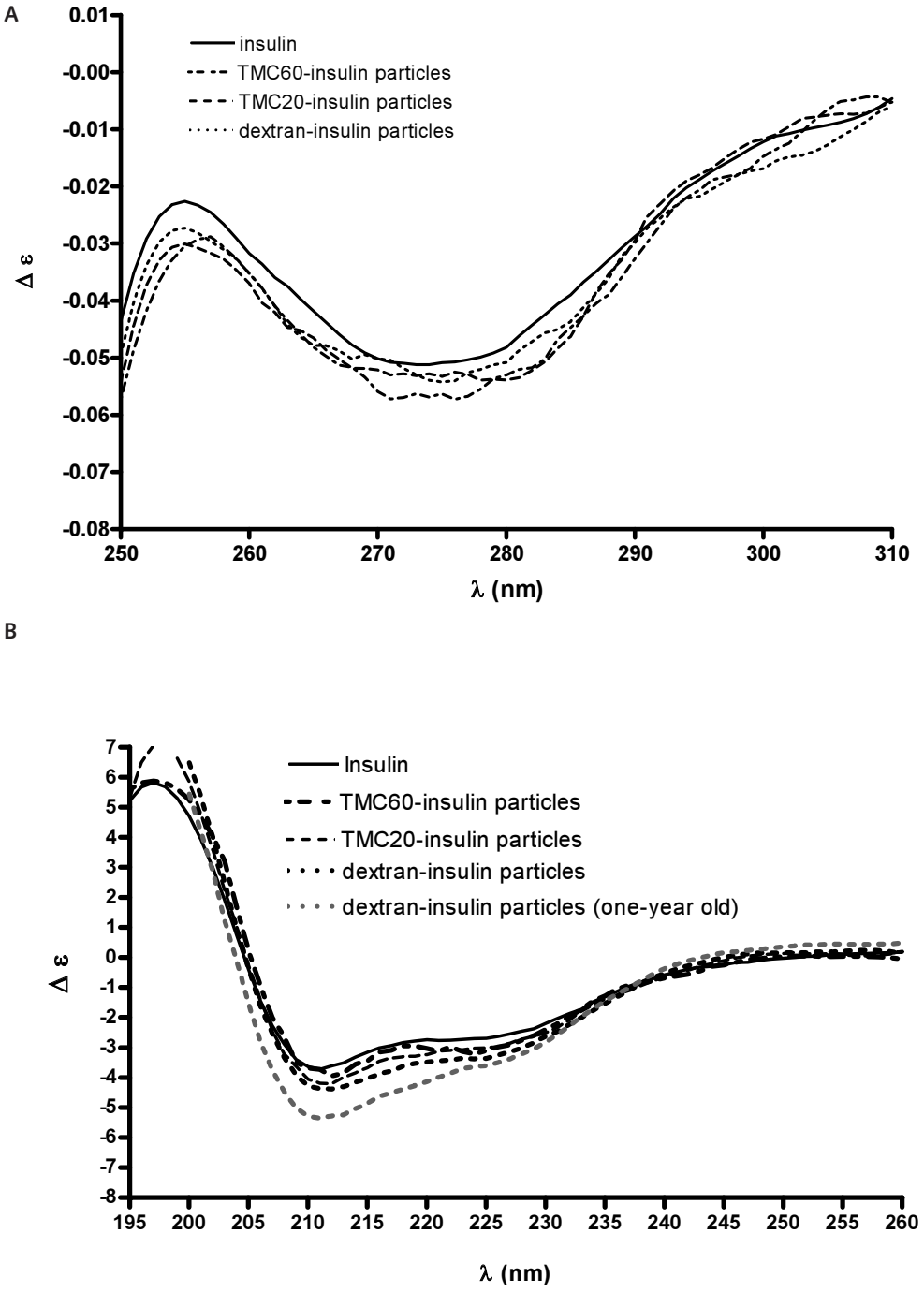

Figure 6. Conformational analysis of insulin dry powders by CD spectroscopy. (A) Near-UV CD spectra; (B) far-UV CD spectra

The tertiary structure of the insulin was also studied by fluorescence spectroscopy. Figure 7 shows the fluorescence spectra of the samples, dissolved in 0.01 M HCl. Dextran- and TMC-insulin formulations showed similar fluorescence intensities as native insulin with an emission maximum at 305 nm, indicating that the tertiary structure of insulin was preserved. These results are in agreement with the near-UV CD data.

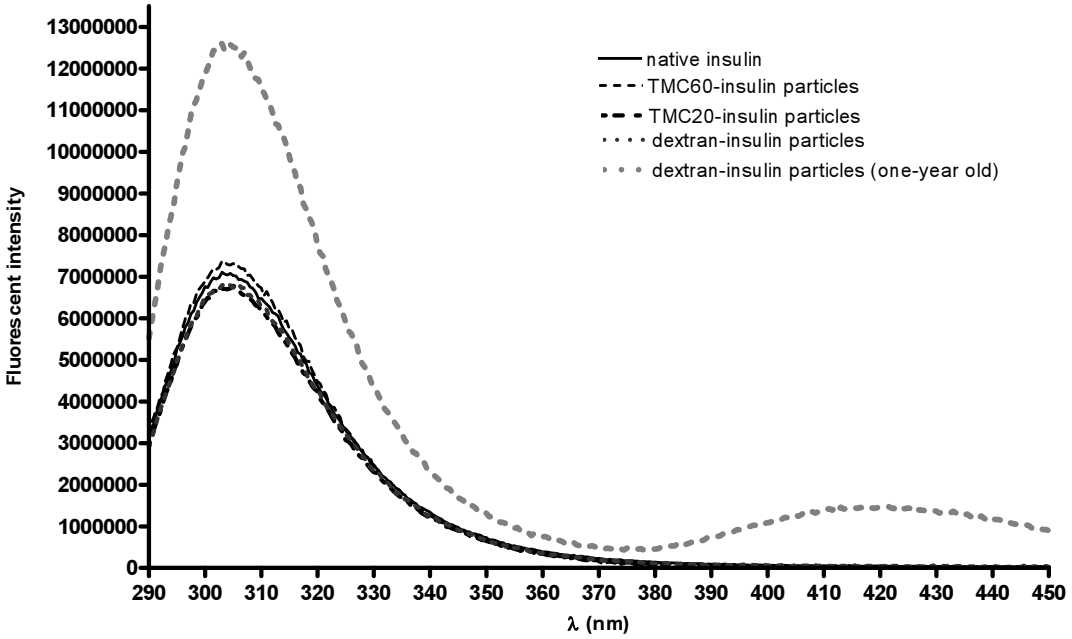

Figure 7. Fluorescence emission spectra of the insulin dried formulations.

3.4 Characterization of the aged insulin microparticle formulations

3.4.1 Particle size

After one year storage at 4 °C in closed bottles, the powders were still free flowing. Moreover, the particle size distributions, as measured by laser diffraction analysis, were comparable to those of the freshly prepared particles (shown in table 1), indicating that the dried particles were stable in time and that neither aggregation nor particle collapse had occurred upon storage.

3.4.2 Structural integrity of insulin

The insulin integrity in the formulations stored for 1 year at 4 ºC was compared with the insulin structure in the freshly prepared batches. The HPLC chromatograms of the aged TMC-insulin particles showed a single peak, representative of insulin. In contrast, the dextran-insulin formulation showed an extra peak at higher retention time of insulin (data not shown), which might be due to degraded (e.g., deamidation

of asparagine residues) insulin (38). The percentage of the degradation product was less than 10% (w/w) of the total insulin content. Fluorescence spectroscopic analysis of the aged insulin powders indicates some extent of tyrosine oxidation (see the fluorescence spectrometry results, below). These oxidized products are more hydrophilic than native insulin and consequently are expected to have a shorter retention time in HPLC. However, such peaks were not detected and likely these oxidized products co-elute with native insulin as previously demonstrated for methionine oxidized interleukin 2 (39).

Possible formation of covalent insulin aggregates during the storage of the dried formulations was studied with GPC analysis. The recovery of insulin was 100% which means that all insulin present in the formulation was dissolved and eluted afterwards. The GPC chromatograms of the aged insulin formulations are shown in figure 5B and C. The chromatograms of the aged dextran- and TMC60-insulin powders largely overlapped with those of the freshly prepared formulations. No other peaks were detected that correspond to higher or lower molecular weight components, indicating that neither chain cleavage occurred nor covalent aggregates were formed. Both the TMC60 and dextran peak showed tailing and partly overlapped with the insulin peak (figure 5). The secondary and tertiary structures of insulin after one-year storage of the dried insulin formulations were investigated by far and near UV CD. The CD spectra of TMC60- and TMC20-insulin and the near-UV CD spectrum of dextran-insulin did not substantially change, except that there was a slight increase in intensity, which may either be due to slight conformational changes but more likely reflect a calibration error in the protein assay because different insulin standards were used. In comparison with native insulin, the far-UV CD spectrum of the dissolved insulin-loaded dextran particles (figure 6B) showed an increase of the signals particularly at a vicinity of 210 nm, showing increase of α-helical structure and reduced accessibility of tyrosines (29, 36) and consequently, subtle changes in the secondary structure of insulin.

The tertiary structure of insulin after storage for 1 year at 4 ºC was also studied by fluorescence spectroscopy. Both TMC-insulin powders showed after dissolution a slight increase in fluorescence intensity compared to that of native insulin. The fluorescence peaks (emission maximum 305 nm) did not shift to a higher or lower wavelength, which indicates that the tertiary structure of insulin was preserved (data not shown). These results are in agreement with the near-UV CD data. Dextran-insulin particles showed a significant increase in fluorescence intensity at 305 nm plus an extra peak around 410 nm (figure 7). The increase in the intensity of the tyrosine emission peak suggests a conformational change (40), whereas the newly formed emission peak at higher wavelengths (ca. 410 nm) is indicative of tyrosine oxidation (41).

Altogether, the aging study revealed that the insulin structure of the TMC-insulin formulations was essentially preserved after storage for 1 year at 4 ºC, whereas the aged dextran-insulin formulations showed both chemical and physical degradation of the protein.

4 Conclusions

This study demonstrates that SCF drying is a suitable method to produce inhalable insulin powders with defined particle characteristics and preserved structure of insulin. Porous spherical TMC and dextran particles had similar VMAD of approx. 4 μm, which should yield a comparable pulmonary deposition and consequently allow a direct comparison of the particles in *in vivo* studies under comparable inspiratory conditions. The applicability and potential of these polymeric-insulin powders as pulmonary delivery systems will be studied in the following chapter.

Acknowledgments

We thank Bas Vermeulen (Feyecon D & I B.V.) for his technical help to prepare SCF dried powders. Paul Hagedoorn (Department of Pharmaceutical Technology and Biopharmacy, University of Groningen) is acknowledged for the LD measurements of the insulin powders. We are grateful to Mies J. van Steenbergen (Department of Pharmaceutics, Utrecht Institute for Pharmaceutical Sciences, Utrecht University) for GPC measurements of insulin.

References

1. J. S. Patton. Mechanisms of macromolecules absorption by the lungs. *Adv Drug Del Rev* 19: 3-36 (1996).

2. D. R. Owens, B. Zinman, and G. Bollit. Alternative routes of insulin delivery. *Diabet Med* 20: 886-898 (2003).

3. J. S. Patton, C. S. Fishburn, and J. G. Weers. The lungs as a portal of entry for systemic drug delivery. *Proc Am Thorac Soc* 1: 338-44 (2004).

4. S. P. Newman, A. Hollingworth, and A. R. Clark. Effect of different modes of inhalation on drug delivery from a dry powder inhaler. *Int J Pharm* 102: 127-132 (1994).

5. M. C. Manning, K. Patel, and R. T. Borchardt. Stability of protein pharmaceuticals. *Pharm Res* 6: 903-918 (1989).

6. J. F. Carpenterand M. C. Manning. *Rational Design of Stable Protein Formulations, Theory and Practice*, Kluwer Academic/ Plenum Publishers, New York, 2002.

7. A. Hussain, Q. H. Majumder, and F. Ahsan. Inhaled insulin is better absorbed when administered as a dry powder compared to solution in the presence or absence of alkylglycosides. *Pharm Res* 23: 138-47 (2006).

8. S. D. Yeo, G. B. Lim, P. G. Debenedetti, and H. Bernstein. Formation of microparticulate protein powders using a supercritical fluid antisolvent. *Biotech Bioeng* 41: 341-346 (1993).

9. N. Elvassore, A. Bertucco, and P. Caliceti. Production of insulin-loaded poly(ethylene glycol)/poly(l-lactide) (PEG/PLA) nano-particles by gas antisolvent techniques. *J Pharm Sci* 90: 1628–1636 (2001).

10. N. Jovanovic, A. Bouchard, G. W. Hofland, G. J. Witkamp, D. J. A. Crommelin, and W. Jiskoot. Distinct effects of sucrose and trehalose on protein stability during supercritical fluid drying and freeze-drying. *Eur J Pharm Sci* 27: 336-45 (2006).

11. N. Jovanovic, A. Bouchard, G. W. Hofland, G. J. Witkamp, D. J. A. Crommelin, and W. Jiskoot. Stabilization of proteins in dry powder formulations using supercritical fluid technology. *Pharm Res* 21: 1955-69 (2004).

12. M. Tservistas, M. S. Levy, M. Y. Lo-Yim, R. D. O'Kennedy, P. York, G. O. Humphrey, and M. Hoare. The formation of plasmid DNA loaded pharmaceutical powders using supercritical fluid technology. *Biotech Bioeng* 72: 12-18 (2001).

13. E. Reverchon. Supercritical antisolvent precipitation of micro-and nano-particles. *J Supercrit Fluids* 15: 1-21 (1999).

14. P. M. Gallagher, M. P. Coffey, V. J. Krukonis, and N. Klasutis. Gas antisolvent recrystallization: new process to recrystallize compounds insoluble in supercritical fluids. *ACS Symp Ser* 406: 334–354 (1989).

15. H. Todo, H. Okamoto, K. Iida, and K. Danjo. Improvement of stability and absorbability of dry insulin powder for inhalation by powder-combination technique. *Int J Pharm* 271: 41-52 (2004).

16. I. M. van der Lubben, G. Kersten, M. M. Fretz, C. Beuvery, J. C. Verhoef, and H. E. Junginger. Chitosan microparticles for mucosal vaccination against diphtheria: oral and nasal efficacy studies in mice. *Vaccine* 28: 1400-1408 (2003).

17. I. M. van der Lubben, F. A. Konings, G. Borchard, J. C. Verhoef, and H. E. Junginger. In vivo uptake of chitosan microparticles by murine Peyer's patches: visualization studies using confocal laser scanning microscopy and immunohistochemistry. *J Drug Target* 9: 39-47 (2001).

18. P. Calvo, C. Remunan-Lopez, J. L. Vila-Jato, and M. J. Alonso. Chitosan and chitosan/ethylene oxide-propylene oxide block copolymer nanoparticles as novel carriers for proteins and vaccines. *Pharm Res* 14: 1431-1436 (1997).

19. R. Fernandez-Urrusuno, P. Calvo, C. Remunan-Lopez, J. L. Vila-Jato, and J. A. Alonso. Enhancement of nasal absorption of Insulin using chitosan nanopartocles. *Pharm. Res.* 16: 1576-1581 (1999).

20. M. Amidi, S. G. Romeijn, G. Borchard, H. E. Junginger, W. E. Hennink, and W. Jiskoot. Preparation and characterization of protein-loaded N-trimethyl chitosan nanoparticles as nasal delivery system. *J Control Release* 111: 107-116 (2006).

21. A. Vila, A. Sanchez, K. Janes, I. Behrens, T. Kissel, J. L. Vila Jato, and M. J. Alonso. Low molecular weight chitosan nanoparticles as new carriers for nasal vaccine delivery in mice. *Eur. J. Pharm. Biopharm.* 57: 123-131 (2004).

22. J. H. Hamman, M. Stander, and A. F. Kotzé. Effect of the degree of quaternization of N-trimethyl chitosan chloride on absorption enhancement: in vivo evaluation in rat nasal epithelia. *Int J Pharm* 232: 235-242 (2002).

23. M. Thanou, J. C. Verhoef, J. H. M. Verheijden, and H. E. Junginger. Intestinal absorption of octeriotide: N-trimethyl chitosan chloride (TMC) ameliorates the permeability and absorption properties of the somatostatin analogue in vitro and in vivo. *J Pharm Sci* 89: 951-957 (2000).

24. D. Snyman, J. H. Hamman, and A. F. Kotze. Evaluation of the mucoadhesive properties of N-trimethyl chitosan chloride. *Drug Dev. Ind. Pharm.* 29: 61-9 (2003).

25. X. Jiang, A. van der Horst, M. J. van Steenbergen, N. Akeroyd, C. F. van Nostrum, P. J. Schoenmakers, and W. E. Hennink. Molar-mass characterization of cationic polymers for gene delivery by aqueous size-exclusion chromatography. *Pharm Res* 23: 595-603 (2006).

26. A. B. Sieval, M. Thanou, A. F. Kotzé, J. C. Verhoef, J. Brussee, and H. E. Junginger. Preparation and NMR- characterisation of highly substituted N-trimethyl chitosan chloride. *Carbohydr Polym* 36: 157-165 (1998).

27. Y. Pérez de Diego, H. C. Pellikaan, F. E. Wubbolts, G. Borchard, G. J. Witkamp, and P. J. Jansens. Opening new operating windows for polymer and protein micronisation using the PCA process. *J Supercrit Fluids* 36: 216-224 (2006).

28. Y. Pérez de Diego, F. E. Wubbolts, G. J. Witkamp, P. J. Jansens, and T. W. de Loos. Improved PCA process for the production of nano- and microparticles of polymers. 50: 2408-2417 (2004).

29. A. Ahmad, I. S. Millett, S. Doniach, V. N. Uversky, and A. L. Fink. Stimulation of insulin fibrillation by urea-induced intermediates. *J Biol Chem* 279: 14999-5013 (2004).

30. B. Metz, G. F. Kersten, G. J. Baart, A. de Jong, H. Meiring, J. ten Hove, M. J. van Steenbergen, W. E. Hennink, D. J. A. Crommelin, and W. Jiskoot. Identification of formaldehyde-induced modifications in proteins: reactions with insulin. *Bioconjug Chem* 17: 815-22 (2006).

31. J. Demeester, S. S. de Smedt, N. N. Sanders, and J. Haustraete. Light scattering. In D. J. A. Crommelin (ed), *Methods for structural analysis of protein pharmaceuticals* (D. J. A. Crommelin, ed), AAPS Press, Arlington, 2005, pp. 245-76.

32. M. Bloemendaland W. Jiskoot. Circular dichroism spectroscopy. In D. J. A. Crommelin (ed), *Methods for structural analysis of protein pharmaceuticals* (D. J. A. Crommelin, ed), AAPS Press, Arlington, 2005, pp. 83-130.

33. Y. Pérez de Diego, F. E. Wubbolts, G. J. Witkamp, T. W. de Loos, and P. J. Jansens. Measurements of the phase behaviour of the system dextran/DMSO/CO2 at high pressures. *J Supercrit Fluids* 35: 1-9 (2005).

34. M. P. Timsina, G. P. Martin, C. Marriott, D. Ganderton, and M. Yianneskis. Drug delivery to the respiratory tract using dry powder inhalers. *Int J Pharm* 101: 1-13 (1994).

35. K. Huus, S. Havelund, H. B. Olsen, M. van de Weert, and S. Frokjaer. Thermal dissociation and unfolding of insulin. *Biochemistry* 44: 11171-7 (2005).

36. A. Ahmad, I. S. Millett, S. Doniach, V. N. Uversky, and A. L. Fink. Partially folded intermediates in insulin fibrillation. *Biochemistry* 42: 11404-16 (2003).

37. E. H. Stricklandand D. Mercola. Near-ultraviolet tyrosyl circular dichroism of pig insulin monomers, dimers, and hexamers. Dipole-dipole coupling calculations in the monopole approximation. *Biochemistry* 15: 3875-84 (1976).

38. J. Brange. Chemical stability of insulin. 4. Mechanisms and kinetics of chemical transformations in pharmaceutical formulation. *Acta Pharm Nord* 4: 209-22 (1992).

39. J. A. Cadee, M. J. van Steenbergen, C. Versluis, A. J. Heck, W. J. Underberg, W. den Otter, W. Jiskoot, and W. E. Hennink. Oxidation of recombinant human interleukin-2 by potassium peroxodisulfate. *Pharm Res* 18: 1461-7 (2001).

40. J. R. Lakowicz. *Principles of fluorescence spectroscopy*, Kluwer/Plenum Press, New York, 1999.

41. C. Arigita, L. Bevaart, L. A. Everse, G. A. Koning, W. E. Hennink, D. J. A. Crommelin, J. G. van de Winkel, M. J. van Vugt, G. F. Kersten, and W. Jiskoot. Stability of mono- and trivalent meningococcal outer membrane vesicle vaccines. *Infect Immun* 71: 5210-8 (2003).

Chapter five

Efficacy of pulmonary insulin delivery in diabetic rats: Use of a model-based approach in the evaluation of insulin powder formulations

Maryam Amidi[1]
Kevin M. Krudys[2]
Cor J. Snel[1]
Daan J.A. Crommelin[1]
Oscar E. Della Pasqua[2,3]
Wim E. Hennink[1]
Wim Jiskoot[1,4]

[1] Department of Pharmaceutics, Utrecht Institute for Pharmaceutical Sciences, Utrecht University, PO Box 80082, 3508 TB Utrecht, The Netherlands

[2] Division of Clinical Pharmacology and Discovery Medicine, GlaxoSmithKline (GSK), Greenford, United Kingdom.

[3] Division of Pharmacology, Leiden/Amsterdam Center for Drug Research (LACDR), Leiden University, P.O. Box 9502, 2300 RA Leiden, The Netherlands

[4] Division of Drug Delivery Technology, Leiden/Amsterdam Center for Drug Research (LACDR), Leiden University, P.O. Box 9502, 2300 RA Leiden, The Netherlands

Submitted for publication

Abstract

In the present study, the potential of N-trimethyl chitosan (TMC) with two degree of quaternization (DQ), TMC20 (DQ 20%, as a mucoadhesive) and TMC60 (DQ 60%, as a mucoadhesive and a permeation enhancer), and dextran (as a non-mucoadhesive and non-permeation enhancer) microparticles as carriers for pulmonary delivery of insulin were studied in diabetic rats. Using a population pharmacokinetic-pharmacodynamic (PKPD) model, we have evaluated the impact of different delivery forms on insulin bioavailability as well as on its pharmacological effects, as measured by insulin sensitivity and glucose disappearance. In addition, possible acute adverse effects of these microparticles were examined by histological studies of the lungs of the treated rats.

The insulin loaded microparticles were prepared by supercritical fluid (SCF) drying technique. The median volume diameter of the particles, as determined by laser diffraction technique and median volume aerodynamic of the particles, as measured by time-of-flight technique were 6-10 μm and about 4 μm, respectively. Pulmonary administration of TMC60-insulin microparticles showed significant systemic absorption of insulin, compared to those of dextran- and TMC20-insulin microparticles. The bioavailability of the pulmonarily administered dextran-, TMC20- and TMC60-insulin microparticles relative to subcutaneous (SC) administered insulin, was 0.48, 0.59 and 0.95, respectively. A decrease of blood glucose concentration after SC and pulmonary administration of insulin formulations was observed.

The insulin powders did not result in toxicity or inflammatory reaction on the respiratory epithelium. The PD model (the minimal model of glucose disappearance) could describe the insulin-glucose relationship and pharmacodynamic efficiency of insulin formulations, which was about 0.6 independent of the formulations. The current findings suggest that TMC microparticles are a promising vehicle for pulmonary delivery of insulin.

Keywords: N-Trimethyl chitosan microparticles; super critical carbon dioxide; pulmonary delivery; insulin; pharmacokinetic; pharmacodynamic

1 Introduction

Currently, chronic insulin therapy is based on multiple daily subcutaneous (SC) injections, which cause discomfort for patients. In addition, SC administered insulin is absorbed rather slowly from the injection site, which does not reflect its natural secretion profile by the pancreas. Therefore, in recent years alternative dosage forms for injectable insulin formulations have been pursued which avoid the regular injections and give a faster absorption rate (1, 2). In this respect studies have been initiated to develop oral (3, 4), intranasal (5) and pulmonary formulations. In particular, pulmonary administration of insulin has recently demonstrated an acceptable glucose control in diabetic patients (1, 2, 6).

The respiratory tract, with a large surface area (~75 m^2), extensive vasculature, a thin membrane and low enzymatic activity, is an attractive site for the delivery of peptides and proteins (2, 7). The transport of these macromolecular therapeutics across the absorptive area, the alveolar wall, occurs through tight-junctional paracellular processes for protein < 22 kDa (7). Protein/peptide loaded particles, either in the form of droplets (aerosol) or powders, with an aerodynamic diameter between 1.5-3 μm deeply deposit into the lung and have access to a large absorptive site, the alveoli (7-9). The major factors limiting pulmonary absorption of the proteins are the poor deposition of the protein formulations at the alveolar region, the low absorption across these epithelial barriers and the mucociliary escalator, by which process protein formulations are removed from the central respiratory tract and that prevents the access of the protein to the alveoli. Small proteins, such as insulin, are able to cross the alveoli, without the use of penetration enhancers, and enter the systemic circulation. However, in humans the bioavailability of pulmonary administered insulin without penetration enhancer is low (8), which is to a large extent due to enzymatic degradation of insulin in the lung. In animals, it has been shown that addition of protease inhibitors (referred to 'absorption enhancers') to inhalable insulin formulations substantially improved the relative bioavailability up to 70% (10-14) and also reduces the risk of adverse effects of insulin on the tissue of patients undergoing chronic diabetic therapy (15). The absorption of insulin from the respiratory epithelium likely can be improved by using permeation enhancers, compounds which are capable to open the tight junctions between the epithelial cells. Chitosan is a mucoadhesive polymer and able to open the tight junctions only at low pH. Both properties may help to enhance the uptake of protein formulated in chitosan microparticles (3, 5, 16, 17). In contrast to chitosan, which is soluble at low pH and insoluble at neutral pH, N-trimethyl chitosan chloride (TMC), a partially quaternized chitosan derivative, shows good water solubility over a wide pH range. Hence, soluble TMC has mucoadhesive properties and, dependent on its degree of quaternization, also absorption enhancing effects even at neutral pH (18-20). TMC with a low degree of quaternization (DQ 20%) has only mucoadhesive properties and with a higher DQ (60%), it has shown strong mucoadhesive and absorption enhancing effect (18, 21, 22). Because of these properties, TMC is an attractive alternative to chitosan for the

design of protein-loaded particles.
In the present study, TMC20 (as a mucoadhesive), TMC60 (as a mucoadhesive and a permeation enhancer) and dextran (as a non-mucoadhesive and non-permeation enhancer) microparticles were prepared by supercritical fluid (SCF) drying technique. This process, using carbon dioxide as an anti-solvent, has been used to prepare dried protein formulations and offers the possibility to produce small microparticles suitable for inhalation (14, 23, 24). The potential of the dried insulin formulations on promoting pulmonary absorption of insulin was studied in diabetic rats and compared to that of subcutaneous administration. Furthermore, the relative bioavailability and pharmacodynamic efficiency of the inhaled insulin formulations were determined and safety and possible acute adverse effects of these microparticles were examined by histological evaluation of the lungs of the treated rats.
The description of the pharmacokinetic (PK) and pharmacodynamic (PD) properties of non-injectable insulin formulations is often performed in terms of a non-compartmental analysis in which parameters such as maximal insulin concentration (C_{max}), time of maximum serum insulin concentration (t_{max}), minimum glucose concentration and time to reach minimum glucose concentration are obtained (11). However, this approach does not describe the pharmacological action of absorbed insulin on glucose disappearance. Therefore, we used an integrated PKPD model to describe the pharmacological effects of the administered insulin in terms of glucose disposition, and insulin sensitivity.

2 Materials and methods

2.1 Materials

Chitosan (M_n = 40 kDa, M_w = 177 kDa, determined by gel permeation chromatography (GPC) using poly(ethylene glycol) (PEG) standards (25); degree of deacetylation 93%) was a generous gift from Primex (Avaldsnes, Norway). N-Trimethyl chitosan with degrees of quaternization (DQ) of 20 and 60% were synthesized by methylation of chitosan by using CH_3I in the presence of a strong base (NaOH) and analyzed by ^{1}H-nuclear magnetic resonance (NMR) spectroscopy, as previously described (26). Dextran (Mw: 64-76 kDa), recombinant human insulin (M=5807 g/mol, 29 IU/mg), Streptozocin (STZ), hematoxylin and eosin were purchased from Sigma-Aldrich (Schnelldorf, Germany). Dimethyl sulfoxide (DMSO) was purchased from Across Organics. All other chemicals used were obtained from commercial suppliers and were of analytical grade.

2.2 Preparation and characterization of dextran- and TMC-insulin microparticles

Insulin-loaded TMCs (DQ: 20 & 60%) and dextran microparticles were prepared by supercritical fluid (SCF) CO_2 drying process, and characterized as described in Chapter four of this thesis.

2.3 Induction of diabetes in rats

Male Sprague-Dawley rats weighing 250-300 g (Charles River, Netherlands) were housed in groups of 4 rats and maintained in the animal facility of Utrecht University with a 12 h day and night schedule, while food and water were ad libitum. The rats received intravenously Streptozocin (STZ), 45 mg/kg dissolved in an ice-cold 0.5 molar citrate buffer (pH 4.5). Induction of diabetes was confirmed by monitoring the blood glucose levels using a glucose-meter, Accu-Chek Sensor System (Roche Diagnostics Inc., Almere, The Netherlands). A blood glucose concentration above 250 mg/dl (15 mmol/l) was used as the cutoff for diabetes. Insulin treatments were initiated after allowing the diabetes state to stabilize over 3-4 days and the rats were fasted for 12 hours prior to experiments but had free access to water.

2.4 Intratracheal and subcutaneous administrations of insulin formulations

Dextran- or TMC20/60-insulin microparticles containing 1.25 IU of insulin were administered intratracheally in the rats (4 per group) using a dry powder inhaler device, DP-4 insufflator™ (PENN CENTURY Inc, Philadelphia, USA). Prior to administration of the formulations the animals were anaesthetized by an intraperitoneal injection of urethane (1.5 g/kg) in physiological saline. Ninety minutes later, the rat was rested on its back at an angle of 45°. A clear view of the trachea was provided by inserting a fiber optic laryngoscope (Penn Century Inc., Philadelphia, USA) into the mouth of the animal. Then, the needle of the DP-4 insufflator attached to an air pump (AP-1™, PENN CENTURY Inc, Philadelphia, USA) was inserted into the trachea. Subsequently, the insulin powder particles deposited in the insufflator were delivered into the rat's lungs. As controls, two groups of diabetic rats received placebo microparticles (dextran and TMC60). For subcutaneous (SC) administration, first insulin was dissolved in 0.01 M HCl, subsequently the pH was adjusted to 7.4 with NaOH 1 M and diluted with 10 mmol PBS. Afterwards, four anesthetized rats received insulin injections (volume 200µl, dose 1.25 IU) into their dorsal flank.
Blood samples (200 µl) were collected from the jugular vein of the animals at time 0 (prior to administration) and 15, 30, 45, 60, 90, 120, 150 and 180 minutes after the administration of the insulin formulation. The blood samples were collected in heparinized micro-centrifuge tubes supplemented with complete mini EDTA-free protease inhibitor cocktail (Roch Diagnostics, Almere,The Netherlands) to prevent insulin degradation. The blood glucose concentration in the samples was determined shortly after collection using

a glucose meter (Roche Diagnostics Inc., Almere, The Netherlands). Plasma was obtained by centrifugation of the blood samples at 2000 ´ g for 3 min and stored at – 20 °C until analysis. The insulin concentration in the different plasma samples was determined using a human insulin-specific ELISA kit (Linco Research Inc., St. Charles, USA). The rats were sacrificed by withdrawing their entire blood volume through their jugular vein. Thereafter, the lungs were excised, inflated with a formaldehyde solution 4% (v/w) in physiological saline, fixed and stored at 4 °C until further histological examination.

2.5 Lung histology

The formaldehyde-treated lungs were dehydrated and embedded in paraffin. Slices of 5 µm thickness were sectioned and stained with a regular hematoxylin/eosin staining. Histological evaluation was performed by using a light microscope equipped with a digital camera. Photographs were taken using a 40 x magnification objective.

2.6 Pharmacokinetic & pharmacodynamic analysis

2.6.1 Pharmacokinetic analysis

The pharmacokinetics of insulin in the diabetic rats was analyzed by a one-compartment disposition model with first-order absorption using the following equation:

$$I(t) = \frac{K_a FD}{V(K_a - K)}\left[e^{-Kt} - e^{-K_a t}\right] \quad (1)$$

where V is the volume of distribution (ml), D is dose, F is the relative bioavailability and K_a and K (min^{-1}) are the absorption and elimination rate constants of insulin from plasma, respectively. The bioavailability of the dextran, TMC60 and TMC20 insulin formulations ($F_{dextran}$, F_{TMC60} and F_{TMC20}) are reported as relative to the subcutaneous dose, for which F was set equal to 1. Otherwise, the formulation was assumed to have no effect on the other parameters of the PK model. A proportional error model was used to describe residual variability in insulin concentrations. Similar to a previous study (Gopalakrishnan et al., 2005), we observed an unexpected rise in insulin concentration at the last sampling time in two animals. Since the rise in insulin did not correspond to changes in plasma glucose concentration, these data points were excluded from the modeling analysis. Statistical analysis was performed by one-way ANOVA test.

2.6.2 Pharmacodynamic analysis

The minimal model of glucose disappearance (27) was used to describe the effect of insulin on glucose kinetics. Glucose disappearance is enhanced by glucose independent of insulin as well as by glucose dependent on insulin acting from a compartment remote from plasma. Remote insulin levels increase as a result of rising

plasma insulin levels and insulin is cleared through a first-order process. The minimal model of glucose disappearance is given by the following equations:

$$\frac{dG(t)}{dt} = -[S_G + X(t)]G(t) + S_G G_b \qquad G(0) = G_0 \tag{2}$$

$$\frac{dX(t)}{dt} = -p_2\{X(t) - S_I[I(t) - I_b]\} \qquad X(0) = 0 \tag{3}$$

where G(t) (mg/dl) is the plasma glucose concentration, I(t) (μU/ml) is the plasma insulin concentration and G_b and I_b are their basal values. X(t) (min^{-1}) is insulin action. The model equations yield four uniquely identifiable parameters: G_0 (mg/dl), the baseline level of glucose; p_2 (min^{-1}), the insulin action parameter; S_G (min^{-1}), glucose effectiveness; and S_I (min^{-1} μU^{-1} ml), insulin sensitivity parameter. Equation 2 represents two interacting factors which determine the lowering of plasma glucose, namely, the glucose effectiveness (S_G), reflecting the ability of glucose *per se* to stimulate glucose disposal and inhibit glucose production and insulin action (X(t)), which is the effect of insulin in the interstitial compartment. Equation 3 represents the flux of insulin from plasma into the interstitial compartment where it acts; the insulin action parameter (p_2) controls the rate with which insulin moves from plasma to interstitial fluid, where it exerts its action on glucose uptake and the insulin sensitivity parameter (S_I) represents the ability of insulin to enhance the stimulation of glucose disposal and/or inhibition of glucose production indicating how efficient insulin can facilitate glucose uptake. A combined additive and proportional error model was used to describe residual variability in glucose concentrations.

2.6.3 Parameter estimation

A population approach was used for numerical identification of model parameters. PK and PD model parameters were estimated sequentially from glucose and insulin data using the first order conditional estimation (FOCE) method in NONMEM (28). PK model parameters were estimated in the first step, and were subsequently used as the input to the PD model. Inter-individual variability was quantifiable for the parameters K, G_0, p_2 and S_I which were assumed to arise from lognormal distributions. The goodness of fit was assessed by examining plots of predicted *versus* observed concentrations and weighted residuals versus time.

2.6.4 Pharmacodynamic efficiency

Pharmacodynamic efficiency is defined as:

$$Efficiency = \frac{AAEC}{AUC} \tag{4}$$

where AUC is the area under the plasma insulin concentration curve and AAEC is the concentration above the effect curve (normalized for baseline glucose levels). Pharmacological efficiency is a weighted measure of response per unit concentration. It is particularly useful to assess improvement in drug delivery or formulations.

3 Results

3.1 Histological evaluation of lung tissue

Administration of the various formulations directly into the lung did not result in any tissue damage and/or infiltration of immune cells like neutrophils (figure 1). From figure 1 it can also be seen that the bronchioles and alveolar cells in treated animals do not differ from those of the non-treated animals.

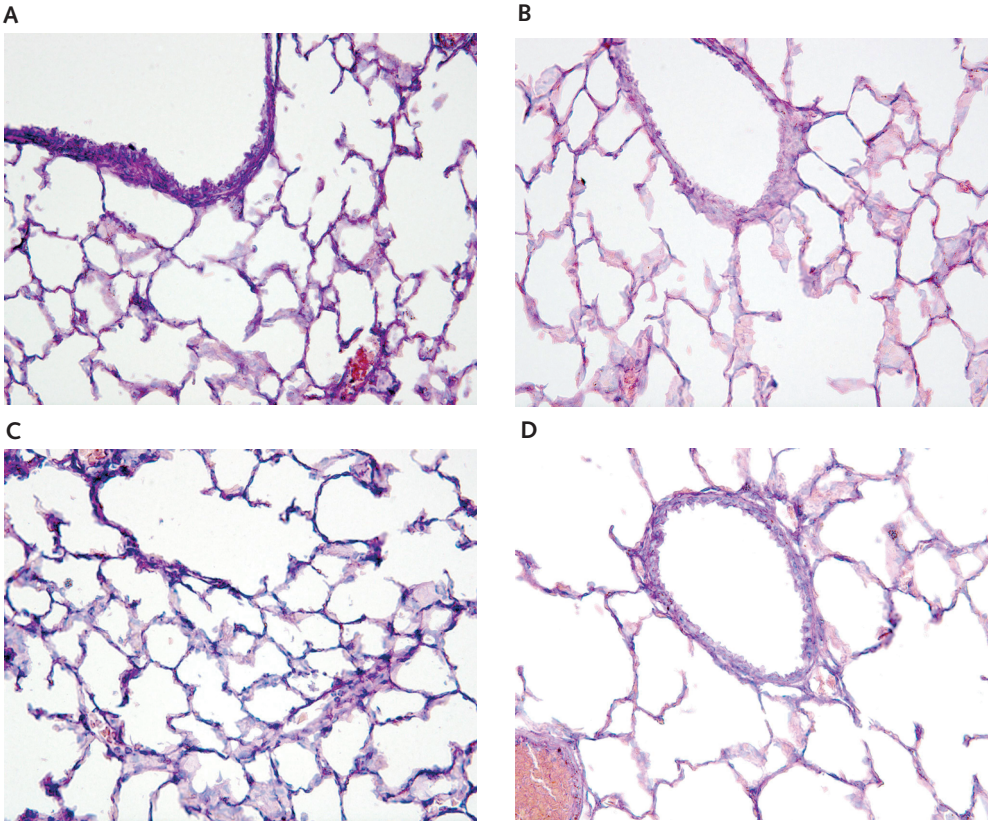

Figure 1. Representative photographs of lung tissue 3 hours post administration of the different formulations (A: TMC60-insulin, B: TMC20-insulin C: dextran-insulin); D: untreated.

Table 1. Particle characteristics of the dried insulin formulations

Dried insulin formulations	Characteristic laser diffraction mean diameter VMD (µm)	VMAD (µm)
TMC60-insulin microparticles	7.9	4.0
TMC20-insulin microparticles	9.9	4.1
Dextran-insulin microparticles	6.1	3.9

3.2 Preparation and characterization of the insulin microparticles

Full details about particle preparation and characterization are given in Chapter four of this thesis. Table 1 summarizes the main characteristics of the particles. The volume median diameters (VMDs) of the TMC20/60- and dextran-insulin microparticles, as determined by laser diffraction technique, and the volume median aerodynamic diameters (VMADs), as determined by time-of-flight technique were about 4 µm, which is the appropriate aerodynamic size for reaching peripheral lungs (7-9).

3.3 Pharmacokinetics

Plasma insulin concentration-time profiles of the rats receiving the different insulin formulations are shown in figure 2A. Pulmonary administration of TMC20 and TMC60-insulin microparticles (further referred to as 'TMC20/60-insulin') and SC insulin injections (further referred to as 'SC-insulin') resulted in maximum plasma concentration at about 30 minutes, whereas for pulmonary administered dextran-insulin (further referred to as 'dextran-insulin') peak was reached at 45 minutes post administration. The plasma insulin concentration for the SC-insulin showed a rapid decrease after having reached its maximum. In contrast, after TMC60- or dextran-insulin the plasma concentration showed a plateau for around one hour (30-90 min post administration), whereas for TMC20-insulin the plasma concentration remained constant for the investigated time, 30-180 minutes post administration. The pharmacokinetics of insulin could be described by a one-compartment disposition model with first-order absorption (equation 1). The estimated fixed effect parameters and respective inter-individual variability are listed in table 2. The residual proportional error of insulin was 22% (standard error (SE), 21%). TMC60-insulin had the highest relative bioavailability to SC-insulin (F; 0.96), whereas F for TMC20-insulin and dextran-insulin were significantly lower (0.59 and 0.48, $p < 0.05$, respectively). Distinct observations, population predictions and individual predictions for PK model in representative rats for the four different administration groups are shown in figure 3A.

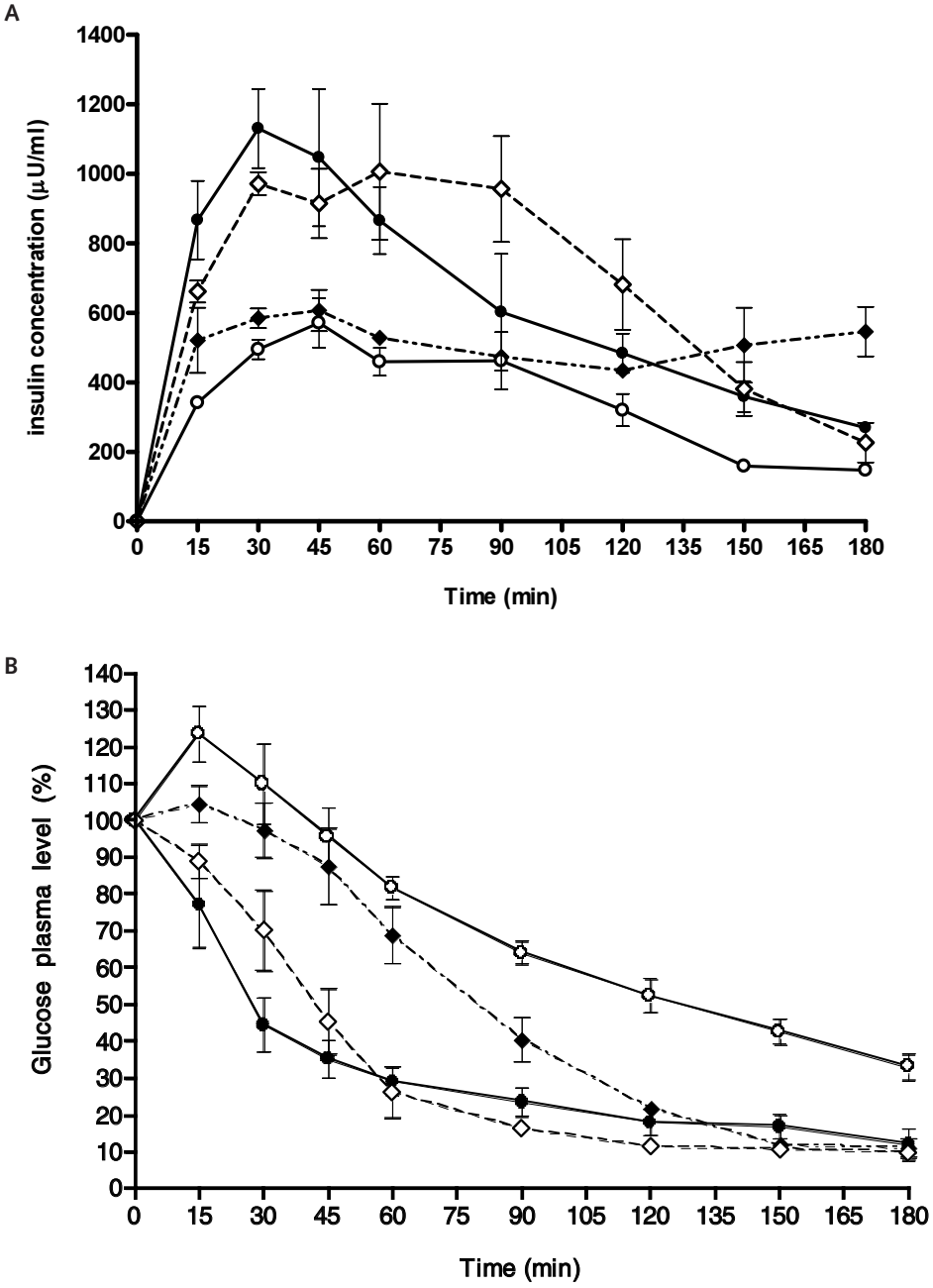

Figure 2. Plasma insulin concentration-time curve (A) and plasma glucose level-time curve (B) of rats that received pulmonarily TMC60-insulin microparticles (◊), TMC20-insulin microparticles (□), dextran-insulin microparticles (○) or SC free insulin in PBS (●). The insulin dose was 1.25 IU per animal. Data are expressed as mean ± SD (n = 4). Glucose plasma concentrations are normalized to baseline levels prior to insulin administration.

3.4 Pharmacodynamics

The time course of blood glucose after administration of the different insulin formulations is shown in figure 2B. During the first 60 minutes post-administration, a rapid decrease of the blood glucose levels for SC- and TMC60-insulin was observed. This was followed by a subsequent slow decrease, which lasted for up to 2 hours. In contrast, the reduction of blood glucose levels occurred with substantially slower kinetics for TMC20- and dextran-insulin. For TMC20-insulin, glucose levels comparable to TMC60- and SC-insulin were reached 120 minutes post-administration, while for dextran-insulin the glucose levels remained significantly higher. Rats that received placebo TMC or dextran particles showed constant glucose levels throughout the experiment (results not shown). Blood glucose levels were analyzed using the minimal model of glucose disappearance (equations 2 and 3). The population pharmacodynamic parameters and their inter-individual variability are presented in the table 2.
The residual proportional error of glucose was 9% (SE, 49%) and the additive error was 20 mg/dl (SE, 68%). Distinct observations, population predictions and individual predictions for PD model in representative rats for the four different administration groups are shown in figure 3B. The pharmacodynamic efficiency (calculated using equation 4) was about 0.6, independent of the formulation (table 3).

Table 2. Pharmacokinetic (PK) and pharmacodynamic (PD) parameter estimates

Parameter	Population mean (SE%)	Inter-individual variability CV% (SE%)
V/F[1] (ml)	668 (25)	
K (min^{-1})	0.012 (25)	19 (66)
K_a (min^{-1})	0.039 (33)	
$F_{dextran}$	0.48 (13)	
F_{TMC20}	0.59 (14)	
F_{TMC60}	0.95 (15)	
G_0 (mg/dl)	485 (12)	46 (43)
S_G (min^{-1})	0.002 (20)	
p_2 (min^{-1})	0.10 (88)	201(75)
S_I (10^4 min^{-1} μU^{-1} ml)	0.33 (13)	32 (66)

[1] V/F: apparent volume distribution (since we did not administer insulin intravenously, it was not possible to calculate the real volume distribution); CV: coefficient of variation; SE: standard error; for explanation of other symbols, see sections 2.6.1 and 2.6.2.

Table 3. Pharmacodynamic efficiency of the different insulin formulations

Formulation	Pharmacodynamic efficiency
TMC60-insulin	0.60 ± 0.01
TMC20-insulin	0.62 ± 0.03
dextran-insulin	0.64 ± 0.09
Insulin in PBS	0.58 ± 0.01

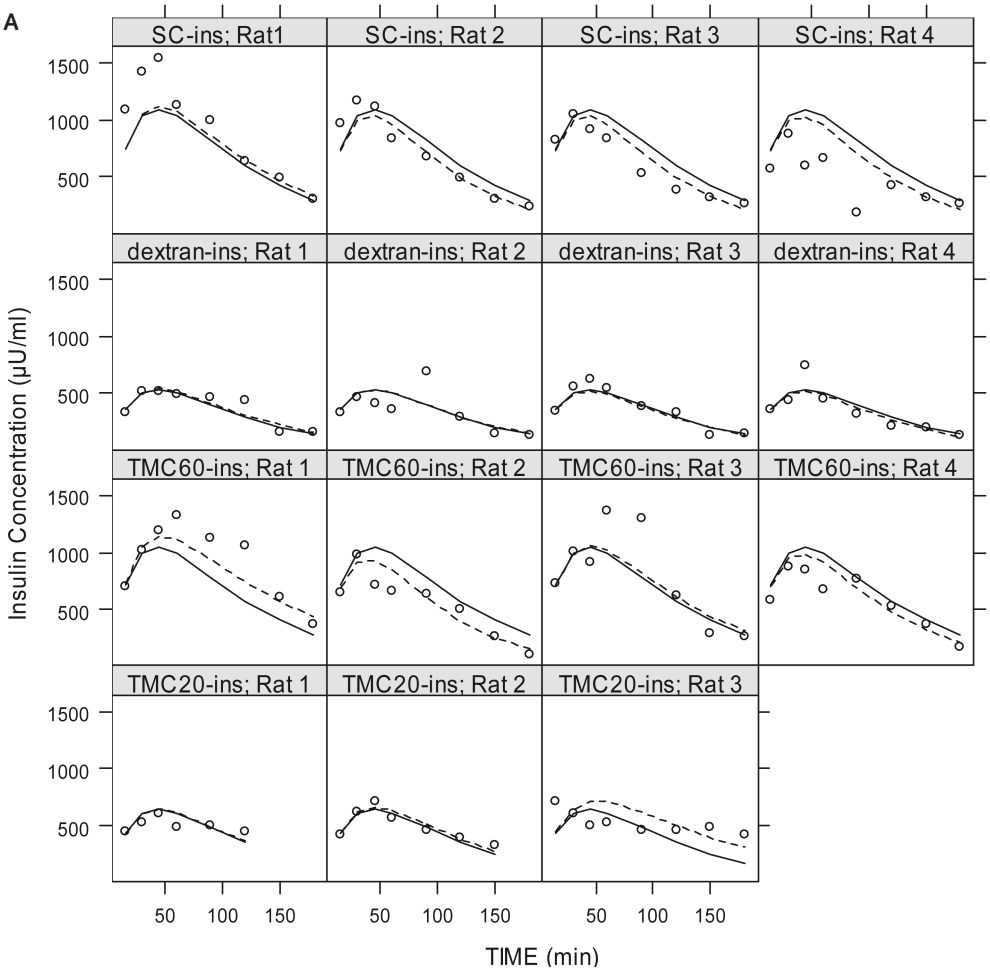
A
SC-ins; Rat1
SC-ins; Rat 2
SC-ins; Rat 3
SC-ins; Rat 4
dextran-ins; Rat 1
dextran-ins; Rat 2
dextran-ins; Rat 3
dextran-ins; Rat 4
TMC60-ins; Rat 1
TMC60-ins; Rat 2
TMC60-ins; Rat 3
TMC60-ins; Rat 4
TMC20-ins; Rat 1
TMC20-ins; Rat 2
TMC20-ins; Rat 3
Insulin Concentration (µU/ml)
1500
1000
500
50
100
150
TIME (min)

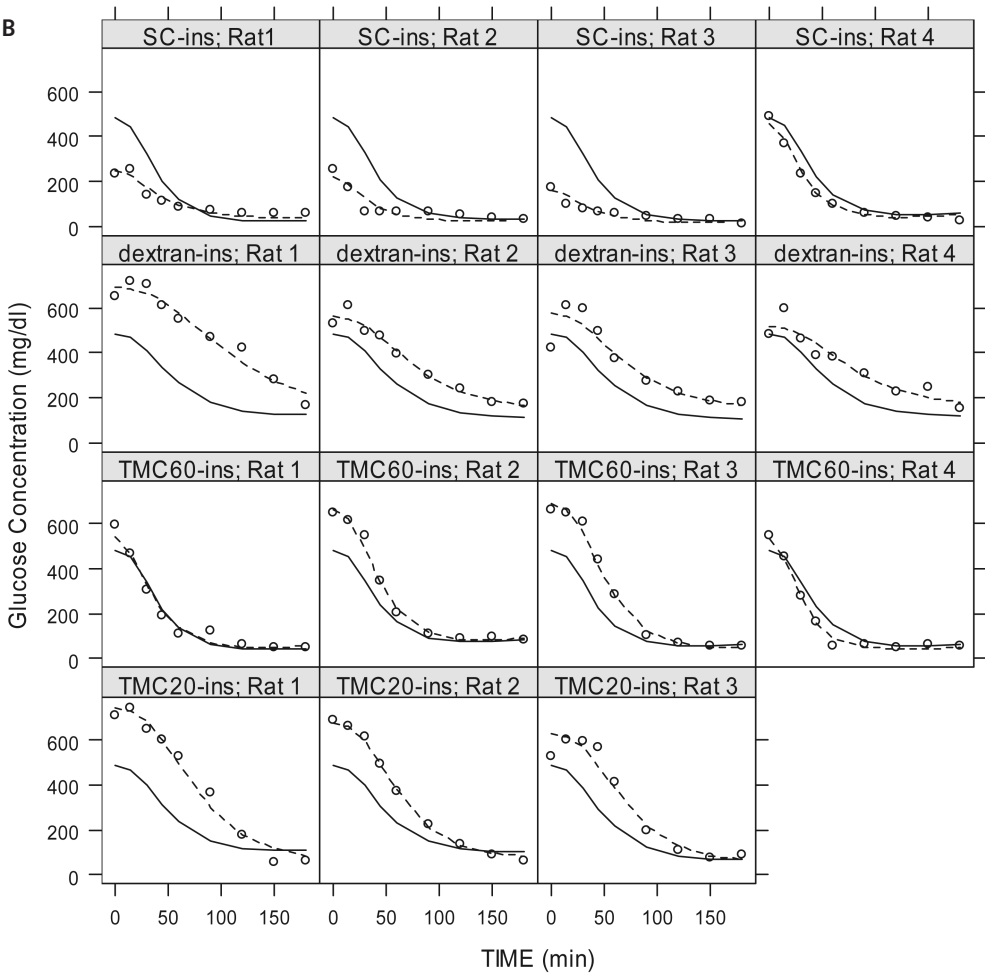

Figure 3. Population (dash line) and individual (solid line) predictions and observations (○) for PK (A) and PD (B) models in representative rats for the four different administrations.

Goodness-of-fit for insulin are illustrated in figures 4A and 5A. Goodness-of-fit for glucose are shown in figures 4B and 5B.

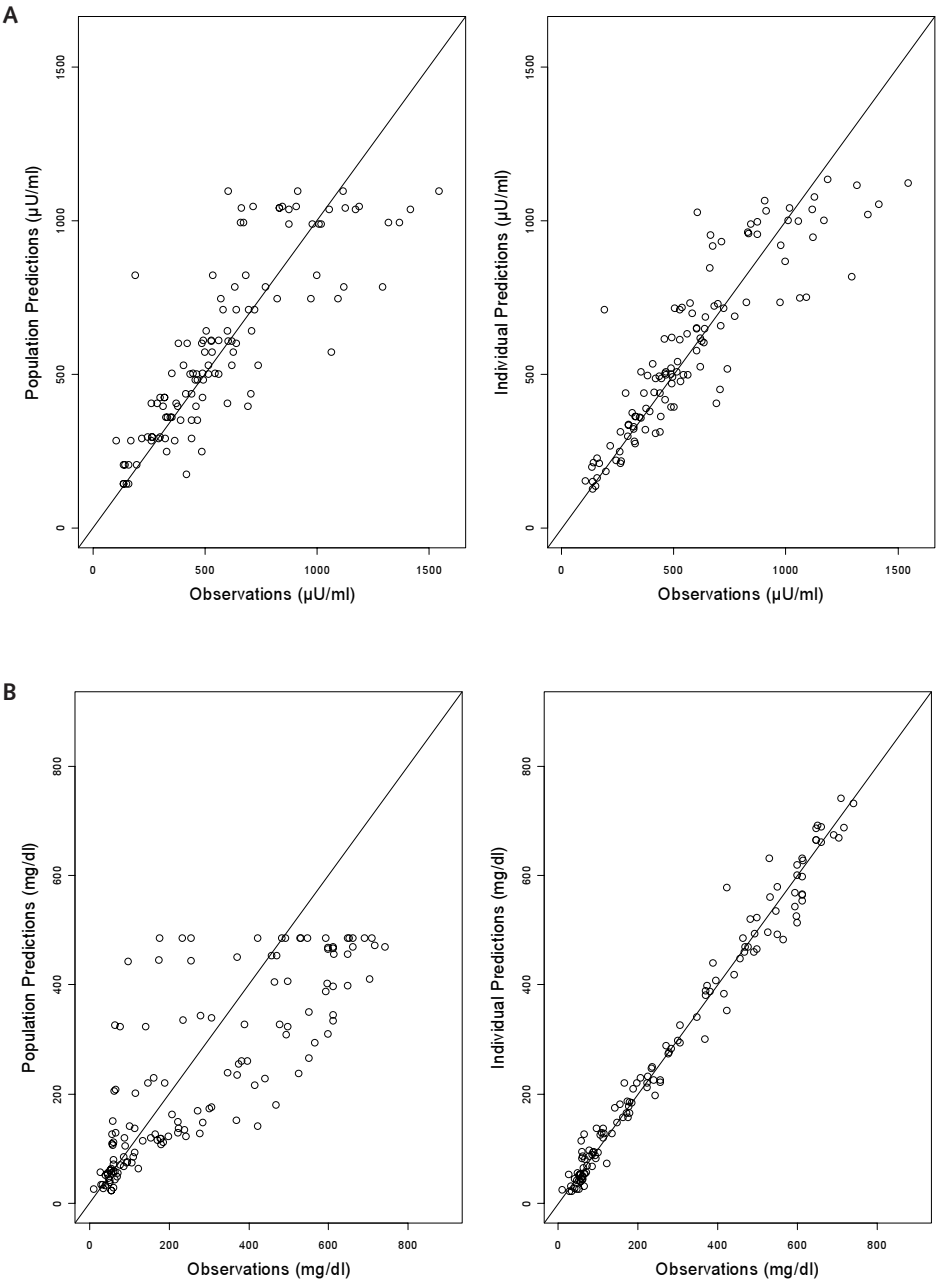

Figure 4. Population and individual predictions versus observations for PK (plasma insulin concentration; A) and PD (plasma glucose concentration; B) models for the four different formulations.

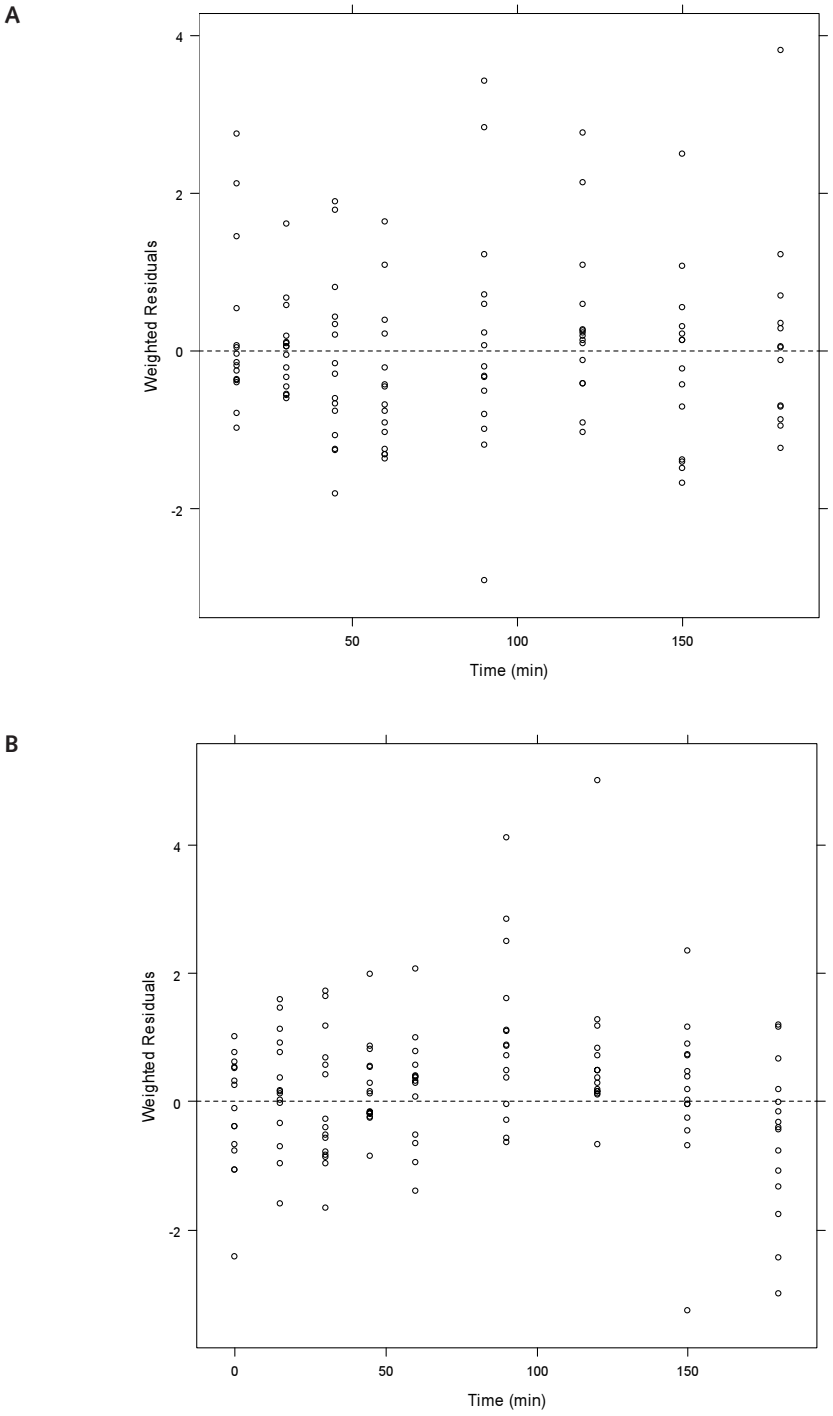

Figure 5. Weighted residuals versus time for PK (plasma insulin concentration; A) and PD (plasma glucose concentration; B) models for the four different formulations.

4 Discussion

In this study, the potential of microparticles composed of soluble, mucoadhesive and permeation enhancing polymers (TMC 20 and 60) for the pulmonary delivery of insulin was investigated. TMC20 and TMC60 loaded insulin as well as dextran (a non-permeation enhancing polymer) microparticles were prepared by SCF. In chapter 4 it was demonstrated that the insulin microparticles had comparable aerodynamic diameters (VMAD of 4 μm) suitable for pulmonary delivery, whereas their VMDs were significantly larger (table 1). This is favorable, because it has been shown that particles with a geometric mean diameter >3 μm are barely taken up by alveolar macrophages (29). The alveolar epithelium is covered with a very thin aqueous layer (less than 1 μm) and the central respiratory epithelium is covered with a mucous layer of about 5 μm (7). In both media the microparticles will dissolve slowly. The larger particles likely stay longer as they might not be taken up rapidly by alveolar macrophages.

The pharmacokinetic analysis showed that TMC20- and dextran-insulin had a relative bioavailability of 0.59 and 0.48, respectively (table 2), which were comparable or superior to those of previous studies also using non-penetration enhancers (13, 30). It has been shown that after pulmonary administration of powders, different fractions are deposited in the different areas of the lungs, depending on the aerodynamic size of the particles, their physical characteristics and the physiology of the recipient. For the insulin-loaded particles that reached the alveoli, insulin molecules can be absorbed through paracellular passive diffusion into the blood (7, 8). In contrast, the permeability of the central respiratory epithelium is markedly less than that of the alveoli. Moreover, the mucus layer, covering the epithelium and the mucociliary escalator, which rapidly removes protein formulations from the lungs, are additional barriers for protein absorption. This means that for the TMC20- and dextran-insulin the absorbed insulin is likely due to the fraction of particles deposited in the alveoli. The observed higher bioavailability for the TMC60-insulin (0.95 table 2) as compared to TMC20- and dextran-insulin can be ascribed to the mucoadhesive and the permeation enhancing activity of TMC60 (19, 21, 22, 31), which contribute to improve the absorption of the insulin at the alveoli and the epithelium in the central respiratory tract. The observed relative bioavailability of the insulin formulations also show, as pointed out above, that enzymatic degradation due to particle uptake by alveolar macrophages is probably low. Moreover, ionic interactions of positively charged TMC with insulin (pI: 5.3) might protect the protein against enzymatic degradation by proteases present in the lung lumen.

Figure 2 shows that the insulin plasma concentration after SC administration decreased rapidly after its maximum at 30 min. This profile is rather different from those previously reported, which show delayed and prolonged absorption (6).

The plasma insulin concentration of TMC60-insulin also had a short lasting peak which was maintained for one hour, whereas TMC20-insulin showed a lower, but a long lasting (up to 3 hours) plateau insulin level. Dextran-insulin showed a time

course similar to that of TMC60-insulin but at a lower insulin plasma concentration. Subcutaneous and/or pulmonary absorption of the insulin are complex processes, which are influenced by many factors such as local blood flow and/or local insulin degradation (32). The observed insulin concentration-time profiles indicate that the pulmonarily administered insulin is absorbed for a prolonged period, which may be due to the slow dissolution of the particles in the thin fluid layer covering the lung epithelium. The prolonged plasma insulin concentration after administration of TMC20-insulin particles is likely due to their slower dissolution as compared to the TMC60 and dextran particles (unpublished results). Unfortunately, the PKPD model could not estimate an individual absorption constant for the formulations, because the number of data points for plasma insulin concentrations during the absorption phase was too low.

From figure 2A and 2B it appears that in the different groups the maximum glucose suppression occurred at a later time than the insulin concentration peak. In several studies, effect compartmental models have been used to describe the action of insulin on glucose (33). These models presume a distributional delay for insulin to reach its site of action, but do not explicitly describe the different physiological effects of insulin and glucose to inhibit glucose production and stimulate glucose uptake. In the minimal model of glucose disappearance used in our study, two important physiological facts are considered. Firstly, the effect of glucose itself to normalize its own concentration (e.g. mass action plus allosteric effect of hexose on protein kinase C) as well as the catalytic effect of insulin to allow glucose to self-normalize due to mobilization of glucose transporter four (GLUT4). Secondly, the effect of insulin on glucose disappearance, which is a slow process, since insulin must first move from plasma to a remote compartment (e.g. interstitial fluid) to exert its action on glucose disposal (34).

Table 2 shows that the PD model provides reliable estimates for G_0 and S_I with inter-individual variability (CV%) of 46% and 32%, respectively. The population mean and inter-individual variability of p_2, however, were poorly estimated, which may be due to the experimental design or the inability of the data to clearly distinguish the contributions of the related parameters p_2 and S_I. The PD model could estimate an S_G value equal to 0.002 min^{-1} for all rats. In this study, the glucose effectiveness (S_G) and insulin sensitivity (S_I) values are considerably lower than those previously reported (35). To our knowledge, this is first time that estimates for insulin-glucose homeoastasis are generated for STZ-induced diabetic rats. The lower values found for S_G and S_I are likely to reflect disease status in this experimental model of diabetes, whereas the data from Natalucci et al were obtained in healthy animals (35) . In fact, Blondeland et al. and Kasuga et al. have reported that STZ-diabetic rats are resistant to insulin (36, 37) and in other studies it was found that in diabetic rats with severe hyperglycemia, S_G is substantially decreased due to low muscle glucose clearance and down-regulation of glucose transporter (GLT4) (38).

Another important aspect of the integrated pharmacokinetic-pharmacodynamic approach used in the current investigation was the estimation of pharmacodynamic

efficiency, as assessed after SC and pulmonarily administered insulin. Our results reveal that despite differences in route of administration and delivery rate, pharmacodynamic efficiency was around 0.6. This means that glucose response per unit systemic insulin was comparable in all groups irrespective of the differences in the time course profile. This also demonstrates that, the biological activity of insulin was not adversely affected by the supercritical drying process. These findings are in agreement with the previous study (Chapter 4), where it was shown with spectroscopic and chromatographic techniques that the structural integrity of insulin was essentially preserved during the drying process.

In this study we have also considered safety aspects of drug delivery using histology techniques to assess inflammation markers in lung tissue. As it is evident from the photographs (figure 1), there was neither injury of the epithelial surfaces and bronchioles nor infiltration of neutrophils, both of which are indicators for acute toxicity after pulmonary administration of the polymeric particles. These results are in accordance with previous observations for TMC20 and TMC60 carriers (20, 39), which show the safety of TMC as carriers for pulmonary delivery of proteins. However, chronic toxicity tests should be performed to evaluate the long term applicability of microparticles for the pulmonary delivery of insulin.

In conclusion, pulmonary administration of TMC60-insulin microparticles as compared to dextran- and TMC20-insulin microparticles, enhanced significantly the systemic absorption of insulin, with a relative bioavailability of about 91% relative to SC insulin. TMC20-insulin powder showed an extended release of insulin, which may result from differences in dissolution and diffusion properties. The PKPD analysis of the insulin formulations enabled characterization of insulin sensitivity and glucose homeostasis in STZ-induced diabetes. Moreover, we have shown that the insulin microparticles do not induce acute inflammatory reaction on the respiratory epithelium. This makes the use of TMC microparticles a promising vehicle for pulmonary delivery of insulin and other therapeutic proteins.

Acknowledgments

We thank Marcel Fens (Department of Pharmaceutics, Utrecht Institute for Pharmaceutical Sciences, Utrecht University) for his help with histology.

References

1. J. S. Skyler, W. T. Cefalu, I. A. Kourides, W. H. Landschulz, C. C. Balagtas, S. L. Cheng, and R. A. Gelfand. Efficacy of inhaled human insulin in type 1 diabetes mellitus: a randomised proof-of-concept study. *Lancet* 357: 331-5 (2001).

2. T. K. Mandal. Inhaled insulin for diabetes mellitus. *Am J Health Syst Pharm* 62: 1359-64 (2005).

3. Z. Ma, T. M. Lim, and L. Y. Lim. Pharmacological activity of peroral chitosan-insulin nanoparticles in diabetic rats. *Int J Pharm* 293: 271-80 (2005).

4. F. Cui, K. Shi, L. Zhang, A. Tao, and Y. Kawashima. Biodegradable nanoparticles loaded with insulin-phospholipid complex for oral delivery: preparation, in vitro characterization and in vivo evaluation. *J Control Release* 114: 242-50 (2006).

5. R. Fernandez-Urrusuno, P. Calvo, C. Remunan-Lopez, J. L. Vila-Jato, and J. A. Alonso. Enhancement of nasal absorption of Insulin using chitosan nanopartocles. *Pharm. Res.* 16: 1576-1581 (1999).

6. J. S. Patton, J. G. Bukar, and M. A. Eldon. Clinical pharmacokinetics and pharmacodynamics of inhaled insulin. *Clin Pharmacokinet* 43: 781-801 (2004).

7. J. S. Patton. Mechanisms of macromolecules absorption by the lungs. *Adv Drug Del Rev* 19: 3-36 (1996).

8. J. S. Patton, C. S. Fishburn, and J. G. Weers. The lungs as a portal of entry for systemic drug delivery. *Proc Am Thorac Soc* 1: 338-44 (2004).

9. S. P. Newman, A. Hollingworth, and A. R. Clark. Effect of different modes of inhalation on drug delivery from a dry powder inhaler. *Int J Pharm* 102: 127-132 (1994).

10. H. Todo, H. Okamoto, K. Iida, and K. Danjo. Effect of additives on insulin absorption from intratracheally administered dry powders in rats. *Int J Pharm* 220: 101-10 (2001).

11. A. Hussain, Q. H. Majumder, and F. Ahsan. Inhaled insulin is better absorbed when administered as a dry powder compared to solution in the presence or absence of alkylglycosides. *Pharm Res* 23: 138-47 (2006).

12. A. Hussain, J. J. Arnold, M. A. Khan, and F. Ahsan. Absorption enhancers in pulmonary protein delivery. *J Control Release* 94: 15-24 (2004).

13. S. Suarez, L. Garcia-Contreras, D. Sarubbi, E. Flanders, D. O'Toole, J. Smart, and A. J. Hickey. Facilitation of pulmonary insulin absorption by H-MAP: pharmacokinetics and pharmacodynamics in rats. *Pharm Res* 18: 1677-84 (2001).

14. H. Todo, K. Iida, H. Okamoto, and K. Danjo. Improvement of insulin absorption from intratracheally administrated dry powder prepared by supercritical carbon dioxide process. *J Pharm Sci* 92: 2475-86 (2003).

15. T. C. Woods, B. Zhang, F. Mercogliano, and S. M. Dinh. Response of the lung to pulmonary insulin dosing in the rat model and effects of changes in formulation. *Diabetes Technol Ther* 7: 516-24 (2005).

16. I. M. van der Lubben, G. Kersten, M. M. Fretz, C. Beuvery, J. C. Verhoef, and H. E. Junginger. Chitosan microparticles for mucosal vaccination against diphtheria: oral and nasal efficacy studies in mice. *Vaccine* 28: 1400-1408 (2003).

17. A. Vila, A. Sanchez, K. Janes, I. Behrens, T. Kissel, J. L. Vila Jato, and M. J. Alonso. Low molecular weight chitosan nanoparticles as new carriers for nasal vaccine delivery in mice. *Eur. J. Pharm. Biopharm.* 57: 123-131 (2004).

18. M. Thanou, J. C. Verhoef, J. H. M. Verheijden, and H. E. Junginger. Intestinal absorption of octeriotide: N-trimethyl chitosan chloride (TMC) ameliorates the permeability and absorption properties of the somatostatin analogue in vitro and in vivo. *J Pharm Sci* 89: 951-957 (2000).

19. J. H. Hamman, M. Stander, and A. F. Kotzé. Effect of the degree of quaternization of N-trimethyl chitosan chloride on absorption enhancement: in vivo evaluation in rat nasal epithelia. *Int J Pharm* 232: 235-242 (2002).

20. M. Amidi, S. G. Romeijn, G. Borchard, H. E. Junginger, W. E. Hennink, and W. Jiskoot. Preparation and characterization of protein-loaded N-trimethyl chitosan nanoparticles as nasal delivery system. *J Control Release* 111: 107-116 (2006).

21. J. H. Hamman, C. M. Schultz, and A. F. Kotzé. N-trimethyl chitosan chloride: optimum degree of quaternization for drug absorption enhancement across epithelial cells. *Drug Dev Ind Pharm* 29: 161-172 (2003).

22. D. Snyman, J. H. Hamman, and A. F. Kotze. Evaluation of the mucoadhesive properties of N-trimethyl chitosan chloride. *Drug Dev. Ind. Pharm.* 29: 61-9 (2003).

23. N. Elvassore, A. Bertucco, and P. Caliceti. Production of insulin-loaded poly(ethylene glycol)/poly(l-lactide) (PEG/PLA) nano-particles by gas antisolvent techniques. *J Pharm Sci* 90: 1628–1636 (2001).

24. N. Jovanovic, A. Bouchard, G. W. Hofland, G. J. Witkamp, D. J. A. Crommelin, and W. Jiskoot. Stabilization of proteins in dry powder formulations using supercritical fluid technology. *Pharm Res* 21: 1955-69 (2004).

25. X. Jiang, A. van der Horst, M. J. van Steenbergen, N. Akeroyd, C. F. van Nostrum, P. J. Schoenmakers, and W. E. Hennink. Molar-mass characterization of cationic polymers for gene delivery by aqueous size-exclusion chromatography. *Pharm Res* 23: 595-603 (2006).

26. A. B. Sieval, M. Thanou, A. F. Kotzé, J. C. Verhoef, J. Brussee, and H. E. Junginger. Preparation and NMR- characterisation of highly substituted N-trimethyl chitosan chloride. *Carbohydr Polym* 36: 157-165 (1998).

27. R. N. Bergman, Y. Z. Ider, C. R. Bowden, and C. Cobelli. Quantitative estimation of insulin sensitivity. *Am J Physiol* 236: E667-77 (1979).

28. S. L. Bealand S. L. B. NONMEM User Guide, NONMEM Project Group, Univ. of California San Francisco, San Francisco, CA, 1992.

29. Y. Tabataand Y. Ikada. Effect of the size and surface charge of polymer microspheres on their phagocytosis by macrophage. *Biomaterials* 9: 356-62 (1988).

30. M. Gopalakrishnan, S. Suarez, A. J. Hickey, and J. V. Gobburu. Population pharmacokinetic-pharmacodynamic modeling of subcutaneous and pulmonary insulin in rats. *J Pharmacokinet Pharmacodyn* 32: 485-500 (2005).

31. J. Smith, E. Wood, and M. Dornish. Effect of chitosan on epithelial cell tight junctions. *Pharm Res* 21: 43-9 (2004).

32. G. Nucciand C. Cobelli. Models of subcutaneous insulin kinetics. A critical review. *Comput Methods Programs Biomed* 62: 249-57 (2000).

33. M. Miyazaki, H. Mukai, K. Iwanaga, K. Morimoto, and M. Kakemi. Pharmacokinetic-pharmacodynamic modelling of human insulin: validity of pharmacological availability as a substitute for extent of bioavailability. *J Pharm Pharmacol* 53: 1235-46 (2001).

34. R. N. Bergman. Minimal model: perspective from 2005. *Horm Res* 64 Suppl 3: 8-15 (2005).

35. S. Natalucci, P. Ruggeri, C. E. Cogo, V. Picchio, and R. Burattini. Insulin sensitivity and glucose effectiveness estimated by the minimal model technique in spontaneously hypertensive and normal rats. *Exp Physiol* 85: 775-81 (2000).

36. O. Blondeland B. Portha. Early appearance of in vivo insulin resistance in adult streptozotocin-injected rats. *Diabete Metab* 15: 382-7 (1989).

37. M. Kasuga, Y. Akanuma, Y. Iwamoto, and K. Kosaka. Insulin binding and glucose metabolism in adipocytes of streptozotocin-diabetic rats. *Am J Physiol* 235: E175-82 (1978).

38. J. M. Mathoo, Z. Q. Shi, A. Klip, and M. Vranic. Opposite effects of acute hypoglycemia and acute hyperglycemia on glucose transport and glucose transporters in perfused rat skeletal muscle. *Diabetes* 48: 1281-8 (1999).

39. B. I. Florea, M. Thanou, H. E. Junginger, and G. Borchard. Enhancement of bronchial octereotide absorption by chitosan and N-trimethyl chitosan shows linear in vitro/in vivo correlation. *J Control Rel* 110: 353-361 (2006).

Chapter six

Diphtheria toxoid-containing microparticulate powder formulations for pulmonary vaccination: preparation, characterization and evaluation in guinea pigs

Maryam Amidi[1]
Hubert C. Pellikaan[2]
Hoang Hirschberg[3]
Anne H. de Boer[4]
Daan J.A. Crommelin[1]
Wim E. Hennink[1]
Gideon Kersten[3]
Wim Jiskoot[1,5]

[1] Department of Pharmaceutics, Utrecht Institute for Pharmaceutical Sciences, Utrecht University, PO Box 80082, 3508 TB Utrecht, The Netherlands

[2] Feyecon D & I B.V., Rijnkade 17A, 1382 GS, Weesp, The Netherlands

[3] Unit Research and Development, The Netherlands Vaccine Institute (NVI), Bilthoven, P.O. Box 457, 3720 AL, Bilthoven, The Netherlands.

[4] Department of Pharmaceutical Technology and Biopharmacy, University of Groningen, Ant. Deusinglaan 1, 9713 AV Groningen, The Netherlands

[5] Division of Drug Delivery Technology, Leiden/Amsterdam Center for Drug Research (LACDR), Leiden University, P.O. Box 9502, 2300 RA Leiden, The Netherlands

Submitted for publication

Abstract

In this study, the potential of N-trimethyl chitosan (TMC, degree of quaternization 50%) and dextran microparticles for pulmonary delivery of diphtheria toxoid (DT) was investigated. The antigen-containing microparticles were prepared by drying of an aqueous solution of polymer and DT through a supercritical fluid (SCF) spraying process. The median volume diameter of the dry particles, as determined by laser diffraction analysis, was between 2-3 μm and the fine particle mass fractions smaller than 5 μm, as determined by cascade impactor analysis, were 35% and 56% for the dextran and TMC formulations, respectively. The water content of the particles as measured by Karl Fischer titration was 2-3% (w/w). Pulmonary immunization with DT-TMC microparticles containing 2 or 10 Lf of DT resulted in a strong immunological response as reflected by the induction of IgM, IgG, IgG subtypes (IgG1 and IgG2) antibodies as well as neutralizing antibody titers comparable to or significantly higher than those achieved after subcutaneous (SC) administration of alum-adsorbed DT (2 Lf). Moreover, the IgG2/IgG1 ratio after pulmonary immunization with DT-TMC microparticles was substantially higher as compared to SC administered alum-adsorbed DT. In contrast, pulmonarily administered DT-dextran particles were poorly immunogenic. Among the tested formulations only pulmonarily administered DT-containing TMC microparticles induced detectable pulmonary secretory IgA levels. In conclusion, in this paper it is demonstrated that TMC microparticles are a potent new delivery system for pulmonary administered DT antigen.

Keywords: N-trimethyl chitosan (TMC) microparticles; supercritical carbon dioxide; pulmonary vaccine delivery; diphtheria toxoid

1 Introduction

Recent advances in biotechnology have resulted in the availability of a large number of protein-based antigens. Up to now, most vaccines are administered by injection because of their instability in the gastrointestinal tract and a low absorption at mucosal sites in general. Obvious disadvantages of parenteral vaccination are low immunization coverage, high cost production and need for trained personnel to administer the vaccine. Although parenterally administered vaccines have contributed to the substantial reduction of the incidence of human infectious diseases, there is a need for more potent and refined vaccines, including non-invasive vaccines.

Pulmonary immunization has been recently explored as an alternative for parenteral vaccination. The respiratory tract has a large absorptive surface area (~ 75 m^2), extensive vasculature, a thin, relatively permeable membrane and low proteolytic activity (1, 2). Importantly, pulmonarily administered vaccines can induce both systemic and local immune responses (3, 4). The extensive dendritic cells (DCs) network lining the respiratory epithelium (in the submucosa and on the alveolar surface) and the macrophages network (in the interstitium as well as the alveoli) have important roles in generating both systemic and local immune responses (1, 5). Moreover, pathogen-specific secretory IgA (S-IgA) antibodies in the respiratory tract are of particular importance for the prevention and control of infection at the respiratory mucosa (6). S-IgA antibodies can inhibit adherence of viruses, bacteria and bacterial toxins to the respiratory mucosal surfaces as well as neutralize infectious agents or antigens in the mucosal tissues (6-10). In spite of the attractive features of pulmonary immunization, most pulmonary vaccines are poorly immunogenic when administered as solutions, either in the form of aerosols or by intratracheal instillation. The major factors limiting pulmonary antigen delivery are poor deposition of the antigen at the alveolar region, low absorption from the epithelial barriers in the peripheral airways and the central lungs and the presence of a mucociliary escalator in the central and upper lung, which rapidly removes antigens or particles from the central respiratory tract. To overcome these barriers, mucoadhesive antigen-containing particles with an aerodynamic size range 1.5 to 3 micron should be used. When they are inhaled with an appropriate manoeuvre, they can penetrate deeply in the lung and have access to the alveoli and the broncho associated lymphoid tissue (BALT) and are therefore attractive vaccine carriers (1, 5). Particles composed of chitosan or chitosan derivatives have been shown to enhance the absorption of macromolecules, including antigens and DNA, across mucosal epithelia and subsequently induce strong immune responses (11-15). It has been shown that chitosan based polymers are mucoadhesive and capable of opening the tight junctions between epithelial cells. Both properties may help to stimulate the uptake of antigens by mucosal epithelium as well as antigen presenting cells (APCs) (12, 13, 16-18). N-trimethyl chitosan chloride (TMC), a partially quaternized chitosan derivative, is particularly attractive because it has both mucoadhesive properties and excellent absorption enhancing effects even at neutral pH (19, 20). Among TMC with different degrees of quaternization (DQ), TMC with a DQ of 50-60% showed strong

mucoadhesive and absorption enhancing properties (19, 20). Previously, we showed the efficacy and safety of TMC nanoparticles as a nasal delivery system for ovalbumin and influenza hemagglutinin (17, 21). In these studies, the TMC nanoparticles were able to enhance the uptake of the loaded albumin in rat nasal mucosa and induce strong systemic and local anti-hemagglutinin antibody responses in intranasally immunized mice with encapsulated influenza hemagglutinin.

The aim of the present work was to investigate the potential of TMC (DQ 50%) microparticles loaded with diphtheria toxoid (DT), as a model antigen, for pulmonary immunization studies. Diphtheria is an acute contagious and often fatal disease caused by the gram positive bacterium *Corynebacterium diphtheriae*, which is transmitted through inhalation of aerosolized respiratory secretions. The virulence of *Corynebacterium diphtheriae* results from the action of its potent exotoxin, which interferes with mammalian protein synthesis (22, 23). Diphtheria toxin is absorbed into the blood circulation and distributed throughout the body, which cause severe systemic complications (22, 24). Prophylactic vaccination is the most effective means to prevent the infection. Currently available parenteral diphtheria vaccines consist of alum adsorbed-DT, the formaldehyde treated diphtheria toxin, which is non-toxic but still immunogenic. Alum-adsorbed DT vaccines induce strong systemic antibody responses but are incapable of inducing S-IgA antibodies. The latter would be advantageous, as DT-specific IgA can bind to the exotoxin released by *Corynebacterium diphtheriae*, thereby preventing it from penetrating into the mucosal sites (10). Therefore, non-parenteral DT vaccines with suitable characteristics for pulmonary deposition, which are capable to induce strong serum IgG as well as S-IgA responses are highly desirable. In the present work, DT associated with TMC50 (as an absorption enhancer) and dextran (as a non-permeation enhancer) microparticles for pulmonary immunization were prepared by a supercritical fluid (SCF) spraying process. This process, using carbon dioxide as an anti-solvent for hydrophilic molecules, has been used as an attractive technique to prepare dried protein formulations and offers the possibility to produce small microparticles suitable for inhalation (25-29). Here, we show that the SCF process allows the production of antigen-loaded TMC microparticles that are suitable for pulmonary administration in a model animal (guinea pigs), and capable of inducing both strong systemic and local immune responses.

2 Materials and methods

2.1 Materials

Chitosan (M_n = 40 kDa, M_w = 177 kDa, determined by gel permeation chromatography (GPC) using poly(ethylene glycol) (PEG) standards (30); degree of deacetylation 93%) was a generous gift from Primex (Avaldsnes, Norway). N-Trimethyl chitosan with a degree of quaternization of 50% (TMC50) was synthesized by methylation of chitosan

by using CH_3I in the presence of a strong base (NaOH) and analyzed by ^{1}H-nuclear magnetic resonance (NMR) spectroscopy as previously described (31). Dextran (Mw = 68.8 kDal) was purchased from Sigma-Aldrich (Schnelldorf, Germany). Horseradish peroxidase-conjugated immunoglobulin class and subtype-specific antibodies were from Gentaur (Brussels, Belgium). Diphtheria toxoid (DT) (5.05 mg/ml) and reference $AlPO_4$ (alum) adsorbed DT vaccine, (Dta 93/1 (9 mg/ml)), were supplied by the Laboratory for Product and Process Development, Netherlands Vaccine Institute (NVI) (Bilthoven, the Netherlands). All other chemicals used were obtained from commercial suppliers and were of analytical grade.

2.2 Preparation of DT-loaded microparticles

DT-loaded microparticles were prepared by spraying of an aqueous solution of DT and dextran or TMC into a supercritical mixture of carbon dioxide (CO_2) and ethanol. First, a solution of 2% (w/w) dextran or TMC in water was prepared. Then the desired amount of DT solution in water (5.05 mg/ml) was mixed with the dextran or TMC solutions to obtain a DT/dextran ratio of 0.0056 or DT/TMC ratios of 0.0056 and 0.028.

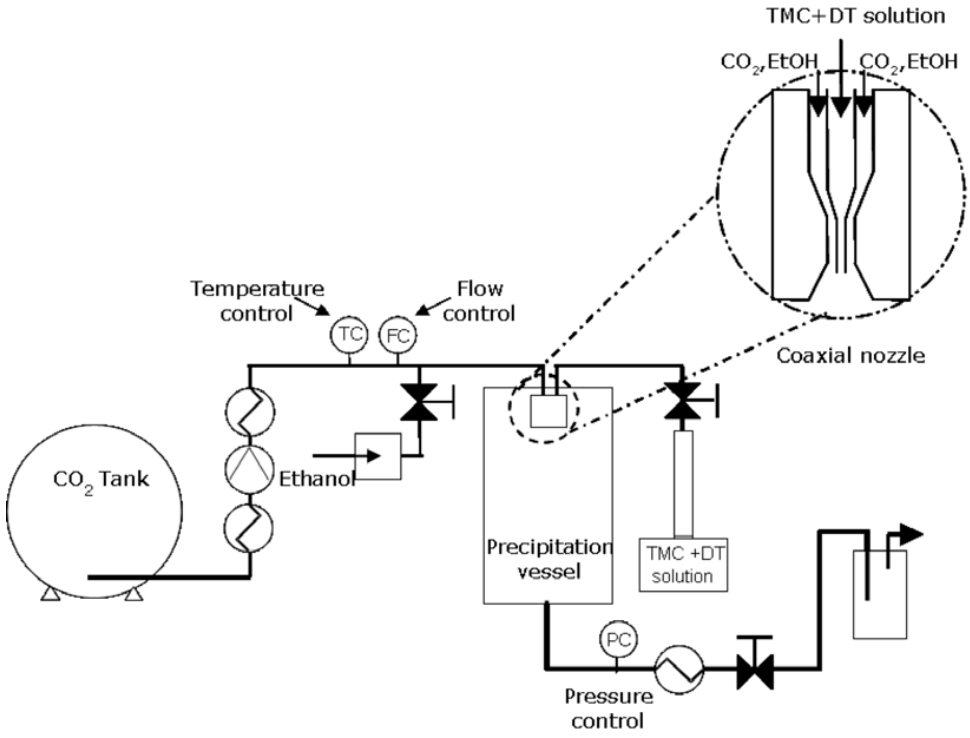

Figure 1. Scheme of experimental set-up of the SCF drying system

A scheme of the experimental setup is presented in figure 1 and details about the apparatus and the method were reported before (28, 29).
At the selected operating temperature (38 °C) and pressure (100 bar), CO_2 and ethanol are fully miscible resulting in a single supercritical phase. The following experimental conditions gave spherical microparticles. First, at 38 °C SC-CO_2 was introduced with a constant flow rate of 367 g/min using a diaphragm pump (Lewa) into a 4-liter precipitation vessel until the pressure reached 100 bar. Then, ethanol was added with a piston pump (Gilson) at a flow rate of 25 ml/min and mixed in a T-mixer with the SC-CO_2 (367 g/min). The ethanol/CO_2 mixture was directly fed into the atomization device (concentric coaxial two-fluid nozzle, inner diameter 0.08 mm) and sprayed into the vessel for 5 min. Next, the aqueous polymer-DT solution was pumped into the T-mixer with a flow rate of 0.5 ml/min using two ISCO 260 syringe pumps, mixed with SC-CO_2 (367 g/min) and ethanol (25 ml/min) and introduced into the precipitation vessel through the atomization device. Once the polymer-DT solution was entirely sprayed into the precipitation vessel, the solution line was closed. Subsequently, SC-CO_2 and ethanol were sprayed into the precipitation vessel for 10 min in order to extract the residual solvent (H_2O). Finally, the vessel was flushed for 30 min with SC-CO_2 (367 g/min) to further extract residual solvents including ethanol. Once the pressure was released, the formed dry powder was collected from the filter at the bottom of the vessel and stored in a closed container at 4 °C.

2.3 Characterization of the DT-loaded microparticles

2.3.1 Particle shape and appearance

The dextran and TMC microparticles were analyzed by scanning electron microscopy (SEM) by using a JEOL JSM-5400 scanning electron microscope (SEM) (Peabody, USA). Samples of the particles were fixed onto aluminum SEM stubs using self-adhesive carbon disks, and were subsequently sputter-coated with a conducting gold layer.

2.3.2 Particle size analysis

Volume median particle diameters and size distributions were determined with a laser diffraction apparatus (HELOS BF MAGIC, Clausthal-Zellerfeld, Germany) equipped with a dry powder dispersion system RODOS (Sympatec GmbH, Germany). Approximately 3 mg of powder was placed into the RODOS ring and dispersed through a laser beam (628 nm) with 3 bar of air pressure. Measurements were performed with a 100 mm lens and calculations of size distributions from the complex diffraction patterns were based on the Fraunhofer theory. In another measurement the same amount of particles was introduced via a DP-4 insufflator (PENN CENTURY Inc, Philadelphia, USA), designed for pulmonary vaccination studies in guinea pigs, into the laser diffraction apparatus.
The deposition properties of the powders from the insufflator were evaluated with a glass constructed 4-stage Fisons cascade impactor, a multistage liquid impinger

(MSLI) type, which was described previously (32, 33). The mass fractions obtained on different impactor stages were used to calculate the fine particle fractions (FPF's). In this study, the FPF was defined as the mass fraction smaller than 5 μm, expressed as percentage of the real (metered) dose. The impactor was connected to a flow control system having a flow controller, a solenoid valve with timer and vacuum pump (Edwards pump, type E1M40, UK) and it was operated at a flow rate of 30 l/min for 5 s. Thirty mg of the different DT powders was introduced into the impactor using a DP-4 insufflator (10 individual insufflations of 3 mg of microparticles) to deposit enough powder on the impactor stages for further chemical analysis. The TMC- and dextran-DT particles deposited on each stage of the impactor were dissolved in water. The total particle masses deposited onto the different stages were derived from determination of the TMC and dextran concentrations in the resulting solutions. The TMC concentration was measured by reversed-phase HPLC analysis as described below and the dextran concentration was determined by a colorimetric carbohydrate assay. The experiments were carried out in duplicate at 20 °C and a relative humidity of 34%. The theoretical cut-off points of the impactor, which are normally presented as particle diameters with 50% collection efficiency, were determined using an equation previously described (34). The fine particle fraction ($FPF_{<5\mu m}$) for each sample was calculated from the theoretical cutpoints and mass fractions on the impactor stages.

Laser diffraction diameters are the same as equivalent volume diameters when spherical particles are measured, whereas cascade impactors measure aerodynamic diameters. The relationship between equivalent volume diameters (D_E) and aerodynamic diameters (D_A) is described by the following equation:

$$D_A = D_E \times (\rho/\chi)^{1/2} \quad (1)$$

where ρ is density of the particles and χ is dynamic shape factor of the particles, which equals to one for spherical particles (33, 34).

2.3.4 Water content determination

The water content of the microparticles was determined by Karl-Fischer titration. In brief, 3 mg powder, accurately weighed, was dissolved or suspended in 500 μl of methanol. Fifty μl of sample was injected into the titration cell and the amount of water of the powders was calculated after subtraction of the background (methanol only) signal.

2.4 Quantification of DT and TMC by reversed-phase HPLC

DT content of the DT microparticles and TMC content of the soluble samples of the DT-TMC powders from the cascade impactor analyses were determined by reversed-phase (RP) HPLC. A Jupiter C_4 (300 Å; 5 μm, 150 × 4.6 mm) column in combination with an All-guard C_4 pre-column (Bester Amstelveen, the Netherlands) was used.

The column was equilibrated for one hour at a flow rate of 1 ml/min with a solvent mixture consisting of 95% acetonitrile/5% H_2O/0.1% trifluoro acetic acid (TFA). For determination of TMC, 50 µl of the different samples collected from the cascade impactor devices were injected onto column. Calibration curves were made for DT and TMC by injecting volumes of 0.5-50 µl of solutions of DT (1 mg/ml) in 0.01 M HCl and TMC (3 mg/ml) in water onto the column. A gradient was run from the starting composition, acetonitrile/H_2O (95/5%)/TFA 0.1%, to acetonitrile/H_2O (5/100%)/TFA 0.1% in 15 minutes. The mobile phase was delivered onto the column at a flow rate of 1 ml/min by a Waters 600 gradient pump equipped with a Waters 717 plus autosampler (Waters Corporation, Milford, MA, USA). Chromatograms were recorded with a Waters 600 absorbance detector set at 280 nm.

2.5 Immunization studies

Specified pathogen free (SPF) female and male (HsdPoc:DH) guinea pigs weighing 600-800 grams were obtained from the breeding facility of the Netherlands Vaccine Institute (NVI) (Bilthoven, the Netherlands). They were maintained at group-housing, females and males separately, in the animal facility of the NVI with a 12 h day and night schedule, while food and water were ad libitum. The experiments were approved by the Ethical Committee for Animal Experimentation of the NVI. Before each immunization, guinea pigs (7 per group) were anesthetized intramuscularly with a mixture of ketamine (30 mg/ml), xylazine (6 mg/ml) and atropine (0.1 mg/ml) in physiological saline (1 ml per guinea pig), and then immunized once intratracheally or SC (table 1). For the pulmonary immunizations, approximately two mg of powder, corresponding with 2 or 10 Lf of DT, were administered intratracheally with a DP-4 insufflator. Each anesthetized guinea pig was rested on its back at an angle of 45°. A clear view of the trachea was provided by inserting a fiber optic laryngoscope (Penn Century Inc., Philadelphia, USA) into the mouth of the animal. Then the needle of the DP-4 insufflator attached to an air pump, AP-1™ (PENN CENTURY Inc, Philadelphia, USA), was inserted into the trachea. Subsequently, the DT powder which was placed in the dry powder inhaler and quickly delivered into the guinea pig's lungs. The amount of delivered dose was determined by subtracting the weight of the insufflator after intratracheal administration from that of the loaded insufflator before administration. If the animals had not received a sufficient dose, a second administration was done to compensate for the missing dose.

For the SC immunizations, anesthetized guinea pigs received 1 ml of a freshly prepared alum-adsorbed DT in physiological saline (2 Lf) or a reference alum-adsorbed DT vaccine, Dta 93/1, diluted in physiological saline (2 Lf) by injecting in their groin flanks (0.5 ml per each groin). Four weeks after the immunizations, the guinea pigs were anesthetized as mentioned above, bled through heart punctures and sacrificed by withdrawing their entire blood volume through their hearts. Individual serum samples were separated from blood cells and coagulated proteins by centrifugation for 5 min at 14000 g and 4 ºC, and stored at -20ºC. After blood samples

were taken, the broncho-alveolar lavages (BAL) were collected by gently washing the lungs with a volume of 6-8 ml of PBS (10 ml/kg of animal weight) supplemented with complete mini EDTA-free protease inhibitor cocktail (one tablet per 10 ml) (Roch Diagnostics, Almere, the Netherlands) by use of a catheter inserted into the trachea. The BAL were centrifuged (10 min at 3000 g) to remove debris and the supernatants were stored at -20 ºC till the day of analysis.

Table 1. Immunization study design

Formulation	Antigen (DT) dose (Lf)	Route of administration[1)]	Serum sampling (day)	Lung washes (day)
1. DT-Dextran microparticles	2	pulmonary	1, 29	29
2. DT-TMC microparticles	2	pulmonary	1, 29	29
3. DT-TMC microparticles	10	pulmonary	1, 29	29
4. Alum-adsorbed DT vaccine	2	SC	1, 29	29
5. Alum-DT reference vaccine	2	SC	1, 29	29

[1)] Groups of 7 guinea pigs were immunized once with the formulations indicated in the table.

2.6 Anti-DT antibody assays

DT-specific antibody responses were determined by using an enzyme-linked immunosorbent assay (ELISA). Briefly, ELISA plates (high binding capacity Greiner, Alphen a/d Rijn, Netherlands) were coated overnight at ambient temperature with diphtheria toxoid antigen (0.5 Lf in 100 µl/well) in coating buffer (0.05 M carbonate/bicarbonate, pH 9.6). Plates were washed and blocked by incubation with 2.5% (w/v) bovine serum albumin (BSA) in coating buffer (200 µl/well) for 1 hour at 37°C. Subsequently, the plates were washed with PBS containing 0.05% Tween, pH 7.6 (PBS/Tween). Appropriate dilutions of sera and non-diluted BAL or nasal lavages of each individual guinea pig were applied to the plates, serially diluted two-fold in PBS/Tween and incubated for 2 h at 37 °C. Plates were then washed and incubated with horseradish peroxidase-conjugated goat antibodies directed against either guinea pigs IgG, IgG1, IgG2, IgM (all diluted 1:5000 in PBS/Tween, 100 µl/well) or IgA (diluted 1:1000 in PBS/Tween, 100 µl/well) for 1 h at 37 °C. Thereafter, the plates were washed twice with PBS/Tween and once with PBS. Specific antibodies were detected by adding 100 µl of 3,3',5,5'-tetra methyl benzidine (TMB, 0.1 mg/ml) in 10 mM sodium acetate pH 5.5 buffer also containing 0.06% (v/v) hydrogen peroxide to each well. After 10 minutes, the reaction was stopped by adding 50 µl 2M H_2SO_4 to each well. IgM, IgG, IgG1 and IgG2 antibody titers are expressed as the reciprocal serum dilution giving an A_{450} of (or 50% of the saturation value). The IgA titer is expressed as the reciprocal sample dilution corresponding with an A_{450} of 0.2 above the background (35, 36). Comparison between guinea pigs of different groups with positive titers was made by a one-way ANOVA test.

2.7 Neutralizing antibody assay

The diphtheria toxin-specific neutralizing antibodies in guinea pigs sera were assessed in a Vero cell assay as previously described (37). Briefly, serially two-fold dilutions of guinea pig sera were prepared in complete medium 199 and applied to microplates (50 µl / well). Then, 50 µl of diphtheria toxin (0.0005 Lf/ml) in complete medium 199 was added to the wells. The plates were covered and incubated for 2 hours at 37 ºC. Subsequently, 50 µl of complete medium 199 containing 5×10^5 Vero cells/ml were added to each well. A reference antitoxin as well as an untreated cell control was included in each plate. The plates were incubated for 6 days at 37 ºC and 5% CO_2. Each well was checked for the presence of living cells by using a microscope. The neutralizing antibody titer is expressed as the last serum dilution that gives protection against diphtheria toxin.

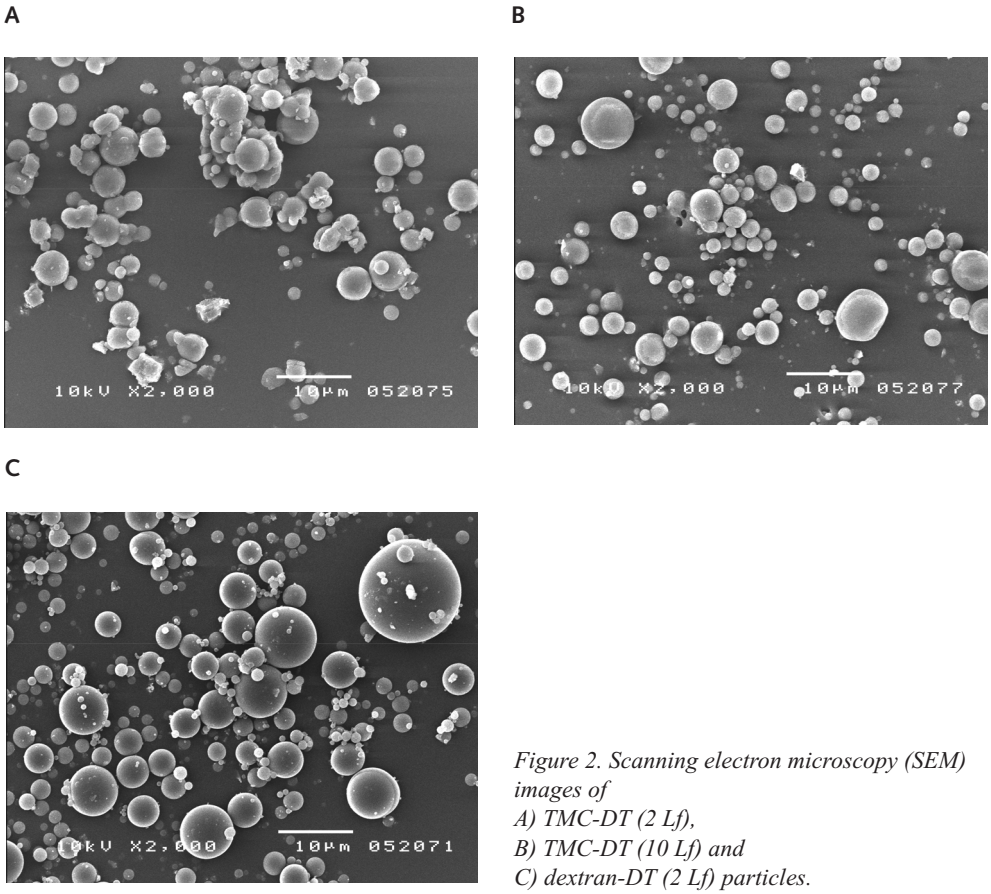

Figure 2. Scanning electron microscopy (SEM) images of
A) TMC-DT (2 Lf),
B) TMC-DT (10 Lf) and
C) dextran-DT (2 Lf) particles.

3 Results

3.1 Preparation and characterization of the DT-loaded dextran and TMC microparticles

The DT-containing TMC and dextran microparticles prepared by SCF spraying were fine and free flowing powders, which dissolved slowly in water. SEM photographs show smooth, spherical particles in the low micrometer range (ca. 0.5-10 μm) for the three formulations (figure 2). Their cumulative volume distributions as function of the particle diameter from laser diffraction technique (RODOS dispersion) are shown in figure 3. The three different DT powders showed rather narrow and unimodal size distributions, indicating the absence of strong agglomerates (figure 3). From figure 3 it appears that 90% of the particles had a size between 1 and 8 μm, which is in excellent agreement with SEM analysis. The size distributions of the particles introduced into the laser diffraction apparatus with a DP-4 insufflator were similar to those of the particles introduced with the RODOS dry powder air dispersion system at an air pressure of 3 bar (data not shown).

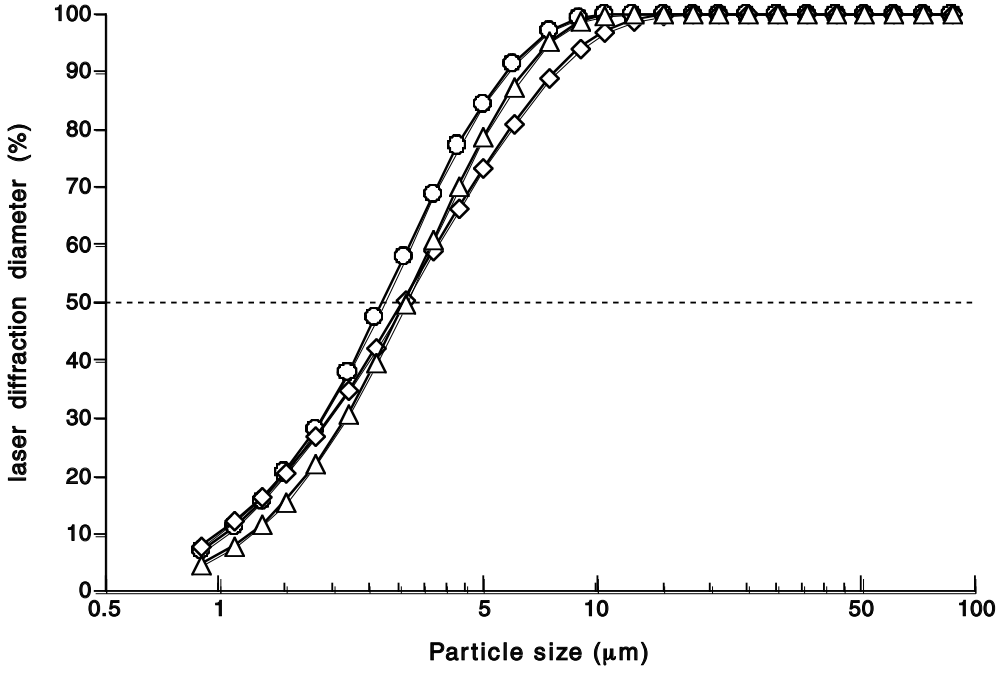

Figure 3. Cumulative volume distribution curves of dried DT formulations measured by laser diffraction; (○) TMC-DT (2 Lf), (Δ) TMC20-DT (10 Lf) and (◊) dextran-DT (2 Lf) microparticles. The particles were dispersed with 3 bar air-pressure into the laser diffraction analyzer using a RODOS dry powder disperser.

This comparison was important to evaluate the potential of the insufflator in its ability to properly disperse the powders into the cascade impactor. The FPF's of the microparticles, as determined by cascade impactor analysis and the median volume diameters (VMD), as determined by laser diffraction are given in table 2. The FPF values of the TMC and dextran particles were about 35 and 56% of the nominal dose, respectively and 54.5 and 63.5% of the emitted dose. This indicates that these powders have a substantial mass fraction of particles below 5 μm suitable for reaching peripheral lung regions (1, 5). Table 2 also shows that the water content of the powders was 2-3% (w/w), which apparently is sufficiently low to avoid particle agglomeration or particle collapse for these types of powders.

Table 2. Characteristics of the dried DT formulations

Dried formulations	Characteristic laser diffraction diameters X10, X50, X90 (μm)[1]			FPF < 5 μm (percentage of the real dose)[2]	FPF < 5 μm (percentage of the emitted dose)[2]	Water content (%)[3]
TMC-DT microparticles (2 Lf)	1.21	3.11	6.49	ND	ND	2.1 ± 0.4
TMC-DT microparticles (10 Lf)	1.35	3.46	6.73	56.0	54.5	2.3 ± 0.2
Dextran-DT microparticles (2 Lf)	0.86	3.22	8.5	35.0	63.5	2.3 ± 0.7

[1] Determined by laser diffraction (LD) analyses (n=2)
[2] Determined by cascade impactor analysis (n=2); ND (not determined); It was not possible to analyze the TMC-DT (2 Lf) because of insufficient amount of powder available.
[3] According to Karl Fischer titration (n=3)

3.2 DT loading

RP-HPLC analyses of DT after dissolution of the powders showed that the DT contents for the dextran and the two TMC powders were 0.52, 0.58 and 2.5% (w/w), respectively. These values are close to the feed ratios (0.56 and 2.8%).

3.3 Immunization studies

The immune responses of guinea pigs to DT (2 Lf) associated with dextran microparticles or TMC microparticles upon pulmonary immunization were evaluated in comparison with conventional, alum-adsorbed DT vaccine administered SC. Moreover, since pulmonary vaccination usually requires higher amounts of antigen in order to induce strong immune responses similar to conventional SC immunization (11), the effect of pulmonary immunization with a

five fold higher dose of DT (10 Lf) associated with TMC microparticles on systemic immune responses was also investigated.

Protection against diphtheria has been shown to correlate with DT-neutralizing serum antibodies (38). Interestingly, after a single intratracheal immunization, DT-TMC microparticles were able to induce high neutralizing antibody titers in all guinea pigs (figure 4). In contrast, pulmonarily administered DT-dextran microparticles were poorly immunogenic, showing undetectable neutralizing antibody titers (figure 4). Importantly, the neutralizing antibody responses elicited by pulmonary immunization with DT-TMC microparticles (2 and 10 Lf) were comparable and significantly stronger than those generated with the conventional SC delivered DT vaccines ($p < 0.01$; $p < 0.001$) (figure 4). In addition, both controls (SC alum-adsorbed DT vaccine and reference vaccine) showed non-responders for neutralizing antibodies.

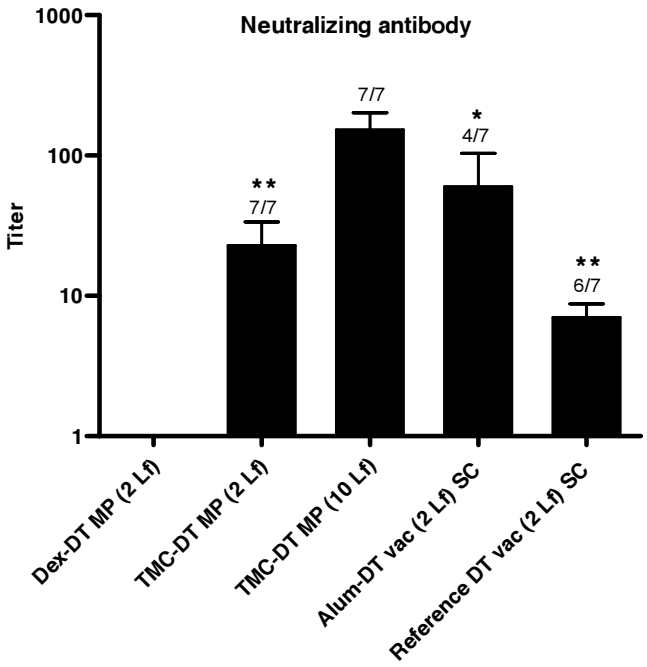

Figure 4. Serum DT-neutralizing response, as determined by Vero cell test, in guinea pigs immunized once pulmonarily with DT-dextran microparticles (Dex-DT MP (2 Lf)), DT-TMC microparticles (TMC-DT MP (2 Lf)), DT-TMC microparticles (TMC-DT MP (10 Lf)) or SC with alum-adsorbed DT vaccine (Alum-DT vac (2 Lf)), reference alum-adsorbed DT vaccine (reference DT vac (2 Lf)). Antibody titers are expressed as mean of the responding guinea pigs; the bars represent the 95% confidence intervals. The numbers above the columns indicate the number of responders per group. Asterisks indicate titers significantly ($P < 0.01$; ** $P < 0.001$) lower than those of the group immunized pulmonarily with TMC-DT MP (10 Lf).*

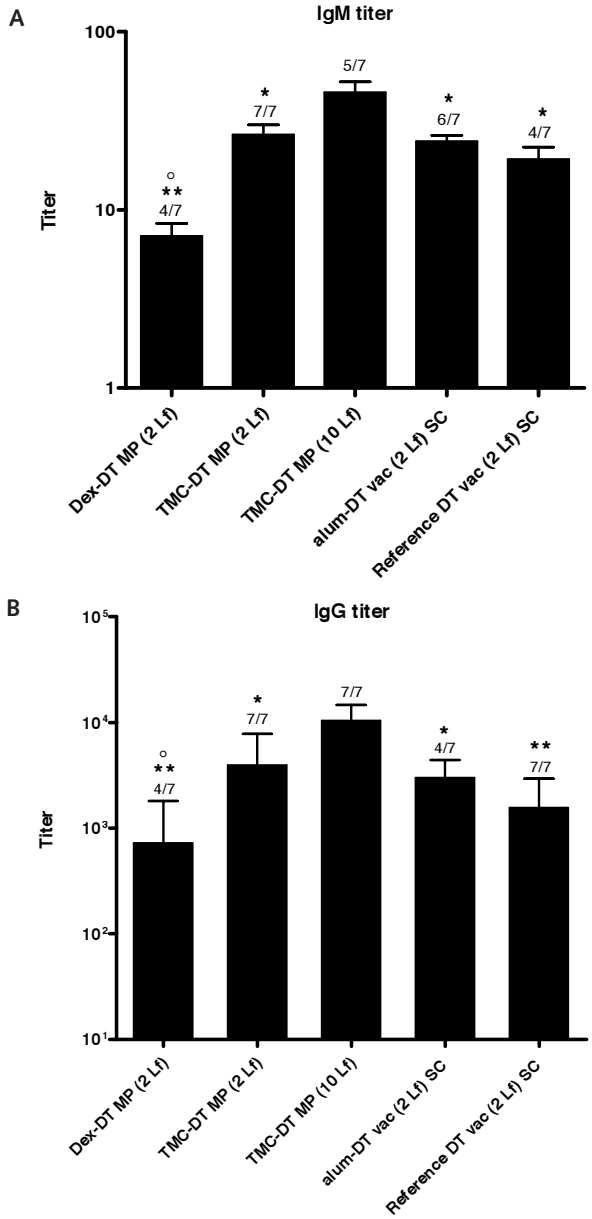

Figure 5. Serum anti DT-specific serum IgM (A) and IgG (B) responses in guinea pigs immunized once pulmonarily with DT-dextran microparticles (Dex-DT MP (2 Lf)), DT-TMC microparticles (TMC-DT MP (2 Lf)), DT-TMC microparticles (TMC-DT MP (10 Lf)) or SC with alum-adsorbed DT vaccine (Alum-DT vac (2 Lf)), reference alum-adsorbed DT vaccine (reference DT vac (2 Lf)). Antibody titers are expressed as mean of the responding guinea pigs; the bars represent the 95% confidence intervals. The numbers above the columns indicate the number of responders per group. Circles indicate titers significantly (° $P < 0.05$) lower than those of the group immunized pulmonarily with TMC-DT MP (2 Lf). Asterisks indicate titers significantly ($P < 0.01$; ** $P < 0.001$) lower than those of the group immunized pulmonarily with TMC-DT MP (10 Lf).*

To gain more insight into the nature of the DT-neutralizing response, antibody class (figure 5) and IgG subclass titers (figure 6) were also determined. When comparing figure 5 with figure 4, it becomes apparent that the IgM titers (figure 5A) and IgG titers (figure 5B) are in qualitative agreement with the neutralizing antibody titers: low or undetectable titers were found in the pulmonarily administered DT-dextran group, pulmonary immunizations with DT-TMC microparticles (2 Lf) induced serum IgM and IgG antibody titers in all animals comparable to those of SC alum-adjuvanted vaccines, and SC immunization with alum-adsorbed DT led to incomplete responses or no response at all in some of the animals. Consistent with the neutralizing antibody results (figure 4), pulmonary immunization with a five-fold higher dose of DT-TMC microparticles (10 Lf) induced stronger IgG immune responses as compared to the low (2 Lf) dose ($p< 0.01$). Although the higher-dose group showed two non-responders for IgM, the average IgG response was significantly higher than that achieved after SC injection of alum-adsorbed DT ($p < 0.01$) or reference DT vaccine ($p < 0.001$) (figure 5).
To investigate the quality of the immune response, the IgG1 and IgG2 subtypes of the DT-specific antibodies were determined (figure 6). The IgG1 responses of the tested formulations largely corresponded to the total IgG responses (cf. figures 5B and 6A). As compared to SC administered DT vaccines and pulmonarily administered DT-dextran microparticles, pulmonarily administered DT-loaded TMC microparticles showed comparable or superior IgG1 responses. Remarkably, the pulmonarily administered DT-TMC microparticles induced significantly higher IgG2 antibody levels in all guinea pigs as compared to the SC controls and the DT-dextran group (figure 6B). Consequently, the IgG2/IgG1 ratios after pulmonary immunizations were significantly higher than those after SC immunization ($p < 0.001$) (figure 6C).
Altogether, these results demonstrate that pulmonary immunization with DT-loaded TMC microparticles induced strong systemic antibody responses comparable or superior to SC administered alum-adsorbed DT.

6A

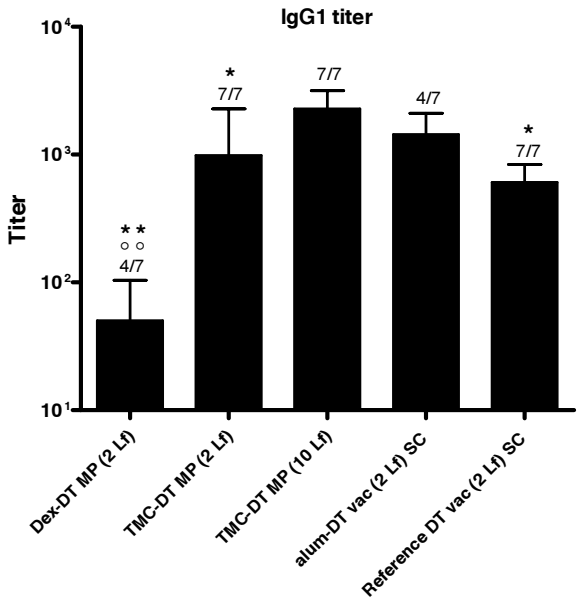
IgG1 titer
Titer
10⁴
10³
10²
10¹
* *
○ ○
4/7
*
7/7
7/7
4/7
*
7/7
Dex-DT MP (2 Lf)
TMC-DT MP (2 Lf)
TMC-DT MP (10 Lf)
alum-DT vac (2 Lf) SC
Reference DT vac (2 Lf) SC

6B

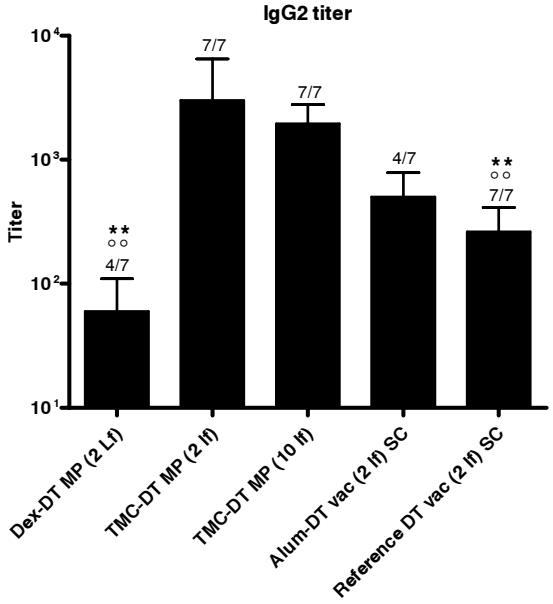
IgG2 titer
Titer
10⁴
10³
10²
10¹
* *
○ ○
4/7
7/7
7/7
4/7
* *
○ ○
7/7
Dex-DT MP (2 Lf)
TMC-DT MP (2 lf)
TMC-DT MP (10 lf)
Alum-DT vac (2 lf) SC
Reference DT vac (2 lf) SC

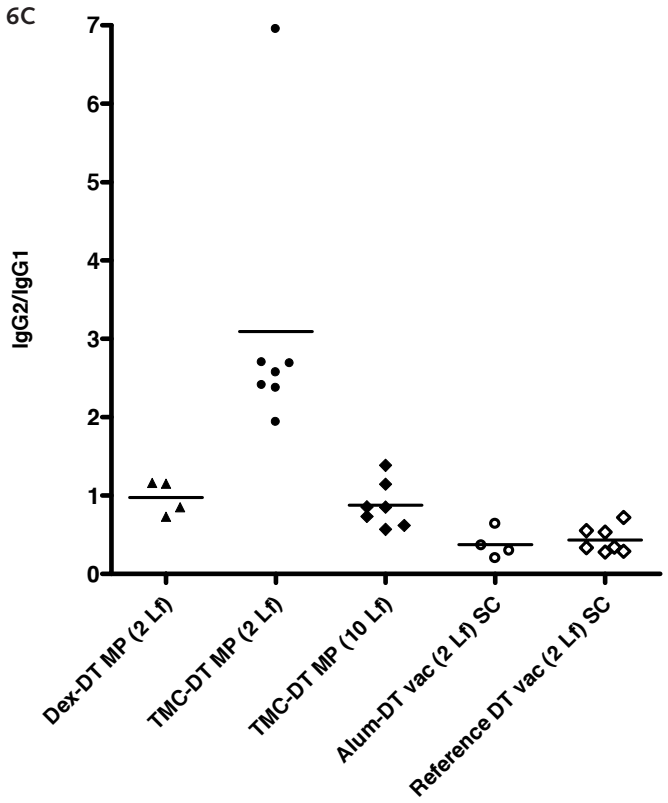

Figure 6. Serum anti DT-specific serum IgG1 (A) and IgG2 (B) responses and corresponding IgG2/IgG1 ratios (C) of guinea pigs immunized once pulmonarily with DT-dextran microparticles (Dex-DT MP (2 Lf)), DT-TMC microparticles (TMC-DT MP (2 Lf)), DT-TMC microparticles (TMC-DT MP (10 Lf)) or SC with alum-adsorbed DT vaccine (Alum-DT vac (2 Lf)), reference alum-adsorbed DT vaccine (reference DT vac (2 Lf)). Antibody titers are expressed as mean of the responding guinea pigs; the bars represent the 95% confidence intervals. The numbers above the columns indicate the number of responders per group. Circles indicate titers significantly (° $P < 0.05$) lower than those of the group immunized pulmonarily with TMC-DT MP (2 Lf). Asterisks indicate titers significantly ($P < 0.01$; ** $P < 0.001$) lower than those of the group immunized pulmonarily with TMC-DT MP (10 Lf).*

Since mucosal immunization has the potential of inducing local immune responses, particularly S-IgA, the IgA levels were measured in the lung lavages of the immunized guinea pigs. Figure 7 shows that only the groups pulmonarily vaccinated with DT-TMC microparticles showed detectable S-IgA titers.

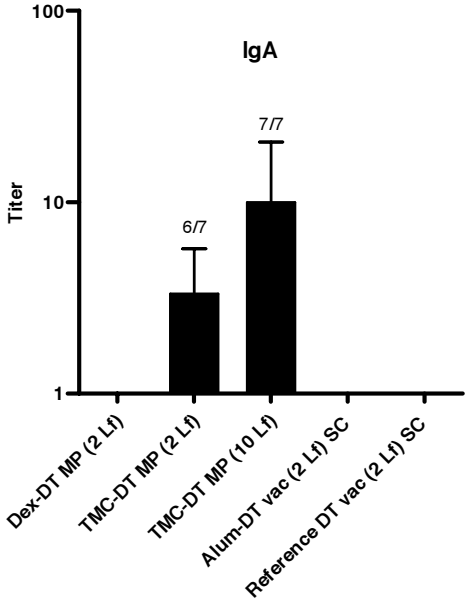

Figure 7. Anti DT-specific S-IgA titers in BAL of guinea pigs immunized once pulmonarily with DT-dextran microparticles (Dex-DT MP (2 Lf)), DT-TMC microparticles (TMC-DT MP (2 Lf)), DT-TMC microparticles (TMC-DT MP (10 Lf)) or SC with alum-adsorbed DT vaccine (Alum-DT vac (2 Lf)), reference alum-adsorbed DT vaccine (reference DT vac (2 Lf)). Antibody titers are expressed as mean of the responding guinea pigs; the bars represent the 95% confidence intervals. The numbers above the columns indicate the number of responders per group.

4 Discussion

The results presented here demonstrate that TMC particles in the correct aerodynamic size range hold great promise for pulmonary vaccination. It has been found that DT-TMC particles can successfully and reproducibly be made by SCF drying. Cascade impactor and laser diffraction analyses revealed that high mass fractions of the DT particles produced for this study were in a size range suitable for reaching peripheral lung regions (1, 5) where they can be efficiently taken up by APCs such as alveolar macrophages and DCs (39, 40). The VMDs of the particles, as determined by laser diffraction analysis were between 2 and 3 μm, which is suitable for uptake by APCs in the respiratory tract.

The FPF values of the powders were calculated as percentage of the real dose. Because a large amount of the dextran powder remained in the insufflator after spraying into the impactor, dextran powder showed a smaller FPF (35%) than TMC-DT (56%). However, the FPF of dextran and TMC powders calculated as percentage of the emitted dose were comparable (54.5% and 63.5%), which shows that the aerodynamic behavior of the dispersed fractions of the dextran and TMC powders were comparable. This comparison based on the emitted dose is important, because in the *in vivo* experiments it was assured that each animal precisely received the same amount of the dextran or TMC powders intratracheally (see section 2.5).

It is possible to obtain information about the porosity of the particles by comparing the mass FPF (as percentage of the emitted dose) to the volume fraction of particles < 5 μm, which can be calculated from the laser diffraction size distribution data (33). In our study, DT particles are spherical (figure 2) and therefore laser diffraction diameters are the same as equivalent volume diameters (D_E). Also, when assuming that the density of the particles is independent of their size, there is a constant relationship between the mass and volume for particles of different sizes, so the cumulative mass distributions (as obtained by cascade impact analysis) and volume distributions (from laser diffraction analysis) are the same as function of the same diameter (D_A or D_E; equation 1)). If spherical particles have non-unit density, there is a difference between D_E and the aerodynamic diameter (D_A) (see equation 1). The fine particle volume fraction (< 5 μm) of TMC-DT and dextran-DT particles (as percentage of the emitted doses) was 72 and 78%, respectively, which is higher than their respective fine particle mass fraction (FPF, 54.5 and 63.5%). Therefore, D_A is larger than D_E. This indicates that both TMC and dextran particles have a density above one. Since the true density of saccharides is around 1.6 g/cm^3, this indicates that the DT microparticles are likely solid or at least have a low porosity.

The DT-containing powders had a low residual water content. The powders had lower dissolution rates than the starting materials, dextran and TMC. This is probably related to the compactness of the particles, which would cause water to slowly penetrate into the polymer network of the particles.

As opposed to pulmonary vaccination with DT-dextran microparticles, single pulmonary immunization with DT-loaded TMC microparticles resulted in strong

dose-dependent systemic immune responses. These results clearly demonstrate that TMC particles have an intrinsic immunostimulating effect for locally administered vaccines, which is in line with previous studies using TMC as adjuvant (14, 21, 41). Furthermore, a single pulmonary immunization with DT-TMC microparticles induced comparable or significantly higher specific anti-DT antibody levels than those obtained with the conventional SC administered DT vaccines (figure 4, 5 and 6). This is remarkable, because non-parenterally administered vaccines usually need booster immunizations to reach high antibody titers comparable to those of single parenteral immunizations (12, 14, 18, 42-45). Factors that may contribute to the immunostimulating effect of TMC microparticles on pulmonary administration include prolonged exposure of the antigen to immunoeffector sites in lungs such as BALT and alveoli, higher absorption of the antigen at the absorptive area and the alveolar region, improved uptake by M-cell type cells present among epithelia cells covering BALT, dendritic cells (DCs) and other APCs in the respiratory epithelium, more efficient delivery to mucosal lymph nodes, and/or more efficient stimulation of APCs after antigen uptake (46-51) (1, 3, 4, 49, 52, 53). According to previous studies with TMC (degree of quaternization > 40%), the polymer is able to efficiently enhance the paracellular transport of proteins by opening the tight junctions of the epithelial cells (19, 20, 54). TMC is mucoadhesive and positively charged and electrostatic interactions between TMC and the negatively charged antigen are likely. TMC attaches to the mucus and/or the epithelial cell membranes and thereby can prolong the residence and probably facilitate the antigen absorption by opening the tight junctions (14, 17, 20, 55). Moreover, it has been reported that particulate antigens are efficiently taken up by APCs in the respiratory epithelium (1, 3, 4, 49, 52, 53) and cationic microparticles are particularly effective for uptake into macrophages and DCs (56). Previously we showed that influenza antigen-loaded TMC nanoparticles were efficiently taken up by nasal epithelium and NALT and were able to induce strong immune responses (21). In this study the DT powders showed slow dissolution *in vitro*, which may imply that in the lungs, where only a thin water layer covering the epithelium is available, the microparticles might be taken up by APCs before they dissolve. Therefore, the absorption-enhancing capacity, the positive charge and the particulate nature of TMC presumably contribute to improved interaction with respiratory mucosa and epithelium, uptake and processing of the encapsulated antigen by APC as well as a more efficient delivery to peripheral lymph nodes (46-51). In contrast, dextran as an inert and neutral polymer lacking mucoadhesive properties is incapable of efficient antigen delivery across the respiratory epithelium.

Currently, most of the commercially available parenteral vaccine formulations consist of antigens adsorbed to aluminium salts (alum), as an adjuvant. Aluminium salts have several limitations in terms of the nature of the immunological responses they promote (57, 58). Parenteral alum adjuvanted vaccines predominantly induce IgG1 subclass antibodies with lower IgG2 antibody titers. In this study both pulmonary and SC immunizations resulted in a mixed Th_2/Th_1 immune response, which may be advantageous for protection against diphtheria in humans (18). As expected, SC

administered alum-adsorbed DT vaccines induced strong IgG1 and weaker IgG2 responses. Pulmonary administered DT-loaded TMC microparticles were able to markedly enhance both the IgG1 and the IgG2 responses and changed the subtype profile compared to SC conventional vaccine (see figure 6). The IgG2/IgG1 ratios were significantly higher after pulmonary immunizations compared to those of SC vaccinations (figure 6C). The highest IgG2 antibody level was achieved after pulmonary vaccination with lower dose f DT (2 Lf) associated to TMC microparticles (see figure 6), which infers that IgG2 production likely needs less antigen dose when administered pulmonarily. Altogether, these data suggest that the quality of the immune response to DT vaccine is substantially affected by the antigen dose, the delivery vehicle and the route of administration.

A major advantage of pulmonary vaccination is the potential induction of S-IgA antibodies at the respiratory epithelium and mucosal sites. S-IgA not only has an important role as the first defense line against many pathogens at the portal of their entry in the respiratory tract but also has been proven to elicit cross-protective immunity more effectively than serum IgG (59). DT-specific S-IgA can bind to exotoxin released by *Corynebacterium diphtheriae*, which may prevent the exotoxin from penetrating inside the mucosal sites (10, 18, 45). It is clear from the results that the pulmonarily administered DT-TMC microparticles were the only formulations that induced S-IgA titers in guinea pigs (figure 7). In contrast, pulmonary administered DT-Dextran microparticles and SC administered antigen formulations did not show S-IgA response, which is consistent with published observations that SC administrations of antigen formulations were not able to induce any S-IgA response (36, 42). In conclusion, pulmonary administration of encapsulated DT antigen in TMC microparticles enhanced significantly the systemic and local immune response, compared to SC administration of conventional alum-DT vaccine or pulmonary immunization with DT-dextran microparticles. This makes the TMC microparticles a promising vehicle for pulmonary delivery of DT antigen and, most likely, other antigens.

Acknowledgments

We thank Hans Strootman and Piet van Schaaik (the Netherlands Vaccine Institute) for their help with the animal studies. Paul Hagedoorn (Department of Pharmaceutical Technology and Biopharmacy, University of Groningen) is acknowledged for the LD measurements of the DT powders and his technical help in the cascade impactor analysis. We are grateful to Mies J. van Steenbergen (Department of Pharmaceutics, Utrecht Institute for Pharmaceutical Sciences, Utrecht University) for his help in HPLC.

References

1. J. S. Patton. Mechanisms of macromolecules absorption by the lungs. *Adv Drug Del Rev* 19: 3-36 (1996).

2. D. R. Owens, B. Zinman, and G. Bollit. Alternative routes of insulin delivery. *Diabet Med* 20: 886-898 (2003).

3. J. Bienenstockand M. R. McDermott. Bronchus- and nasal-associated lymphoid tissues. *Immunol Rev* 206: 22-31 (2005).

4. H. O. Alpar, S. Somavarapu, K. N. Atuah, and V. W. Bramwell. Biodegradable mucoadhesive particulates for nasal and pulmonary antigen and DNA delivery. *Adv Drug Deliv Rev* 57: 411-30 (2005).

5. J. S. Patton, C. S. Fishburn, and J. G. Weers. The lungs as a portal of entry for systemic drug delivery. *Proc Am Thorac Soc* 1: 338-44 (2004).

6. C. Pilette, Y. Ouadrhiri, V. Godding, J. P. Vaerman, and Y. Sibille. Lung mucosal immunity: immunoglobulin-A revisited. *Eur Respir J* 18: 571-88 (2001).

7. M. L. Clements, S. O'Donnel, M. M. Levine, R. M. Chanock, and B. R. Murphy. Dose response of A/Alaska/6/77 (H3N2) cold-adapted reassortant vaccine virus in adult volunteers: role of local antibody in resistance to infection with vaccine virus. *Infect. Immun.* 40: 1044-1051 (1983).

8. F. Y. Liew, S. M. Russel, G. Appleyard, C. M. Brand, and J. Beale. Cross protection in mice infected with influenza A virus by the respiratory route is corrected with local IgA antibody rather than serum antibody or cytotoxic T cell reactivity. *Eur. J. Immunol.* 14: 350-356 (1984).

9. B. J. Underdownand J. M. Schiff. Immunoglobulin A:strategic defense initiative at the mucosal surface. *Annu. Rev. Immunol.* 4: 389-417 (1986).

10. D. D. Ourth. Neutralization of diphtheria toxin by human immunoglobulin classes and subunits. *Immunochemistry* 11: 223-5 (1974).

11. M. Bivas-Benita, M. Laloup, S. Versteyhe, J. Dewit, J. De Braekeleer, E. Jongert, and G. Borchard. Generation of Toxoplasma gondii GRA1 protein and DNA vaccine loaded chitosan particles: preparation, characterization, and preliminary in vivo studies. *Int J Pharm* 266: 17-27 (2003).

12. I. M. van der Lubben, G. Kersten, M. M. Fretz, C. Beuvery, J. C. Verhoef, and H. E. Junginger. Chitosan microparticles for mucosal vaccination against diphtheria: oral and nasal efficacy studies in mice. Vaccine 28: 1400-1408 (2003).

13. A. Vila, A. Sanchez, K. Janes, I. Behrens, T. Kissel, J. L. Vila Jato, and M. J. Alonso. Low molecular weight chitosan nanoparticles as new carriers for nasal vaccine delivery in mice. *Eur. J. Pharm. Biopharm.* 57: 123-131 (2004).

14. I. M. van der Lubben, J. C. Verhoef, M. M. Fretz, F. A. C. van Opdorp, I. Mesu, G. Kersten, and H. E. Junginger. Trimethyl chitosan chloride (TMC) as novel excipient for oral and nasal immunization against diphtheria. *STP Pharm Sci* 12: 235-242 (2002).

15. M. Bivas-Benita, K. E. van Meijgaarden, K. L. Franken, H. E. Junginger, G. Borchard, T. H. Ottenhoff, and A. Geluk. Pulmonary delivery of chitosan-DNA nanoparticles enhances the immunogenicity of a DNA vaccine encoding HLA-A*0201-restricted T-cell epitopes of Mycobacterium tuberculosis. *Vaccine* 22: 1609-15 (2004).

16. I. M. van der Lubben, F. A. Konings, G. Borchard, J. C. Verhoef, and H. E. Junginger. In vivo uptake of chitosan microparticles by murine Peyer's patches: visualization studies using confocal laser scanning microscopy and immunohistochemistry. *J Drug Target* 9: 39-47 (2001).

17. M. Amidi, S. G. Romeijn, G. Borchard, H. E. Junginger, W. E. Hennink, and W. Jiskoot. Preparation and characterization of protein-loaded N-trimethyl chitosan nanoparticles as nasal delivery system. *J Control Release* 111: 107-116 (2006).

18. E. A. McNeela, I. Jabbal-Gill, L. Illum, M. Pizza, R. Rappuoli, A. Podda, D. J. Lewis, and K. H. Mills. Intranasal immunization with genetically detoxified diphtheria toxin induces T cell responses in humans: enhancement of Th2 responses and toxin-neutralizing antibodies by formulation with chitosan. *Vaccine* 22: 909-14 (2004).

19. J. H. Hamman, M. Stander, and A. F. Kotzé. Effect of the degree of quaternization of N-trimethyl chitosan chloride on absorption enhancement: in vivo evaluation in rat nasal epithelia. *Int J Pharm* 232: 235-242 (2002).

20. M. Thanou, J. C. Verhoef, J. H. M. Verheijden, and H. E. Junginger. Intestinal absorption of octeriotide: N-trimethyl chitosan chloride (TMC) ameliorates the permeability and absorption properties of the somatostatin analogue in vitro and in vivo. *J Pharm Sci* 89: 951-957 (2000).

21. M. Amidi, S. G. Romeijn, J. C. Verhoef, H. E. Junginger, L. Bungener, A. Huckriede, D. J. Crommelin, and W. Jiskoot. N-Trimethyl chitosan (TMC) nanoparticles loaded with influenza subunit antigen for intranasal vaccination: Biological properties and immunogenicity in a mouse model. *Vaccine* 25: 144-53 (2007).

22. H. O. Alpar, J. E. Eyles, E. D. Williamson, and S. Somavarapu. Intranasal vaccination against plague, tetanus and diphtheria. *Adv Drug Deliv Rev* 51: 173-201 (2001).

23. N. Rydelland I. Sjoholm. Oral vaccination against diphtheria using polyacryl starch microparticles as adjuvant. *Vaccine* 22: 1265-74 (2004).

24. N. Rydelland I. Sjoholm. Oral vaccination against diphtheria using polyacryl starch microparticles as adjuvant. *Vaccine* 22: 1265-74 (2004 Mar).

25. S. D. Yeo, G. B. Lim, P. G. Debenedetti, and H. Bernstein. Formation of microparticulate protein powders using a supercritical fluid antisolvent. *Biotech Bioeng* 41: 341-346 (1993).

26. N. Elvassore, A. Bertucco, and P. Caliceti. Production of insulin-loaded poly(ethylene glycol)/poly(l-lactide) (PEG/PLA) nano-particles by gas antisolvent techniques. *J Pharm Sci* 90: 1628–1636 (2001).

27. M. Tservistas, M. S. Levy, M. Y. Lo-Yim, R. D. O'Kennedy, P. York, G. O. Humphrey, and M. Hoare. The formation of plasmid DNA loaded pharmaceutical powders using supercritical fluid technology. *Biotech Bioeng* 72: 12-18 (2001).

28. N. Jovanovic, A. Bouchard, G. W. Hofland, G. J. Witkamp, D. J. A. Crommelin, and W. Jiskoot. Stabilization of proteins in dry powder formulations using supercritical fluid technology. *Pharm Res* 21: 1955-69 (2004).

29. N. Jovanovic, A. Bouchard, G. W. Hofland, G. J. Witkamp, D. J. A. Crommelin, and W. Jiskoot. Distinct effects of sucrose and trehalose on protein stability during supercritical fluid drying and freeze-drying. *Eur J Pharm Sci* 27: 336-45 (2006).

30. X. Jiang, A. van der Horst, M. J. van Steenbergen, N. Akeroyd, C. F. van Nostrum, P. J. Schoenmakers, and W. E. Hennink. Molar-mass characterization of cationic polymers for gene delivery by aqueous size-exclusion chromatography. *Pharm Res* 23: 595-603 (2006).

31. A. B. Sieval, M. Thanou, A. F. Kotzé, J. C. Verhoef, J. Brussee, and H. E. Junginger. Preparation and NMR- characterisation of highly substituted N-trimethyl chitosan chloride. *Carbohydr Polym* 36: 157-165 (1998).

32. G. W. Hallworthand U. G. Andrews. Size analysis of suspension inhalation aerosols by inertial separation methods. *J Pharm Pharmacol* 28: 898-907 (1976).

33. A. H. de Boer, D. Gjaltema, P. Hagedoorn, and H. W. Frijlink. Characterization of inhalation aerosols: a critical evaluation of cascade impactor analysis and laser diffraction technique. *Int J Pharm* 249: 219-31 (2002).

34. W. C. Hinds. Acceleration and curvilinear particle motion. In *Aerosol Technology.* Properties, behavior and measurement of airborne particles (W. C. Hinds, ed), John Wiley & Sons, New York, 1982, pp. 104-126.

35. W. R. Verweij, L. de Haan, M. Holtrop, E. Agsteribbe, R. Brands, G. J. van Scharrenburg, and J. Wilschut. Mucosal immunoadjuvant activity of recombinant Escherichia coli heat-labile enterotoxin and its B subunit: induction of systemic IgG and secretory IgA responses in mice by intranasal immunization with influenza virus surface antigen. *Vaccine* 16: 2069-2076 (1998).

36. L. de Haan, W. R. Verweij, M. Holtrop, R. Brands, G. J. van Scharrenburg, A. M. Palache, E. Agsteribbe, and J. Wilschut. Nasal or intramuscular immunization of mice with influenza subunit antigen and the B subunit of Escherichia coli heat-labile toxin induces IgA- or IgG-mediated protective mucosal immunity. *Vaccine* 19: 2898-2907 (2001).

37. K. Miyamura, S. Nishio, A. Ito, R. Murata, and R. Kono. Micro cell culture method for determination of diphtheria toxin and antitoxin titres using VERO cells. I. Studies on factors affecting the toxin and antitoxin titration. *J Biol Stand* 2: 198-201 (1974).

38. R. Rappuoli. New generation vaccines. In G. S. Cobon (ed), New and improved vaccines against diphtheria and tetanus (G. S. Cobon, ed), Marcel Dekker, New York, 1997, pp. 417–36.

39. M. Kanke, I. Sniecinski, and P. P. DeLuca. Interaction of microspheres with blood constituents: I. Uptake of polystyrene spheres by monocytes and granulocytes and effect on immune responsiveness of lymphocytes. J Parenter Sci Technol 37: 210-7 (1983).

40. Y. Tabataand Y. Ikada. Effect of the size and surface charge of polymer microspheres on their phagocytosis by macrophage. Biomaterials 9: 356-62 (1988).

41. B. C. Baudner, M. Morandi, M. M. Giuliani, J. C. Verhoef, H. E. Junginger, P. Costantino, R. Rappuoli, and G. Del Giudice. Modulation of immune response to group C meningococal conjugate vaccine given intranasally to mice together with trimethyl chitosan delivery system. *J Infect Dis* 189: 828-832 (2004).

42. M. Singh, M. Briones, and D. T. O'Hagan. A novel bioadhesive intranasal delivery system for inactivated influenza vaccines. *J. Control. Release* 70: 267-76 (2001).

43. A. Coulter, R. Harris, R. Davis, D. Drane, J. Cox, D. Ryan, P. Sutton, S. Rockman, and M. Pearse. Intranasal vaccination with ISCOMATRIX adjuvanted influenza vaccine. *Vaccine* 21: 946-9 (2003).

44. V. W. Bramwell, S. Somavarapu, I. Outschoorn, and H. O. Alpar. Adjuvant action of melittin following intranasal immunisation with tetanus and diphtheria toxoids. *J Drug Target* 11: 525-30 (2003).

45. M. Isaka, Y. Yasuda, S. Kozuka, T. Taniguchi, K. Matano, J. Maeyama, T. Komiya, K. Ohkuma, N. Goto, and K. Tochikubo. Induction of systemic and mucosal antibody responses in mice immunized intranasally with aluminium-non-adsorbed diphtheria toxoid together with recombinant cholera toxin B subunit as an adjuvant. *Vaccine* 18: 743-51 (2000).

46. P. G. Jenkins, A. G. Coombes, M. K. Yeh, N. W. Thomas, and S. S. Davis. Aspects of the design and delivery of microparticles for vaccine applications. *J. Drug. Target* 3: 79-81 (1995).

47. A. G. Coombes, E. C. Lavelle, P. G. Jenkins, and S. S. Davis. Single dose, polymeric, microparticle-based vaccines: the influence of formulation conditions on the magnitude and duration of the immune response to a protein antigen. *Vaccine* 14: 1429-1438 (1996).

48. I. Jabbal-Gill, W. Lin, P. Jenkins, P. Watts, M. Jimenez, L. Illum, S. Davis, J. Wood, D. Major, P. Minor, X. Li, E. Lavelle, and A. Coombes. Potential of polymeric lamellar substrate particles (PLSP) as adjuvants for vaccines. 18: 238-250 (2000).

49. Q. Vu, K. M. McCarthy, M. McCormack, and E. E. Schneeberger. Lung dendritic cells are primed by inhaled particulate antigens, and retain MHC class II/antigenic peptide complexes in hilar lymph nodes for a prolonged period of time. *Immunology* 105: 488–498 (2002).

50. K. D. Newman, P. Elamanchili, G. S. Kwon, and J. Samuel. Uptake of poly(D,L-lactic-co-glycolic acid) microspheres by antigen-presenting cells in vivo. *J Biomed Mater Res* 60: 480-6 (2002).

51. R. Audran, K. Peter, J. Dannull, Y. Men, E. Scandella, M. Groettrup, B. Gander, and G. Corradin. Encapsulation of peptides in biodegradable microspheres prolongs their MHC class-I presentation by dendritic cells and macrophages in vitro. *Vaccine* 21: 1250–1255 (2003).

52. L. Vidard, M. Kovacsovics-Bankowski, S. K. Kraeft, L. B. Chen, B. Benacerraf, and K. L. Rock. Analysis of MHC class II presentation of particulate antigens of B lymphocytes. *J. Immunol.* 156: 2809–2818 (1996).

53. H. F. Sun, K. G. J. Pollock, and J. M. Brewer. Analysis of the role of vaccine adjuvants in modulating dendritic cell activation and antigen presentation in vitro. *Vaccine* 21: 849–855 (2003).

54. A. F. Kotzé, H. L. Lueßen, B. J. de Leeuw, A. G. de Boer, J. C. Verhoef, and H. E. Junginger. Enhancement of paracellular drug transport with highly quaternised N-trimethyl chitosan chloride in neutral environments: in vitro evaluation in intestinal epithelial cells (Caco-2). *J Pharm Sci* 88: 253-257 (1999).

55. D. Snyman, J. H. Hamman, and A. F. Kotze. Evaluation of the mucoadhesive properties of N-trimethyl chitosan chloride. *Drug Dev Ind Pharm* 29: 61-9 (2003).

56. L. Thiele, H. P. Merkle, and E. Walter. Phagocytosis and phagosomal fate of surface-modified microparticles in dendritic cells and macrophages. *Pharm Res* 20: 221-8 (2003).

57. R. K. Gupta. Aluminum compounds as vaccine adjuvants. *Adv Drug Deliv Rev* 32: 155-172 (1998).

58. J. Coxand A. Coulter. Prospects for the development of new vaccine adjuvants. *Biodrugs* 12: 439-53 (1999).

59. R. Ito, Y. A. Ozaki, T. Yoshikawa, H. Hasegawa, Y. Sato, Y. Suzuki, R. Inoue, T. Morishima, N. Kondo, T. Sata, T. Kurata, and S. Tamura. Roles of anti-hemagglutinin IgA and IgG antibodies in different sites of the respiratory tract of vaccinated mice in preventing lethal influenza pneumonia. *Vaccine* 21: 2362-2371 (2003).

Chapter seven

7 Summary and perspectives

1 Summary

Therapeutic peptides/proteins and proteins-based antigens are labile compounds, which are almost exclusively administered by parenteral injections, because of their instability and/or poor absorption when using non-parenteral routes of administration. However, injections are inconvenient for patients and injectable formulations are expensive. Therefore, in recent years alternative routes of administration and dosage forms for therapeutic proteins and antigens have been pursued to avoid regular injections and give high absorption of the proteins and/or uptake of vaccines. Among the nonparenteral delivery routes, nasal and pulmonary delivery of proteins and antigens is particularly attractive, because the respiratory tract, including the nasal mucosa and pulmonary epithelium, has large absorptive surfaces, especially in the lungs, extensive vasculature and low proteolytic activity (1-3). Despite these advantages, there are major factors limiting the absorption and/or uptake of proteins from the respiratory epithelia. These limitations include the inherent impermeability of the respiratory epithelia for proteins and antigens, the short residence time of the proteins/antigens in the nasal cavity and central respiratory tract because of mucociliary clearance, and poor accessibility of protein and vaccine formulations to the absorptive sites, especially the alveoli (3, 4). Moreover, soluble antigens are hardly taken up by the MALT. In order to tackle these difficulties, proper delivery systems have to be developed that protect proteins/antigens against degradation, prevent their rapid elimination from administration sites and enhance their absorption and/or uptake across epithelial barriers.

Chitosan microparticles and nanoparticles loaded with proteins and antigens have shown to enhance the absorption and/or cellular uptake of macromolecules across mucosal sites (5-8). Chitosan is mucoadhesive and capable of opening the tight junctions between epithelial cells (9, 10). However, it is insoluble and inactive at physiological pH. In contrast to chitosan, N-trimethyl chitosan chloride (TMC), a partially quaternized chitosan derivative, shows good water solubility over a wide pH range with mucoadhesive properties and excellent absorption enhancing effects even at neutral pH (11, 12). Therefore, TMC particulate carrier systems are excellent candidates for intranasal and pulmonary delivery of proteins and antigens. Since the nose and lungs have their own specific physiological conditions and barriers, in terms of type of epithelial cells, presence or absence of a mucous layer and ease of access, the physicochemical characteristics of delivery systems for therapeutic proteins and antigens have to be tailored according to the route of administration.

The research described in this thesis was aimed at evaluating the potential of TMC particulate carrier systems for delivery of therapeutic proteins and antigens across respiratory (nasal and pulmonary) epithelia. To this end, TMC loaded nanoparticles and microparticles with different model proteins as well as a therapeutically relevant protein (insulin) and antigens (influenza subunit antigen and diphtheria toxoid) were prepared and characterized, and their efficacy for nasal and pulmonary delivery of these proteins was investigated in animal models.

Chapter 1 gives a review on the current literature of chitosan-based polymeric carrier systems for non-parenteral delivery of proteins and antigens, focusing on nasal and pulmonary routes of administration. The principles behind nasal and pulmonary absorption and/or cellular uptake of proteins/antigens are discussed. Absorption of a soluble protein/antigen can occur via the paracellular pathway, by opening the epithelial tight junctions using penetration enhancers. Moreover, via the transcellular pathway, soluble proteins/antigens as well as protein/antigen-loaded particles can be taken up by epithelia and the M-cells present in MALT. Practical issues for nasal and pulmonary delivery of therapeutic proteins and antigens are discussed, such as the use of mucoadhesive particulate carrier systems with defined particle size in order to reach the sites of absorption/uptake. Chitosan, as a mucoadhesive and absorption enhancer, has functional groups for chemical modifications, which has resulted in a large variety of chitosan derivatives with several tailored properties, e.g. solubility, hydrophobicity, etc. The physicochemical and biological properties of chitosan-based polymers, in particular TMC, for non-parenteral protein and antigen delivery are summarized. **Chapter 1** also discusses techniques for preparation of chitosan-based particulate carriers, such as ionic crosslinking and supercritical drying processes, which are the principal techniques used in this thesis to prepare TMC nanoparticles and microparticles. Finally, *in vivo* evaluations of chitosan-based particulate delivery systems for proteins and antigens are reviewed. These studies have shown benefits in terms of improved stability and efficient delivery of these macromolecules.

Chapter 2 reports on preparation and characterization of TMC nanoparticles as a carrier system for the nasal delivery of proteins. TMC nanoparticles were prepared by ionic crosslinking of TMC in an aqueous solution (with or without ovalbumin) with tripolyphosphate, at ambient temperature while stirring. Since small positively charged nanoparticles generally show a higher uptake by nasal epithelia than larger and/or negatively charged ones, the criteria size, size distribution and zeta-potential of the nanoparticles were used to select the best formulation parameters to prepare nanoparticles. The nanoparticles had an average size of about 350 nm and a positive surface charge. The nanoparticles showed an excellent loading efficiency (95%) and loading capacity (50% (w/w)) for ovalbumin. More than 70% of the protein remained associated with the TMC nanoparticles for at least 3 hours on incubation in PBS (pH 7.4) at 37 °C. Polyacrylamide gel electrophoresis and immunoblotting techniques suggested that the protein structure was preserved during preparation of the protein-loaded TMC nanoparticles. Ciliary beat frequency (CBF) measurements of chicken embryo trachea and *in vitro* cytotoxicity assays revealed no cell toxicity of the nanoparticles, whereas a partially reversible cilio-inhibiting effect on the CBF of chicken trachea was seen *in vitro*. *In vivo* experiments showed that intranasally administered TMC nanoparticles loaded with FITC-albumin were able to cross the mucosal layer, taken up by rat nasal epithelia and NALT cells, and transported to sub-mucosal layers. These results led us to conclude that TMC nanoparticles are a potential new delivery system for transport of proteins through the nasal mucosa.

In **Chapter 3** the potential of TMC nanoparticles as a carrier system for the nasal

delivery of a monovalent influenza subunit vaccine was investigated. The antigen-loaded nanoparticles were prepared by an ionic gelation technique as described in **Chapter 2**. The nanoparticles had an average size of about 800 nm with a narrow size distribution, a positive surface charge, a loading efficiency of 78% and a loading capacity of 13% (w/w). It was shown that more than 75% of the protein remained associated with the TMC nanoparticles upon incubation of the particles in PBS for 3 hours. The molecular weight and antigenicity of the entrapped hemagglutinin was maintained as shown by polyacrylamide gel electrophoresis and Western blotting, respectively. Intranasally administered soluble antigen alone or co-administered with soluble TMC was poorly immunogenic. However, single intranasal (i.n.) or intramuscular (i.m.) administration of encapsulated influenza antigen in TMC nanoparticles resulted in strong hemagglutination inhibition and in total IgG responses that were significantly higher than those achieved after i.m. administration of the subunit antigen. The IgG1/IgG2a profiles after i.n. or i.m. immunizations were similar. Immune responses were significantly enhanced after i.n. booster vaccinations. Moreover, among the tested formulations only antigen-loaded TMC nanoparticles induced significant IgA levels in nasal washes of all mice after i.n. administration. These findings make TMC nanoparticles a potential carrier for nasal delivery of influenza antigens and, most likely, other antigens.

Chapter 4 describes the preparation and physicochemical characterization of TMC (as a polymeric mucoadhesive absorption enhancer) and dextran (as a non-permeation enhancer) microparticles as carriers for pulmonary delivery of insulin. Insulin-loaded microparticles suitable for pulmonary administration were prepared by a supercritical fluid (SCF) drying process. This process involved spraying of an acidic water/DMSO solution of insulin and dextran or TMC into supercritical carbon dioxide. The mean size of the particles, as determined by laser diffraction analysis, was between 6-10 μm and their volume median aerodynamic diameter (VMAD) as determined by time-of-flight measurement was ca. 4 μm. The water content of the particles as measured by Karl Fischer titration was ca. 4% (w/w), but this resulted in neither collapse nor aggregation of the particles. In the freshly prepared dried insulin powders, the SCF drying process did not cause insulin degradation as detected by HPLC and GPC analysis. Moreover, the secondary and tertiary structure of insulin as determined by circular dichroism (CD) and fluorescence spectroscopy was essentially preserved in all formulations. After one year storage at 4 ºC, the particle characteristics were maintained and the insulin structure was largely preserved in the TMC powders. This study demonstrates that SCF drying is a suitable method to produce stable inhalable insulin powders.

In **Chapter 5**, the potential of the microparticles described in **Chapter 4** as carriers for pulmonary delivery of insulin was studied in diabetic rats. The insulin-loaded microparticles were administered intratracheally into the lungs of the rats. A population pharmacokinetic-pharmacodynamic (PKPD) model was used to evaluate the impact of different delivery systems on insulin bioavailability as well as on its pharmacological effects, as measured by insulin sensitivity and glucose

disappearance. In addition, possible acute adverse effects of these microparticles were examined by histological studies of the lungs of the treated rats. Pulmonary administration of TMC60-insulin microparticles resulted in significant systemic absorption of insulin, compared to the absorption using dextran- and TMC20-insulin microparticles. TMC20-insulin powder showed an extended release of insulin, which may result from differences in dissolution and/or absorption properties. The bioavailability of the pulmonarily administered dextran-, TMC20- and TMC60-insulin particles relative to subcutaneously (SC) administered insulin, was 0.47, 0.57 and 0.91, respectively. The insulin powders did not induce acute inflammatory reactions on the respiratory epithelium of the insulin formulations. The PKPD model (the minimal model of glucose disappearance) could describe the insulin-glucose relationship and the pharmacodynamic efficiency of insulin formulations, which was about 0.6 independent of the formulations. The current findings suggest that TMC microparticles are a promising vehicle for pulmonary delivery of insulin and perhaps other therapeutic proteins.

In **Chapter 6**, TMC (DQ 50%, as a mucoadhesive and permeation enhancer) and dextran (as a non-mucoadhesive and non-permeation enhancer) microparticles associated with diphtheria toxoid (DT, as a model antigen) were studied for their capability to induce systemic and local immune responses after pulmonary immunization in guinea pigs. The antigen-containing microparticles were prepared by spraying an aqueous solution of DT and TMC or dextran into supercritical carbon dioxide. The median volume diameter of the dry particles, as determined by laser diffraction, was between 2-3 μm and the fine particle fraction smaller than 5 μm, as determined by cascade impactor analysis, was about 55%. The water content of the particles as measured by Karl Fischer titration was 2-3% (w/w). Immunizations with DT-TMC microparticles containing 2 or 10 Lf of DT resulted in a strong immunological response as reflected by the induction of IgM, total IgG, IgG subtypes (IgG1 and IgG2) antibodies as well as neutralizing antibody titers comparable to or superior to those achieved after subcutaneous (SC) administration of alum-adsorbed DT (2 Lf). In contrast, pulmonarily administered DT-dextran particles were poorly immunogenic. Interestingly, pulmonary immunization with DT-TMC microparticles resulted in an improved Th_1 response, with a significantly higher IgG2/IgG1 ratio as compared to SC administered alum-adsorbed DT. Importantly, only pulmonarily administered DT-containing TMC microparticles induced detectable pulmonary secretory IgA levels.

2 Discussion and perspectives

The results presented in this thesis demonstrate that TMC particles are promising delivery systems for nasal and pulmonary delivery of therapeutic proteins and protein-based antigens. TMC particles are easy to prepare and have a high loading capacity for antigens and proteins. Moreover, the preparation methods used appeared to be

compatible with the proteins: the physicochemical characteristics and the biological activity of a pharmaceutically relevant protein (insulin) as well as the antigenicity and the immunogenicity of two antigens (hemagglutinin and diphtheria toxoid) were preserved. However, as outlined below several issues need to be addressed when further developing the concept of using TMC in pharmaceutical products.

In this thesis, the TMC polymers used were obtained by methylation of chitosan. The chitosan we used had a residual degree of N-acetylation of 7%. Under the applied reaction conditions, quaternization is not quantitative and also mono- and dimethylated amines are present. It has been also reported that methylation of hydroxyl groups at position 3 and 6 might occur (13). This means that the obtained TMCs are poorly defined and difficult to fully characterize. Moreover, chain cleavage of chitosan may take place using the synthetic method. The reproducible production of TMC forms a challenge and therefore, alternative methods to synthesize well-defined TMCs reproducibly and with a narrow molecular 'dispersion' spectrum are needed. Jia et al reported on the modification of the primary groups of chitosan with formaldehyde and a reducing agent to yield a fully dimethylated chitosan which in a subsequent step, using methyl iodide, was converted under relatively mild conditions to partially quaternized TMC (14). This method is potentially suitable to synthesize better defined TMCs, but needs further investigations. Important questions are whether the degree of quaternization can be controlled and O-methylations are avoided. In a recent study, the synthesis of an N-sulfonated chitin polymer catalyzed by chitinase was reported (15). Starting from a disaccharide, the enzymatic polymerization proceeded homogeneously and provided polysaccharides with total control over region-selectivity and stereochemistry. It might be interesting to investigate enzymatic (co)polymerization of well-defined building blocks to yield TMC. An additional advantage of this method is that TMCs synthesized in this way are devoid of (in particular protein-related) impurities normally present in chitosan from natural resources.

The biodegradability of polymeric carriers is an important issue for potential drug delivery applications. Biodegradation can occur through either chemical pathways and/or by enzymatic actions. It has been shown that chitosan is mainly degraded via enzymatic routes. Chitosan is susceptible to degradation with different human enzymes such as lysozyme, pectinase, lipase, amylase, N-acetylglucosaminidase and chitinase (16, 17). The presence of lysozyme and chitinase in human lungs has been reported, whereas chitinase is present in blood and leukocytes. Moreover, macrophages produce lysozyme and chitinase, which depolymerize chitosan to chitosan oligomers and finally to N-acetyl glucosamine and glucosamine. It has been shown that chicken egg white lysozyme exerts a maximum activity on chitosan with a degree of acetylation around 20% and is ineffective on fully deacetylated chitosan (17). So far, the enzymatic degradability of TMC has not been studied. Therefore, the enzymatic degradation of TMCs with model enzymes has to be investigated.

In **Chapter 2 and 3** of this thesis, we successfully applied colloidal TMC nanoparticles for nasal protein and vaccine delivery. However, the stability and shelf-

life of these colloidal systems have not been investigated yet. For a commercial product, a shelf-life of at least two years is desired. Since aqueous colloidal systems generally have limited stability, freeze-drying is an option to improve the shelf-life of colloidal TMC nanoparticles (18). In addition, supercritical drying, as a relatively new and mild technique, is another option for drying these nanoparticle suspensions. However, these and other drying processes have to be further investigated for their capability of stabilizing protein-loaded TMC nanoparticles regarding their particle characteristics (size, charge), protein release profiles, and preservation of the structural integrity and biological activity of the protein/antigen. This can be done by optimizing the freeze-drying conditions, i.e. freeze rate, primary and secondary drying phase or the SCF drying process i.e. pressure, temperature and the use of co-solvents. The aggregation of the nanoparticles and structural damage of the loaded protein can be prevented by the use of proper non-reducing sugars (trehalose, sucrose and/or mannitol) as lyoprotectants (18).

In **Chapter 4**, we have shown that TMC-loaded insulin microparticles, with suitable median aerodynamic diameters, can be prepared by a supercritical drying process. The particles were stable during one year storage at 4 °C and the structural integrity of the protein was essentially preserved. However, more elaborate studies are needed to fully determine the long-term stability of TMC-protein powder formulations, both at refrigerated and ambient temperature conditions. The preferred physico-chemical characteristics of the powders in the product manufacturing process, e.g. flow properties and hygroscopicity, have to be assessed as well

The results of toxicity tests of TMC particulate carriers presented in the **Chapter 2 and 5** showed the absence of *in vitro* cytotoxicity, *ex vivo* ciliostatic effects, *in vivo* tissue damage and acute inflammatory reactions on the respiratory epithelium. It should be noted that the cell type should be selected according to the application and route of administration. In **Chapter 2**, cytotoxicity studies were performed with Calu-3 cells, which present essential characteristics of the respiratory epithelia such as intra-cell tight junctions, apically located cilia and mucus production. It is recommended to also perform cytotoxicity assays in an alveolar cell line lacking the mucus layer. *In vitro* and *ex vivo* toxicity tests are valuable tools for preliminary safety evaluations of drug delivery systems, but they do not fully assess their safety *in vivo*. So far, no long-term *in vivo* safety evaluations of TMC formulations have been reported. Therefore, to investigate in more depth the safety of TMC particles for nasal and pulmonary protein delivery, long-term toxicity evaluations in particular after repeated administrations in different animal models and, eventually, humans are needed.

As pointed out previously, the TMCs used in the current studies are relatively not well defined and characterized. It has been shown for TMC that with increasing molecular weight and degree of quaternization (DQ), its *in vitro* cytotoxicity increases (19, 20). However, along with higher the N-methylation degrees, the extent of O-methylation may increase. The separate effects of N- and O-methylation on the cytotoxicity of TMC formulations have not been investigated yet. Therefore, it is

recommended to carry out future *in vitro* and *in vivo* toxicity studies with well-defined TMCs. To mask possible toxic effects of TMC, pegylation is an obvious approach. Besides, pegylation might also improve the colloidal stability of TMC nanoparticles (20).

The results presented in **Chapter 3 and 6** show that TMC nanoparticles and microparticles hold great potential for nasal and pulmonary vaccine delivery. Additionally, in **Chapter 6**, we demonstrated that pulmonary immunization with DT-loaded TMC microparticles showed an enhanced Th_1 type immune response, as the IgG2/IgG1 ratios were significantly higher than those after alum-adjuvanted SC immunizations. The latter shows an attractive adjuvant effect of TMC upon pulmonary vaccination. As discussed in **Chapter 1**, the mechanism behind the adjuvant activity of chitosan has been studied. However, for TMC mechanistic studies such as TMC-specific activation of antigen presenting cells (APCs) and T-cell proliferation assays are lacking and need to be carried out. Such studies may also shed light onto structure-adjuvant relationships of TMC, which are crucial to rationally optimize TMC-based vaccine delivery systems.

The effects of TMC particles on the immune response can likely be improved by using TMC particles with ligands at their surface which actively target these particles to M-cells, APCs such as dendritic cells (DCs), and macrophages. For instance, mannose and glucomannan interact with mannose receptors on APCs and these molecules can thus be used as targeting ligands, e.g. by conjugating mannose to TMC or by coating preformed TMC nanoparticles with the negatively charged phosphorylated glucomannan. Furthermore, specific ligands such as monoclonal antibodies, directed to specific receptors on APCs can be attached to the surface of TMC particles, which may result in targeted delivery and improved immunogenicity of the vaccine. Another approach to enhance the efficacy of TMC particles as vaccine delivery systems is co-incorporation of adjuvants, e.g. CpG motifs, non-toxic or attenuated forms of heat-labile bacterial enterotoxins of Escherichia coli or Vibrio cholerae in the particles.

In the TMC nanoparticles, the protein interacts with positively charged TMC by electrostatic forces. As shown in **Chapter 2 and 3**, these nanoparticles displayed a burst release likely caused by loosely associated protein in the nanoparticle matrix. Subsequently, no further protein release occurred in the investigated time frame; the remaining protein was stably associated with the TMC nanoparticles. Mechanistic studies, e.g. using surface plasmon resonance (SPR) analysis, towards protein-TMC interactions should be performed to better understand the protein loading and release characteristics of TMC particles. Moreover, biocompatible anionic polymers, e.g alginate, can be added to TMC particle formulations as release modifiers (21). Also thiolated TMC can be applied to prepare crosslinked particles, from which the release of proteins can be modulated (22). Coating of protein-loaded TMC nanoparticles with lipid bilayers results in TMC nanovesicles, which may show an improved colloidal stability and a decreased burst release of the loaded protein. Moreover, in these vesicles the protein/antigen is protected against attack of proteases.

In **Chapter 5** of this thesis pulmonarily administered TMC20-insulin microparticles, unlike TMC60- and dextran-insulin powders, showed a long-lasting (up to 3 hours) plateau insulin plasma level, which is likely due to their slower dissolution or absorption as compared to the TMC60 and dextran particles. This might be interesting when a controlled release and long-lasting effect of a protein drug is desired, but the exact mechanism of this observation still has to be unraveled.

In conclusion, the studies described in this thesis demonstrate that TMC particulate carrier systems hold great promise for mucosal delivery of therapeutic proteins and protein antigens. Further characterization and stabilization, as well as mechanistic studies on the biological and pharmacological effects of protein-loaded TMC nanoparticles and microparticles are needed to provide better insights into the safety and efficacy of TMC-based protein/antigen formulations and, ultimately, to assess their clinical value.

References

1. S. S. Davis. Nasal Vaccines. *Drug Deliv Rev* 51: 21-42. (2001).

2. J. S. Patton, C. S. Fishburn, and J. G. Weers. The lungs as a portal of entry for systemic drug delivery. *Proc Am Thorac Soc* 1: 338-44 (2004).

3. J. S. Patton. Mechanisms of macromolecules absorption by the lungs. *Adv Drug Del Rev* 19: 3-36 (1996).

4. R. J. Soane, M. Hinchcliffe, S. S. Davis, and L. Illum. Clearance characteristics of chitosan based formulation in the sheep nasal cavity. *Int J Pharm* 217: 183-191 (2001).

5. R. Fernandez-Urrusuno, P. Calvo, C. Remunan-Lopez, J. L. Vila-Jato, and M. J. Alonso. Enhancement of nasal absorption of insulin using chitosan nanoparticles. *Pharm Res* 16: 1576-81 (1999).

6. I. M. van der Lubben, F. A. Konings, G. Borchard, J. C. Verhoef, and H. E. Junginger. In vivo uptake of chitosan microparticles by murine Peyer's patches: visualization studies using confocal laser scanning microscopy and immunohistochemistry. *J Drug Target* 9: 39-47 (2001).

7. I. M. van der Lubben, G. Kersten, M. M. Fretz, C. Beuvery, J. C. Verhoef, and H. E. Junginger. Chitosan microparticles for mucosal vaccination against diphtheria: oral and nasal efficacy studies in mice. *Vaccine* 28: 1400-1408 (2003).

8. Y. Pan, Y. J. Li, H. Y. Zhao, J. M. Zheng, H. Xu, G. Wei, J. S. Hao, and F. D. Cui. Bioadhesive polysaccharide in protein delivery system: chitosan nanoparticles improve the intestinal absorption of insulin in vivo. *Int J Pharm* 249: 139-147 (2002).

9. M. Thanou, J. C. Verhoef, and H. E. Junginger. Oral drug absorption enhancement by chitosan and its derivatives. *Adv Drug Deliv Rev* 52: 117-26 (2001).

10. C. M. Lehr, J. A. Browstra, E. H. Schacht, and H. E. Junginger. In vitro evaluation of mucoadhesive properties of chitosan and some other natural polymers. *Int J Pharm* 78: 43-48 (1992).

11. J. H. Hamman, M. Stander, and A. F. Kotzé. Effect of the degree of quaternization of N-trimethyl chitosan chloride on absorption enhancement: in vivo evaluation in rat nasal epithelia. *Int J Pharm* 232: 235-242 (2002).

12. M. Thanou, J. C. Verhoef, J. H. M. Verheijden, and H. E. Junginger. Intestinal absorption of octeriotide: N-trimethyl chitosan chloride (TMC) ameliorates the permeability and absorption properties of the somatostatin analogue in vitro and in vivo. *J Pharm Sci* 89: 951-957 (2000).

13. A. Polnok, G. Borchard, J. C. Verhoef, N. Sarisuta, and H. E. Junginger. Influence of methylation process on the degree of quaternization of N-trimethyl chitosan chloride. *Eur J Pharm Biopharm* 57: 77-83 (2004).

14. Z. Jia, D. shen, and W. Xu. Synthesis and antibacterial activities of quaternary ammonium salt of chitosan. *Carbohydr Res* 333: 1-6 (2001).

15. A. Makino, H. Nagashima, M. Ohmae, and S. Kobayashi. Chitinase-catalyzed synthesis of an alternatingly N-sulfonated chitin derivative. *Biomacromolecules* 8: 188-95 (2007).

16. H. Onishiand Y. Machida. Biodegradation and distribution of water-soluble chitosan in mice. *Biomaterials* 20: 175-82 (1999).

17. R. A. Muzzarelli. Human enzymatic activities related to the therapeutic administration of chitin derivatives. *Cell Mol Life Sci* 53: 131-40 (1997).

18. S. Mao, U. Bakowsky, A. Jintapattanakit, and T. Kissel. Self-assembled polyelectrolyte nanocomplexes between chitosan derivatives and insulin. *J Pharm Sci* 95: 1035-48 (2006).

19. T. Kean, S. Roth, and M. Thanou. Trimethylated chitosans as non-viral gene delivery vectors: cytotoxicity and transfection efficiency. *J Control Release* 103: 643-53 (2005).

20. S. Mao, X. Shuai, F. Unger, M. Wittmar, X. Xie, and T. Kissel. Synthesis, characterization and cytotoxicity of poly(ethylene glycol)-graft-trimethyl chitosan block copolymers. *Biomaterials* 26: 6343-56 (2005).

21. F. Chen, Z. R. Zhang, and Y. Huang. Evaluation and modification of N-trimethyl chitosan chloride nanoparticles as protein carriers. *Int J Pharm* in press (2006).

22. A. Bernkop-Schnurch, M. Hornof, and D. Guggi. Thiolated chitosans. *Eur J Pharm Biopharm* 57: 9-17 (2004).

Appendices

Nederlandse samenvatting

List of abbreviations

List of publications

Curriculum Vitae

Acknowledgments

Nederlandse samenvatting

Eiwitten vormen een belangrijke categorie van farmaca die toegepast worden voor de behandeling van chronische en levensbedreigende ziekten. Zo wordt bijvoorbeeld het eiwithormoon insuline gebruikt voor de behandeling van suikerziekte. Ook worden eiwitten in de vorm van vaccins toegediend aan met name kinderen en volwassenen ter voorkoming van virale en bacteriële infecties. Vanwege hun ongunstige biofarmaceutische eigenschappen worden deze eiwitmoleculen bijna zonder uitzondering via injecties aan patiënten gegeven. Dit is niet alleen pijnlijk voor de patiënt, maar ook zijn hier nogal hoge kosten aan verbonden. Er is derhalve grote behoefte aan afgiftesystemen waarmee deze eiwitten via niet-invasieve routes aan patiënten kunnen worden toegediend. Aangezien eiwitten erg gevoelig zijn voor chemische en fysische degradatieprocessen, moeten voor de vervaardiging van dergelijke afgiftesystemen vaak bestaande technologieën geoptimaliseerd worden of compleet nieuwe ontwikkeld worden.
In dit proefschrift is onderzocht of TMC (tri-gemethyleerd chitosan) geschikt is voor de bereiding van nasale en pulmonale toedieningsvormen voor therapeutische eiwitten en vaccins. TMC is een semi-synthetisch en wateroplosbaar polymeer dat verkregen wordt door chemische modificaties van chitine, een polysaccharide dat na cellulose het meest voorkomende polymeer in de natuur is en geïsoleerd wordt uit het exoskelet van o.a. garnalen. Dit polymeer hecht zich vanwege het kationogene karakter sterk aan het slijm waarmee epitheelcellen in onze neus en longen bedekt zijn. Hierdoor wordt de verblijftijd van aan TMC gebonden eiwitten in de luchtwegen verlengd. Bovendien verhoogt TMC de permeabiliteit van neus- en longepitheel. Door deze effecten kunnen therapeutische macromoleculen, die toegediend worden in combinatie met TMC, geabsorbeerd worden. Ook kunnen complete TMC-nanodeeltjes, die beladen zijn met eiwitmoleculen, door cellen worden opgenomen en vervolgens hun inhoud afgeven. In dit proefschrift zijn verschillende aspecten van TMC-eiwitformuleringen onderzocht.
Hoofdstuk 1 van dit proefschrift geeft een overzicht van de huidige literatuur van op chitosan gebaseerde afgegiftesystemen voor toediening van eiwitten via niet-parenterale routes. De principes die ten grondslag liggen aan de nasale en pulmonale absorptie van eiwitten en/of cellulaire opname van met eiwit beladen deeltjes worden bediscussieerd.
In **Hoofdstuk 2** worden TMC-nanodeeltjes onderzocht als dragersysteem voor de nasale toediening van eiwitten. Nanodeeltjes die beladen waren met het modeleiwit ovalbumine en met een afmeting van ongeveer 350 nm, werden vervaardigd door al roerende aan een waterige oplossing van TMC en ovalbumine, tripolyfosfaat toe te voegen. Experimenten met luchtpijpen van kippenembryo's en celcultures lieten weinig toxische effecten van deze deeltjes zien. Aangetoond werd dat nasaal toegediende TMC-nanodeeltjes werden opgenomen door het epitheel en verder getransporteerd werden naar de onderliggende cellagen. Deze studie toonde aan dat TMC-nanodeeltjes geschikte systemen zijn voor de nasale toediening van eiwitten.

In **Hoofdstuk 3** wordt onderzocht of TMC-nanodeeltjes die beladen zijn met een influenza-antigeen in staat zijn een goede immuunrespons op te wekken. Nasale toediening van een waterige oplossing van het antigeen met en zonder TMC resulteerde in een zeer geringe immuunrespons. Echter, zowel het intramusculair als nasaal toegediende antigeen dat ingebouwd was in TMC-nanodeeltjes met een afmeting van ongeveer 800 nm, gaf een zeer sterke immuunreactie te zien.
In **Hoofdstuk 4** staat de vervaardiging en karakterisering van met insuline beladen TMC-microdeeltjes beschreven. Deze deeltjes werden verkregen door een oplossing van TMC/insuline in DMSO/water te drogen met superkritisch CO_2. Aangezien deze microdeeltjes bedoeld zijn voor pulmonale toediening, is onderzocht of het middels deze techniek mogelijk is deeltjes te verkrijgen met een geschikte aerodynamische afmeting onder behoud van de structuur van het eiwit. Het bleek dat deeltjes met een geschikte grootte inderdaad vervaardigd kunnen worden en met een aantal geavanceerde technieken werd aangetoond dat het eiwit zijn structurele integriteit behouden heeft. Deze gunstige resultaten gaven aanleiding om deze formuleringen te testen in diabetische ratten, waarvan de resultaten in **Hoofdstuk 5** staan beschreven. Pulmonale toediening van de met insuline beladen TMC-microdeeltjes resulteerde in een significante systemische insuline-absorptie. Voor één formulering werd zelfs een relatieve biologische beschikbaarheid van 0,97 gevonden ten opzichte van subcutaan toegediend insuline. Het geabsorbeerde insuline was biologisch actief, hetgeen resulteerde in een sterke verlaging van de bloedsuikerspiegel. Histologische analyses lieten geen acute ontstekingsreacties of andere toxische effecten zien.
Hoofdstuk 6 beschrijft een studie over de pulmonale toediening van TMC-microdeeltjes die beladen zijn met difterietoxoïd (DT), een modelantigeen. De met eiwit beladen deeltjes werden vervaardigd door droging van een oplossing van DT en TMC in water gebruikmakend van superkritisch CO_2. Deze deeltjes hadden de goede aerodynamische afmetingen en gaven na pulmonale toediening aan hamsters zowel een sterke lokale als een systemische immuunrespons te zien. De gevonden immuunrespons was zelfs sterker dan die werd waargenomen na intramusculaire toediening van een standaard DT-formulering.
Samenvattend kan geconcludeerd worden dat de studies die beschreven staan in dit proefschrift hebben aangetoond dat op TMC gebaseerde nano- en microdeeltjes veelbelovende systemen zijn voor de toediening van therapeutische eiwitten en vaccins via niet-invasieve toedieningsroutes.

List of abbreviations

ANOVA	Analysis of Variance
APC	antigen presenting cell
APS	aerodynamic particle sizer
AUC	area under the curve
BAL	broncho-alveolar lavages
BALT	broncho-alveolar lymphoid tissue
BSA	bovine serum albumin
CBF	ciliary beat frequency
CD	circular dichroism
CLSM	confocal laser scanning microscopy
CO2	carbon dioxide
CSF	colony-stimulating factor
DC	dendritic cell
DCM	dichloromethane
DD	degree of deacetylation
DLS	dynamic light scattering
DM	dimethylation
DMEM	Dulbecco's Modified Eagle's Medium
DMSO	dimethyl sulfoxide
DT	diphtheria toxoid
DQ	degree of quaternization
ELISA	enzyme-linked immunosorbent assay
FCS	fetal calf serum
FITC	fluorescein isothiocyanate
FPF	fine particle fraction
GPC	gel permeation chromatography
HA	hemagglutinin
HAU	hemagglutination unit
HBSS	Hank´s balanced salt solution
HEPES	N-[2-hydroxyethyl] piperazine-N´-[2-ethanesulphonic acid]
HI	hemagglutination inhibition
HPLC	high-performance liquid chromatography
HTCC	N-(2-hydroxyl) propyl-3-trimethyl ammonium chitosan chloride
Ig	immunoglobulin
i.m.	intramuscular
i.n.	intranasal
INF	interferon α
LC	loading capacity
LD	laser diffraction
LE	loading efficiency
LR	Locke-Ringer solution

MALT	mucosal associated lymphoid tissue
MCC	carboxymethyl chitosan
M-cell	microfold cell
MLSI	multistage liquid impinger
MMAD	mass median aerodynamic diameter
Mw	molecular weight
NA	neuraminidase
NALT	nasal associated lymphoid tissue
NMR	nuclear magnetic resonance
PBS	phosphate buffer saline
PBS-T	phosphate buffer saline-Tween
PDI	polydispersity index
PEC	polyelectrolyte complexes
PEI	poly(ethylene imine)
PEG	poly(ethylene glycol)
pI	isoelectric point
PLGA	poly(lactide-co-glycolide)
γ-PGA	poly-γ-glutamic acid
RALS	right angle light scattering
RP-HPLC	reversed phase high-performance liquid chromatography
SEM	scanning electron microscopy
SC	subcutaneous
SC-CO2	supercritical carbon dioxide
SCF	supercritical fluid
SDS	sodium dodecyl sulfate
SDS- PAGE	sodium dodecyl sulfate polyacrylamide gel electrophoresis
SPF	specified pathogen free
TEER	transepithelial electrical resistance
TFA	trifluoro acetic acid
TMB	3,3',5,5'-tetra methyl benzidine
TMC	N-trimethyl chitosan
TPP	tripolyphosphate
TT	tetanus toxoid
UV	ultra violet
VMD	volume median diameter
VMAD	volume median aerodynamic diameter

List of publications

M. Amidi, S. G. Romeijn, G. Borchard, H. E. Junginger, W. E. Hennink, and W. Jiskoot. Preparation and characterization of protein-loaded N-trimethyl chitosan nanoparticles as nasal delivery system. *J Control Release* 111: 107-116 (2006).

O. Borges, A. Cordeiro-da-Silva, S. G. Romeijn, **M. Amidi**, A. de Sousa, G. Borchard and H. E. Junginger. Uptake studies in rat Peyer's patches, cytotoxicity and release studies of alginate coated chitosan nanoparticles for mucosal vaccination. *J Control Release.*114: 348-58 (2006).

M. Amidi, S. G. Romeijn, J. C. Verhoef, H. E. Junginger, L. Bungener, A. Huckriede, D. J. A. Crommelin, and W. Jiskoot. N-Trimethyl chitosan (TMC) nanoparticles loaded with influenza subunit antigen for intranasal vaccination: Biological properties and immunogenicity in a mouse model. *Vaccine* 25: 144-53 (2007).

M. Amidi, H. C. Pellikaan, A. H. de Boer, D. J. A. Crommelin, W. E. Hennink, and W. Jiskoot. Preparation and physicochemical characterization of supercritically dried insulin-loaded microparticles for pulmonary delivery. *Submitted for publication* (2007).

M. Amidi, K. M. Krudys, C. J. Snel, D. J.A. Crommelin, O. E. Della Pasqua, W. E. Hennink and W. Jiskoot. Efficacy of pulmonary insulin delivery in diabetic rats: Use of a model-based approach in the evaluation of insulin powder formulations. *Submitted for publication* (2007).

M. Amidi, H. C. Pellikaan, H. Hirschberg, A. H. de Boer, D. J. A. Crommelin, W. E. Hennink, G. Kersten and W. Jiskoot. Diphtheria toxoid-containing microparticulate powder formulations for pulmonary vaccination: preparation, characterization and evaluation in guinea pigs. *Submitted for publicatio*n (2007).

M. Amidi, D.J.A.Crommelin, W. E. Hennink, and W. Jiskoot. Non-parenteral delivery systems based on chitosan and its derivatives for protein therapeutics and antigens. *Manuscript in preparation.*

Curriculum Vitae

Maryam Amidi was born on May 5th 1974 in Tehran, Iran. In June 1993 she finished high school and subsequently she passed the National Academic Entrance Exam for Medical Sciences. In February 1994, she started to study pharmacy at the Free University of Tehran where she obtained her pharmacy doctor degree (Pharm. D.) in May 2000. After her graduation she worked in public and hospital pharmacies where she was responsible for reorganization and management issues.

In April 2002, she started her Ph.D. research project within the Division of Pharmaceutical Technology of the Leiden/Amsterdam Center for Drug Research, Leiden University, where she worked on the design and characterization of polymeric micro- and nanoparticles for mucosal protein and vaccine delivery, under supervision of Prof. Dr. H.E. Junginger, Prof. Dr. G. Borchard and Dr. J.C. Verhoef. In January 2004, she moved to the Department of Pharmaceutics, Utrecht University, where she continued her Ph.D. project under supervision of Prof. Dr. W. Jiskoot, Prof. Dr. D.J.A. Crommelin and Prof. Dr. W. E. Hennink, resulting in a thesis entitled *N-trimethyl chitosan (TMC) carriers for nasal and pulmonary delivery of therapeutic proteins and vaccines*. During her Ph.D. training she presented a number of lectures and posters at different international congresses, symposia and meetings.

Currently, she is working as a post doctoral researcher at the Department of Pharmaceutics, Utrecht University.

Acknowledgments

My Ph.D. story began in August 2000 when I attended the FIP conference in Vienna, Austria. At that time, I was following my dream, pursuing a Ph.D. abroad. It was a great challenge for me and finally my dream became true. I met Prof. Hans Junginger, who gave me the opportunity to start my Ph.D. in The Netherlands. Destiny?
Thinking back with gratitude on the last five years, I had one of the most challenging and extraordinary period of my life. Doing a Ph.D. at two different universities (Leiden and Utrecht) was a very wonderful and constructive experience, which gave me a chance to work with different persons and to make very good friends. Therefore, I would like to acknowledge all who supported me during my Ph.D. study.
First, I would like to express my appreciation to Prof. Dr. Hans Junginger for being my supervisor in the first year of my Ph.D. project and also for his hearty support and concern during this period and thereafter. Hans, I was so delighted because you always gave me compliments and were so positive about my work.
I would like to thank my other supervisors, Prof. Dr. Gerrit Borchard and Dr. Coos Verhoef for their advice and guidance during my research in Leiden. Special thanks for Gerrit and Christiane for inviting me to Germany and their generous hospitality.
Thanks to all my colleagues in Leiden: Miranda, Marytal, Julia, Mojgan, Gert and Stefan for their encouragement, support and courteousness. Special acknowledgments have to be given to Stefan for his assistance and patience during the animal experiments.
I wish to express my sincere gratitude to my promotor Prof. Dr. Wim Hennink for his patient guidance and instructive advice throughout my research project. Wim, you inspired me to reach my goal and I truly appreciate your scientific and genial support during these years. I enjoyed your hospitality, sense of humor and the fruitful discussions we had in our meetings.
I am deeply indebted to my second promotor Prof. Dr. Wim Jiskoot for supervising my research and his perceptive advice. Wim, your strong enthusiasm and critical discussions had a great impact on my work. You enlightened me with your extensive knowledge and I learnt so much from you.
I am very grateful to my third promotor, Prof. Dr. Daan Crommelin for his essential role in the transfer of my project from Leiden to Utrecht and his critical scientific discussions. Daan, you guided me how to be become an objective scientist and I appreciate your sharp and useful comments on the results I obtained.
I am thankful to my collaborators, who greatly contributed to accomplish this thesis: Dr. Anke Huckriede and Dr. Laura Bungener of the Department of Microbiology, Molecular Virology Section, University of Groningen are sincerely acknowledged for their essential and fruitful participation in my influenza vaccination studies, and also Wouter ter Veer for his assistance with the ELISA assays.
An important part of my research project would not be possible without collaboration of Feyecon D & I B.V. Special thanks goes to Hubert Pellikaan and Bas Vermeulen for their help with the supercritical experiments.

I would like to express my appreciation to Dr. Anne H. de Boer and Paul Hagedoorn of the Department of Pharmaceutical Technology and Biopharmacy, University of Groningen for their technical help with the characterization of the different powders and their professional comments to direct me through this part of my research.
I am also thankful to the people of the Netherlands Vaccine Institute (NVI), Hans Strootman and Piet van Schaaik for helping me to perform pulmonary immunizations and Dr. Gideon Kersten and Hoang Hirschberg for their valuable contributions, which resulted in a great piece of work.
The success in performing pharmacological analysis as described in chapter five of this thesis is the outcome of an excellent collaboration with Dr. Oscar Della Pasqua of the Division of Pharmacology, Leiden University and Dr. Kevin Krudys of the Division of Clinical Pharmacology and Discovery Medicine, GlaxoSmithKline (GSK). I am grateful for their precious contribution and guiding me through the difficult pharmacological aspects of this analysis.
Well, thanks to all colleagues and friends at the Department of Pharmaceutics, Utrecht University, for providing such a wonderful, cheerful and cooperative environment.
Special acknowledgments have to be given to Mies for his kind help with the HPLC and GPC experiments, Cor for his patient assistance in the animal experiments and two great ladies, Barbara and Lidija, who helped me with the different bureaucratic procedures during my Ph.D. and always cheered me up by their funny emails. I also would like to thank Dr. Herre Talsma for his help and kind support during these years, Dr. Raymond Schiffelers for discussion on statistics and Marcel for his assistance with the histological evaluations. Further I wish to thank other colleagues and friends: Marion for her kindness and Ellen for her cheerful attitude and organizing all those social activities. Cristianne and Birgit, I enjoyed having interesting and fruitful discussions with you. I thank Manuela for her kindness, generosity and sharing ups and downs in research. I should not forget Niels. I appreciate your warm and open-minded personality and I always enjoyed our witty and interesting conversations. I would like to express my warm thanks to Sabrina and Marc, my friends and room-mates at work. You created a friendly atmosphere in the lab and were always supportive. Sabrina thanks for inviting me to Portugal and your hospitality. I had a wonderful time there with you and Ellen.
My hearty thanks go to Natasa, my friend. I had a great time with you in the lab as well as outside the lab and we shared our fun, stress and happy and sad moments during these years. I am fortunate to have met my precious friend, Poupak, who always takes care about me.
I am grateful to my relatives in The Netherlands, Zari joon and amou Bagher, who made me feel at home. I never forget their warm welcome and also generous support during these years. Gelare and Matt, thank you for being there for me and the wonderful time I spent with you in all birthday parties, great Christmas dinners and weekend movie-marathons.
As well, I want to thank my great friends Sima and Farzin for their cordial friendship and taking care of me as their sister.

My warm thanks go to my closest friend, Amirhossein, who always inspired me during this period despite the distance. I am always delighted with your massive knowledge and fruitful conversations. I will cherish this friendship forever.
Finally, my greatest strength and inspiration is my family. It is impossible to say by words how grateful I am to them. My everlasting love and appreciation goes to my younger sister, Medya, for her enduring support and enormous love. I am thankful to my parents, who made everything in my life feasible with their huge encouragement, sacrifices and endless love. You are the meaning of love for me.

Iedereen ontzettend bedankt

Maryam